

Heavy products formation in free radical systems during thermal conversion of heavy oil

by

Joy Hikmat Tannous

A thesis submitted in partial fulfillment of the requirements for the degree of

Doctor of Philosophy

In

Chemical Engineering

Department of Chemical and Materials Engineering

University of Alberta

© Joy Hikmat Tannous, 2019

Abstract

Thermal cracking of heavy oils is important industrially in processes such as visbreaking, coking and residue hydroconversion. In these processes, residue conversion is limited by formation of heavy products. Heavy product formation also contributes to industrially relevant problems such as fouling and gum formation. In this study, heavy product formation in free radical systems was investigated.

The study of free radical systems requires preparatory work for the quantification of free radical content. Electron spin resonance spectroscopy (ESR) was employed to perform quantitative analysis of the free radical content of oilsands bitumen, asphaltenes, deasphalted oil, vacuum residue and vacuum gas oil fractions, as well as thermally converted product fractions. The main contribution from this work was to show that for bitumen and bitumen derived materials the bulk liquid properties affected the measured free radical concentration, even after compensating for effects that could affect the spectroscopy. These differences were explained in terms of the “equilibrium” composition that resulted from dimerization and decomposition of free radical pairs. It suggested that the free radical concentration and availability of reactive free radicals could be independently manipulated through temperature and the bulk liquid properties in thermal conversion of bitumen. This was a noteworthy contribution, because it suggested a new way to approach the control of free radical availability during thermal conversion.

Naphtheno-aromatics were suspected to be one of the compound classes responsible for heavy products formation. The reactivity of indan, indene, thianaphthene, indole and benzofuran was investigated at thermal cracking conditions of 400 °C and 2 MPa under nitrogen environment and provided relevant information about the reactivity of such compound classes for the rest of the study. Several of the test compounds were capable of self-reacting and forming heavy products.

Heavy product formation caused by free radical addition reactions was evaluated. The importance of hydrogen transfer reactions were highlighted, and how the bulk liquid properties affected the probability of free radical chain transfer, two aspects that are seldom captured in models describing thermal cracking for visbreaking processes.

However, it was speculated that hydrogen transfer was not the only type of transfer that could take place and that methyl transfer could also take place. There was a large body of literature on intramolecular methyl migration, but little mention of intermolecular methyl transfer as a potentially important reaction type in free radical systems. In a series of reactions, the potential transfer of a methyl group in free radical systems was tested using indene, 2-methylindene and α -methylstyrene. Besides the formation of products typical of hydrogen transfer, evidence of methyl transfer was provided. When methyl transfer was favored by the presence of methylated compounds in the feed, there was less heavy products formed in the vacuum residue range, the products were of lower density, and there was less free radical content in the products. This was a noteworthy and new contribution, because it not only showed the importance of intermolecular methyl transfer in free radical systems, but also indicated that methyl transfer as opposed to hydrogen transfer affected the properties of the reaction product.

Tracking the effect of methyl and hydrogen transfer as well as addition reactions in free radical systems was suspected to be possible using traceable compounds. A new way of synthesis of ^{13}C -labelled indene was evaluated. The synthesis of ^{13}C -labelled indene provided a method to use labelled compounds to track addition reactions in bitumen and deasphalted oil. This work can serve as the starting point for future investigations related to heavy products formation in free radical systems.

Preface **(mandatory due to collaborative work)**

Chapter 3 of this thesis was published as “Tannous, J. H.; De Klerk, A. Quantification of the free radical content of oilsands bitumen fractions. *Energy and Fuels* **2019**, 33(8), 7083-7093”. I was responsible for concept formation, experimental design, data collection and analysis as well as manuscript composition. Kaushik Sivaramakrishnan, Priscila Nascimento and Shirley Fong assisted with data collection. Arno de Klerk acted as the supervisory author and corresponding author and was involved in the concept formation, data interpretation and manuscript composition.

Chapter 4 of this thesis was done in collaboration with Riya. We were responsible for concept formation, experimental design, data collection and analysis as well as manuscript composition. Arno de Klerk acted as the supervisory author and was involved in the concept formation, data interpretation and manuscript composition. The work produced a research lead to indicate that halogenated organics might have a role to play in sulfur ring-opening. This research lead is being pursued with Raquel Reolon, but has been omitted from the thesis, because it is not complete yet. I was responsible for presenting this work at Petrophase 2018.

Chapter 5 of this thesis was published as “Tannous, J. H.; De Klerk, A. Asphaltenes formation during thermal conversion of deasphalted oil. *Fuel* **2019**, 255, 1-10.” I was responsible for concept formation, experimental design, data collection and analysis as well as manuscript composition; I was the corresponding author. I was also responsible for presenting this paper at the 67th Canadian Chemical Engineering Conference. A part of Chapter 7 of this thesis was also included in the oral presentation at the conference. Cloribel Santiago and Priscila Nascimento assisted with data collection. Arno de Klerk acted as the supervisory author and was involved in the concept formation, data interpretation and manuscript composition.

To my grandma Hélène, for her unconditional love.

To my parents, Hikmat and Samar, and my brother Georges for always believing in me.

Acknowledgments

First and foremost, I would like to show gratitude to my supervisor, Prof. Arno de Klerk. His guidance, patience and immense knowledge were, mostly, all that kept me going. His enthusiasm and thirst for knowledge changed my view of research and were the source of motivation for the four years of PhD. Besides his continuous support in science, I must thank him for all the long random chats we had about music, life matters, and philosophy that were omitted from this thesis and may never be published. The secret being revealed, I might as well apologize to everyone that wanted to meet with him and had to wait outside the office thinking we were discussing science.

I thank my small family for being there for me on a daily basis throughout the four years; Dad, for all the sacrifices, his trust and for his sense of humor; Mom, for being my secret keeper and for all her spam calls; Georges for his piano plays when I am stressed and for always bothering me with random topics; my grandma H el ene, my aunts Sira and Moli and my cousins Lynn and Sara for all the love and care.

I thank Dory, for all the joy he brought to my life, for lifting me up when I could not reach. Thanks for giving me faith when I lost it, for being my strength and for believing in me since day one. I stood tall because he stood by me.

I could not have made it without my big family: aunts, uncles, cousins and second cousins in Lebanon and around the world. Thanks for being such a great support system.

I am grateful to my best friends Cynthia and Nagham for being there at my best and at my worst; Alyanna for all the laughter especially during thesis writing; Dany for always teasing me; Johnny for tolerating my stupid health questions and all my other friends that if I name all of them, my acknowledgements would be a chapter.

I am blessed to have such amazing people around me here. I thank my family in Edmonton Jennifer, Jenny, Natalia, Shirley, Lina, Riya, Jose, Giselle, and Daniel for always being there.

I thank CNOOC, Alberta Innovates and NSERC for the financial support.

Table of Contents

Chapter 1: Introduction	1
1.1 Background	1
1.2 Objective and scope of work	2
1.2.1 Objective	2
1.2.2 Scope of work	3
Chapter 2: Literature review on heavy products formation in free radical systems during thermal conversion of heavy oil	5
2.1 Introduction	5
2.2 Asphaltenes phase separation	6
2.3 Study of mesophase formation	8
2.4 Suppression of coke formation	9
2.5 Free radical chemistry	11
2.5.1 Free radicals: definition and types	11
2.5.2 Free radical reactions	12
2.5.3 Chain growth reactions	16
2.6 Hydrogen donor solvents and hydrogen transfer	17
2.6.1 Hydrogen donation and abstraction abilities of petroleum residues	18
2.6.2 Hydrogen transfer in petroleum conversion	21
2.6.3 Ability of maltenes to donate hydrogen to asphaltenes	24
2.7 Industrial relevance of heavy products formation in thermal processes	26
Chapter 3: Quantification of the free radical content of oilsands bitumen fractions	35
3.1 Introduction	36
3.2 Experimental	38
3.2.1 Materials	38
3.2.2 Analyses	39
3.3 Results	41
3.3.1 ESR calibration	41
3.3.2 Oilsands bitumen	44

3.3.3	Asphaltenes	46
3.3.4	Deasphalted oil (DAO)	48
3.3.5	Bitumen heavy fractions	50
3.3.6	Upgraded bitumen fractions	52
3.4	Discussion	55
3.4.1	Dilution and solvent effects	55
3.4.2	Concentration of free radicals in oilsands bitumen fractions	59
3.4.3	Implications for bitumen upgrading	62
3.5	Conclusions	64
Chapter 4: Reaction of 5-membered ring naphtheno-aromatics at thermal cracking conditions		68
4.1	Introduction	69
4.2	Experimental	70
4.2.1	Materials	70
4.2.2	Equipment and procedure	71
4.2.3	Analyses	72
4.3	Results	74
4.3.1	Self-reaction of model compounds at thermal cracking conditions	74
4.3.1.1	Physical observations and <i>n</i> -pentane insoluble content of the products	74
4.3.1.2	Chemical structure identification by GC-MS	76
4.3.1.3	High boiling compounds identification using SimDist	83
4.3.1.4	Free radical content by ESR	84
4.3.2	Reaction of mixture of model compounds at thermal cracking conditions	85
4.3.2.1	Analysis of gaseous products	85
4.3.2.2	<i>n</i> -pentane insoluble content	86
4.3.2.3	Chemical structure identification by GC-MS	86
4.3.2.4	Quantification of indan and thianaphthene by GC-NPD	92
4.3.2.5	High boiling compounds identification using SimDist	93
4.3.2.6	Free radical content by ESR	94

4.4	Discussion	94
4.4.1	Effect of reactor walls on cracking and addition	94
4.4.2	Self-reactivity of model compounds	95
4.4.3	Reactivity of model compounds in mixtures	97
4.4.4	Sulfur ring-opening	98
4.5	Conclusions	99
Chapter 5: Asphaltenes formation during thermal conversion of deasphalted oil		102
5.1	Introduction	103
5.2	Experimental	105
5.2.1	Materials	105
5.2.2	Equipment and procedure	108
5.2.3	Analyses	109
5.3	Results	111
5.3.1	Effect of indene on <i>n</i> -pentane insoluble content	111
5.3.2	¹ H NMR characterization of products	113
5.3.3	ESR characterization of products	116
5.3.4	Refractive index measurement of products	118
5.3.5	Self-reaction of indene	119
5.3.6	Impact of dilution on reaction of indene	121
5.4	Discussion	125
5.4.1	Heavier product formation during thermal conversion	125
5.4.2	Contribution of indene to asphaltenes formation in VR DAO	126
5.4.3	Reaction of indene	128
5.4.4	Impact of bulk liquid properties on free radical combination	130
5.4.5	Implications for modelling of thermal conversion	132
5.5	Conclusions	133
Chapter 6: Methyl transfer in free radical reactions		138
6.1	Introduction	139
6.2	Experimental	141

6.2.1	Materials	141
6.2.2	Equipment and procedure	142
6.2.3	Analyses	143
6.3	Results	144
6.3.1	Reaction of α -methylstyrene with indene	144
6.3.1.1	Identification of reaction products by GC-MS	144
6.3.1.2	Characterization by simulated distillation and <i>n</i> -pentane insoluble content	148
6.3.1.3	Spectroscopy of reaction products	150
6.3.2	Reaction of α -methylstyrene with 2-methylindene	152
6.3.2.1	Identification of reaction products by GC-MS	152
6.3.2.2	Characterization by simulated distillation and <i>n</i> -pentane insoluble content	156
6.3.2.3	Spectroscopy of reaction products	158
6.3.3	Self-reactions	159
6.4	Discussion	160
6.4.1	Reaction chemistry taking place in the reaction of indene with α -methylstyrene	160
6.4.2	Reaction chemistry taking place in the reaction of 2-methylindene with α -methylstyrene	163
6.4.3	Comparison of the tendency of indene, 2-methylindene and α -methylstyrene to form asphaltenes precursors	165
6.4.4	Methyl transfer taking place in free radical chemistry	167
6.4.5	Effect of the methyl group in the feed on the formation of light and heavy products	168
6.5	Conclusions	171
Chapter 7: Synthesis of carbon-labelled indene		176
7.1	Introduction	177
7.2	Experimental	179
7.3	Results and Discussion	179

7.3.1	Synthesis of 3-chloropropiophenone from benzene	179
7.3.2	Synthesis of indanone from 3-chloropropiophenone	181
7.3.3	Synthesis of indene from indanone	187
7.3.3.1	Through the enol triflate intermediate	187
7.3.3.1.1	Indanone to enol-triflate:	188
7.3.3.1.2	Enol-triflate to indene	189
7.3.3.2	Direct synthesis of indene from indanone	190
7.3.3.3	Through the indanol intermediate	192
7.3.3.3.1	Synthesis of indanol from indanone	192
7.3.3.3.2	Synthesis of indene from indanol	193
7.4	Finalized synthesis of indene from benzene and challenges	194
7.5	Cost estimation of synthesis of ^{13}C -labelled indene	195
7.6	Conclusions	196
Chapter 8: Conclusions		200
8.1	Introduction	200
8.2	Major conclusions and insights	200
8.3	Recommended future work	203
8.3.1	Impact of bulk liquid properties on free radicals	203
8.3.2	Sulfur-ring opening	204
8.3.3	Synthesis of ^{13}C -labelled indene	204
8.3.4	Application of ^{13}C -labelled indene in oil systems	204
8.3.5	Tracking of methyl group in oil systems	205
Bibliography		206
Appendix A: Chapter 3 Support Information		224
A.1	Power saturation study	224
A.2	ESR tube selection	225
A.3	ESR resonant cavity and probe filling	228

Appendix B: Chapter 4 Support Information	230
Appendix C: Chapter 6 Support Information	238
C.1 Calculation of the wt% of each light product in the light fraction (b.p < 240 °C excluding gases)	238
C.2 Calculation of the mol% of each feed that reacted to form light fraction and heavy fraction	239

List of Tables

Table 2.1. Canadian specifications for bitumen for pipeline transportation.	27
Table 3.1. List of chemicals employed in this study.	39
Table 3.2. Free radical content and <i>g</i> -values measured for different bitumen samples. ^a	44
Table 3.3. Free radical content and <i>g</i> -values measured for different asphaltenes samples. ^a	46
Table 3.4. Free radical content and <i>g</i> -values measured for different deasphalted oil (DAO) samples. ^a	49
Table 3.5. Free radical content and <i>g</i> -values measured for different heavy distillation fractions from bitumen. ^a	51
Table 3.6. Free radical content and <i>g</i> -values of different thermally converted and hydroprocessed products from bitumen upgrading. ^a	53
Table 4.1. Model compounds purities.	70
Table 4.2. Compounds used for peak identification in GC-MS.	71
Table 4.3. Concentration of model compounds in mixtures.	72
Table 4.4. <i>n</i> -pentane insolubles for the product of the self-reaction of model compounds.	75
Table 4.5. Composition of the reactor walls.	76
Table 4.6. Compound classes present in the product of the self-reaction of indene, the self-reaction of benzofuran and the reaction of the mixture of indene and indan.	78
Table 4.7. Free radical content in the products of the self-reaction of indene and benzofuran for the reaction times indicated.	85
Table 4.8. <i>n</i> -pentane insoluble content in the products of the mixtures of model compounds for a 60 minutes reaction time.	86
Table 4.9. Chemical structures of peaks of reaction of indan+thianaphthene and indene+thianaphthene (Fig 4.10-4.12).	89
Table 4.10. Mass of indan and thianaphthene in the feed and product.	93
Table 4.11. Free radical content for product of the mixtures of model compounds at 60 min.	94
Table 4.12. Self-reaction of indene with and without glass vial.	94
Table 5.1. Characterization of the industrial VR DAO feed.	107

Table 5.2. Feed materials prepared for thermal conversion experiments.	109
Table 5.3. Free radical content in products after thermal conversion at 400 °C for the reaction times indicated.	116
Table 5.4. Free radical content in <i>n</i> -pentane insoluble (asphaltenes) fraction separated from the products after thermal conversion at 400 °C for the reaction times indicated.	117
Table 5.5. Results from the self-reaction of indene by thermal conversion at 400 °C for 30 and 60 min.	119
Table 5.6. Product distribution from self-reaction of indene at 400 °C for 30 and 60 min reaction time.	121
Table 5.7. <i>n</i> -Pentane insoluble content after thermal conversion of model mixtures at 400 °C for the reaction times indicated.	122
Table 5.8. Free radical content in the total reaction product after thermal conversion of the model mixtures at 400 °C for the reaction times indicated.	125
Table 6.1. Model compounds purities.	141
Table 6.2. Compounds used for peak identification in GC-MS.	142
Table 6.3. Concentration of model compounds in mixtures.	143
Table 6.4. Compound classes present in the product of the reactions of indene with α -methylstyrene in different percentages.	146
Table 6.5. Simulated distillation results for indene-MST (4:2), indene-MST (3:3) and indene-MST (2:4)	149
Table 6.6. <i>n</i> -pentane insoluble content.	150
Table 6.7. Type of hydrogens in the products of indene-MST (2:4), indene-MST (3:3) and indene-MST (4:2).	151
Table 6.8. Analyte spin content in the products of the reactions of indene with α -methylstyrene.	152
Table 6.9. Chemical structure of peaks in chromatogram of Figures 6.5 and 6.6.	153
Table 6.10. <i>n</i> -pentane insoluble and simulated distillation results for indene-MST (1:2) and 2MI-MST (1:2).	157
Table 6.11. Type of hydrogens in the products of indene-MST (1:2) and 2MI-MST (1:2).	158

Table 6.12. Analyte spin content in the products of the reactions of indene with α -methylstyrene and 2-methylindene with α -methylstyrene.	159
Table 6.13. Analyte spin content in the products of the self-reactions of indene, α -methylstyrene and 2-methylindene	160
Table 6.14. wt% of light compounds in light fraction.	154
Table 6.15. mol% of each feed that reacted to form light and heavy products.	156
Table 6.16. Hydrogen transfer vs. methyl transfer.	169
Table 7.1. Indanone synthesis at different conditions.	184
Table 7.2. Indene synthesis at different conditions.	191
Table 7.3. Cost estimation for synthesis of 1 gram of ^{13}C -labelled indene.	195
Table A.1. Comparison of Norell and PQ tubes for quantitative ESR analysis of 24 wt% bitumen (Bit-6, Cold Lake bitumen) in toluene solution at 15 mW microwave power.	226

List of Figures

Figure 2.1: Example of pendent-core model.	7
Figure 2.2: Block flow diagram for CNOOC's field upgrader. ⁶⁷	26
Figure 3.1. Organic free radical substances employed for calibration of ESR spectrometer.	38
Figure 3.2. Calibration of the ESR spectrometer with different calibration substances.	42
Figure 3.3. Concentration dependence of measured free radical content of heavy gas oil diluted in toluene.	54
Figure 3.4. Free radical dimerization "equilibrium" illustrated by the triphenylmethane radical.	58
Figure 3.5. Relative abundance of free radicals in bitumen and bitumen derived fractions at an analyte concentration of 3–6 wt%.	60
Figure 4.1. Pictures captured by Zeiss microscope for products of thermally cracked (a) indene, (b) indole and (c) benzofuran.	76
Figure 4.2. Chromatogram of the <i>n</i> -pentane soluble fraction of the product of the self-reaction of indene at 60 minutes showing cracking products.	77
Figure 4.3. Chromatogram of the <i>n</i> -pentane soluble fraction of the product of the self-reaction of indene at 60 minutes showing addition products. Unlabeled peaks from retention time 9-20 min are indicative of column bleeding.	81
Figure 4.4. Chromatogram of the product of the self-reaction of benzofuran at 60 minutes showing cracking products.	82
Figure 4.5. Chromatogram of the product of the self-reaction of benzofuran at 60 minutes showing addition products. Unlabeled peaks from retention time 9-20 min are indicative of column bleeding.	82
Figure 4.6. Distillation curve of the products of the self-reaction of indole at 30 and 60 minutes reaction times.	83
Figure 4.7. Distillation curve of the products of the self-reaction of benzofuran at 30 and 60 minutes reaction times.	84
Figure 4.8. Chromatogram of the product of the thermal conversion of indene+indan at 60 minutes showing cracking products.	87

- Figure 4.9.** Chromatogram of the product of the thermal conversion of indene+indan at 60 minutes showing addition products. Unlabeled peaks from retention time 9-20 min are indicative of column bleeding. 87
- Figure 4.10.** Chromatogram of the low boiling compounds of the product of the thermal conversion of indan+thianaphthene at 60 minutes. 88
- Figure 4.11.** Chromatogram of the high boiling compounds of the product of the thermal conversion of indan+thianaphthene at 60 minutes. 88
- Figure 4.12.** Chromatogram of the product of the thermal conversion of indene+thianaphthene at 60 minutes. 89
- Figure 4.13.** Indan free radical formation and termination. 96
- Figure 5.1.** Hydrogen transfer from indene leading to the formation of a resonance stabilized indenyl radical. (Note: The hydrogen radical is usually transferred and not released as an isolated free radical species). 104
- Figure 5.2.** Experimental setup used for thermal conversion. 108
- Figure 5.3.** *n*-Pentane insoluble content after thermal conversion at 400 °C of VR DAO spiked with no indene (■), 5.6 wt% indene (◆) and 11.1 wt% indene (●). Error bars indicate one sample standard deviation. 112
- Figure 5.4.** Change in the distribution of non-aromatic hydrogen (●) and aromatic hydrogen (■) due to thermal conversion at 400 °C of VR DAO. Error bars indicate one sample standard deviation. 114
- Figure 5.5.** Change in the aromatic hydrogen content of VR DAO spiked with 5.6 wt% indene (◆) and 11.1 wt% indene (●) due to thermal conversion at 400 °C. Error bars indicate one sample standard deviation. 115
- Figure 5.6.** Refractive index of total product after thermal conversion at 400 °C of VR DAO spiked with no indene (■), 5.6 wt% indene (◆) and 11.1 wt% indene (●). 118
- Figure 5.7.** Simulated distillation of *n*-pentane soluble product after thermal conversion of indene at 400 °C for 60 min. 120
- Figure 5.8.** Heavy product formation indicated by simulated distillation analysis of the *n*-pentane soluble products after thermal conversion of indene-containing model mixtures at 400 °C. 123

- Figure 5.9.** Section of the chromatogram from the GC-MS analysis of *n*-pentane soluble product after thermal conversion of an indane with 5.6 wt% indene mixture at 400 °C for 30 min. 124
- Figure 5.10.** Free radical formation by indene by (i) hydrogen disproportionation, but not by (ii) homolytic bond dissociation. 129
- Figure 6.1.** Indene double bond alteration. 140
- Figure 6.2.** Chromatograms of the products of the reactions of indene with α -methylstyrene in different percentages for (a) light products, the solvent delay = 2.5 minutes (b) addition products. Values of intensities in y-axis multiplied by a factor of 1.5 for Indene-MST (3:3) and 2 for Indene-MST (4:2) for clear presentation. 145
- Figure 6.3.** SimDist curve for the product of the ratio of indene to α -methylstyrene of 4:2 in feed, showing the main three plateaus. 148
- Figure 6.4.** Chromatogram of the products of the reaction of 2-methylindene with α -methylstyrene (light products); the solvent delay = 8 minutes. 153
- Figure 6.5.** Chromatogram of the products of the reaction of indene with α -methylstyrene (light products); the solvent delay = 8 minutes. 153
- Figure 6.6.** Possible structures of addition products that could be detected by GC-MS. 156
- Figure 6.7.** SimDist curves for the reactions indene-MST (1:2) and 2MI-MST (1:2). 158
- Figure 6.8.** wt% of each light product in the light fraction for all reactions of indene with α -methylstyrene. 161
- Figure 6.9.** Free radical pathway for formation of cumene from α -methylstyrene. 162
- Figure 6.10.** Free radical pathway for formation of ethylbenzene from α -methylstyrene. 162
- Figure 6.11.** Free radical pathway for formation of indane from indene. 162
- Figure 6.12.** Free radical pathway for formation of propylbenzene from ethylbenzene. 164
- Figure 6.13.** Free radical pathway for formation of *sec*-butylbenzene from cumene. 164
- Figure 6.14.** Free radical pathway for formation of 1-methylindane from indane. 165
- Figure 6.15.** Free radical pathway for formation of indane from 2-methylindene. 165
- Figure 7.1.** Pathway for synthesis of ¹³C-labelled indene. 178
- Figure 7.2.** Synthesis of radioactive indene from benzene.² 178
- Figure 7.3.** Reaction of benzene with 3-chloropropionyl chloride. 180
- Figure 7.4.** Chromatogram of synthesized 3-chloropropiophenone. 181

Figure 7.5. Cyclization of 3-chloropropiophenone.	181
Figure 7.6. Chromatogram of the product of indanone-7.	186
Figure 7.7. Enol intermediate for synthesis of indene from indanone.	187
Figure 7.8. Manual fragmentation of mass spectrum of the peak of the enol-triflate.	189
Figure 7.9. Chromatogram showing hexaethyl-disiloxane as main product.	190
Figure 7.10. Synthesis of indene from indanone through the indanol intermediate.	192
Figure 7.11. Chromatogram of synthesized indanol.	193
Figure 7.12. Chromatogram of synthesized indene.	194
Figure 7.13. Finalized pathway for synthesis of indene from benzene.	194
Figure A.1. Microwave power saturation study with an asphaltenes sample.	221
Figure A.2. Comparison of signal-to-noise ratio obtained with (a) Norell tubes (top), and (b) PQ tubes (bottom), for the analysis of an <i>n</i> -pentane soluble maltenes sample (DAO-5).	223
Figure A.3. Illustration of ESR tube filling requirements for quantitative ESR analysis.	225
Figure B.1. GC-MS of indan product.	230
Figure B.2. GC-MS of indole product.	231
Figure B.3. GC-MS of thianaphthene product.	231
Figure B.4. Chromatogram of benzofuran product spiked with phenol.	232
Figure B.5. Chromatogram of benzofuran product spiked with 2-ethylphenol.	232
Figure B.6. FTIR results for products of the self-reaction of benzofuran.	233
Figure B.7. Screenshot of the Proton-NMR results for products of the self-reaction of benzofuran at 60 minutes.	233
Figure B.8. Distillation curve for the self-reaction of indan product.	234
Figure B.9. Distillation curve of the self-reaction of thianaphthene product.	234
Figure B.10. Distillation curve of the self-reaction of indene product.	235
Figure B.11. Chromatograms of the product of indene and thianaphthene along with two other products of the same samples spiked with 2-methylbenzenethiol and 3-methylbenzenethiol.	235
Figure B.12. Chromatograms of the product of indene and thianaphthene along with the same samples spiked with 2-ethylbenzenethiol.	236

Figure B.13. Distillation curve of the product of the reaction of indan and thianaphthene at 60 min. 236

Figure B.14. Distillation curve of the product of the reaction of indene and indan at 60 min. 237

Figure B.15. Distillation curve for the n-pentane soluble fraction of the product of the reaction of indene with thianaphthene at 60 min. 237

Chapter 1: Introduction

1.1 Background

Within the same concept of creation of the so-called three-age system, by Christian Thomsen,¹ that classifies the pre-history into discrete periods, some scientists suggest we currently belong to the Petroleum Age — the age in which oil became a necessity for humans. However, the extensive use of petroleum caused depletion of conventional light oils. This shifted the focus to heavy and extra heavy oils.

Compared to light oils, the challenges that heavy oils bring are the higher boiling point ranges due to the nature of the heavy oils that contains mainly molecules of high molecular mass. They, therefore, tend to be denser and more viscous. Thus, transporting oils, like Canadian Oil Sands bitumen and Venezuelan heavy oils, at ambient temperatures, is challenging. Residue processing technologies, are used to increase their fluidity by converting them into lighter compounds using catalysts, hydrogen and/or high temperatures. Due to the large capital cost associated with the use of hydrogen and regeneration of catalysts, pure non-catalytic thermal cracking (or visbreaking) is one of the cheapest technologies currently employed in industries.²

The purpose of visbreaking is the cracking of macromolecules into lighter compounds of higher value. However, the formation of products heavier than the feed material constitutes a major drawback of these technologies. These low commercial value heavy compounds, such as “asphaltenes” or “coke” decrease the conversion ability of the unit and cause fouling. Such bulky molecules are formed by addition reactions, the opposite of breakdown, and this was discussed in the book by Sachanen.³

In non-catalytic thermal conversions, the equilibrium between cracking reactions and condensation/polymerization resembles the competition between two elite athletes. Athletes can always train more, come prepared and do their best to win. However, the performance of athletes and their chances to win depend on several factors: the athlete’s genetic potential, training level, sleep quality and duration, social life, injuries as well as the physical environment. All these elements may not always be manageable or considered. Similarly, one can always manipulate

reaction conditions or feed material in order to shift the equilibrium towards desirable cracking reactions, but the complexity of the matrix imposes the presence of uncontrollable aspects which will lead to the formation of addition products. As long as the race is on, there will be fluctuation of the winning chances of each athlete, exactly like the equilibrium between cracking and addition that keeps on changing throughout the reaction time. Just like the performance of athletes could be ameliorated by performing more studies, the better the complex matrix in thermal cracking is understood, the more controllable the factors are and the easier it is to expand on ways to improve thermal conversion.

Thermal conversion is limited by the addition reactions that form condensation products, precursors of asphaltenes and coke. Asphaltenes are the products of condensation/polymerization that are formed by a free radical mechanism. They are like bumpers in the race, if the athlete hits a bumper and falls, his chances to win are less. Similarly, the formation of asphaltenes is an obstacle that may lead to coke formation, thus limiting the conversion of cracking reactions. The formation of asphaltenes means that heavier oils with higher viscosity than the feed are being formed from the thermal conversion, that is undesirable. When looking at the literature, there are little studies on the chemistry of formation of heavy compounds and the ways to suppress addition products formation in non-catalytic conversions. There is also no clear indication on the compounds classes in heavy oils that have tendency to undergo addition reactions and form coke precursors. The literature that is relevant to heavy products formation in thermal processes is cited and discussed in Chapter 2.

1.2 Objective and scope of work

1.2.1 Objective

The objective of this thesis is to provide a fundamental understanding of the asphaltenes formation in thermal conversions by studying the behavior of free radicals at visbreaking conditions and emphasizing the chemistry of free radical addition reactions.

1.2.2 Scope of work

In order to meet the objective of this study, free radicals had to be measured and quantified. Electron spin resonance spectroscopy (ESR) was employed to perform quantitative analysis of the free radical content of oilsands bitumen, asphaltenes, deasphalted oil, vacuum residue and vacuum gas oil fractions, as well as thermally converted product fractions. The amount of free radicals was reported in spins/g. The effect of bulk liquid properties on the measured free radical concentration was highlighted. This will be elaborated in Chapter 3.

It is known that 5-membered ring naphtho-aromatic compounds have tendency to undergo addition reactions in auto-oxidation of bitumen.⁴ Therefore, it was worthwhile checking their reactivity under thermal cracking conditions (Chapter 4). The next study was done on one of the 5-membered ring naphtho-aromatic compounds, indene, a molecule that could self-react and undergo addition reactions to form asphaltenes. Indene has been reacted with industrial deasphalted oil. Indene was employed to exacerbate asphaltenes formation during thermal conversion of deasphalted oil. The prevalence of addition reactions and the importance of hydrogen transfer reactions were emphasized, which had implications for modelling reaction chemistry describing thermal conversion of heavy oil (Chapter 5).

To better understand the chemistry of free radicals, the postulate that methyl transfer may be taking place in parallel with hydrogen transfer was tested. Model compounds were used to test this hypothesis and the main outcomes of this study are described in Chapter 6.

The study in Chapter 5 could not tell whether indene induced increased asphaltenes formation, or whether it formed addition products with the deasphalted oil, therefore, it was suggested to use carbon-labelled indene instead to track the effect of such molecules on thermal conversions. Due to the high cost of commercial ¹³C-labelled indene, Chapter 7 dealt with the synthesis of ¹³C-labelled indene from ¹³C-labelled benzene. A new pathway is developed and tested. The overall conclusions and recommendations for future work can be found in Chapter 8.

Literature cited

- (1) Thomsen, C. J. *A Guide to Northern Antiquities*; London, 1848.
- (2) Maples, R. E. *Petroleum Refinery Process Economics*; PenWell: Tulsa, 2003.
- (3) Sachanen, A. N. *Conversion of Petroleum: Production of Motor Fuels by Thermal and Catalytic Processes*; Reinhold Publishing Corporation, 1948.
- (4) Siddiquee, M. N.; De Klerk, A. Hydrocarbon Addition Reactions during Low-Temperature Autoxidation of Oilsands Bitumen. *Energy and Fuels* **2014**, 28 (11), 6848–6859.

Chapter 2: Literature review on heavy products formation in free radical systems during thermal conversion of heavy oil

2.1 Introduction

The depletion of light oils shifted the interest to heavy oils as a major source of energy. For heavy oils to be used by the consumers, they need to be fluid enough (i.e. have a low viscosity) in order to be transported in pipelines. Thus, heavy oils need to be treated and cracked into smaller molecules. Converting macromolecules (heavy molecules) into valuable products occurs by thermal conversions.

One of the oldest thermal conversion technologies for the upgrading of heavy oils that came to market in the 1930s was visbreaking (viscosity breaking). Visbreaking uses only heat — typically temperatures in the range of 400-500 °C — to crack large molecules into smaller ones. Some other cracking processes, use besides heat, either hydrogen only, catalyst only (e.g. fluid catalytic cracking — FCC) or both hydrogen and catalyst (e.g. hydrocracking). Hydrogen and catalyst increase the conversion of light products at high temperatures.

Light valuable products are formed upon thermal cracking of heavy products. However, one major drawback in thermal processes is the formation of products heavier than the feed. The formation of heavier products occurs by addition reactions (i.e. polymerization). The formation of heavy products defeats the purpose of thermal cracking. It decreases the selectivity towards light desirable products. In addition, some heavier products formed tend to precipitate as solids. The heavy products that have tendency to precipitate are referred to as asphaltenes or aggregates. Heavy oils fed to the thermal cracker unit contain, by nature, aromatic compounds. Asphaltenes are characterized by the presence of condensed poly-aromatic rings formed by addition of many mono-aromatic rings. They are defined as a solubility class (soluble in light aromatics such as toluene but not soluble in *n*-alkane) but are generally known to be rich in carbon and deficient in hydrogen. Asphaltenes are one type of heavy product. The precipitation of asphaltenes with further thermal conversion leads to what is called coke. Coking causes deposits leading to restrictions in equipment and piping and is, therefore, not desirable.

Due to the high capital cost associated with the use of hydrogen, new partial upgrading processes for heavy oils are shifting to the use of visbreaking.¹ In visbreaking, the cracking and addition reactions take place by a free radical mechanism. Therefore, the formation of heavier products is referred to as free radical addition reactions. Since such thermal cracking processes were not designed to form coke, but rather to break down molecules into valuable products, the formation of coke is a problem. The topic of heavy product formation in free radical systems during thermal conversion is consequently of practical industrial interest.

2.2 Asphaltenes phase separation

The formation of asphaltenes and coke in thermal processes has long been recognized as a major drawback that causes increase in viscosity of the product as well as fouling.

Earlier, the formation of coke was believed to be taking place following a series of condensation steps where molecules keep on undergoing addition reactions until they get to their heaviest version called “coke”.^{2,3} The first investigators that described the coke formation process as a type of phase separation were Magaril et al.^{4,5,6} The coke formation was thought to be starting to form when the asphaltenes concentration in solution reaches a maximum. Other studies on the mechanism of coke formation and inhibition of onset of coking have been published.^{7,8,9,10,11,12,13,14}

However, Wiehe¹⁵ was the first to develop in 1993, a kinetic model to describe the phase separation process in the formation of asphaltenes during thermal conversions. This was after a study in 1992¹⁶ in which the insolubility of species in the bulk oil was attributed to a low hydrogen content and high molecular mass.

In 1994, Wiehe¹⁷ introduced the principle of pendant core for asphaltenes structures. The model divides the pseudo components in petroleum residues into two basic pseudo building blocks: the core and the pendants. Asphaltenes are the aromatic core building block and the pendants are the part of the asphaltenes that would become light components as thermal conversion proceeds (Figure 2.1). When asphaltenes are more soluble in the matrix, they do not phase separate.

Therefore, the better the matrix is able to play the role of a solvent for the asphaltenes, the less the coke formed.

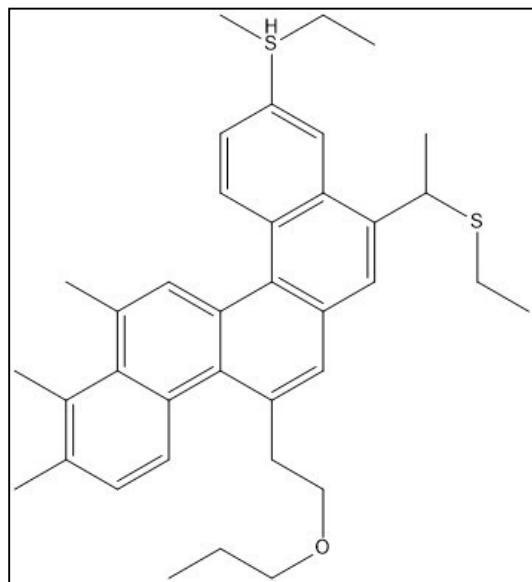


Figure 2.1. Example of pendent-core model.

In thermal conversions, besides light liquid products and coke, there are some gases formed. Gases have a high H:C ratio. The more extreme the operating conditions are, the more the coke and gases formed and the less the light liquid products. The pendent core model¹⁷ gave explanation to the relation between the Conradson Carbon Residue (CCR) content and the hydrogen content in petroleum macromolecules. It has been shown that the decrease of coke formation is achieved when the amount of gases produced is decreased, or when hydrogen is added (i.e. hydrotreating).

In 1998, Wiehe¹⁸ employed the separation of petroleum into fractions of saturates, small rings aromatics, resins, asphaltenes and coke to investigate coking tendency. Coke were material insoluble in toluene and asphaltenes materials insoluble in *n*-heptane. The separation of the other fractions was described in the paper.¹⁶ He found that the susceptibility for coke formation depended on the amount of hydrogen contained in each fraction. The chemical properties of the feed highly affect the induction period (i.e. onset of mesophase). The heavier the feed, the shorter the induction period.

The literature on asphaltenes phase separation is therefore relevant to this study, because this phase separation is viewed as an analytically tractable surrogate for phase separation that takes place at actual reaction conditions as lighter hydrocarbons are increasingly produced by thermal cracking reactions.

2.3 Study of mesophase formation

It was suggested that understanding the factors that affect the mesophase induction period and properties might assist in manipulating its formation. This ultimately could lead to developing ways to suppress coke formation. This does not rule out the possible contribution of the formation of a second isotropic phase, but there is no direct method to differentiate isotropic phase domains that lead to coke and the possible contribution of a second isotropic phase is only speculative.

In 1998, Rahimi et al.¹⁹ used hot-stage microscopy while adding hydroaromatics to heavy residues to test their effects on coke formation in hydrocracking. They tested the change of the mesophase spheres size and shape as a function of temperature. They postulated that the mesophase formation was independent of the gas medium used for pressurization but dependent on the temperature.

The mesophase induction period was longer when hydrogen donors were used. When the feed was mixed with hydrotreated bitumen, the mesophase had smaller sphere sizes and appearance of mesophase was further delayed.

In another study,²⁰ they showed the advantage of using hot-stage microscopy to have a real-time observation of thermal cracking. They conducted the reactions at a pressure of 5.3 MPa, and a temperature of 440 °C under nitrogen and hydrogen and they measured the mesophase induction period for different heavy oils. The induction period for a sample that was saturated with asphaltenes was very short. It was proven that the longer the heavy residue components, the higher the induction time for onset of mesophase (that is in accordance with the previous study by Wiehe¹⁸).

It was also demonstrated that the coke induction time for bitumen and the summation of the induction times of 4 different subfractions of the same bitumen, are very close.²⁰ The presence of

clays did not affect the coke induction period but certain clays led to a change in the size of the mesophase. The presence of molecules that can donate hydrogens, increased the coke induction period and decreased the rate of mesophase formation. A partially deasphalted oil was tested in order to investigate the effect of asphaltenes and it was shown that the removal of asphaltenes decreases the propensity to form coke.

Li et al.²¹ also found three different types of mesophases with different shapes and onset points being formed as intermediates prior to coke formation.

The literature on mesophase formation is relevant to this study, because it is a likely precursor phase to coke formation.

2.4 Suppression of coke formation

The suppression of coke formation was attempted by several techniques e.g. the use of catalysts, or direct hydrogen supply or both, to increase the rate of hydrogenation which boosts the formation of light products in the distillate ranges.

However, in non-catalytic processes, the formation of asphaltenes and coke remains a problem. Research has been done on the solvent de-asphalting (e.g.²²) in order to remove asphaltenes from the feed prior to thermal conversion. In parallel, and in order to delay the onset of coking, studies have been done on the addition of additives, surfactants, aromatic hydrocarbons or hydrogen donor solvents. Since there is a direct relation between availability of hydrogen and formation of asphaltenes and their stability, the thermal cracking matrix has been mimicked using hydrogen donor solvents. Hydrogen donor solvents have also been employed as additives to delay the onset of coking and increase product quality (e.g. heteroatom removal and decrease of H:C ratio). The effect of hydrogen donor solvents on the formation of asphaltenes and the hydrogen transfer in the matrix have been extensively reported and will be reviewed in Section 2.6 of this Chapter.

Other studies investigated the effect of presence of maltenes, which are considered by some to be the natural hydrogen donors (i.e. without additives), on asphaltenes stability. Maltenes are defined

as a solubility class (soluble in an *n*-alkane such as *n*-pentane or *n*-heptane). They constitute the matrix in thermal conversions. Maltenes properties change depending on the type of feed.

In fact, making use of these naturally occurring hydrogen donors may be more beneficial money-wise (i.e. no cost associated with buying additives). Chemistry-wise, natural hydrogen donors were found to be as effective as hydrogen donor solvents in delaying the onset of coking.²³ In non-catalytic processes, the alternative way to decrease coke formation is by using a catalyst and hydrogen gas, which by definition, is not an option. On the other hand, the addition of hydrogen donor solvents in the matrix will decrease the amount of heavy products formed thereby increasing the coke induction time (i.e. delay coke formation). Addition of a hydrogen donor solvent will also inhibit cracking by promoting chain transfer reactions. In the presence of hydrogen donors in the matrix, it might be essential to increase the visbreaker temperature to favour cracking. In some instances, the amount of hydrogen donor solvents required to provide enough hydrogen to avoid coke formation is high. The use of large amounts of hydrogen donor solvents necessitates their regeneration. Wiehe²⁴ mentioned that the best choice of hydrogen donors for residue visbreaking are three- or four-ring aromatics that have been partially hydrogenated.

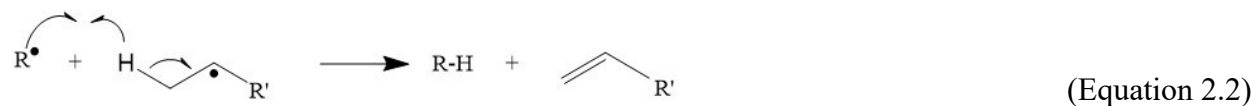
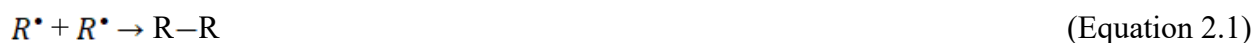
More details on natural hydrogen donors and maltenes-asphaltenes equilibrium will be covered in Section 2.6.3 of this Chapter. Since all reactions taking place during visbreaking follow a free radical mechanism, including heavy products formation that are formed by free radical addition reactions, Section 2.5 of this Chapter will cover free radical basics, types and factors that affect their stabilities.

The literature on coke suppression is directly relevant to the topic of this study, since onset of coke formation limits thermal conversion by visbreaking. This aspect is also of industrial relevance and one of the justifications for conducting the study.

2.5 Free radical chemistry

2.5.1 Free radicals: definition and types

Radicals are species with an unpaired electron. They differ from other types of reactive species by their ability to react with each other. The reactivity of free radicals is classified into transient and persistent. Transient radicals are radicals with short life time that can react with one another at diffusion-controlled rates that rarely exceeds $1 \mu\text{s}$.²⁵ The self-reaction can be either a combination that involves the addition of two like-radicals (Equation 2.1) or a hydrogen disproportionation (Equation 2.2).



Persistent free radicals do not react with each other at diffusion-controlled rate but they may still react over a long period of time. Persistent radicals can be either reactive or not reactive, that is why their lifetime is described by the so-called half-life. The half-life of a radical, at a given concentration, is the time taken for the concentration of radicals to reduce to 50% of the initial value. Radicals used as standards for Electron Spin Resonance (ESR) are persistent, e.g. 2,2-diphenyl-1-picrylhydrazyl (DPPH) and 4-hydroxy-2,2,6,6-tetramethylpiperidin-1-oxyl (TEMPO).²⁶ ESR is the technique used to identify and quantify free radicals in mixtures.

Three factors might play a role in increasing the half-life of a radical making it less reactive: (i) steric hindrance by bulky groups, (ii) electronic effects characterized by the ability of the group attached to the radical to delocalize the unpaired electron, and/or (iii) ability of the radical centre to attain planar conformation.²⁷ The electronic effect reflects a stability defined by the nature of the group attached to the radical. If the attached group is able to create a stable radical, the reaction proceeds towards the formation of the radical. This implies that the product radical is thermodynamically stable (i.e. the bond dissociation energy is low). The electronic effect can be

due to hyperconjugation (overlap of a p orbital with a σ bond) or a resonance (overlap of a p orbital with a π bond or lone pair). In resonance, there is a stronger orbital interaction than in hyperconjugation which makes radicals more stable.²⁶

The stability of carbon radicals follows the same order as carbocations with a tertiary radical being more stable than a methyl radical. This is also due to the steric hindrance that the groups attached to a tertiary carbon radical create.²⁶

Understanding the types of free radicals is crucial when working on systems that operate by a free radical mechanism, that is the case of this thesis study.

2.5.2 Free radical reactions

The generic classification of free radical reactions divides them into initiation, propagation and termination.

Initiation consists of a homolytic bond cleavage that produces two free radicals. This can be achieved by thermolysis (heat driven), photolysis (absorption of ultraviolet radiation) or radiolysis (high energy radiation sources like X-rays, γ -rays or high-energy electrons.).

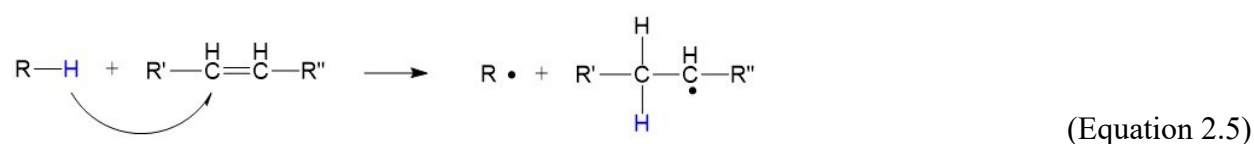
The generic homolytic bond cleavage via thermolysis is illustrated in Equation 2.3.



Radical initiation can also happen by redox reactions upon interaction with alkali metal or transition metal salt.²⁶ For instance, Equation 2.4 shows a reduction due to the presence of a metal reductant or cathode that gives an electron and converts a non-radical into a radical anion as intermediate that later decomposes into a radical and an anion.



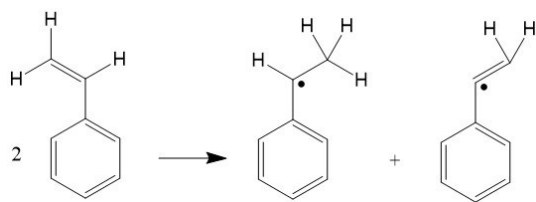
One other type of initiation in the liquid phase, that is not much considered in literature, is the molecule-induced free radical formation, also called bimolecular free radical formation or molecule-assisted homolysis. The molecule-induced radical formation (MIRF) usually takes place at low temperatures where the highly endothermic chemical bond dissociation may not be possible. It consists of a bimolecular reaction between two or more neutral molecules (i.e. non-radicals). In the bimolecular reaction, the two molecules are in contact and a hydrogen transfer occurs. The two interacting molecules may or may not be of the same identity. Due to the transfer of the hydrogen, a radical is formed (Equation 2.5).



However, the occurrence of the bimolecular radical formation is independent of the concentration of hydrogen donors.²⁸ MIRF does not necessarily require a hydrogen transfer to occur. The other types of MIRF is the diradical formation. For instance, Flory²⁹ suggested that the initiation in the thermal polymerization of styrene to polystyrene, occurs by an MIRF mechanism where a diradical is formed by the interaction between two styrene molecules (Equation 2.6).^{28,30}



Ever since then, the molecule-induced initiation of styrene has been debatable. Other researchers claimed that the initiation step in styrene polymerization is a third-order reaction, in which three styrene molecules form two radicals.^{31,32} Later, Walling³³ proved that the initiation takes place by the formation of monoradicals (Equation 2.7) from the interaction between two styrene molecules, a mechanism that was previously ruled out by Flory, but which, with several studies later, had the most support (e.g.³⁴).



(Equation 2.7)

Other examples of studies that covered the MIRF include the thermal decomposition of dihydronaphthalenes³⁵, and isotoluene³⁶, as well as the non-catalyzed hydrogenation of α -methylstyrene.³⁷

MIRF is also described as a redox reaction, that involves an oxidizing agent and a reducing agent. One example is the reaction of metal ions with peroxides the mechanism for which is well established to be a transfer of an electron from the metal ion to the peroxide. However, in the absence of metal ions and with a low ionization potential of molecules, the mechanism of the molecule-induced reaction between neutral molecules might get complicated. Factors such as temperature, solvent and reactant concentration may affect the MIRF phenomenon.²⁸ MIRF will be discussed in more details in Chapters 3 and 5.

In bitumen, in general, as well as in vacuum residues, free radicals are present naturally even before any thermal conversion is performed.³⁸ Therefore, initiation is not required to produce free radicals during thermal conversions. However, these free radicals, that are present in bitumen, are not transient but they belong to the persistent category, some reactive and some not reactive.

Propagation includes all reactions in which products still contain radicals. The reactions can either be unimolecular or bimolecular. Bimolecular reactions among free radicals is what leads to termination by formation of neutral molecules.²⁶

Besides the possibility of oxidation of a radical to a cation by losing an electron, or reduction to an anion by gaining an electron, propagation reactions can be classified into five types:^{26,27}

- Abstraction: a bimolecular reaction where a hydrogen or halogen transfers between a neutral molecule and a radical creating a new radical and a new neutral molecule.



- Substitution: a bimolecular reaction where an atom from a neutral molecule attacks a radical and changes its identity.



- Addition: a bimolecular reaction where addition of a radical to a neutral molecule occurs forming a larger radical.



- Fragmentation: a unimolecular reaction where a radical is broken apart into another radical and a neutral molecule.



- Rearrangement: a unimolecular reaction where migration of the free radical occurs within the same molecule. The rearrangement may come in the form of an intramolecular cyclization.



Termination reactions occur either by *(i)* a combination or coupling characterized by addition of two like-radicals, also called dimerization or homocoupling (Equation 2.1) or two different radicals, also called heterocoupling, or *(ii)* a disproportionation by transfer of a hydrogen from one radical to the other that results in two neutral molecules, one saturated and the other unsaturated (Equation 2.2).^{26,27}

Free radical reactions constitute the core of this study since visbreaking takes place by a free radical mechanism. Understanding initiation, propagation and termination of free radicals allows manipulating free radical chemistry in the system to favor cracking over addition reactions.

2.5.3 Chain growth reactions

The free radical addition reaction is a type of propagation reaction. As suggested by the title of this PhD study, this reaction type was of particular interest. As described earlier, free radical addition could involve the addition of a radical to an olefin. This type of addition reaction is referred to as chain growth reactions.

Propagation reactions can undergo either chain growth or chain transfer. When a reactant R-R' is added to an olefin (C=C), the chain reaction starts by the addition of the free radical R· to the olefin (Equation 2.13a). Please note that although C=C is used as shorthand to indicate an olefin; the intent was not to limit the example to ethylene. Chain transfer occurs when the free radical formed (i.e. R-C-C·) is terminated (Equation 2.13b) leaving behind another radical (R·) to start a new chain. However, if the matrix favors chain growth to take place, the formed radical R-C-C· will add to another olefin molecule to become bulkier (Equations 2.14a). Depending on the chemistry and the concentration of each reactant in the mixture, R-C-C-C· formed may add to another olefin and grow more or may react with R-R' (Equations 2.14b) and undergo chain transfer.³⁹ Chain growth is boosted when the bond dissociation energy of R-R' is high since this makes chain transfer (Equation 2.13b) unfavorable. In addition, when R-R' reactant is present in low concentration, the chance that free radical R-C-C· meets with an olefin molecule instead of R-R' in the matrix and undergoes chain growth is high. Chain transfer and growth will be further discussed in Chapter 5.



Free radical addition reactions are of importance in organic synthesis especially the addition of a radical to an alkene to transform a π -bond to a σ -bond that polymer chemists use to synthesize new materials. Chain growth reactions are used for polymer synthesis.^{25,40}

In the context for thermal conversion of heavy oil, which is conducted at temperatures > 350 °C, free radical addition reactions are undesirable. In visbreaking, the formation of heavier products is contrary to the objective of converting heavier to lighter products (i.e. cracking). Therefore, the equilibrium must be shifted in a way to allow homolytic bond cleavage rather than chain growth by free radical addition reactions.

Chain growth reactions are relevant to this study since they constitute one of the major pathways for heavy products formation in thermal cracking processes.

2.6 Hydrogen donor solvents and hydrogen transfer

Hydrogen donor solvents are commonly described as molecules, that due to their structure, can donate more than one hydrogen during reactions without becoming an olefin or a free radical after all transferrable hydrogen has been donated. The importance of such solvents is their ability to favor chain transfer over chain growth since the hydrogen donated is capable of capping free radicals in the propagation step and terminating them. It should be pointed out that during the process of hydrogen donation by a hydrogen donor, the intermediate product from single hydrogen donation may be an olefin or free radical.

Hydrogen donor solvents have been vastly employed. While hydrogen donor solvents form stable non-radical molecules upon donation of all transferrable hydrogen, other molecules that are able to donate hydrogen — but that are not hydrogen donors — are susceptible for addition or combination since they form a radical or an alkene upon donation of all transferrable hydrogen. In addition, hydrogen donors can still degrade when in mixture or by self-reactions.

Tetralin is considered a prototypical hydrogen donor solvent that converts to naphthalene once it donates all four hydrogens. Tetralin has been extensively employed to test several hypotheses in complex matrices including thermal conversions. It has also been used as a source of hydrogen in desulfurization processes.⁴¹ Hydrogen donor solvents have been widely used for the liquefaction of coal⁴² but this review will not cover references for coal processing.

Varga et al.⁴³ were some of the first investigators that used tetralin as a hydrogen donor and proved that there was less coke formed in the thermal cracking of a Hungarian crude oil of high asphaltene content than in the absence of tetralin. Langer et al.⁴⁴ were some of the first investigators to use tetralin as a hydrogen donor in the visbreaking of residues. The conversion of residues was increased and the coke yield decreased.

2.6.1 Hydrogen donation and abstraction abilities of petroleum residues

Besides tetralin, anthracene and its hydrogenated products have been vastly employed to study the hydrogen donation and abstraction abilities of oil residues.

Uemasu et al.⁴⁵ studied the hydrogen donation ability of 9,10-dihydroanthracene. Billmers et al.⁴⁶ covered the kinetics of the migration of hydrogen under what they introduced to be a molecular disproportionation concept. The transfer occurred at a temperature range of 224-400 °C between 9,10-dihydroanthracene and an ethyl anthracene molecule where the products were anthracene and the ethyl 9,10-dihydroanthracene. They concluded that the transfer of a single hydrogen atom that is on the benzylic position by a free radical mechanism, from the 9,10-dihydroanthracene to the ethyl anthracene, was the rate-determining step. Therefore, the activation energy for hydrogen transfer is lower than that of cracking a carbon-carbon bond.

Rüchard et al.³⁷ found that hydrogen transfer occurs between the two closed-shell organic molecules 9,10-dihydroanthracene and α -methylstyrene in biphenylether between temperatures of 280-310 °C. Cumene and anthracene were formed. The initiation is a molecule-induced radical formation.

Guo et al.⁴⁷ used dihydroanthracene as a hydrogen donor and a probe molecule to study the mechanism of thermal cracking of heavy residues. When measuring the hydrogen abstraction ability of residues, the vacuum residue with high sulfur content was found to have the highest value. It was postulated that the presence of hydrogen sulfide, due to the organic sulfur decomposition, catalyzes the transfer of hydrogen from the hydrogen donor molecule dihydroanthracene to the vacuum residue. The hydrogen transfer at lower temperatures was shown to be abstracted mainly by the aromatic part of the residue since not much cracking happens. In contrast, at higher temperatures, the hydrogen is used to terminate free radical fragments formed due to cracking.

Gould and Wiehe⁴⁸ used 2,3-dichloro-5,6-dicyano-*p*-benzoquinone (DDQ), a great hydrogen acceptor, to measure the ability of petroleum residues to donate hydrogens for the purpose of proving that petroleum residues have natural hydrogen donors. They used 9,10-dihydroanthracene as a probe molecule for quantification of the amount of DDQ unreacted. They concluded that the reactivity and concentration of hydrogen donors present in petroleum residues are relatively large. An interesting observation was that the reactivity of the hydrogen donors in the asphaltenes fraction is high in a way that depletes their presence in the asphaltenes pretty quickly, which makes them heavier. This is not the case for the petroleum residues, that maintain a constant concentration of these hydrogen donors for some time before decreasing. They concluded that asphaltenes were better hydrogen donors than tetralin at 110 °C. The comparison was made only at 110 °C.

In another study, Guo et al.⁴⁹ proved that hydrogen transfer takes place during visbreaking. They tested the ability of petroleum vacuum residues and their Saturates, Aromatics, Resins, and Asphaltenes (SARA) fractions to donate hydrogen to a probe molecule, anthracene. The 9,10-dihydroanthracene was used as a hydrogen donor to study the ability of the asphaltenes fraction of the same residues to accept hydrogen at 400 °C and 3 MPa. The ratio of residue to model probe compounds was 1:1 in mass and reactions took place in a microautoclave under nitrogen.

It was concluded that the ability of residue to donate hydrogen increases at the beginning as the anthracene converts to 9,10-dihydroanthracene and 1,2,3,4-tetrahydroanthracene. When the matrix is rich with the hydrogenated products, the ability of the residue to donate hydrogen starts

decreasing because of both the abundance of the hydrogenated compounds and the decrease of donatable hydrogens in the residue. When the reaction between formation of 9,10-dihydroanthracene and 1,2,3,4-tetrahydroanthracene and formation of anthracene is in equilibrium, the maximum hydrogen donation ability (HDA) of residue is reached. Thermal conversion also takes place in the background matrix. Therefore, when the hydrogenated molecules are formed, they provide hydrogen to the heavy molecules making them less susceptible to form coke. In that way, 9,10-dihydroanthracene and 1,2,3,4-tetrahydroanthracene form anthracene again. 0.3-0.7 mg hydrogen/g of vacuum residues could be transferred from vacuum residues over the temperature range 360-430 °C.

They have also proved that the maximum HDA is reached faster and has a higher value at higher temperatures. Aromatics, resins and asphaltenes have a higher HDA than saturates that barely donate any hydrogen at lower temperatures. The HDA of all four fractions increases with temperature. The HDA of the residue as a whole is higher than the summation of the HDAs of each fraction of the SARA.

Naghizada et al.⁵⁰ used α -methylstyrene, cumene, anthracene and 9,10-dihydroanthracene as model compounds to study the reactivity of asphaltenes at 100 and 250 °C and 4 MPa under nitrogen. Using proton-NMR, hydrogen disproportionation was proven to take place during the reaction conditions in the absence of any additive. There was also an increase in aromatic carbon content measured by ¹³C-NMR. When α -methylstyrene was reacted with asphaltenes, the ability of the latter to donate hydrogen was obvious by the conversion of α -methylstyrene to cumene even at temperatures as low as 120 °C. The opposite did not take place when asphaltenes were reacted with cumene (i.e. asphaltenes did not abstract hydrogen from cumene). The same happens when asphaltenes were reacted with anthracene or 9,10-dihydroanthracene. The amount of hydrogen donated by asphaltenes was double to 9,10-dihydroanthracene than to anthracene.

The hydrogen donation and abstraction abilities of petroleum residues is of importance since it directly affects the formation of coke. If the petroleum residues are not capable of abstracting the hydrogen provided from hydrogen donors, it defeats the purpose of using these additives.

2.6.2 Hydrogen transfer in petroleum conversion

Carlson et al.⁵¹ tested the transfer of hydrogen from tetralin to cracked residues. They suggested that the formation of condensed poly-aromatic rings by free radical mechanisms can be decreased by the presence of a source that can readily donate more reactive hydrogen than that from the asphaltene structure. West Texas residue was used for this study with 1:1 ratio of solvent to residue and reactions conducted at 450 °C for 2.5 hours. Six different hydrogen donor solvents have been evaluated in the absence of hydrogen: *n*-heptane, benzene, methylcyclohexane, decalin, tetralin and naphthalene. The amount of coke formed increases when *n*-heptane or naphthalene were used but decreased with other solvents. The lowest amount of coke obtained was with tetralin followed by decalin. This is due to the formation of tetralin from decalin under pyrolysis conditions. The rest of the solvents had little effect on the conversions.

Tetralin was then reacted with multiple residues to prove its effectiveness in coke reduction. The conclusion elucidated was the ability of tetralin to readily donate hydrogen, thus decreasing the formation of condensed polyaromatic rings. They also found that naphthenic-aromatic compounds are better hydrogen donors than condensed-ring naphthenic compounds under the conditions used in the study.

Ignasiak et al.⁵² studied the reaction of tetralin with Athabasca asphaltene between the temperatures 195-390 °C. The amount of light compounds is increased with the presence of tetralin and as the temperature increased. At 390 °C under argon, half of the asphaltene amount was converted to materials that are soluble in *n*-pentane. Tetralin played the role of a stabilizer of the cracked products formed from asphaltene to avoid their transformation to coke.

Sanford et al.⁵³ studied the effect of the presence of hydrogen or tetralin (as hydrogen donor additives) and the combination of both in the feed (Athabasca bitumen) on the amount of coke in the product of thermal conversion. Coke amount was cut in half when either hydrogen or tetralin was used, and cut in half again when both were used. This confirms hydrogen transfer taking place. The purpose was to trap radical intermediates, formed during thermal conversion, using a hydrogen donor solvent rather than direct hydrogen supply that was the conventional method of chain

terminating these radicals. Neither the use of hydrogen donors alone, nor the combination of hydrogen with hydrogen donors, nor the combination of both with catalyst could stop the formation of coke but could only decrease it. The use of a hydrogen acceptor increased the coke yield.

Kubo⁵⁴ measured the radical scavenging ability of hydrogen-donor hydrocarbons in petroleum using the radical 2,2-diphenyl-1-picrylhydrazyl (DPPH). The radical scavenging ability was also compared with other model compounds like tetralin and conventional hindered phenolic antioxidants. The ability of the heavy fraction, specifically of the petroleum, to donate hydrogen was found to be higher or equal to that of both model compounds. This is in accordance with the study by Gould and Wiehe.⁴⁸

The work by Clarke et al.²³ tested the ability of a number of additives to decrease the onset of asphaltene formation when mixed with Cold Lake bitumen: toluene, *p*-xylene, naphthalene, phenanthrene, tetralin, decalin, nonyl-phenol, quinolone, indole, benzothiophene and others. It was found that phenanthrene and the surfactant nonyl-phenol had the highest effects in increasing the onset of asphaltene and coke formation by keeping asphaltene soluble in the matrix. They were added at high concentrations (10-25 wt%). The rest of the additives were found to be ineffective. One interesting observation in this study is that maltene fractions of the same bitumen was as effective as the added surfactants to delay the formation of asphaltene. This will be further elaborated in Section 2.6.3.

Morgenthaler et al.⁵⁵ demonstrated that some polycyclic aromatic hydrocarbons are great hydrogen donors and can catalyze hydrogen transfer when 9,10-dihydroanthracene is reacted in excess with α -methylstyrene using diphenylether as solvent at 250 °C. The catalysis effect of these compounds is characterized by their ability to decrease the required temperature for hydrogen transfer to occur. At 250 °C and in the absence of polycyclic aromatic hydrocarbon compounds, no hydrogen transfer occurs from 9,10-dihydroanthracene to α -methylstyrene. The hydrogen donor compounds played the role of the catalyst as their amount did not change between feed and product. This was contrary to the observations by Naghizada, et al.⁵⁰ that reported that hydrogen transfer took place in the same system at 250 °C.

Rahimi et al.⁵⁶ demonstrated that the presence of hydrogen donor materials in the amount of 5 wt% with Athabasca bitumen vacuum residue increased the induction period of the mesophase and significantly decreased the rate of appearance and the amount of mesophase formed.

Shi et al.⁵⁷ studied the behavior of normal alkanes and phenanthrene in the presence of a hydrogen donor (tetralin) and an aromatic solvent (1-methylnaphthalene) in order to mimic hydrogen transfer in coal and oil systems. Reactions took place under nitrogen at 7 MPa and 300 °C with equal masses of hydrogen donor and sample. It was concluded that the presence of tetralin inhibited the cracking of *n*-C₂₀ leading to small amounts of olefins compared to hydrocracking. The solvent also played the role of an inhibitor but to a lower extent than tetralin. The presence of tetralin with phenanthrene led to the hydrogenation of phenanthrene to dihydrophenanthrene and octahydrophenanthrene. It was also proved that longer paraffinic chains can crack easier than shorter ones in the presence of hydrogen donors. Deuterium labeling was used to study the mechanism of hydrogen transfer and it was found that there was more hydrogen transfer at higher temperatures. They claimed that the reason that tetralin inhibits the cracking of the *n*-C₂₀ molecule is that, as soon as the radical is formed, the hydrogen is donated from the tetralin to cap the radical.

Aleman-Vasquez et al.⁵⁸ studied the effect of use of hydrogen donor solvents, tetralin, decalin and naphthalene, to decrease the formation of heavy compounds in residue upgrading in the presence of hydrogen or methane. A ratio of 1:20 of solvent to heavy crude oil was used and reactions were conducted at 1.1 MPa at 420 °C in an autoclave. The amount of coke (toluene insoluble) decreased significantly in the product due to the ability of these solvents to donate hydrogen. This decrease was more significant when hydrogen donor solvents were used with hydrogen than with methane. In the case of hydrogen, naphthalene showed the highest decrease in coke yield followed by decalin then tetralin. Besides coke yield, the presence of the solvents and the change of temperature affected the API gravity and the viscosity. They have also concluded that there was obvious interconversion between the three solvents. However, there were no control experiments performed for the reaction of heavy crude oils with the solvents without hydrogen in order to give evidence whether the decrease of coke yield was due to hydrogen or hydrogen donors. The investigation on the ability of each solvent to delay onset of coking in absence of hydrogen or methane was also not performed in this study.

The study of hydrogen donor solvents was originated from the idea that maltenes, when present with asphaltenes, contain some hydrogen donors. In order to mimic this, hydrogen donor solvents were used. However, other literature used actual maltenes to test their hydrogen donation ability and their role in solvating asphaltenes (Section 2.6.3). In fact, bitumen inherently contains free radicals and contains some carbon-hydrogen bonds that are weaker than the carbon-hydrogen bonds in tetralin, the prototypical hydrogen donor solvent. The use of hydrogen donor solvents seems to be more beneficial in terms of dilution than in terms of chemistry (i.e. hydrogen availability),⁵⁹ which could potentially be better accomplished by natural hydrogen donors present in the bitumen.⁴⁸

The literature on hydrogen transfer is relevant to this study since the formation of heavier products is directly dependent on the abundance of hydrogen in the system. The formation of carbon rich and hydrogen depleted material is dependent on the type of matrix. If hydrogen donor materials are present in the matrix, the formation of heavier products can be suppressed.

2.6.3 Ability of maltenes to donate hydrogen to asphaltenes

The ability of resins to solvate asphaltenes has long been recognized.^{60,61,62}

Rahimi et al.⁶³ separated bitumen into asphaltenes and maltene fraction and performed thermal conversion for the two fractions separately due to the complexity of the matrix as a whole. Higher temperatures led to formation of condensed rings of asphaltenes. However, the donation of hydrogen from the maltenes fraction prevented the transformation of asphaltenes to coke over the period studied. Thus, the factor that affects the precipitation of asphaltenes is the matrix that might or might not act as a good solvent. Maltenes were found to be good solvents for asphaltenes while hexadecane was a poor hydrogen donor.

During thermal conversion in the presence of hydrogen, both asphaltenes and maltenes compete for the hydrogen which is provided by catalytic hydrogenation and hydrogen transfer. Throughout the reaction, the amount of asphaltenes gradually increases, which makes the availability of hydrogen decrease. Thus, the ability of maltenes to solvate asphaltenes becomes insufficient and

asphaltenes precipitation to coke happens. This is in accordance with Wiehe's phase-separation model.¹⁵ This study⁶³ also emphasizes the importance of the equilibrium between maltenes and asphaltenes during thermal conversions to delay the onset of coking.

In terms of free radicals, Rahimi et al.⁶³ observed that when the free radical concentration in the matrix is high, the ability to keep free radicals soluble so they can gain a hydrogen and terminate, is lower. Therefore, free radicals tend to undergo addition/combination reactions. The presence of asphaltenes in a higher concentration in the matrix does not only lead to hydrogen starvation and coke formation, but also to an increased viscosity that makes radicals less mobile and thus more prone to undergo addition reactions than termination reactions. This will be further studied in Chapters 5 and 6.

Wiehe et al.⁶⁴ showed that the amount of coke formed from the thermal cracking of asphaltenes is ten times larger than that formed when maltenes were present.

Di Carlo et al.⁶⁵ developed a model to predict the behaviour of residues during visbreaking. The model was created mainly using proton resonance spectroscopy and reflects the importance of the maltenes fraction in the mixture to create a thermodynamic equilibrium that keeps the asphaltenes stability index high. It was shown that the tendency of asphaltenes to peptize (i.e. precipitate) is higher when the aromatic content of asphaltenes is higher or when the aromatic content of maltenes is lower.⁶⁵ Thus, asphaltenes are more stable after thermal cracking when initially the aromaticity of maltenes and asphaltenes in the feed is more similar. The heavier the feedstock, the more extreme is the boiling range of products (i.e. a high amount of light products and a high amount of heavy products and less atmospheric and vacuum gasoil boiling range products).

Jamaluddin et al.⁶⁶ also studied the effect of maltenes fractions and gas oils on the solvation of asphaltenes and delay of onset of coking. It was proven that de-asphalted oil has a higher ability to solubilize asphaltenes than toluene due to their high resins content (30 wt%). Gas oils produced from vacuum distillation had the highest solvation ability.

The literature on the ability of maltenes to donate hydrogen to asphaltenes is related to coke formation. If the maltenes fraction was able to keep asphaltenes rich enough in hydrogen to stay solvated in the matrix, the induction period of coke formation is extended.

2.7 Industrial relevance of heavy products formation in thermal processes

In the BituMax™ partial upgrader process of CNOOC (previously Nexen),⁶⁷ shown as a block flow diagram in Figure 2.2, thermal cracking constitutes the heart of the field upgrader.

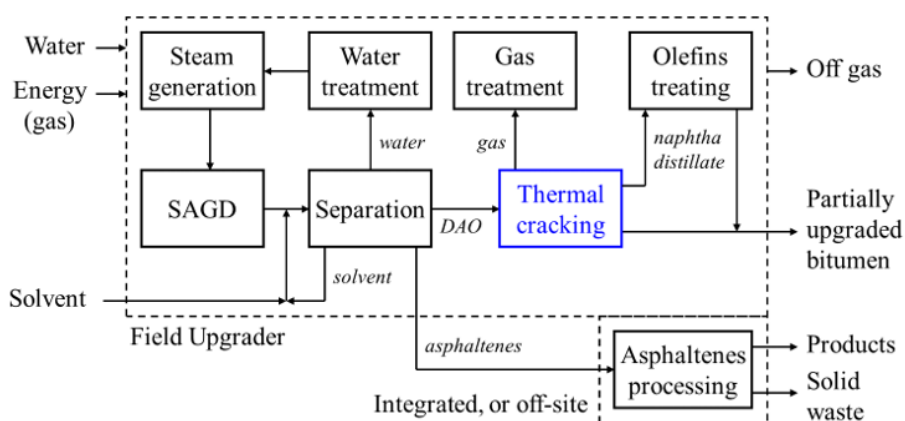


Figure 2.2. Block flow diagram for CNOOC's field upgrader.⁶⁷

The diagram highlights general equipment and process streams. After bitumen is recovered by steam assisted gravity drainage (SAGD), bitumen upgrading starts with removing the asphaltenes that will retain most of the metals, impurities and much of the material responsible for the Conradson carbon content of the bitumen feed. This separation process decreases the carbon content by carbon rejection using a solvent. Asphaltenes produced from the separation are further processed to get as much as possible of useful products from it, thus reclaiming some of the oil yield that would otherwise be lost due to asphaltenes rejection. Water is re-used for SAGD after treatment.

The main process feed stream is the de-asphalted oil (DAO), sent to oil upgrading, which consists of a thermal cracking (visbreaking) unit and an olefin treatment unit. The thermal cracking process

produces the partially upgraded oil that, after olefin treating of the cracked naphtha, meets the pipeline specifications in terms of density, viscosity and olefins content (Table 2.1).⁶⁸

Though the visbreaker is preceded by a solvent de-asphalting unit, the formation of new asphaltenes in the thermal conversion of de-asphalted oil, defeats the purpose of performing solvent de-asphalting. The formation of asphaltenes, that are considered to be coke precursors, limits the conversion, increases the product instability (i.e. due to phase separation), increases the product viscosity and the risk of fouling.

Table 2.1. Canadian specifications for bitumen for pipeline transportation

Property	Specification
Viscosity	<350 cSt at 7.5 °C
Density	>19° API (or <940 kg/m ³)
Olefin Content	<1 wt% as 1-decene equivalent
Water and sediments	<0.5 wt%

The formation of products heavier than the feed in visbreaking was studied. For instance, Rahimi et al.⁶⁹ investigated the chemistry of thermal cracking of polyaromatic fractions of oil residues and showed that the polyaromatic fractions cracked to form smaller molecules. However, the feed also underwent addition reactions to form heavier products that led to coke formation. They postulated that hydrogen transfer and side-chain cracking were major routes in thermal cracking since the products formed had a smaller molecular weight than the feed and were more aromatic.

Several process innovations have been performed to the visbreaking unit like optimizing parameters for different feeds, removing volatile nonsolvent, preventing adhesion of coke to the visbreaking surface.²⁴ Some models have been developed to predict the yield and mechanism of thermal conversion in visbreaking (e.g.^{70,71}). However, these models did not solve the problem from its origin. In other words, there was not much effort invested on the study of the reason of formation of heavier products leading to asphaltenes.

Asphaltenes are formed when molecules approaches the solubility limit that leads to their separation and precipitation. Asphaltenes are formed when addition reactions take place leading

to formation of condensed polyaromatic rings. The solubility of asphaltenes in the visbreaker matrix is well described by the equilibrium between addition and cracking reactions as introduced in Chapter 1. In fact, changes in the solubility of the feed in the complex matrix of visbreaking occur. Solubility is also highly dependent on the bulk liquid properties. This will be covered in more details in Chapters 3 and 5.

In order to avoid asphaltenes formation, it is useful to better understand the precursors of asphaltenes. There is a large body of literature on the coke formation mechanism and characterization as well as use of hydrogen donating solvents, but there was less literature on the potential contribution of lower boiling fractions. In fact, prior to mesophase formation, condensation reactions take place. These reactions start by forming dimers that further add up forming asphaltenes by a free radical mechanism. This thesis will focus on studying compounds lighter than asphaltenes but that are potential precursors of coke. In order to understand the heavy products formation in thermal conversions, we will focus on developing a better understanding of the chemistry behind the free radical addition reactions.

Literature cited

- (1) Keesom, B.; Gieseman, J. *Bitumen Partial Upgrading 2018 Whitepaper*; Report AM0401A for Alberta Innovates, rev.8, April 13, 2018.
- (2) Levinter, M. E.; Medvedeva, M. I.; Panchenkov, G. M.; Aseev, Y. G.; Nedoshivin, Y. N.; Finkel'shtein, G. B.; Galiakbarov, M. F. Mechanism of Coke Formation in the Cracking of Component Groups in Petroleum Residues. *Chem. Technol. Fuels Oils* **1966**, 2 (9), 628–632.
- (3) Levinter, M. E.; Medvedeva, M. I.; Panchenkov, G. M.; Agapov, G. I.; Galiakbarov, M. F.; Galikeev, R. K. The Mutual Effect of Group Components during Coking. *Chem. Technol. Fuels Oils* **1967**, 3 (4), 246–249.
- (4) Magaril, R. Z.; Aksenova, E. I. Study of Mechanism of Coke Formation in Cracking of Petroleum Resins. *Int. Chem. Eng.* **1968**, 8 (4), 727.
- (5) Magaril, R. Z.; Aksenova, E. I. Investigation of the Mechanism of Coke Formation during Thermal Decomposition of Asphaltenes. *Chem. Technol. Fuels Oils* **1970**, 6 (7), 509–512.
- (6) Magaril, R. Z.; Ramazaeva, L. F.; Aksenova, E. I. Kinetics of Coke Formation in the Thermal Processing of Petroleum. *Khim. Tekhnol. Topl. Masel* **1970**, 15 (3), 15–16.
- (7) Speight, J. G. Thermal Cracking of Athabasca Bitumen, Athabasca Asphaltenes, and Athabasca Deasphalted Heavy Oil. *Fuel* **1970**, 49 (2), 134–145.
- (8) Yan, T. Y. Coke Formation in Visbreaking Process. *Am. Chem. Soc. Div. Pet. Chem. Prepr.* **1987**, 32, 490–495.
- (9) Mansoori, G. A.; Jiang, T. S.; Kawanaka, S. Asphaltene Deposition and Its Role in Petroleum Production and Processing. *Arab. J. Sci. Eng.* **1988**, 13 (1), 17–34.
- (10) Sanford, E. C. Influence of Hydrogen and Catalyst on Distillate Yields and the Removal of Heteroatoms, Aromatics, and CCR during Cracking of Athabasca Bitumen Residuum over a Wide Range of Conversions. *Energy and Fuels* **1994**, 8 (6), 1276–1288.
- (11) Srinivasan, N. S.; McKnight, C. A. Mechanism of Coke Formation from Hydrocracked Athabasca Residuum. *Fuel* **1994**, 73 (9), 1511–1517.
- (12) Storm, D. A.; Barresi, R. J.; Sheu, E. Y. Evidence for the Micellization of Asphaltenic Molecules in Vacuum Residue. *Prepr. Chem. Soc. Div. Pet. Chem.* **1995**, 40 (4), 776–779.
- (13) Tong, Y.; Poindexter, M. K.; Rowe, C. T. Inhibition of Coke Formation in Pyrolysis

- Furnaces. *Prepr. Chem. Soc. Div. Pet. Chem.* **1995**, *40* (4), 612–617.
- (14) Nagaishi, H.; Chan, E. W.; Sanford, E. C.; Gray, M. R. Kinetics of High-Conversion Hydrocracking of Bitumen. *Energy and Fuels* **1997**, *11* (2), 402–410.
- (15) Wiehe, I. A. A Phase-Separation Kinetic Model for Coke Formation. *Ind. Eng. Chem. Res.* **1993**, *32* (11), 2447–2454.
- (16) Wiehe, I. A. A Solvent-Resid Phase Diagram For Tracking Resid Conversion. *Ind. Eng. Chem. Res.* **1992**, *31* (2), 530–536.
- (17) Wiehe, I. A. The Pendant-Core Building Block Model of Petroleum Residua. *Energy and Fuels* **1994**, *8* (3), 536–544.
- (18) Wiehe, I. A. The Chemistry of Coke Formation from Petroleum: A Tutorial. *Prepr. Chem. Soc. Div. Pet. Chem.* **1998**, *43* (4), 612–615.
- (19) Rahimi, P.; Gentzis, T.; Fairbridge, C.; Khulbe, C. Chemistry of Petroleum Residues in the Presence of H-Donors. *Prepr. Chem. Soc. Div. Pet. Chem.* **1998**, *43* (4), 634–636.
- (20) Rahimi, P. M.; Gentiz, T.; Delbianco, A. Application of Hot-Stage Microscopy in the Investigation of the Thermal Chemistry of Heavy Oils and Bitumen: An Overview. *Prepr. Chem. Soc. Div. Pet. Chem.* **2001**, *46* (4), 341–343.
- (21) Li, S.; Liu, C.; Que, G.; Liang, W.; Zhu, Y. Phenomena Occurring before Coke Formation in the Thermal Reaction System of Gudau Vacuum Residuum. *Prepr. Chem. Soc. Div. Pet. Chem.* **1995**, *40* (4), 736–740.
- (22) Brons, G.; Yu, J. M. Solvent Deasphalting Effects on Whole Cold Lake Bitumen. *Prepr. Chem. Soc. Div. Pet. Chem.* **1995**, *40* (4), 785–793.
- (23) Clarke, P. F.; Pruden, B. B. Asphaltene Precipitation from Cold Lake and Athabasca Bitumens. *Pet. Sci. Technol.* **1998**, *16* (3–4), 287–305.
- (24) Wiehe, I. A. Visbreaking. In *Process chemistry of petroleum macromolecules*; Speight, J. G., Ed.; CRC press, 2008; pp 369–376.
- (25) Subramanian, H.; Landais, Y.; Sibi, M. P. Radical Addition Reactions. *Compr. Org. Synth. Second Ed.* **2014**, *4*, 699–741.
- (26) Parsons, A. F. *An Introduction to Free Radical Chemistry*; Wiley-Blackwell., 2000.
- (27) Nonhebel, D. C.; Walton, J. C. *Free-Radical Chemistry: Structure and Mechanism*; 1974.
- (28) Harmony, J. A. K. Molecule-Induced Radical Formation. In *Methods in free-radical chemistry vol. 5*; Huyser, E. S., Ed.; Marcel Dekker, Inc: New York, 1974; pp 101–176.

- (29) Flory, P. J. The Mechanism of Vinyl Polymerizations. *J. Am. Chem. Soc.* **1937**, *59* (2), 241–253.
- (30) Pryor, W. A.; Lasswell, L. D. Diels-Alder and 1,4-Diradical Intermediates in the Spontaneous Polymerization of Vinyl Molecules. In *Advances in free-radical chemistry vol.5*; Williams, G. H., Ed.; Academic Press: New York, 1975; pp 27–100.
- (31) Mayo, F. R. Chain Transfer in the Polymerization of Styrene. VIII. Chain Transfer with Bromobenzene and Mechanism of Thermal Initiation. *J. Am. Chem. Soc.* **1953**, *75* (24), 6133–6141.
- (32) Hiatt, R. R.; Bartlett, P. D. The Thermal Reaction of Styrene with Ethyl Thioglycolate; Evidence for the Termolecular Thermal Initiation of Styrene Polymerization. *J. Am. Chem. Soc.* **1959**, *81* (5), 1149–1154.
- (33) Walling, C. *Free Radicals in Solution*; Wiley, 1957.
- (34) Chong, Y. K.; Rizzardo, E.; Solomon, D. H. Confirmation of the Mayo Mechanism for the Initiation of the Thermal Polymerization of Styrene. *J. Am. Chem. Soc.* **1983**, *105* (26), 7761–7762.
- (35) Kopecky, K. R.; Lau, M. P. Thermal Reaction between 5-Methylene-1,3-Cyclohexadiene and Styrene. *J. Org. Chem.* **1978**, *43* (3), 525–526.
- (36) Gajewski, J. J.; Gortva, A. M. Bimolecular Thermal Reactions of 5-Methylene-1,3-Cyclohexadiene (o-Isotoluene) and 3-Methylene-1,4-Cyclohexadiene (p-Isotoluene). *J. Am. Chem. Soc.* **1982**, *104* (1), 334–335.
- (37) Rüchardt, C.; Gerst, M.; Nölke, M. The Uncatalyzed Transfer Hydrogenation of *p*-Methylstyrene by Dihydroanthracene or Xanthene—a Radical Reaction. *Angew. Chem. Int. Ed. Engl.* **1992**, *31* (11), 1523–1525.
- (38) Strausz, O. P.; Lown, E. M. *The Chemistry of Alberta Oil Snads, Bitumes and Heavy Oils*; Alberta Energy Research Institute, 2003.
- (39) Abell, P. I. Addition to Multiple Bonds. In *Free radicals Vol.2*; Kochi, J. K., Ed.; John Wiley & Sons, 1973; pp 63–68.
- (40) Giese, B. Synthetic Applications of Radical C-C Bond Forming Reactions. *Res. Chem. Intermed.* **1986**, *7* (1), 3–11.
- (41) Doyle, G. Desulfurization via Hydrogen Donor Reactions. *Am. Chem. Soc., Div. Pet. Chem., Prepr.* **1976**, *21*, 165–172.

- (42) Bockrath, B. C. Chemistry of Hydrogen Donor Solvents. In *Coal Science Vol.2*; Gorbaty, M. L., Larsen, J. W., Wender, I., Eds.; Academic Press: New York, 1983; pp 65–124.
- (43) Varga, J.; Rabo, G.; Zalai, A. Thermal Decomposition of Asphalt-Containing Crude Oils in the Presence of Diluents and Hydrogen. *Brennst.-Chem* **1956**, *37*, 244.
- (44) Langer, A. W.; Stewart, J.; Thompson, C. E.; White, H. T.; Hill, R. M. Hydrogen Donor Diluent Visbreaking of Residua. *Ind. Eng. Chem. Process Des. Dev.* **1962**, *1* (4), 309–312.
- (45) Uemasu, I.; Kushiyama, S. Analysis of 9,10-Dihydroanthracene by Capillary Gas Chromatography for Evaluation of Transferable Hydrogen in Heavy Oils. *J. Chromatogr. A* **1986**, *368* (C), 387–390.
- (46) Billmers, R.; Griffith, L. L.; Stein, S. E. Hydrogen Transfer between Anthracene Structures. *J. Phys. Chem.* **1986**, *90* (3), 517–523.
- (47) Guo, A.; Wang, Z.; Feng, J.; Que, G. Mechanistic Analysis on Thermal Cracking of Petroleum Residue Using H-Donor as a Probe. *Prepr. Chem. Soc. Div. Pet. Chem.* **2001**, *46* (4), 344–347.
- (48) Gould, K. A.; Wiehe, I. A. Natural Hydrogen Donors in Petroleum Resids. *Energy and Fuels* **2007**, *21* (3), 1199–1204.
- (49) Guo, A.; Wang, Z.; Zhang, H.; Zhang, X.; Wang, Z. Hydrogen Transfer and Coking Propensity of Petroleum Residues under Thermal Processing. *Energy and Fuels* **2010**, *24* (5), 3093–3100.
- (50) Naghizada, N.; Prado, G. H. C.; De Klerk, A. Uncatalyzed Hydrogen Transfer during 100–250 °C Conversion of Asphaltenes. *Energy and Fuels* **2017**, *31* (7), 6800–6811.
- (51) Carlson, C. S.; Langer, A. W.; Stewart, J.; Hill, R. M. Thermal Hydrogenation. Transfer of Hydrogen from Tetralin to Cracked Residua. *Ind. Eng. Chem.* **1958**, *50* (7), 1067–1070.
- (52) Ignasiak, T. M.; Strausz, O. P. Reaction of Athabasca Asphaltene with Tetralin. *Fuel* **1978**, *57* (10), 617–621.
- (53) Sanford, E. C.; Xu, C. M. Relationship between Solids Formation, Residuum Conversion, Liquid Yields and Losses during Athabasca Bitumen Processing in the Presence of a Variety of Chemicals. *Can. J. Chem. Eng.* **1996**, *74* (3), 347–352.
- (54) Kubo, J. Radical Scavenging Abilities of Hydrogen-Donating Hydrocarbons from Petroleum. *Ind. Eng. Chem. Res.* **1998**, *37* (11), 4492–4500.
- (55) Morgenthaler, J.; Rüdhardt, C. New Hydrogen Transfer Catalysts. *European J. Org. Chem.*

- 1999**, *1999* (9), 2219–2230.
- (56) Rahimi, P.; Gentzis, T.; Kubo, J.; Fairbridge, C.; Khulbe, C. Coking Propensity of Athabasca Bitumen Vacuum Bottoms in the Presence of H-Donors - Formation and Dissolution of Mesophase from a Hydrotreated Petroleum Stream (H-Donor). *Fuel Process. Technol.* **1999**, *60* (2), 157–170.
- (57) Shi, B.; Wang, L. Q.; Lin, D. L.; Que, G. H. Hydrogen-Transfer between Hydrogen Donors and Model Compounds with Steady Isotope. *Prepr. Chem. Soc. Div. Pet. Chem.* **2001**, *46* (4), 325–328.
- (58) Alemán-Vázquez, L. O.; Cano-Domínguez, J. L.; García-Gutiérrez, J. L. Effect of Tetralin, Decalin and Naphthalene as Hydrogen Donors in the Upgrading of Heavy Oils. *Procedia Eng.* **2012**, *42*, 532–539.
- (59) Zachariah, A.; Wang, L.; Yang, S.; Prasad, V.; De Klerk, A. Suppression of Coke Formation during Bitumen Pyrolysis. *Energy and Fuels* **2013**, *27* (6), 3061–3070.
- (60) Nellensteyn, F. J. The Colloidal Structure of Bitumens. In *The science of petroleum, Vol. 4*; Dunstan, A. E., Nash, A. W., Brooks, B. T., Tizard, H., Eds.; Oxford university press, 1938; pp 2760–2763.
- (61) Pfeiffer, J. P.; Saal, R. N. J. Asphaltic Bitumen as Colloid System. *J. Phys. Chem.* **1940**, *44*, 139–149.
- (62) Schabron, J. F.; Speight, J. G. The Solubility and Three-Dimensional Structure of Asphaltenes. *Pet. Sci. Technol.* **1998**, *16* (3–4), 361–375.
- (63) Rahimi, P. M.; Gentzis, T. Thermal Hydrocracking of Cold Lake Vacuum Bottoms Asphaltenes and Their Subcomponents. *Fuel Process. Technol.* **2003**, *80* (1), 69–79.
- (64) Wiehe, I. A.; Yarranton, H. W.; Akbarzadeh, K.; Rahimi, P. M.; Teclemariam, A. The Paradox of Asphaltene Precipitation with Normal Paraffins. *Energy and Fuels* **2005**, *19* (4), 1261–1267.
- (65) Di Carlo, S.; Janis, B.; Migliorati, P. Tendency of Petroleum Residues to Be Processed in Visbreaking: A Prediction Model. *Prepr. Chem. Soc. Div. Pet. Chem.* **1995**, *40* (4), 730–735.
- (66) Jamaluddin, A. K. M.; Nazarko, T. W.; Sills, S.; Fuhr, B. J. Deasphalted Oil - A Natural Asphaltene Solvent. *SPE Prod. Facil.* **2007**, *11* (03), 161–165.
- (67) De Klerk, A.; Zerpa Reques, N. G.; Xia, Y.; Omer, A. A. Integrated Central Processing

- Facility (CPF) in Oil Field Upgrading (OFU). US 9,650,578 B2, 2014.
- (68) National Energy Board. Crude Petroleum Tariff No. 391.
- (69) Rahimi, P. M.; Dettman, H.; Nowlan, V.; DelBianco, A. Molecular Transformation during Heavy Oil Upgrading. *Prepr. Chem. Soc. Div. Pet. Chem.* **1997**, *42* (1), 23–26.
- (70) Castellanos, J.; Cano, J. L.; Del Rosal, R.; Briones, V. M.; Mancilla, R. L. Kinetic Model Predicts Visbreaker Yields. *Oil gas J.* **1991**, *89* (11), 76.
- (71) Trauth, D. M.; Yasar, M.; Neurock, M.; Nigam, A.; Klein, M. T.; Kukes, S. G. Asphaltene and Resid Pyrolysis: Effect of Reaction Environment. *Fuel Sci. Technol. Int.* **1992**, *10* (7), 1161–1179.

Chapter 3: Quantification of the free radical content of oilsands bitumen fractions

Abstract

Electron spin resonance (ESR) spectroscopy was employed to perform quantitative analysis of the free radical content of oilsands bitumen, asphaltenes, deasphalted oil, vacuum residue and vacuum gas oil fractions, as well as thermally converted product fractions. Calibration standards for ESR were compared and 2,2-diphenyl-1-picrylhydrazyl (DPPH) was selected. The heaviest fractions, including asphaltenes, had free radical concentrations in the range 10^{17} – 10^{18} spins/g, whereas lighter fractions such as the lighter gas oil fractions had free radical concentrations in the range 10^{16} – 10^{17} spins/g. It was found that the bulk liquid properties affected the measured free radical concentration, even after compensating for effects that could affect the spectroscopy. These differences were not analytical artifacts and could be explained with reference to literature in terms of the “equilibrium” composition resulting from dimerization and decomposition of free radical pairs. Reported free radical concentrations must consequently be interpreted by considering nature of the bulk liquid that was analyzed. Practically, the results have implications for thermal conversion of bitumen. It appears that the free radical concentration and availability of reactive free radicals can be independently manipulated through temperature and the bulk liquid properties.

Keywords: quantitative electron spin resonance, oilsands bitumen, free radicals.

3.1 Introduction

Electron spin resonance (ESR) or electron paramagnetic resonance (EPR) spectroscopy is an analytical technique that is useful for the analysis of species with unpaired electrons, such as organic free radicals. ESR spectroscopy measures energy absorption by unpaired electrons when they change their spin state under the influence of a magnetic field. ESR spectroscopy is related to nuclear magnetic resonance (NMR) spectroscopy, which measures energy absorption by nuclei with non-integer spin numbers as they change their spin state under the influence of a magnetic field. Coupling between an unpaired electron and nearby nuclei with non-integer spin numbers, such as ^1H , causes hyperfine splitting of the ESR spectrum that is analogous to the effect of spin-spin coupling on an NMR spectrum. It is therefore possible to obtain information about the environment in which the unpaired electron is by analyzing the ESR spectrum.

When ESR is applied to mixtures of radical species, it appears as if there is no hyperfine splitting. Signals of individual species that have g -values close to each other result in overlap of the hyperfine splitting of individual species, causing the spectrum to appear as if there is no hyperfine splitting. Signal overlap and other reasons have been cited as explanations for the lack of hyperfine splitting in oilsands bitumen derived samples,¹ and other heavy materials, such as coal.² Other reasons for the lack of hyperfine splitting being observed in bitumen include molecular tumbling of micelles that increases the width of absorption lines, electron dipole-dipole interactions and occurrence of g -anisotropy. As a consequence, in bitumen the information about the structure of the free radical species that could be obtained from hyperfine splitting is lost, but information about the total energy of absorption, as well as the average energy of the absorption is retained. It is therefore possible to employ ESR spectroscopy to mixtures of free radical species and quantify the concentration of unpaired electrons from the absorption area in the spectrum, as well as obtain some information about the nature of the free radicals from the average Landé g -value. Thus, when ESR spectroscopy is applied to petroleum, the concentration of free radicals can be quantified, which is the main topic of this investigation.

Several applications of ESR spectroscopy to petroleum were found. A number of investigators characterized and quantified organic free radicals in different petroleum fractions.^{3,4,5,6} In addition

to the organic free radicals, paramagnetic metal species can be observed, such as vanadium(IV). Vanadium(IV) is typically present as VO^{2+} in vanadyl porphyrins in petroleum. Since the ESR spectrum of vanadium(IV) does not overlap with carbon centered radicals, quantification of vanadium and organic radicals can both be accomplished. Some investigators used the central line of the vanadium(IV) spectrum to quantify the vanadium content in various bitumen fractions.^{1,7} In a more advanced application of ESR to vanadium(IV), the size distribution of asphaltenes containing vanadyl porphyrins was determined.^{8,9} Differences in the g -value are indicative of the nature of the free radicals. The g -value was correlated to the sulfur content in petroleum asphaltenes,¹⁰ as well as to the overall sulfur, nitrogen and oxygen heteroatom content,¹¹ although the statistical significance of this correlation was questionable.¹² Using the g -values, an even broader relationship between ESR spectral data and petroleum reservoir properties and oil properties was established. In this way ESR spectroscopy was employed to obtain biomarker history, because the ESR spectra provided information that could be related to the origin of the fossil fuels and the geological nature of the source.^{1,10,11,13} ESR spectroscopy was also used to evaluate changes in free radical content subsequent to thermal conversion of petroleum.^{14,15} The diversity of applications of ESR spectroscopy to petroleum hopefully makes it clear that ESR spectroscopy of petroleum is useful.

The use of ESR in the study of oilsands bitumen, apart from characterization, is as a tool to study thermal conversion. In bitumen upgrading, thermal conversions (e.g. visbreaking and coking) take place by a free radical mechanism. Bitumen initially contains free radicals; thus initiation during thermal conversion does not depend only on homolytic bond dissociation to form free radical species. Fouling and asphaltene formation during and after thermal conversion may be caused by free radical reactions that take place. The focus in this case would be on the propagation steps that lead to free radical addition reactions, leading to precursors of coke.

The purpose of this study was twofold. First, it aimed to resolve practical aspects associated with the quantitative ESR spectroscopy of petroleum fractions. Calibration for quantitative ESR measurements is still a topic of discussion, with no definitive recommendation.¹⁶ The approach taken was to compare several different calibration substances and parameters that could affect measurements. In this way an indication of the uncertainty could be established for absolute

values, as well as for the relative uncertainty for measurements with a single set of calibration conditions. Second, it aimed to provide an overview of the distribution of free radicals present in different oilsands bitumen fractions. In this respect it was found that the free radical concentration depended on the properties of the bulk liquid and that solvent dilution affected the measurements. A plausible explanation for these observations was provided and the implications for bitumen upgrading were discussed.

3.2 Experimental

3.2.1 Materials

The calibration of the ESR spectrometer was performed using three different organic substances, namely, 2,2-diphenyl-1-picrylhydrazyl (DPPH), 4-hydroxy-2,2,6,6-tetramethyl-1-piperidine-1-oxyl (TEMPO), and α,γ -bisdiphenylene- β -phenylallyl (BDPA). The structures of these organic free radicals are shown in Figure 3.1.

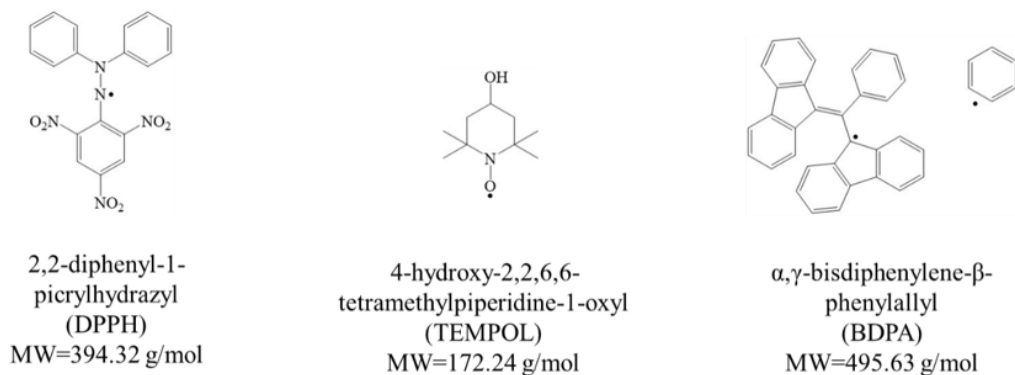


Figure 3.1. Organic free radical substances employed for calibration of ESR spectrometer.

The origin and purity of commercially obtained chemicals employed in this study are listed in Table 3.1. These chemicals were used without further purification.

Table 3.1. List of chemicals employed in this study.

Compound	Formula	CASRN ^a	Mass fraction purity ^b	Supplier
<i>Solvents</i>				
<i>n</i> -pentane	C ₅ H ₁₂	109-66-0	0.994	Fischer Scientific
toluene	C ₇ H ₈	108-88-3	0.999	Fischer Scientific
N-methylpyrrolidine (NMP)	C ₅ H ₁₁ N	120-94-5	0.97	Sigma-Aldrich
<i>Calibration materials for ESR</i>				
2,2-diphenyl-1-picrylhydrazyl (DPPH)	C ₁₈ H ₁₂ N ₅ O ₆	1898-66-4	0.90	Sigma-Aldrich
4-hydroxy-2,2,6,6-tetramethyl-1-piperidine-1-oxyl (TEMPOL)	C ₉ H ₁₈ NO ₂	2226-96-2	0.95	Alfa Aesar
α,γ -bisdiphenylene- β -phenylallyl (BDPA)	C ₃₉ H ₂₇	35585-94-5	0.99	Sigma-Aldrich

^a CASRN = Chemical Abstracts Services Registry Number

^b This is the purity of the material guaranteed by the supplier; the actual purity may be better.

The oilsands bitumen fractions were obtained from various sources. These were grouped into different categories based on their nature. A description of the origin of the samples are given together with the results.

3.2.2 Analyses

The free radical content in the products was measured using an Active Spectrum bench top extended range (X-band, 7000 Gauss) Micro-ESR. All measurements were performed at 9.6×10^9 Hz, 1.2 Gauss coil amplitude, a digital gain of 12 dB, and a microwave power of 15 mW. The analyses were the average of 7 scans with a sweep delay of 30 milliseconds between each scan. Analyses were conducted at ambient temperature, 20 °C. The quantification of the free radical content into number of spins per grams of sample was possible by the double integration of the ESR peak (i.e. the single integration of the absorption peak) using different calibration curves. The

double integration was done using the MicroESR software without base correction but with a filtering done using S-G (Savitzky-Golay) with a Gauss width of 1 and a polynomial order of three.

A saturation curve was created using the same above operating conditions but by arraying the microwave power. The array size is 10 and it includes the values of: 1, 3, 6, 10, 15, 25, 40, 50, 60, 70 mW. The delay between each run is 30 seconds and tuning was also automatically performed before each run. The power saturation study and the power saturation graph are reported in Appendix A.1. It was confirmed that a microwave power of 15 mW was within the power region where the square root of microwave power versus the intensity of the ESR signal was linear.

In addition to these ESR measurements, the naphtha samples were also analyzed using an Elecsys E-500 Electron Paramagnetic Resonance spectrometer at a receiver gain of 60, a 20 mW microwave power, mode coil amplitude of 1 Gauss using 6 scans and a microwave frequency of 9.85×10^9 Hz.

The analyses performed in this study were performed with PQ tubes: 5 mm diameter medium wall quartz, 18 cm (7 inch) long, concentricity ± 0.0102 mm, camber ± 0.102 mm. A study of the influence of different tube types can be found in Appendix A.2.

Toluene was employed as the solvent throughout the study, although asphaltenes were analyzed by dissolving the asphaltenes in either toluene, or N-methylpyrrolidine. Comparison of the quantification in toluene and N-methylpyrrolidine did not reveal a systematic bias, although differences were observed. Nevertheless, with the exception of the asphaltenes samples that employed both solvents, all other measurements employed only toluene as the solvent. The concentration of samples varied between 3 and 50 wt% of sample in the solvent depending on the purpose of the measurement and the type of sample. The exact concentrations are provided with the results. Lighter boiling samples that could not be quantified when diluted in a solvent, were analyzed neat, without the use of a solvent. In all instances care was taken to fill the ESR tube used for analysis to a level that would ensure that the resonant cavity of the ESR was presented with sample throughout the length of the tube in the resonant cavity. The procedure and reasoning behind the approach is discussed in more detail in Appendix A.3. Samples were analyzed at

ambient temperature, 20 °C, in closed tubes, but under air atmosphere. Samples were analyzed as soon as they were prepared. The difference between ESR analyses performed with sample under air and under nitrogen was reported to be measurable, but minor.^{5,7} (It was noted that one study¹⁷ reported a more significant impact of oxygen on measurements).

The density of samples that were analyzed at high concentration or neat, such as the vacuum gas oils, was measured using an Anton Paar DMA 4500M density meter. All density measurements were performed at 20 °C and atmospheric pressure. The instrument was calibrated with ultra-distilled water and the temperature accuracy was 0.01 °C and readability accuracy of density measurements was 0.00001 g/cm³.

Some solubility fractions were freshly prepared for this study. For this purpose the *n*-pentane insoluble fraction (asphaltenes) was precipitated. The precipitation was performed by mixing the sample and *n*-pentane in a 1:40 ratio of sample to *n*-pentane. The mixture was stirred in a closed jar at room temperature for 1 hour and left to settle for 23 hours before filtration. Filtration was done using 0.22 µm filter paper. The collected *n*-pentane insoluble precipitates were dried overnight in a fume hood until achieving a constant mass that was indicative of complete drying. The same procedure was employed for the preparation of all solubility fractions, but it is recognised that this procedure may affect the free radical content compared to preparation conducted under inert conditions. Following on the observations in literature^{5,7} the impact of atmosphere is reportedly minor, but this was not verified in this study.

3.3 Results

3.3.1 ESR calibration

The samples used for calibration were gravimetrically prepared in the concentration range below 1 wt%, with toluene being the solvent of choice. Toluene was selected, because of the good solubility of both the calibration substances, as well as the analytes in toluene. In this way nearly all analyses could be performed with the same solvent. When the solvent is the main component of the sample mixture, the solvent determines the dielectric loss of the sample. By keeping the

solvent the same, it reduces the impact of changes in dielectric loss on the ESR quality factor, Q .¹⁶ When the solvent is the main component, the densities of the calibration mixtures and the samples for analysis are also near the same, i.e. the density approximates that of the solvent and it is not necessary to determine the density of the sample separately. The density is important to relate the measured volumetric spin concentration to the gravimetric spin concentration. When analyzing samples at higher concentration, the density of the mixture potentially changes and must be compensated for by employing the measured densities of the sample and calibration mixtures to relate the spin concentration per volume to spin concentration per mass.

All calibration samples were freshly prepared for calibration. This is pointed out, because it has been reported that the solvent affects storage stability.¹⁶ Calibration curves were determined for each of the calibration substances at the same ESR analysis conditions (Figure 3.2).

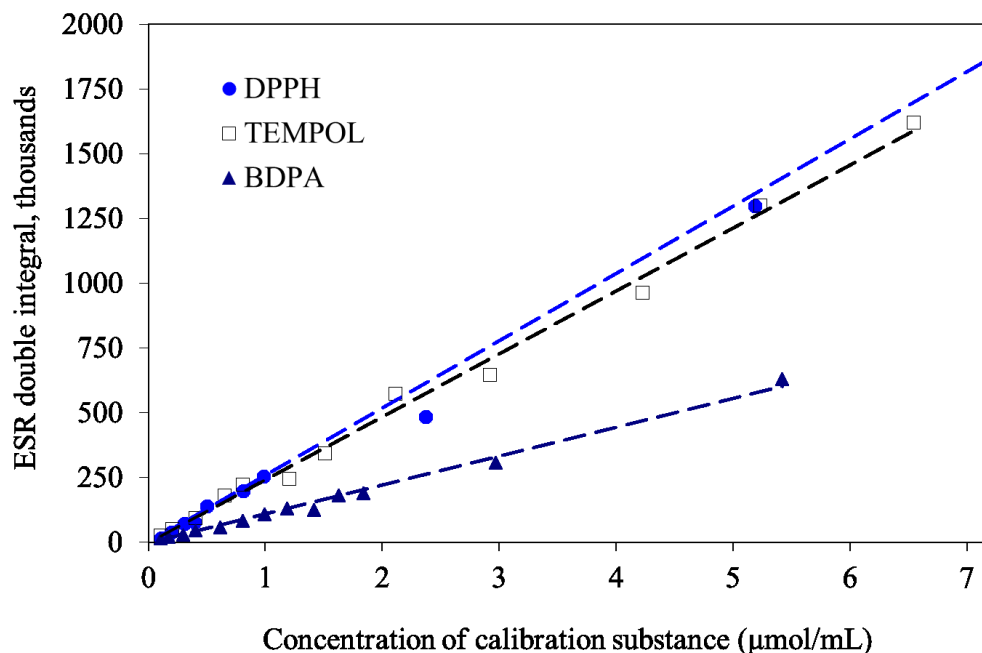


Figure 3.2. Calibration of the ESR spectrometer with different calibration substances.

The relationship between the double integral value, A_{ESR} , and the concentration of the calibration substance, $C_{\text{substance}}$, in units of $\mu\text{mol/mL}$ were linear, with the linear regression coefficients, r^2 , as indicated (Equations 1 to 3).

$$A_{\text{ESR}} = 0.26 \times 10^6 \cdot C_{\text{DPPH}}, r^2 = 0.993 \quad (1)$$

$$A_{\text{ESR}} = 0.24 \times 10^6 \cdot C_{\text{TEMPOL}}, r^2 = 0.994 \quad (2)$$

$$A_{\text{ESR}} = 0.11 \times 10^6 \cdot C_{\text{BDPA}}, r^2 = 0.991 \quad (3)$$

More careful inspection of the calibration curves reveals that there are two regions. The slope of the calibration curve in the concentration region up to around $1 \mu\text{mol/mL}$ is somewhat different to that of the total calibration curve.

There was reasonable agreement between the double integral area response of the ESR measurements and the concentration of DPPH (Equation 1) and TEMPOL (Equation 2). The free radical spin concentration is related to concentration of the calibration substance, with $1 \mu\text{mol/mL}$ of DPPH and TEMPOL in corresponding to $1 \mu\text{mol spins/mL} = 6 \times 10^{17} \text{ spins/mL}$. This relationship presumes that all of the molecules in the calibration substance are present as persistent free radicals of long half-life. The selection of such substances for calibration is based on more guidelines being provided in literature.¹⁶

When unknown samples are analyzed, the free radical concentration is determined relative to the calibration, which will give a value in units of spins/mL. To convert measured values from spins/mL to spins/g, the measured value must be divided by the concentration of the analyte in the sample, with the analyte concentration expressed in units of g/mL.

The double integral area response of BDPA (Equation 3) was contrary to expectation. BDPA has two free radicals (Figure 3.1) and should have had double the response of DPPH and TEMPOL at the same concentration. Instead, it had a lower response than DPPH and TEMPOL. It was reported that the ESR signal intensity of solutions of BDPA in toluene gradually decreased over a period of 8 hours,¹⁸ which implies that BDPA solutions must be prepared and analyzed almost immediately when used for calibration purposes.

For the rest of the study the ESR double integral areas were converted to spin concentrations using the calibration with DPPH. This was an arbitrary selection. This selection does not affect relative comparisons. However, all absolute values for spin concentration are by definition related to and subject to the same uncertainty as introduced by the DPPH calibration.

DPPH also served as *g*-value reference, with a reported *g*-value of 2.0036 ± 0.0001 , where the *g*-value of a free electron is 2.0023.¹⁶

3.3.2 Oilsands bitumen

Oilsands bitumen in its natural state contains stable free radical species. The free radical content of the six bitumen samples was measured (Table 3.2). The samples were prepared to be in the concentration range 4–7 wt% in the solvent. For toluene as solvent this was equivalent to 35–60 mg/mL.

Table 3.2. Free radical content and *g*-values measured for different bitumen samples.^a

Number	Free radical content (spins/g)			<i>g</i> -value		Description
	x	s	n	x	s	
Bit-1	9.3×10^{17}	1.2×10^{17}	3	2.0057	0.0008	Athabasca bitumen, Nexen
Bit-2	1.1×10^{18}	2.4×10^{17}	3	2.0042	0.0007	Athabasca bitumen, Suncor
Bit-3	8.7×10^{17}	7.3×10^{16}	3	2.0055	0.0009	Cold Lake bitumen (#1), >10 years old
Bit-4	9.5×10^{17}	3.8×10^{16}	3	2.0055	0.0004	Cold Lake bitumen (#2), ~5 years old
Bit-5	1.1×10^{18}	1.4×10^{16}	3	2.0049	0.0003	Cold Lake bitumen (#3), ~1 years old
Bit-6	1.0×10^{18}	1.5×10^{17}	6	2.0049	0.0011	Cold Lake bitumen (#4), tight emulsion ~2 years old ^b

^a Average (x), one sample standard deviation (s), and number of samples (n).

^b The presence of water affects the analysis, but the emulsion was tight, stable (two years without any sign of phase separation) and homogenous in appearance.

Samples Bit-1 and Bit-2 were oilsands bitumens from the Athabasca region. The first (Bit-1) was a bitumen from the Nexen Long Lake site, which is now owned and operated by CNOOC

International Ltd. This sample was taken about two years ago. The second (Bit-2) was a bitumen from Suncor.

Samples Bit-3 to Bit-6 were oilsands bitumens from the Cold Lake region. These samples were taken over a period of more than a decade. It may be coincidence, but the free radical content in the Cold Lake bitumen samples appeared correlated with the age of the samples, with older samples having a slightly lower free radical content. In a more recent ongoing investigation a similar observation was made, namely, that there is slight decrease in free radical content of stored samples over time. In one of the samples (Bit-6) there was a tight emulsion of water. The water content by Karl Fischer titration was 9 wt%, but the elemental composition by CHNS analysis indicated that the water content was higher than that.

One sample of bitumen (Bit-6) was also prepared at higher concentration (as indicated in Table 3.2) and analyzed multiple times in different sample tubes to evaluate measurement repeatability and the impact of analysis at higher concentration. Repeatability of measurement of the same sample using different ESR tubes resulted in a relative standard deviation of 4 % compared to the measured value. When different samples were taken from the same bitumen (Bit-6) and analyzed, the relative standard deviation was 15 %. High variability was also found in Bit-1 (13 %) and Bit-2 (21 %), which suggested that the bitumen is not homogeneous in composition. This observation is not just based on the ESR analyses, but also the variability that has been observed in several experimental investigations employing bitumen in our research group.

The g -values for the different bitumen samples were recorded and reported in Table 3.2. The g -value is an average g -value of multiple species and were all in the range 2.0042–2.0057. Apart from the spectroscopic significance of the g -value, the g -value contains information about composition. The g -values for many compounds can be found in literature, e.g.¹⁹ For carbon radicals in multinuclear aromatics, a good correlation was shown between the g -value and the Hückel energy parameter describing the energy of the π orbital of the unpaired electron.²⁰ A correlation between g -value and elemental composition,²¹ and an increase in g -value and heteroatom content,^{10,11} were also proposed. However, according to a different study, the relationship between increase in g -value and heteroatom content appears to be inconclusive.¹²

Since the samples were diluted, no anisotropy based on orientation was anticipated despite the viscous nature of the undiluted samples. Yet, in practice some variation in the recorded g -values for the bitumen samples was found (Table 3.2), with sample standard deviations of the order 0.0010.

3.3.3 Asphaltenes

The asphaltenes were the substances in which the highest free radical concentrations were expected. The free radical content of the eight asphaltenes samples in this study is presented in Table 3.3, and all samples were prepared to be in the concentration range 3–6 wt% in the solvent.

Table 3.3. Free radical content and g -values measured for different asphaltenes samples.^a

Number	Free radical content (spins/g)			g -value		Description
	x	s	n	x	s	
Asph-1	2.1×10^{18}	2.8×10^{17}	4	2.0051	0.0008	Asphaltenes from Nexen Long Lake facility
Asph-2	3.0×10^{18}	2.7×10^{17}	3	2.0033	0.0012	Asphaltenes from Quadrise Corp.
Asph-3	2.4×10^{18}	2.8×10^{17}	2	2.0058	0.0024	C ₅ insoluble, Athabasca bitumen (#1), Suncor
Asph-4	2.4×10^{18}	-	1	2.0051	-	C ₅ insoluble, Athabasca bitumen (#2), Suncor
Asph-5	1.8×10^{18}	-	1	2.0053	-	C ₅ insoluble, Athabasca bitumen (#3), Suncor
Asph-6	1.9×10^{18}	3.4×10^{17}	4	2.0042	0.0002	C ₅ insoluble, Athabasca bitumen (#4), Suncor
Asph-7	2.1×10^{18}	2.5×10^{17}	2	2.0049	0.0003	C ₆ insoluble, Athabasca bitumen (#4), Suncor
Asph-8	1.3×10^{18}	-	1	2.0042	-	C ₅ insolubles in vacuum residue DAO, Nexen

^a Average (x), one sample standard deviation (s), and number of samples (n).

The first two asphaltenes samples in Table 3.3 (Asph-1 and Asph-2) were C₅ insoluble material that was produced by companies. The material from the Nexen Long Lake facility (Asph-1) was produced at large scale from Athabasca bitumen using *n*-pentane precipitation. The density was determined by measurement in toluene at 20 °C and calculated to be 1107 kg/m³. The asphaltenes contained both straight run asphaltenes from the bitumen, as well as asphaltenes from thermal conversion of the bitumen. The value in this study, $(2.1\pm 0.3)\times 10^{18}$ spins/g, compares well with a previous measurement of these asphaltenes, $(2.0\pm 0.1)\times 10^{18}$ spins/g.¹⁵ The material from Quadrise Corporation (Asph-2) was also *n*-pentane precipitated, but the nature of the feed material from Murphy Oil from which these asphaltenes were derived was not indicated. Both samples were at least 4 years old.

The next six asphaltenes samples in Table 3.3 (Asph-3 to Asph-8) were all precipitated from bitumen in our laboratory as part of different studies within the past year.

Different samples from the rigorous *n*-pentane precipitation of asphaltenes (Asph-3 to Asph-7) from Athabasca bitumen from Suncor (Bit-2) provided an indication of the variation when different researchers precipitated asphaltenes at different times from the bitumen of the same origin, but not necessarily the same sample barrel. The difference was of the order 0.5×10^{18} spins/g between the highest value, $(2.4\pm 0.3)\times 10^{18}$, and the lowest value, $(1.9\pm 0.3)\times 10^{18}$. The density of Asph-5 was determined by measurement in toluene at 20 °C and calculated to be 1077 kg/m³. One asphaltene sample was produced from the same bitumen as used for Asph-6, but by rigorous *n*-hexane precipitation (Asph-7). The free radical content in the *n*-hexane insoluble material was slightly higher than the *n*-pentane insoluble material, $(2.1\pm 0.3)\times 10^{18}$ compared to $(1.9\pm 0.3)\times 10^{18}$ spins/g.

The vacuum residue deasphalted oil that remained after asphaltenes (Asph-1) precipitation at the Long Lake facility, still contained some *n*-pentane insoluble material. A rigorous *n*-pentane precipitation of asphaltenes (Asph-8) from the vacuum residue deasphalted oil precipitated *n*-pentane insolubles with a lower free content than present in the asphaltenes (Asph-1) from the same origin, 1.3×10^{18} compared to $(2.1\pm 0.3)\times 10^{18}$ spins/g.

The g -values for the asphaltenes samples were recorded (Table 3.3). For Asph-2, one anomalous low g -value was recorded, and for Asph-3, one anomalous high g -value was recorded. Since there was no rational basis for discarding these measurements, they were retained in the calculated averages, which caused the average g -value of the asphaltenes to have a wide range, 2.0033–2.0058.

3.3.4 Deasphalted oil (DAO)

When the asphaltenes are separated from bitumen, there is a partitioning of free radical species in the bitumen between the asphaltenes and deasphalted oil (maltenes). In the absence of reaction and when the amount of asphaltenes is known, the free radical content of deasphalted oil can be calculated by material balance using the results in Tables 3.2 and 3.3. The n -pentane insoluble content of Athabasca bitumens is around 15–16 wt% and from the results, the free radical content of deasphalted oil from Athabasca bitumen should be of the order $0.7\text{--}0.9 \times 10^{18}$ spins/g.

Five deasphalted oil samples were analyzed (Table 3.4) and all samples for analysis was prepared at a concentration of 3–6 wt%.

The first deasphalted oil (DAO-1) was virgin deasphalted oil prepared at liter-scale from Athabasca bitumen (Bit-1). The free radical content was 9.3×10^{17} spins/g, which was similar to that found for the bitumen (Table 3.2).

The other three deasphalted oil samples (DAO-2 to DAO-4) were vacuum residue deasphalted oil from the Nexen Long Lake site, and included material that was thermally processed. Furthermore, it is only the vacuum residue fraction of the n -pentane soluble material, which makes it a heavier boiling material than DAO-1. The samples were taken at different times about 2 years ago from the same barrel and that were collected using different methods. The vacuum residue deasphalted oil is practically a solid at ambient conditions and samples were removed either by heating to around 80 °C, or by freezing and chipping product from the solid. There was a concern that heating the material to 80 °C, which is the more practical method to obtain larger sub-samples, would result in changes in free radical content. There was a numeric difference between the samples

obtained by heating and freezing, 1.0×10^{18} compared to 9.5×10^{17} spins/g, but considering the variability that was of the order 10^{17} , the difference may not be meaningful.

Table 3.4. Free radical content and *g*-values measured for different deasphalted oil (DAO) samples.^a

Number	Free radical content			<i>g</i> -value		Description
	(spins/g)			x	s	
	x	s	n	x	s	
DAO-1	9.3×10^{17}	2.0×10^{17}	3	2.0046	0.0004	C ₅ solubles in Athabasca bitumen, Nexen
DAO-2	1.0×10^{18}	1.0×10^{17}	6	2.0044	0.0007	Vacuum residue DAO, top of barrel, heated, Nexen
DAO-3	1.0×10^{18}	1.9×10^{17}	3	2.0041	0.0007	Vacuum residue DAO, middle of barrel, heated, Nexen
DAO-4	9.5×10^{17}	8.0×10^{16}	3	2.0050	0.0014	Vacuum residue DAO, middle of barrel, frozen, Nexen
DAO-5	8.6×10^{17}	3.5×10^{16}	3	2.0051	0.0008	C ₅ solubles in vacuum residue DAO, Nexen
DAO-5 ^b	1.8×10^{17}	-	1	2.0041	-	Nexen

^a Average (x), one sample standard deviation (s), and number of samples (n).

^b Sample prepared at 32 wt% concentration for analysis.

It was not clear why a previous investigation²² that employed the same vacuum residue deasphalted oil (DAO-2 to DAO-4) reported a lower free radical content, 1.3×10^{17} , than found in this study. Two noticeable differences in procedure were noted between that investigation²² and the present study: (i) the ESR calibration was performed using TEMPOL, which was shown to be near similar to DPPH (Figure 3.2), and (ii) the samples were prepared at 30 wt% concentration, and not 3–6 wt% as in this study.

The last sample (DAO-5) was the *n*-pentane soluble fraction that was recovered from *n*-pentane precipitation to remove remaining asphaltenes (Asph-8) from the vacuum residue deasphalted oil. Its density was determined by measurement in toluene at 20 °C and was calculated to be 970 kg/m³. As a final test, DAO-5 was analyzed at higher concentration and to our surprise a much lower free radical content was measured (Table 3.4), namely, $(8.6 \pm 0.4) \times 10^{17}$ spins/g at ~5 wt%

concentration, compared to 1.8×10^{17} spins/g at 32 wt% concentration. Although this observation helps to explain the lower free radical concentration previously reported,²² it did not explain why ESR measurement of the bitumen emulsion (Bit-6) in Table 3.2 did not change noticeably when measured at higher concentration. This topic is explored in the discussion (Section 3.4.1).

The *g*-values for the deasphalted oil samples were measured (Table 3.4) and the range of values was 2.0041–2.0050.

3.3.5 Bitumen heavy fractions

Vacuum gas oils and vacuum residue fractions from different facilities were analyzed (Table 3.5). The samples were prepared at 3–6 wt% concentration. Following on the observations about the concentration sensitivity of deasphalted oil seen in Table 3.4, several samples were also prepared and analyzed at higher concentration, as indicated in Table 3.5.

Vacuum residue from Cold Lake bitumen (VR-1) was obtained from Imperial Oil. Vacuum residue (VR-2) and vacuum gas oil (VGO-1) from Athabasca bitumen were obtained from the Syncrude upgrader facility. A flow diagram of the Syncrude upgrader can be found in literature.²³ The density of VGO-1 was measured in toluene at 20 °C and calculated to be 1003 kg/m³. A series of samples of VGO-1 was prepared at higher concentration, 28–42 wt%, and it was found that the measured free radical content was lower (Table 3.5), 8.1×10^{17} compared to 1.4×10^{17} spins/g, like was found with deasphalted oil.

Table 3.5. Free radical content and *g*-values measured for different heavy distillation fractions from bitumen.^a

Number	Free radical content			<i>g</i> -value		Description
	(spins/g)			x	s	
	x	s	n	x	s	
VR-1	1.4×10 ¹⁸	2.9×10 ¹⁷	3	2.0047	0.0015	Cold Lake vacuum residue, Imperial Oil
VR-2	1.4×10 ¹⁸	1.2×10 ¹⁷	3	2.0046	0.0007	Athabasca vacuum residue, Syncrude
VGO-1	8.1×10 ¹⁷	-	1	2.0058	-	Athabasca vacuum gas oil, Syncrude
VGO-1 ^b	1.4×10 ¹⁷	1.8×10 ¹⁶	3	2.0027	0.0022	Athabasca vacuum gas oil, Syncrude
HVGO-1	8.7×10 ¹⁷	7.4×10 ¹⁶	3	2.0043	0.0011	Heavy vacuum gas oil, Nexen Long Lake
HVGO-1 ^c	1.5×10 ¹⁷	-	1	2.0040	-	Heavy vacuum gas oil, Nexen Long Lake
LVGO-1 ^d	7.8×10 ¹⁷	-	1	-	-	Light vacuum gas oil, Nexen Long Lake
LVGO-1 ^e	4.1×10 ¹⁶	-	1	2.0046	-	Light vacuum gas oil, Nexen Long Lake

^a Average (x), one sample standard deviation (s), and number of samples (n).

^b Samples prepared at 28-42 wt% concentration for analysis.

^c Sample prepared at 31 wt% concentration for analysis.

^d Spectrum was very noisy to the extent that it was difficult to obtain an accurate *g*-value.

^e Sample analyzed undiluted, i.e. 100 wt% concentration.

Vacuum residue from Cold Lake bitumen (VR-1) was obtained from Imperial Oil. Vacuum residue (VR-2) and vacuum gas oil (VGO-1) from Athabasca bitumen were obtained from the Syncrude upgrader facility. A flow diagram of the Syncrude upgrader can be found in literature.²³ The density of VGO-1 was measured in toluene at 20 °C and calculated to be 1003 kg/m³. A series of samples of VGO-1 was prepared at higher concentration, 28–42 wt%, and it was found that the measured free radical content was lower (Table 3.5), 8.1×10¹⁷ compared to 1.4×10¹⁷ spins/g, like was found with deasphalted oil.

Heavy vacuum gas oil (HVGO-1) with density of 984.0 kg/m³ at 20 °C and light vacuum gas oil (LVGO-1) with density of 930.4 kg/m³ at 20 °C were obtained from the vacuum distillation unit at the Nexen Long Lake facility. These materials contained both straight run Athabasca bitumen and thermally cracked material. The samples were collected about 5 years ago. When these

samples were analyzed at higher concentration, it was also found that the measured free radical content was lower.

The distilled vacuum residues and vacuum gas oil samples had g -values mostly in the range 2.0043–2.0047 (Table 3.5). One of the measurements of g -value of the VGO-1 sample had an anomalous low value, which accounted for the noticeably lower average g -value of VGO-1.

3.3.6 Upgraded bitumen fractions

A variety of samples of thermally converted and hydroprocessed products produced from bitumen were analyzed (Table 3.6). These samples included lighter fractions that had lower free radical content and to get a clear ESR spectrum had to be analyzed as more concentrated solutions. Considering the observations made based on the results in Tables 3.4 and 3.5, the effect of concentration should not be ignored when interpreting the reported values.

The Syncrude upgrader facility has three fluidized bed coker units. On each coker unit, the fractionator separates the non-coked products from the fluid coker.²³ The heaviest material that may still contain small coke particulates is removed in a scrubber, before it goes to the fractionator. A sample of the coker scrubber (VR-3) was obtained from a coker unit at the Syncrude upgrader. This material had the highest free radical content of the samples from coking, $(1.4 \pm 0.2) \times 10^{18}$ spins/g. A distilled residue fraction (VR-4) was also obtained.

Table 3.6. Free radical content and *g*-values of different thermally converted and hydroprocessed products from bitumen upgrading.^a

Number	Free radical content			<i>g</i> -value		Description
	(spins/g)			x	s	
	x	s	n			
VR-3	1.4×10 ¹⁸	2.2×10 ¹⁷	2	2.0049	0.0003	Coker scrubber bottoms, Syncrude
VR-4	1.1×10 ¹⁸	8.5×10 ¹⁶	3	2.0042	0.0013	Coker residue (distilled), Syncrude
HGO-1 ^b	8.1×10 ¹⁷	7.4×10 ¹⁶	2	-	-	Heavy coker gas oil (#1), 500-550 °C cut point, Syncrude
HGO-1 ^c	2.2×10 ¹⁷	1.1×10 ¹⁶	4	2.0042	0.0003	
HGO-2 ^d	2.2×10 ¹⁷	1.6×10 ¹⁷	3	2.0030	0.0006	Heavy coker gas oil (#2), Syncrude
LGO-1 ^e	3.8×10 ¹⁶	-	1	2.0049	-	Light coker gas oil, 350-400 °C cut point, Syncrude
LGO-2 ^e	3.8×10 ¹⁶	-	1	2.0031	-	Hydrotreated light coker gas oil, Syncrude
LGO-3 ^e	4.8×10 ¹⁶	-	1	2.0049	-	Straight run light gas oil, Syncrude
Naph-1 ^e	none detectable		1	-	-	Thermally cracked naphtha, Nexen

^a Average (x), one sample standard deviation (s), and number of samples (n).

^b Spectrum was very noisy to the extent that it was difficult to obtain an accurate *g*-value.

^c Samples prepared at 20-22 wt% concentration for analysis.

^d Samples prepared at 12-50 wt% concentration for analysis.

^e Sample analyzed undiluted, i.e. 100 wt% concentration.

The heaviest cut from the fractionator after the fluidized bed coker is the heavy coker gas oil, which has a boiling range spanning vacuum gas oil and includes some vacuum residue material. Two different heavy coker gas oils (HGO-1 and HGO-2) were also obtained. The HGO-1 sample came from a Syncrude fluid coker unit and its density was determined by measurement in toluene at 20 °C and calculated to be 1014 kg/m³. The density of HGO-2 sample at 20 °C was 1008 kg/m³. The measured free radical content of HGO-1 was lower when determined in a more concentrated solution, (8.1±0.7)×10¹⁷ spins/g measured at 4–6 wt%, compared to (2.2±0.1)×10¹⁷ spins/g measured at 20–22 wt%. The impact of concentration on the measured free radical content was particularly evident in the heavy gas oil samples (Figure 3.3). It also indicated why the sample standard deviation for measurements with a wider concentration range was higher, e.g. HGO-2 in Table 3.6.

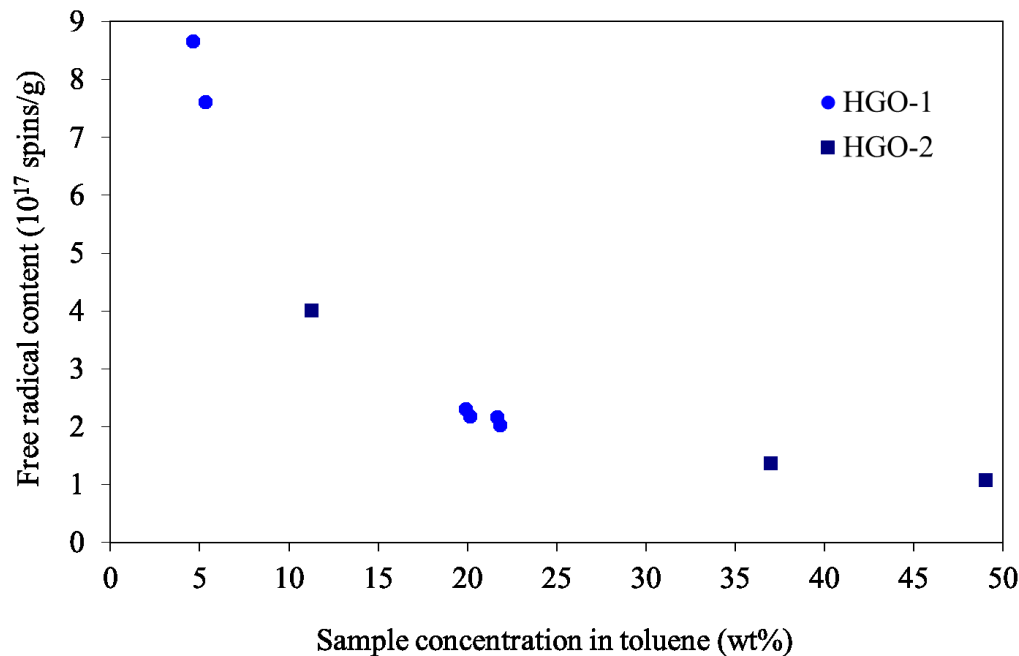


Figure 3.3. Concentration dependence of measured free radical content of heavy gas oil diluted in toluene.

One sample of light coker gas oil (LGO-1) with density at 20 °C of 956.1 kg/m³ was obtained from the Syncrude facility. It was interesting to note that after hydrotreating, the free radical content of this material did not change measurably on a mass basis. The hydrotreated light coker gas oil (LGO-2) originated from unit 18-1 at the Syncrude facility. The density of LGO-2 at 20 °C was 896.3 kg/m³.

The straight run light gas oil (LGO-3), i.e. atmospheric distillate, is a distillate obtained from the Athabasca bitumen feed to the Syncrude facility. The density of LGO-3 at 20 °C was 955.4 kg/m³. The straight run material (LGO-3) had a slightly higher free radical content than the processed materials (LGO-1 and LGO-2), 4.8×10^{16} compared to 3.8×10^{16} spins/g. These values were measured by analysis of undiluted samples. The free radical concentration was low and approached the quantification limit of the spectrometer used, which was around 3×10^{16} spins/g.

The thermally cracked naphtha (Naph-1) was obtained from the Nexen Long Lake facility and it is the product from thermal cracking by visbreaking. The density of the naphtha measured at 20 °C was 743.9 kg/m³. No free radicals were detected using the Active Spectrum Micro-ESR used for all of the work reported. The same sample was also analyzed using an Elexsys E-500 spectrometer, but if free radicals were present, the free radical content was below the detection limit of both spectrometers. This observation corroborated the findings of a previous study with the same material.²⁴

The *g*-values for all of the samples were in the range 2.0030–2.0049 and considering the variability in the measurements, the *g*-value did not appear to change in relation to distillation range of the material that was analyzed.

3.4 Discussion

3.4.1 Dilution and solvent effects

One aspect in the present work that required explanation was the observation that the measured free radical content of the bitumen derived materials changed with solvent dilution. The calibration materials had a linear relationship over a wide free radical concentration range (Figure 3.2). Only the DPPH calibration was employed and it was linear over the free radical concentration range observed in this study. The impact of sample (analyte) concentration on the measured free radical concentration was in some instances observed, with different values for the free radical content of same material being recorded (Figure 3.3).

The origin of the observations did not appear to be related to the analytic procedure. The effect of using toluene or N-methylpyrrolidine as solvent for asphaltenes resulted in no specific analytical bias, even though some difference in dielectric loss of the changed liquid properties on the ESR quality factor was expected. All of the samples after preparation had a low viscosity. Although a change in sample concentration affected liquid properties and thereby the ESR quality factor, and explanation based on a change in liquid properties was inconsistent with the observed halving of

the measured spin concentration when changing the sample concentration from 5 wt% to 11 wt% (Figure 3.3).

The next aspect that was considered, were non-reactive interactions between the solvent and the free radical species. Evidence that the solvent type affected the free radical concentration in Athabasca bitumen and asphaltenes was reported before.²⁵ It was found that when the same material was dissolved in different solvents, the measured free radical content changed. The change in measured spin concentration was correlated with the dipole moment of the solvent. For dilute solutions of asphaltenes (~0.4 wt%) and for dilute solutions of bitumen (7–9 wt%), the measured free radical content decreased as the dipole moment of the solvent increased. For example, when measuring the free radical content of Athabasca asphaltenes in toluene the free radical content was more than four times higher compared to the free radical content measured in dichloromethane, which has a larger dipole moment.

In this study differences were observed between measurement of asphaltenes in N-methylpyrrolidine (dipole moment of 4.1 Debye) and toluene (dipole moment of 0.4 Debye), but no systematic bias was observed, possibly due to the limited number of samples analyzed.

Huyser,²⁶ who classified the solvent interactions into two types, described the effect of solvents on free radicals more generally:

The first type of interaction is the interaction of free radicals with molecules in the bulk liquid. In the case of diluted solutions, solvent molecules constitute most of the bulk liquid. The interaction of solvent molecules with free radicals was expected to dominate free radical interactions in such dilute solutions. These interactions are reversible. Both temperature and the strength of the interaction with the solvent determine the ratio of non-interacting free radicals to interacting free radicals. Interacting free radicals gain additional stability by the interaction with the solvent. In the extreme case, the interacting free radicals are not available to participate in free radical reactions, or the interacting free radicals are less reactive, which affects their reaction selectivity. As temperature increases, or the strength of the interaction with the solvent decreases, the ratio non-interacting free radicals to interacting free radicals increase.

The second type of interaction is the solvation of reactive non-radical species, i.e. species with a weak bond that is subject to homolytic bond dissociation. Solvation of the reactive species can affect its decomposition into free radical products. In the case of dilute solutions, the main solvating species would be the solvent molecules. When the transition state that leads to decomposition of the reactive species requires desolvation of the solvated species, then the enthalpy and the entropy change associated with transition state formation are increased. These two changes largely counter-balance each other and the overall impact of the solvent on the rate of decomposition is not as large as suggested by the enthalpic and entropic contributions viewed in isolation. However, this type of interaction is relevant to labile free radical dimers, as will be explained later on.

There was no indication that these solvent effects would increase or reduce the free radical concentration in the absence of reaction. Both types of solvent interaction affected free radical reactions, but not the free radical concentration in the absence of reaction. There was consequently a reactive process involved that was affected both by the type of solvent,²⁵ as well as the amount of solvent (Figure 3.3).

The properties of the bulk liquid have an impact on the “equilibrium” between species in the free radical state and their association as a dimer.²⁷ For the sake of explanation, this is illustrated by the dimerization of the triphenylmethane radical (Figure 3.4). The forward reaction takes place at rate k_1 and the backward reaction takes place at rate k_{-1} . The ratio of the forward and backward reactions, $K_{\text{eff}} = (k_1/k_{-1})$, determines the steady state concentration of the free radical species relative to the dimerization product.²⁷

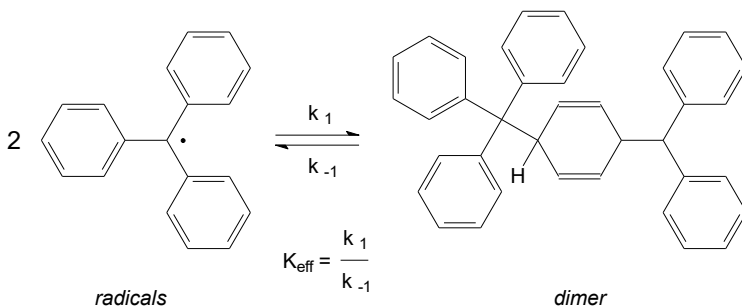


Figure 3.4. Free radical dimerization “equilibrium” illustrated by the triphenylmethane radical.

In the case of bitumen, it is better to consider the dimerization reaction in Figure 3.4 as the radical combination of a radical pair of dissimilar radical species, or potentially even a biradical species where the “dimerization” reaction is an intramolecular coupling reaction.

In addition to temperature, there are several factors that play a role in determining the value of K_{eff} . The bulk liquid, or solvent in the case of dilute solutions, affects the value of K_{eff} in the following ways, which are described in terms of solvents and a free radical pair:²⁷

(a) The solvent determines the effectiveness of free radical solvation, which affects the stability of the free radical in the solvent. Applying the concept of interacting and non-interacting radicals, the reactive radicals are only those radicals that are non-interacting. Radical–solvent interaction thereby reduces the effective concentration of free radicals that can participate in dimerization, without directly reducing the amount of free radicals. Indirectly this affects K_{eff} , because it decreases the rate of the forward reaction (k_1), because the radical must first be desolvated before it can dimerize.

(b) When the solvent is able to stabilize the transition state of free radical formation, it increases the rate of the reverse decomposition reaction (k_{-1}). For example, in the case where the transition state involves partial separation of charge, polar solvents may assist in stabilizing the transition state for free radical formation. Stabilization of the transition state by other means not related to solvent polarity is also possible.

(c) The solvent may interact with species to promote homolytic bond dissociation, i.e. molecule-induced homolysis. In these cases, the solvent interaction promotes the reaction without itself being converted during the reaction. Molecule-induced homolysis is manifested as an apparent increase in the reverse reaction (k_{-1}) to increase the free radical concentration.

(d) The solvent also provides a solvent “cage”, which can affect recombination. When the escape of the radical pair from the solvent cage is slow, the probability of radical recombination is increased. In viscous solvents, or solvents where the solvent species are strongly interacting with each other, the rate of diffusion is slower compared to less viscous and less interacting solvents. Consequently, when the rate of diffusion is decreased, the radical pair may not escape the solvent cage, which increases the probability of the forward reaction (k_1). The overall impact of solvent caging is to decrease the observed free radical concentration.

(e) The solvent can also influence the change in volume that is required for free radical formation. When the change in volume is less, it would favor the reverse reaction (k_{-1}). The volume of activation for the transition state for the reaction is given by the Evans–Polanyi relationship (Equation 4), where ΔV^\ddagger is the molar volume change required in the specific solvent to form the transition state, P is pressure, T is temperature, and R is the universal gas constant.

$$\Delta V^\ddagger = -R \cdot T \cdot (\partial \ln k_{-1} / \partial P)_T \quad (4)$$

When these solvent effects are applied to the results of the ESR analysis, we can say that dilution with toluene decreases K_{eff} and thereby increases the steady state concentration of free radical pairs in the bitumen and derived materials. The exact manner in which dilution in toluene affected K_{eff} is a matter of speculation, since this study was not designed to probe the nature of the solvent interaction.

3.4.2 Concentration of free radicals in oilsands bitumen fractions

The present study highlighted the impact of the bulk liquid properties on the measured free radical content in bitumen and bitumen derived fractions. When comparing the relative abundance of free

radicals in different fractions, the comparison should therefore be at the same analyte concentration. For the purpose of comparing relative abundance of free radicals the comparison was made at an analyte concentration of 3–6 wt% (Figure 3.5).

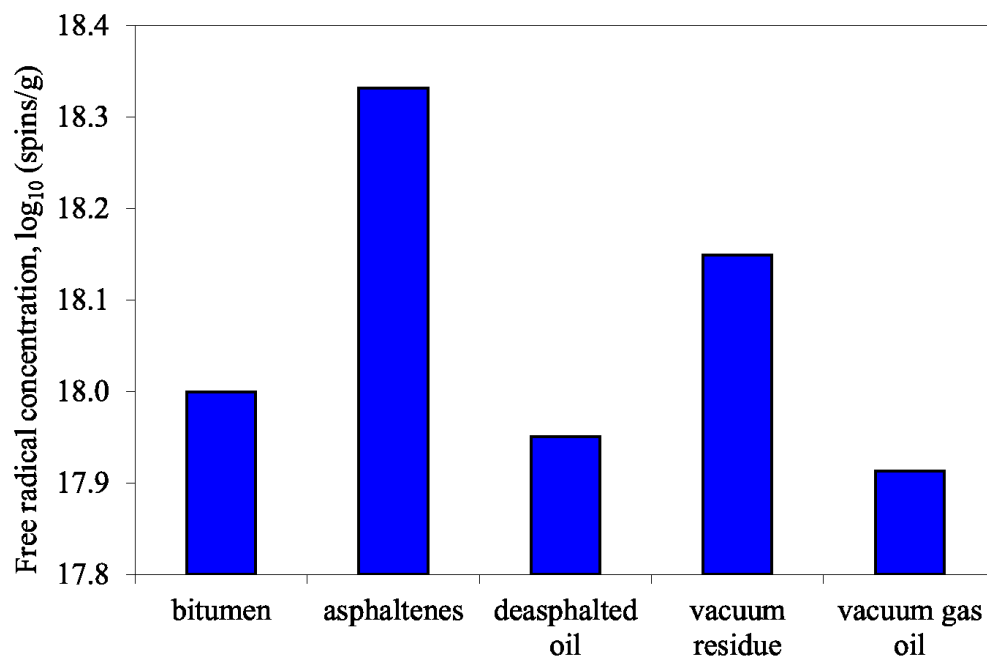


Figure 3.5. Relative abundance of free radicals in bitumen and bitumen derived fractions at an analyte concentration of 3–6 wt%.

The average values for asphaltenes (*n*-pentane insoluble material) and deasphalted oil (*n*-pentane soluble material) were based on laboratory separations and did not include industrially separated material. The vacuum gas oil was the average of full range vacuum gas oil, heavy vacuum gas oil and light vacuum gas oil. Lighter boiling materials were omitted from Figure 3.5, because the free radical content was measured at higher analyte concentration.

The relative comparison (Figure 3.5) indicated that the relative abundance of free radicals were higher in the heaviest products, asphaltenes and vacuum residue. All of the values measured at 3–6 wt% analyte concentration were of the order 10^{18} spins/g analyte.

Differences in the free radical content of bitumen samples based on their age (time period that elapsed since their collection) were measurable, but were minor (Table 3.2). With age, the free

radical content in the bitumen appeared to decrease. For example, in a one year old sample of Cold Lake bitumen (Bit-5) the free radical concentration was 1.1×10^{18} spins/g and in a ten year old sample of Cold Lake bitumen (Bit-3) the free radical concentration was 0.9×10^{18} spins/g. Differences within the same sample and the method of retrieval (Table 3.4, compare DAO-2, DAO-3 and DAO-4) resulted in near similar measured spin concentrations.

The free radical content of bitumen and bitumen derived materials reported in this study was compared with values in literature, as described below.

Values for the free radical content in petroleum derived asphaltene were reported by Yen, et al.^{3,4} and were of the order 10^{18} – 10^{19} spins/g. Their work included two values for Athabasca asphaltene, 5.5 – 5.6×10^{18} . The Athabasca asphaltene spin concentrations came from work performed by Erdman and Dickie that was not published, but was related to a preprint²⁸ that indicated the asphaltene was *n*-pentane insoluble material. ESR analysis was performed without dilution at room temperature and spin concentration was quantified relative to single value for a DPPH solution. The present work (Table 3.3) found the asphaltene to have a lower free radical concentration than reported by Yen, et al.^{3,4} and the difference in reported asphaltene free radical content is even larger if the difference in analyte concentration for measurement is taken into account. Quantification of free radical content depends on the calculation of the double integral value. Considering when the original measurements by Yen, et al.^{3,4} were made, it is speculated that in addition to calibration, calculation of the double integral from the derivative ESR spectrum may explain some of the difference.

The value of 1.3×10^{18} spins/g reported by Niizuma, et al.⁵ for Athabasca asphaltene were close to what was found in the present study (Table 3.3). It appears that they recorded the ESR spectrum of the asphaltene without dilution, although this was not explicitly stated.

Niizuma, et al.⁵ also investigated the temperature dependence of the ESR measurement on the free radical concentration. Measured free radical concentration decreased as measurement temperature was decreased. The explanation that was forwarded for the temperature dependence over the temperature range -200 to $+50$ °C was related to the presence of “close lying singlet and triplet

state biradicals ... in addition to doublet monoradicals". This followed from the explanation by Yen and Young,²⁹ who observed analogous behavior for petroleum samples in the same temperature range. Although temperature effects were not studied in this work, it is relevant to the more general discussion and in particular the observation that at least some of the free radicals are diradicals.

The values for Athabasca and Cold Lake asphaltenes and deasphalted oils that were reported by Schultz and Selucky,⁷ were generally lower than reported in Tables 3.3 and 3.4. Viscous samples were prepared by adding a few drops of dichloromethane, but were otherwise undiluted. The spin concentration for Athabasca *n*-pentane insoluble asphaltenes was 6.0×10^{17} spins/g and for Cold Lake asphaltenes it was 9.2×10^{17} spins/g. The deasphalted oil fraction obtained from Cold Lake bitumen had a spin concentration of 2.9×10^{16} spins/g. The lower spin concentrations reported by Schultz and Selucky⁷ is understandable in the context of the observation that lower spin concentration is observed for more concentrated analytes, as shown in Figure 3.3.

The variance in reported values for the persistent free radical content of oilsands bitumen fractions appears to be related partly to differences in the concentration at which the measurements were performed. Although a plausible explanation for this could be provided (Section 3.4.1), the spin concentrations in oilsands bitumen fractions with fully dissociated free radical species are still not known.

3.4.3 Implications for bitumen upgrading

Thermal conversion technologies employed to upgrade bitumen, such as visbreaking and coking, rely on free radical cracking to convert heavier to lighter products. Free radical cracking is usually explained in terms of initiation, propagation, and cracking reactions, where propagation is considered the most important for determining the rate of thermal conversion of bitumen.³⁰

There are several potential propagation reactions, hydrogen transfer, free radical cracking, and free radical addition. From a thermal conversion perspective, free radical cracking is the most valuable,

because it leads to a decrease in the average molecular mass of the product. Free radical cracking is a monomolecular propagation reaction.

To increase the selectivity of free radical cracking over either propagation or termination by free radical addition, the free radical and olefin content must be kept low to reduce the probability of such bimolecular reactions taking place. Pertinent to the present investigation are reactions involving propagation by free radical addition to a diradical (Equation 3.5) and termination by free radical addition of two monoradicals (Equation 3.6).



In these equations R and R' represent any organic structure, including heteroatom containing organic structures.

Temperature dependent ESR studies reported in literature,^{5,29} interpreted their results to indicate that both monoradical and diradicals were present in bitumen. The presence of diradicals implies that propagation by free radical addition (Equation 3.5) may be an important reaction during thermal conversion of bitumen.

One way of manipulating the free radical concentration is through temperature. The present study showed it might also be possible to manipulate the free radical concentration through the properties of the bulk liquid. When the bulk liquid is considered as a solvent for the free radical species, changes in the bulk liquid properties can be used to manipulate the free radical concentration independent of temperature. It does not matter whether the bulk liquid properties are changed by reaction, by co-feeding other material, or by both — the concentration and the reactive availability of free radical species will be affected.

Another implication of the impact of bulk liquid composition is that it might be worthwhile revisiting the interpretation of thermal conversion data in the published literature. For example, coke yield was reduced when bitumen was thermally converted at 400 °C in the presence of 10

wt% naphthalene.³¹ Such results could potentially be explained by changes in the available reactive free radical concentration as consequence of the changed bulk liquid properties.

3.5 Conclusions

New quantitative measurements of the persistent free radical concentration in oilsands bitumen and bitumen derived materials were provided. The results confirmed published observations that showed free radical concentrations in the range 10^{17} – 10^{18} spins/g, with the highest free radical concentrations found in the heaviest fractions, which included the asphaltenes solubility class. It was found that the light fractions had free radical concentrations in the range 10^{16} – 10^{17} spins/g. The results of the study also contributed observations about the influence of the bulk liquid on the free radical concentration in oilsands bitumen fractions.

The isothermal measurement of free radical concentration in bitumen fractions was affected by the analyte concentration even after compensating for effects that affected the ESR spectroscopy. This could be explained with reference to literature by the impact that the bulk liquid properties have on the “equilibrium” composition between free radical pairs and their corresponding non-radical dimeric product. Reported free radical concentrations in bitumen fractions must consequently be interpreted by taking into consideration that the measurement is affected by the nature of the bulk liquid within which the analysis was performed.

Practically, the results in this study also have implications for bitumen upgrading by thermal conversion processes. The free radical concentration and availability of reactive free radicals are not only affected by temperature, but also by the bulk liquid properties. It should therefore be possible to manipulate selectivity during thermal conversion independent of temperature by manipulating the bulk liquid properties.

Literature cited

- (1) Strausz, O. P.; Lown, E. M. *The Chemistry of Alberta Oil Sands, Bitumens and Heavy Oils*; Alberta Energy Research Institute: Calgary, Alberta, Canada, 2003.
- (2) Zhou, B.; Liu, Q.; Shi, L.; Liu, Z. Electron Spin Resonance Studies of Coals and Coal Conversion Processes: A Review. *Fuel Process. Technol.* **2019**, *188* (March), 212–227.
- (3) Yen, T. F.; Erdman, J. G.; Saraceno, A. J. Investigation of the Nature of Free Radicals in Petroleum Asphaltenes and Related Substances by Electron Spin Resonance. *Anal. Chem.* **1962**, *34* (6), 694–700.
- (4) Yen, T. F.; Sprang, S. R. ESR G-Values of Bituminous Materials. *Prepr. Pap.-Am. Chem. Soc., Div. Pet. Chem.* **1970**, *15* (2), A65–A76.
- (5) Niizuma, S.; Steele, C. T.; Gunning, H. E.; Strausz, O. P. Electron Spin Resonance Study of Free Radicals in Athabasca Asphaltene. **1977**, *56*, 249–256.
- (6) Chang, H.-L.; Wong, G. K.; Lin, J.-R.; Yen, T. F. Electron Spin Resonance Study of Bituminous Substances and Asphaltenes. In *Asphaltenes and asphalts. Vol. 2*; Yen, T. F., Chilingarian, G. V., Eds.; Elsevier: Amsterdam, 2000; pp 229–280.
- (7) Schultz, K. F.; Selucky, M. L. ESR Measurements on Asphaltene and Resin Fractions from Various Separation Methods. *Fuel* **1981**, *60* (10), 951–956.
- (8) Trukhan, S. N.; Yudanov, V. F.; Gabrienko, A. A.; Subramani, V.; Kazarian, S. G.; Martyanov, O. N. In Situ Electron Spin Resonance Study of Molecular Dynamics of Asphaltenes at Elevated Temperature and Pressure. *Energy and Fuels* **2014**, *28* (10), 6315–6321.
- (9) Trukhan, S. N.; Kazarian, S. G.; Martyanov, O. N. Electron Spin Resonance of Slowly Rotating Vanadyls-Effective Tool to Quantify the Sizes of Asphaltenes in Situ. *Energy and Fuels* **2017**, *31* (1), 387–394.
- (10) Eloffson, R. M.; Schulz, K. F.; Hitchon, B. Geochemical Significance of Chemical Composition and ESR Properties of Asphaltenes in Crude Oils from Alberta, Canada. *Geochim. Cosmochim. Acta* **1977**, *41* (5), 567–580.
- (11) Yen, T. F.; Sprang, S. R. Contribution of E.S.R. Analysis toward Diagenic Mechanisms in Bituminous Deposits. *Geochim. Cosmochim. Acta* **1977**, *41* (8), 1007–1018.
- (12) Malhotra, V. M.; Buckmaster, H. A. 9 and 34 GHz EPR Study of the Free Radicals in Various Asphaltenes: Statistical Correlation of the g-Values with Heteroatom Content. *Org.*

- Geochem.* **1985**, 8 (4), 235–239.
- (13) Petrakis, L.; Grandy, D. W. An Electron Spin Resonance Spectrometric Investigation of Natural, Extracted and Thermally Altered Kerogenous Materials. *Geochim. Cosmochim. Acta* **1980**, 44 (5), 763–768.
- (14) Khulbe, K. C.; Mann, R. S.; Lamarche, G.; Lamarche, A.-M. Electron Spin Resonance Study of the Thermal Decomposition of Solvent Extracted Athabasca Tar Sand Bitumen. *Fuel Process. Technol.* **1992**, 31 (2), 91–103.
- (15) Payan, F.; De Klerk, A. Hydrogen Transfer in Asphaltenes and Bitumen at 250 °C. *Energy and Fuels* **2018**, 32 (9), 9340–9348.
- (16) Eaton, G. R.; Eaton, S. S.; Barr, D. P.; Weber, R. T. *Quantitative EPR*; Springer, 2010.
- (17) Adams, J. Q.; Altgelt, K. H.; LeTourneau, R. L.; Lindeman, L. P. Free Radical Concentrations in Gel Permeation Fractions of Asphaltenes from Different Crude Oils. *Prepr. Pap.-Am. Chem. Soc., Div. Pet. Chem* **1966**, 12, B140–B144.
- (18) Meyer, V.; Eaton, S. S.; Eaton, G. R. X-Band Electron Spin Relaxation Times for Four Aromatic Radicals in Fluid Solution and Comparison with Other Organic Radicals. *Appl. Magn. Reson.* **2014**, 45 (10), 993–1007.
- (19) Bielski, B. H. J.; Gebicki, J. M. Atlas of Electronspin Resonance Spectra. Academic Press: New York, 1967.
- (20) Gordy, W. *Theory and Applications of Electron Spin Resonance (Vol. 15)*; Wiley-Interscience: New York, 1980.
- (21) Retcofsky, H. L. Magnetic Resonance Studies of Coal. In *Coal Science Vol.1*; Gorbaty, M. L., Larsen, J. W., Wender, I., Eds.; Academic Press: New York, 1982; pp 43–82.
- (22) Castillo, J.; De Klerk, A. Visbreaking of Deasphalted Oil from Bitumen at 280–400 °C. *Energy and Fuels* **2019**, 33 (1), 159–175.
- (23) Gray, M. R. *Upgrading Oilsands Bitumen and Heavy Oil*; University of Alberta Press: Edmonton, AB, 2015.
- (24) Uzcátegui, G.; Fong, S. Y.; De Klerk, A. Cracked Naphtha Reactivity: Effect of Free Radical Reactions. *Energy and Fuels* **2018**, 32 (5), 5812–5823.
- (25) Khulbe, K. C.; Mann, R. S.; Lu, B. C. Y.; Lamarche, G.; Lamarche, A. M. Effects of Solvents on Free Radicals of Bitumen and Asphaltenes. *Fuel Process. Technol.* **1992**, 32 (3), 133–141.

- (26) Huyser, E. S. Solvent Effects in Free-Radical Reactions. In *Advances in free-radical chemistry. Vol. 1*; Williams, G. H., Ed.; Academic Press: London, 1965; pp 77–135.
- (27) Martin, J. C. Solvation and Association. In *Free radicals Vol.2*; Kochi, J. K., Ed.; John Wiley & Sons, 1973; pp 493–526.
- (28) Erdman, J. G.; Dickie, J. P. Mild Thermal Alteration of Asphaltic Crude Oils. *Prepr. Pap.-Am. Chem. Soc., Div. Pet. Chem.* **1964**, *9*, B69–B79.
- (29) Ten, T. F.; Young, D. K. Spin Excitations of Bitumens. *Carbon N. Y.* **1973**, *11*, 33–41.
- (30) Gray, M. R.; McCaffrey, W. C. Role of Chain Reactions and Olefin Formation in Cracking, Hydroconversion, and Coking of Petroleum and Bitumen Fractions. *Energy and Fuels* **2002**, *16* (3), 756–766.
- (31) Zachariah, A.; Wang, L.; Yang, S.; Prasad, V.; De Klerk, A. Suppression of Coke Formation during Bitumen Pyrolysis. *Energy and Fuels* **2013**, *27* (6), 3061–3070.

Chapter 4: Reaction of 5-membered ring naphtheno-aromatics at thermal cracking conditions

Abstract

When new asphaltenes are formed from deasphalted oil, it erodes the conversion advantage provided by solvent deasphalting prior to visbreaking. Naphtheno-aromatics were suspected to be the compounds responsible for heavy products formation. Five-membered ring naphtheno-aromatics were proved to be susceptible to addition reactions in low temperature autoxidation (oxidation with air). The reactivity of indan, indene, thianaphthene, indole and benzofuran was tested at thermal cracking conditions of 400 °C and 2 MPa under nitrogen environment. Indan and thianaphthene were shown to be unreactive when self-reacted under the operating conditions and in the absence of metals. In the presence of indene as a hydrogen donor, indan and thianaphthene rings were opened, and addition reactions took place. When reacted with indene, sulfur-ring opening of thianaphthene to 2-methylbenzenethiol and 2-ethylbenzenethiol is possible with a 27% decrease in the amount of thianaphthene between reactants and products. The reaction of indan and thianaphthene formed addition products and indan ring opening products. However, the percentage decrease of indan and thianaphthene between reactants and products was low (7 wt% and 3 wt% respectively). Free radical ring opening and addition reactions are products of self-reactions of indene and benzofuran. The ring opening in indole molecule did not take place at the experimental conditions in this study but polymerization occurred without any detectable free radicals in the products.

Keywords: 5-membered ring naphtheno aromatics, pyrolysis, free radical addition, sulfur ring-opening.

4.1 Introduction

The formation of heavy products by free radical mechanisms has been previously used for polymerization processes to manufacture chemical surfactants, adhesives, lubricants as well as plastics such as polyethylene and polystyrene.

In non-catalytic cracking of heavy residues, a series of reactions takes place following a free radical mechanism. In oil refineries, thermal conversions are used for cracking purposes. However, the free radical mechanism induces both cracking and addition reactions. While the former is desirable, the latter is ultimately forming aggregates that are precursors for asphaltenes and coke formation.

In bitumen free radical reactions it was postulated that naphthenic-aromatic classes contribute to addition reactions.¹ It was also shown that indene produces a large amount of indan and that the amount of indan decreases with the reaction time while the percentage of *n*-pentane insoluble compounds increases. This indicated that indan is capable of free radical addition reactions that lead to asphaltenes formation. Siddiquee et al.² stated that five-membered ring compounds are more prone to autoxidize at low temperature. Their study was done on low temperature oxidation of air that also involves a free radical chemistry. In autoxidation, the free radical addition reactions were the primary cause of the increased viscosity of oxidized bitumen. Based on their study, five-membered rings naphtheno-aromatics (e.g. indene and indan) had the highest ability to undergo free radical addition reactions. The susceptibility for oxidation addition reactions for heterocyclic pyrrolic rings was the highest for indole followed by benzofuran and thianaphthene. On the other hand, six membered rings naphtheno-aromatic compounds (e.g. quinoline) were stable and did not have a tendency to autoxidize.

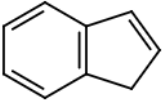
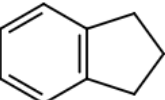
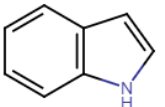
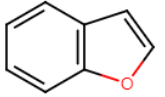
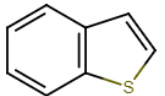
It was thus of interest to investigate the behaviour of these model compounds (i.e. indene, indan, thianaphthene, benzofuran and indole) at thermal cracking conditions. In this study, the aim is to test the reactivity and behaviour of 5-membered ring naphtheno-aromatics in an oxygen-free, catalyst-free and hydrogen-free environment.

4.2 Experimental

4.2.1 Materials

The model compounds used in the batch reactor are summarized in Table 4.1. The purity of the indene was determined by gas chromatography with flame ionization detector and it was found to be 97.71 ± 0.05 % based on total response area without response factor correction (average \pm standard deviation of six analyses).

Table 4.1. Model compounds purities.

Compound Name	2-D chemical structure	CASRN ^a	Purity (%) ^b	Supplier
Indene		95-13-6	≥ 90	Sigma-Aldrich
Indan		496-11-7	95	Sigma-Aldrich
Indole		120-72-9	99	Sigma-Aldrich
Benzofuran		271-89-6	99	Sigma-Aldrich
Thianaphthene		95-15-8	95	Sigma-Aldrich

^a CASRN = Chemical Abstracts Services Registry Number

^b This is the purity of the material guaranteed by the supplier; material was not further purified

The chemicals used for spiking the product for peak identification in GC-MS are listed in Table 4.2.

Table 4.2. Compounds used for peak identification in GC-MS.

Compound Name	Purity (%) ^a	Supplier
Phenol	>99.5	Sigma Aldrich
2-ethylphenol	99	Sigma Aldrich
2,3-Dihydro-1-benzofuran	99	Sigma Aldrich
2-methylbenzenethiol	95	Sigma Aldrich
3-methylbenzenethiol	95	Sigma Aldrich
2-ethylbenzenethiol	>95	Fisher Scientific

^aThis is the purity of the material guaranteed by the supplier; material was not further purified

Toluene (99.9%, Fisher Scientific) and *n*-pentane (99.4%, Fisher Scientific) were used as solvents for the chromatographic analyses. Toluene was also used as the solvent for all Electron Spin Resonance (ESR) analyses. Calibration for electron spin resonance spectrometry was performed with 2,2-diphenyl-1-picrylhydrazyl (~90%, Sigma-Aldrich). The pentane insoluble analysis used *n*-pentane (99.4%, Fisher Scientific) as the solvent. Carbon disulfide (99.99%, Fisher Scientific) was used as the solvent for analyses by simulated distillation (SimDist). Nitrogen (99.999 mol%) used for pressurizing the batch reactors was purchased from Praxair as cylinder gas. Chloroform-D (99.8%, Acros Organics) was used as the solvent for the proton nuclear magnetic resonance measurements.

4.2.2 Equipment and procedure

Thermal cracking reactions of the model compounds were carried out in a batch micro-reactor built with 316 stainless steel Swagelok fittings. Reactions were performed at 400 °C and 2 MPa under nitrogen environment. The self-reactions of 5-membered ring naphtheno-aromatics (i.e. indene, indan, thianaphthene, benzofuran and indole) were conducted at 30 minutes and 60 minutes. The reactions of mixtures of naphtheno aromatics (Table 4.3) were conducted at a reaction time of 60 minutes. All reactions were run using a glass vial inside the reactor to avoid interaction with the reactor walls. Table 4.3 shows the proportions of each reactant in the mixtures.

Table 4.3. Concentration of model compounds in mixtures.

Sample name	Mass of indene (g)	Mass of indan (g)	Mass of thianaphthene (g)
Indene+indan	2.542±0.001	2.553±0.001	-
Indene+thianaphthene	2.515±0.001	-	2.504±0.001
Indan+thianaphthene	-	2.503±0.001	2.523±0.001

4.2.3 Analyses

The gases present in the gaseous reaction product were determined using an Agilent 7890A gas chromatograph with a flame ionization detector for detection of hydrocarbons and a thermal conductivity detector for other gases. In the former, separation was performed using a molecular sieve 13X 45/60 column (10 ft × 1/8 in). In the latter, separation was performed in a HayeSep R 80/100 column (10 ft × 1/8 in). Identification was based on retention time. The oven temperature was initially at 70 °C and was held constant for 7 minutes, then it was increased at a rate of 10 °C/min to 250 °C and it stayed there for 2 minutes before cooling down to 70 °C at a rate of 30 °C/min. It was kept at 70 °C for 8 minutes.

The *n*-pentane insoluble content was determined by mixing 2 g of reaction product with 80 mL of *n*-pentane. The mixture was stirred in a closed jar at room temperature for 1 hour and left to settle for 23 hours before filtration. Filtration was done using 0.22 µm filter papers. The collected *n*-pentane insoluble precipitates were dried overnight in a fume hood until achieving a constant mass that was employed as a measure of complete drying. The mass of the dried *n*-pentane insoluble material was recorded. The percentage of *n*-pentane insoluble material per gram sample was calculated. Both the *n*-pentane insoluble and *n*-pentane soluble fractions were further analyzed.

The free radical content in the products was measured using an Active Spectrum Micro-ESR. For analysis, 20 mg of the sample was diluted in 600 µL toluene and measured at 1.2 Gauss coil amplitude, a digital gain of 12 dB, and a microwave power of 15 mW. The analyses were the average of 7 scans with a sweep delay of 30 seconds. The quantification of the free radical content

into number of spins per grams of sample was possible by the double integration of the ESR peak using a calibration curve of toluene in 2,2-diphenyl-1-picrylhydrazyl (DPPH). The double integration was done using the MicroESR software.

Proton nuclear magnetic resonance spectra were obtained by dissolving 100-150 mg of the benzofuran self-reaction product in 700 μL of chloroform-D. The analysis was performed using a 60 MHz NMReady-60 spectrometer from Nanalysis Corporation. Analyses were the average of 32 scans with a scan delay of 20 seconds. The results were analyzed using MestReNova software to determine whether the alcoholic functional group was detectable or not.

Fourier Transform infra-red spectroscopy (FTIR ABB MB 3000) was used to identify the alcoholic functional group. Spectroscopes were collected for samples in the wavenumber range of 400-4000 cm^{-1} obtained at a resolution of 4 and detector gain of 243.

A Carl Zeiss StereoMicroscope Discovery V20 was used to magnify images of products that underwent visible changes in their appearance and structures.

All products obtained from the self-reaction of model compounds were analysed using Simulated distillation. Only the *n*-pentane soluble fraction of the product of the mixtures of model compounds (Table 4.3) were analysed using this technique. The analyses used for all samples were performed using an Agilent 7890B high temperature gas chromatograph with a flame ionization detector and DB-HT-SIMDIS column (5 m \times 0.53 mm \times 0.15 μm). The injection volume was 0.5 μL using helium as the carrier gas. Sample preparation involved dissolving 100 mg of the reaction product in about 12 g of CS_2 ; the exact mass of the reaction product and CS_2 was measured and recorded at 0.1 mg readability. The temperature program started at 50 $^\circ\text{C}$ and temperature was increased at a rate of 15 $^\circ\text{C}/\text{min}$ to 425 $^\circ\text{C}$ at which temperature it was held constant for 10 minutes.

Gas chromatography coupled with mass spectroscopy was used to identify the compound classes present in reaction products. The apparatus used was an Agilent 7820A coupled with 5977E mass spectrometer. Separation was performed on a HP-5 column (30 m \times 0.25 mm \times 0.25 μm) using helium as the carrier gas at a constant flow rate of 1 mL/min.

The temperature program used for the self-reaction of model compounds (i.e. indene, indan, thianaphthene, benzofuran, indole) in addition to the indene-indan mixture, started at 100 °C then the temperature was increased by 10 °C/min up to 320 °C, then held for 13 min. The injector is split/splitless and the split ratio is 100:1 with an injection volume of 1 µL.

The temperature program used for the reaction of the other mixtures of model compounds (i.e. indene and thianaphthene, indan and thianaphthene) products started at 80 °C, with a hold time of 5 min, after which the temperature was increased by 5 °C/min up to 200 °C, then held for 2 min at 200 °C, and then increased again at a rate of 5 °C/min until 320°C. The injector is split/splitless and the split ratio is 100:1 with an injection volume of 1 µL.

Gas chromatography employed for quantification of indan and thianaphthene in the reaction products uses an Agilent 7890A chromatograph and separation occurs in a HP-PONA column (50m x 0.2 mm x 0.5 µm). The temperature program starts at 80 °C, with a hold of time of 5 min, after which the temperature is increased by 5 °C/min up to 320 °C and then is held for 2 minutes. The injector is split/splitless and the split ratio is 100:1 with an injection volume of 0.2 µL. Calibration curves for both indan and thianaphthene were created.

4.3 Results

4.3.1 Self-reaction of model compounds at thermal cracking conditions

4.3.1.1 Physical observations and *n*-pentane insoluble content of the products

The amount of asphaltenes and coke (referred to as *n*-pentane insolubles) were recorded for the products of the self-reaction of model compounds at different reaction times and are shown in Table 4.4.

Table 4.4. *n*-Pentane insolubles for the product of the self-reaction of model compounds.

Model compound name	Reaction time (min)	Solubility of raw model compound in <i>n</i> -pentane	% <i>n</i> -pentane insoluble in products
Indene	30	Soluble	35
	60		72
Indan	30	Soluble	0
	60		0
Thianaphthene	30	Soluble	0
	60		0
Indole	30	Insoluble	100
	60		100
Benzofuran	30	Insoluble	100
	60		100

The self-reaction of indene is leading to high amounts of asphaltenes and coke. These values differ from the values reported in Chapter 5, which were even higher. In the study in Chapter 5,³ indene was in contact with the walls of the reactor. The amount of asphaltenes and coke decreased when a glass vial was used inside the reactor (i.e. when there was no contact of the indene with the reactor walls). Reactor walls are playing a role in the chemistry, or the higher surface temperature is causing an increase in the rate of this reaction. A generic analysis of stainless steel 316 material obtained from Sandvik Materials Technology is shown in Table 4.5.

The product of indene as shown in the Zeiss microscope is presented in Figure 4.1(a) at a 1000 μm scale. The physical appearance of the product is in accordance with the high asphaltenes and coke content.

The products of the self-reaction of indan and the self-reaction of thianaphthene did not show any physical changes. Table 4.4 shows that these products did not produce any asphaltenes or coke. Indole and benzofuran, which are initially not soluble in *n*-pentane, have formed products with

noticeable physical changes as shown in Figure 4.1 (b) and (c). Both products were not soluble in *n*-pentane.

Table 4.5. Composition of the reactor walls.

Compound Name	Composition (%)
Iron	64
Chromium	17
Nickel	13
Molybdenum	3
Manganese	2
Silica	0.4
Copper	0.3
Phosphorous, Carbon, Sulfur, Aluminum	0.3



Figure 4.1. Pictures captured by Zeiss microscope for products of thermally cracked (a) indene, (b) indole and (c) benzofuran.

4.3.1.2 Chemical structure identification by GC-MS

The GC-MS was used to identify the chemical structure of the products of the self-reaction of the model compounds.

Since indene has formed a large amount of asphaltenes and coke (*n*-pentane insoluble material), part of the product (i.e. coke) was not totally soluble in toluene, the solvent used for analysis in

the GC-MS. Therefore, only the *n*-pentane soluble fraction of the product of this reaction was analyzed using gas chromatography. The chromatogram of both 30 minutes and 60 minutes reaction time look the same. The chromatogram of the 60 minutes reaction time is shown in Figure 4.2. Numbering of peaks were done in such a way that peak numbers were consistent for the self-reaction of indene and benzofuran.

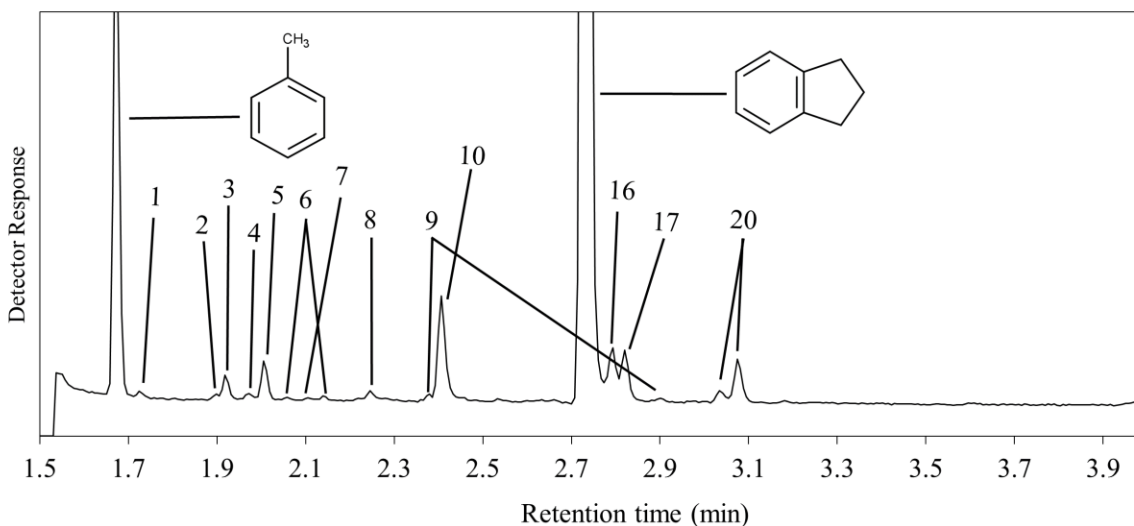
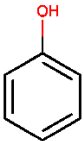
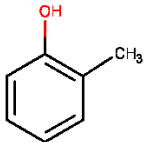
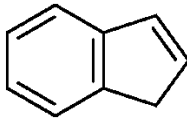
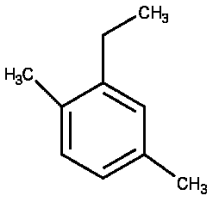
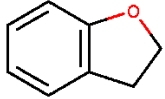
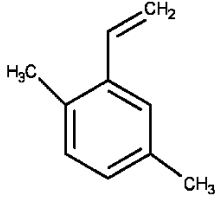
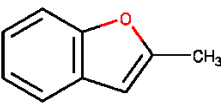
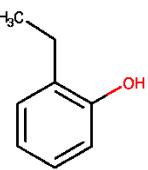
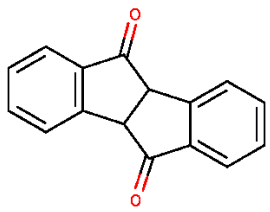


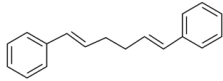
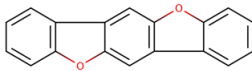
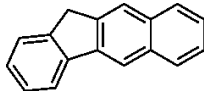
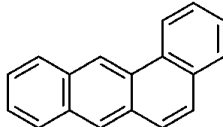
Figure 4.2. Chromatogram of the *n*-pentane soluble fraction of the product of the self-reaction of indene at 60 minutes showing cracking products.

The highest intensity peak corresponds to indan (2.73 minutes), the hydrogenated product of indene. All low boiling compounds (peaks 1-10) eluting between 1.725 and 2.406 are impurities present in the raw indene or in the solvent used as shown in Table 4.6. Some of the indene remains unreacted and shows at around 2.8 minutes. Peaks 17 and 20 were monocyclic products and provided evidence of ring-opening taking place.

Table 4.6. Compound classes present in the product of the self-reaction of indene, the self-reaction of benzofuran and the reaction of the mixture of indene and indan.

	Retention time (min)	Compound name	Chemical structure
1 ^a -10 ^a	1.725 - 2.406	- ^b	-
11 ^d	2.286	Phenol	
12, 13, 14	2.406, 2.547, 2.589	- ^b	Unidentified
15 ^a	2.734	2-Methylphenol	
16	2.787	Indene	
17 ^c	2.814	2-Ethyl-1,4-dimethylbenzene	
18	2.887	- ^b	Unidentified
19	3.048	2,3-Dihydro-1-benzofuran	

20 ^c	3.048, 3.081	Isomers of 2-Ethenyl-1,4-dimethylbenzene	 <p>The structure shows a benzene ring with a vinyl group (-CH=CH₂) at the top position and two methyl groups (-CH₃) at the 1 and 4 positions relative to the vinyl group.</p>
21 ^c	3.258	2-Methyl-1-benzofuran	 <p>The structure shows a benzofuran ring system with a methyl group (-CH₃) attached to the 2-position of the furan ring.</p>
22 ^d	3.349	2-Ethylphenol	 <p>The structure shows a benzene ring with a hydroxyl group (-OH) at the top position and an ethyl group (-CH₂-CH₃) at the 2-position.</p>
23 ^a , 24 ^a , 25 ^a	3.936, 4.110, 4.257	_b	-
26 - 29	10.665- 12.476	_b	Unidentified
30	12.523, 12.837	_b	Unidentified
31	13.231	_b	Unidentified
32 ^c	13.325, 13.946	Isomers of 4b,9b-dihydroindeno[2,1-a]indene-5,10-dione	 <p>The structure shows a complex polycyclic system consisting of two benzene rings fused to a central five-membered ring. Two carbonyl groups (=O) are attached to the central ring at the 5 and 10 positions.</p>

33 ^c	13.331	[(1E,5E)-6-Phenylhexa-1,5-dien-1-yl]benzene	
34	13.585	- ^b	Unidentified
35 ^c	14.133, 16.860	Isomers of benzo[1,2-b:4,5-b']bisbenzofuran	
36 ^c	14.534, 14.694	Isomers of 11H-Benzo[b]fluorene	
37	14.354, 14.668	- ^b	Unidentified
38	15.156	- ^b	Unidentified
39 ^c	16.739	Benz[a]anthracene	

^aPeak present in the pure compound acquired from the supplier as an existing impurity or unidentified compound.

^bNot unambiguously identified.

^cThese compounds should be seen only as being indicative of the nature of the products. The true identities of these compounds have not been confirmed.

^dThese compounds has been spiked and identity has been confirmed (Figures B.4, B.5 in Appendix B).

Figure 4.3 shows addition products from the self-reaction of indene. This product was further analyzed in the Simulated distillation to check the amount of higher boiling point compounds not

detectable by GC-MS. Some compounds point towards two or more different peaks and displayed the same major fragment ion peaks in their mass spectrum reports. Those peaks are representative of presence of isomers for the respective compounds.

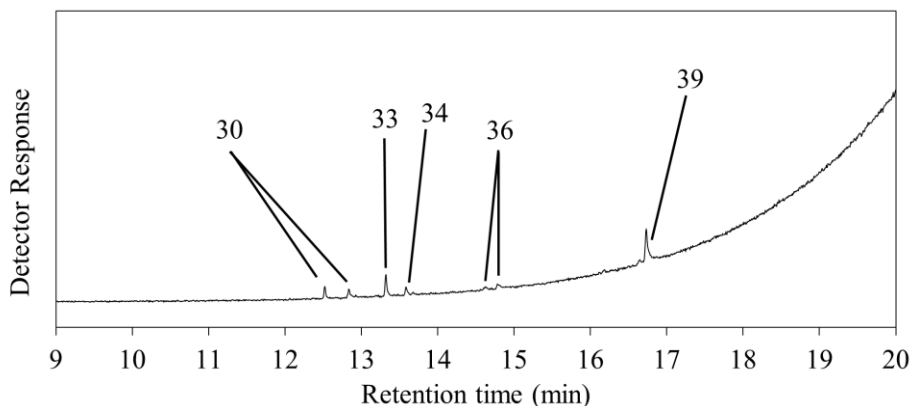


Figure 4.3. Chromatogram of the *n*-pentane soluble fraction of the product of the self-reaction of indene at 60 minutes showing addition products. Unlabeled peaks from retention time 9-20 min are indicative of column bleeding.

The chromatograms of the self-reactions of indan, indole and thianaphthene show only indan, indole and thianaphthene respectively (Figures B.1, B.2 and B.3 in Appendix B) at both reaction temperatures. These products have been further analyzed using Simulated Distillation in order to check whether there are heavier compounds non-detectable by GC-MS.

The chromatogram of the self-reaction of benzofuran at 60 minutes is shown in Figures 4.4 and 4.5. Both reaction times show similar chromatograms. A large amount of benzofuran remains unreacted (2.5 minutes). Part of the benzofuran is hydrogenated to 2,3-dihydrobenzofuran (peak 19). Ring opening products are phenol (2.286 minutes) and 2-ethylphenol (3.349 minutes). These products have been confirmed by spiking the sample (Figures B.4, B.5 in Appendix B). Benzofuran undergoes addition reactions as shown in Figure 4.5. Addition products include dimerization as well as ring opening and recombination. All compounds that were identified are shown in Table 4.6.

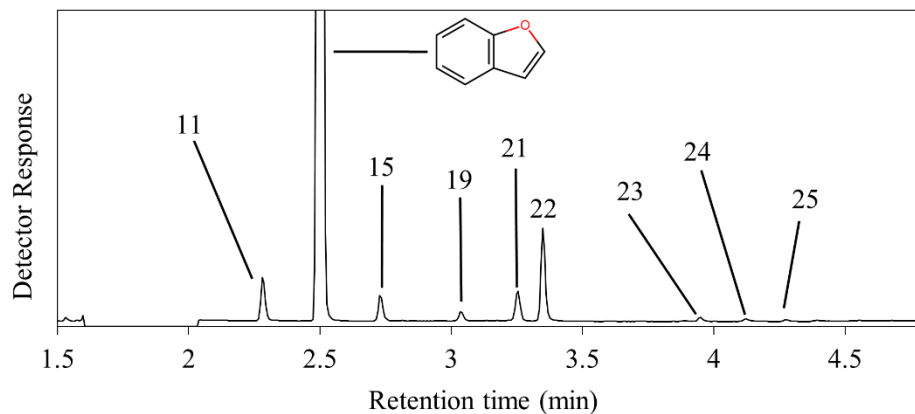


Figure 4.4. Chromatogram of the product of the self-reaction of benzofuran at 60 minutes showing cracking products.

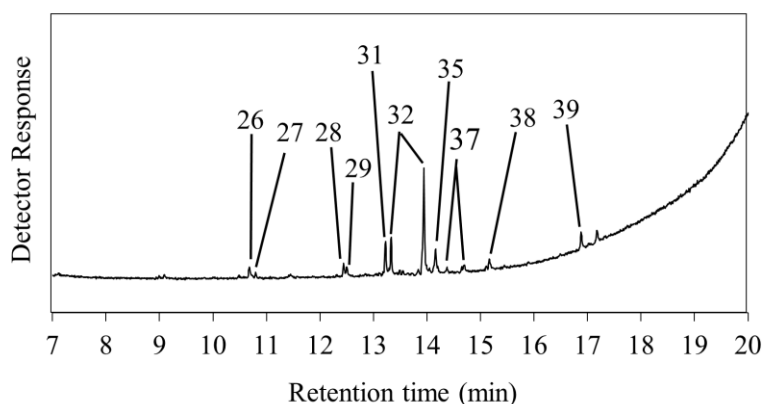


Figure 4.5. Chromatogram of the product of the self-reaction of benzofuran at 60 minutes showing addition products. Unlabeled peaks from retention time 9-20 min are indicative of column bleeding.

FTIR and NMR were used to identify the alcohol functional group. However, the concentration of alcoholic functional groups in the products was lower than the detection limit of the apparatus (Figures B.6 and B.7 in Appendix B). The dominating effect in NMR is that of the peaks were representative of benzofuran, which occupies a large concentration in the product.

4.3.1.3 High boiling compounds determination using SimDist

The product of the self-reaction of indan, at both reaction temperatures, contained compounds that elute totally in a temperature range of 170-192 °C (Figure B.8 in Appendix B). The normal boiling point of indan is 176.5 °C.⁴ Therefore, the only product in the self-reaction of indan is indan, as also confirmed by GC-MS.

The product of the self-reaction of thianaphthene, at both reaction temperatures, contained products that elute totally at temperatures below 222 °C (Figure B.9 in Appendix B). Compounds boiling at temperatures lower than 400 °C are detectable by the GC-MS. Since GC-MS only shows thianaphthene whose normal boiling point is 221 °C,⁴ then it is the only compound present in the product.

Figure 4.6 shows the distillation curves of the product of indole at 30 and 60 minutes. The major compound present is the indole, which has a normal boiling point of 254 °C.⁴ Around 86% of the product boils at a temperature less than 240 °C for the 30 minutes reaction time and 92% for the 60 minutes reaction time. The boiling point is very close to the boiling point of indole, and as confirmed by GC-MS, the only low boiling compound in the product is indole. However, the distillation curve shows that there are heavier compounds (14% for the 30 min reaction and 8% for the 60 min reaction) which are polymerization products. A higher amount of heavier products was present at 30 min than at 60 min, contrary to what one would anticipate.

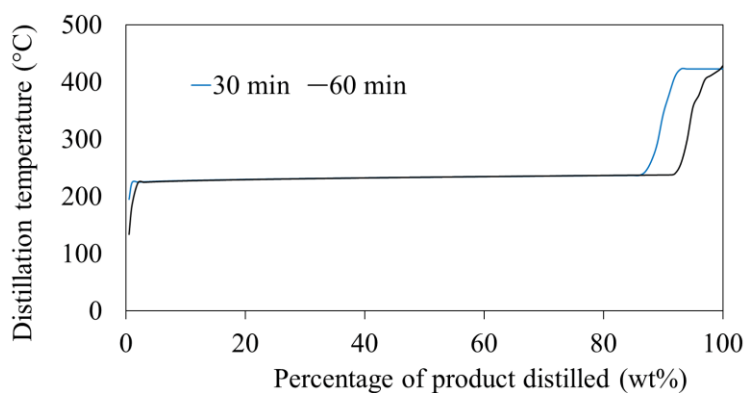


Figure 4.6. Distillation curve of the products of the self-reaction of indole at 30 and 60 minutes reaction times.

Figure 4.7 shows the distillation curves of the product of benzofuran at 30 and 60 minutes. The major compound present is the benzofuran, as confirmed by the GC-MS. The normal boiling point of benzofuran is 165-175°C.⁴ All low boiling compounds showing on GC-MS eluted at boiling points less than 215°C. This constitutes around 72% for the 30 minutes reaction and around 87% for the 60 minutes reaction. Benzofuran has formed addition products, part of which were detectable by the GC-MS.

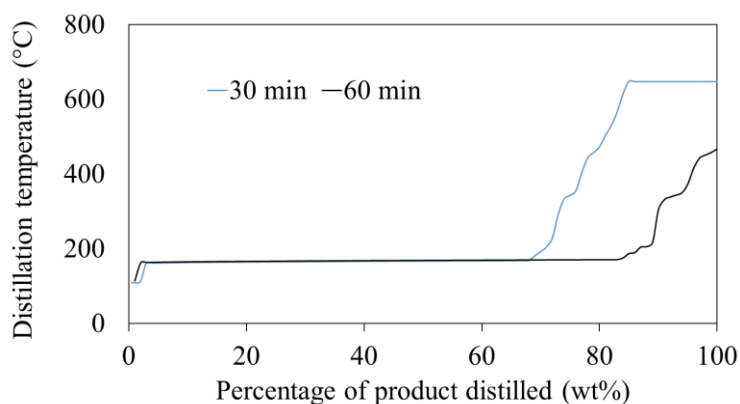


Figure 4.7. Distillation curve of the products of the self-reaction of benzofuran at 30 and 60 minutes reaction times.

The distillation curve of the products of the self-reaction of indene resembles the one in the study in Chapter 5 except with less heavy compounds that were formed (Figure B.10 in Appendix B). This is in accordance with the asphaltenes content that also shows a smaller value compared to the study in Chapter 5. The maximum boiling temperature in the product is around 588 °C.

4.3.1.4 Free radical content by ESR

Knowing that all model compounds initially did not have any free radical content, it was of interest to check whether the products had any free radicals that did not terminate during the reaction. The free radical content for the products was measured immediately after reaction.

The products from the self-reactions of indole, indan and thianaphthene, at both reaction temperatures, have no detectable free radical content. All free radicals, if any, terminated by the end of the reaction time.

A pulse was observed for the products of the self-reactions of indene and benzofuran at a g-factor of 2, characteristic of the carbon free radicals. This indicates that the reactions taking place did not terminate and/or some free radicals are still trapped in the condensed poly-aromatic rings. The free radical content of these products was quantified (Table 4.7). The amount of free radicals is increasing with the reaction time for both compounds materials. The amount of free radicals formed by indene is higher than that formed by benzofuran.

Table 4.7. Free radical content in the products of the self-reaction of indene and benzofuran for the reaction times indicated.

Feed material	Reaction time (min)	Free radical content after conversion (10^{18} spins/g)	g-value
Indene	30	1.22	2.00864
	60	1.32	2.00897
Benzofuran	30	1.09	2.00007
	60	1.17	2.00840

4.3.2 Reaction of mixture of model compounds at thermal cracking conditions

Mixtures of model compounds were thermally converted. Indene, indan and thianaphthene were selected for the study as they are all initially soluble in *n*-pentane. It was worthwhile investigating the behavior of these model compounds when in mixture. The gas products of the reactions were only analyzed qualitatively because it was not possible to get accurate values of the amount of gases produced during the reactions (it was minor). Liquid and solid products obtained were further analyzed.

4.3.2.1 Analysis of gaseous products

The gases that were identified in both indan+thianaphthene and indene+thianaphthene gaseous products include methane, ethylene, ethane, propylene, propane, butenes, *i*-pentane, *n*-

hexane and carbon monoxide. Of these compounds, methane and ethane were present at highest concentrations.

4.3.2.2 *n*-Pentane insoluble content

Indan and thianaphthene were reacted with indene, a hydrogen donor molecule, in order to test their reactivities in the presence of hydrogen sites. They were also reacted together (i.e. indan and thianaphthene). The products of the reactions were analyzed for *n*-pentane insoluble content (Table 4.8). Mixtures that had indene, have formed condensed poly-aromatic rings insoluble in *n*-pentane. Indan and thianaphthene did not form any *n*-pentane insoluble material, though the color of the product was dark brown, indicating that reactions took place.

Table 4.8. *n*-Pentane insoluble content in the products of the mixtures of model compounds for a 60 minute reaction time.

Feed material	<i>n</i> -pentane insoluble content in the product (%)	
	Actual	Normalized to indene in the feed
Indene+Thianaphthene	12.6	25.2
Indan+Thianaphthene	0	-
Indene+Indan	22.9	45.8

4.3.2.3 Chemical structure identification by GC-MS

The chromatograms for the different reaction mixtures of model compounds are shown in Figures 4.8-4.12. Figures 4.8 and 4.9 show products of ring opening and addition reactions of the indene and indan reaction. A series of reactions took place leading to cracking of the rings. A large amount of indan is present in the product (eluting at 2.69 min). It is known that indene forms a large amount of indan at these conditions.³ Some cracking products of undetermined structures were present as peaks 12-14, 17, 18 and 20. Asphaltenes and coke precursors show at the high elution time part of the chromatogram (Figure 4.9).

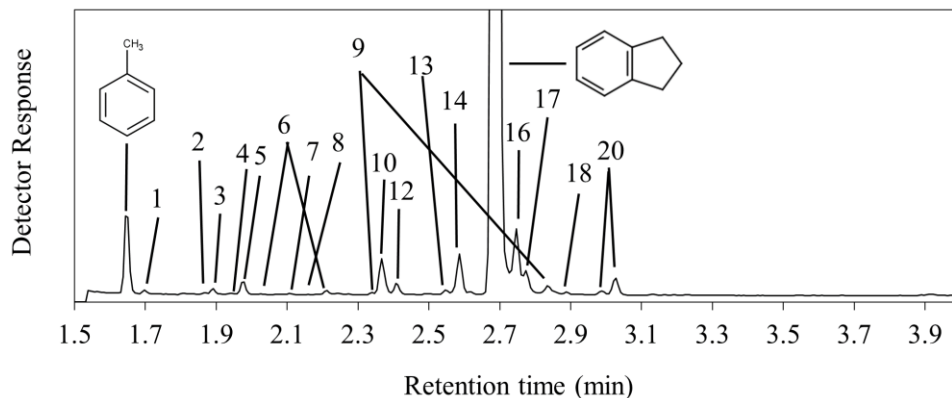


Figure 4.8. Chromatogram of the product of the thermal conversion of indene+indan at 60 minutes showing cracking products.

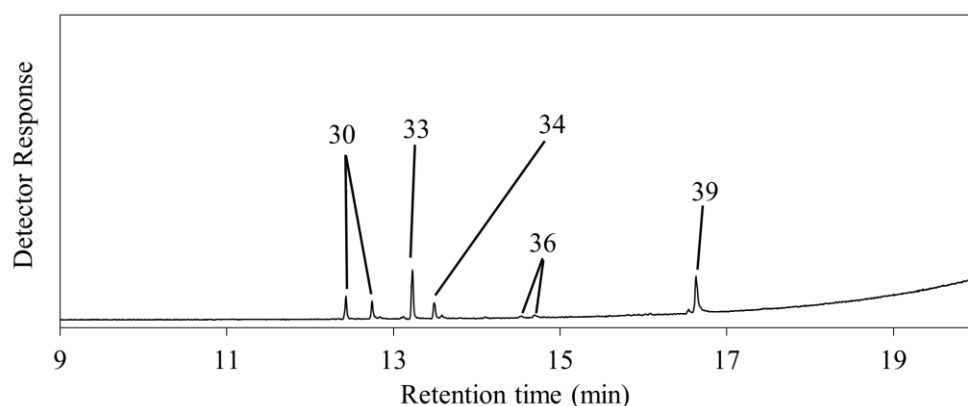


Figure 4.9. Chromatogram of the product of the thermal conversion of indene+indan at 60 minutes showing addition products. Unlabeled peaks from retention time 9-20 min are indicative of column bleeding.

Figures 4.10 and 4.11 show the chromatogram of the product of the thermally converted indan+thianaphthene mixture. The corresponding structures for each peak are in Table 4.9. Indan and thianaphthene are the major products, indicating the stability of these compounds. Other products showing in the chromatogram indicate that reactions took place. Some of the indene (peak 4) might be formed due to the dehydrogenation of indan, or might be initially present in the product. Indene was not quantified in the product. There is clear evidence of thianaphthene hydrogenation into 2,3-dihydrobenzo[b]thiophene (peak 10). Figure 4.11 shows that both indan and thianaphthene underwent addition reactions. SimDist was run to know whether the addition products shown in the GC-MS were the only ones formed.

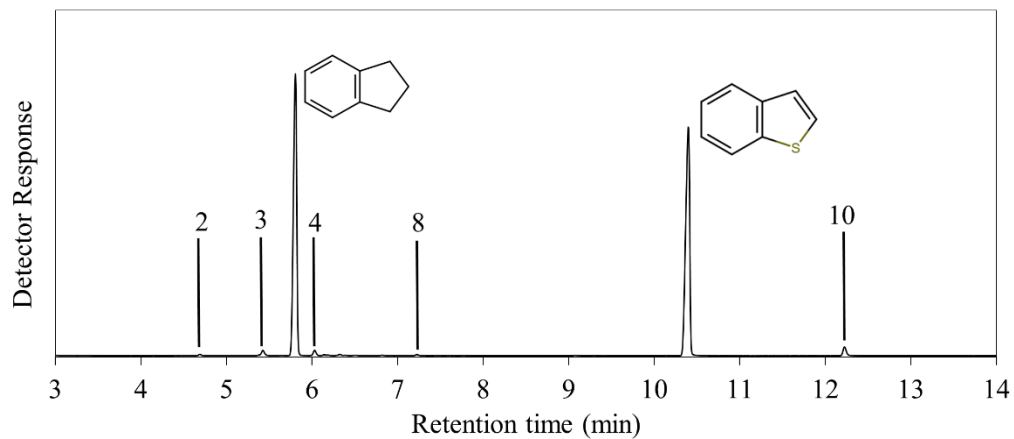


Figure 4.10. Chromatogram of the low boiling compounds of the product of the thermal conversion of indan+thianaphthene at 60 minutes.

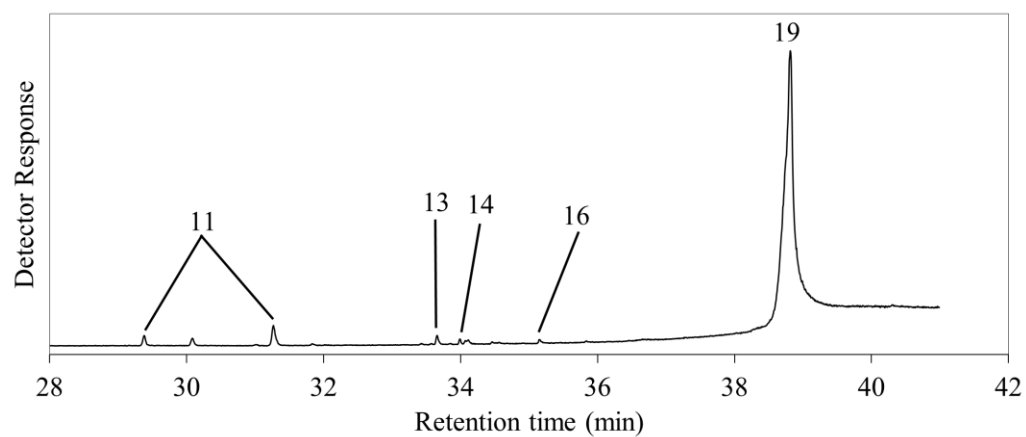


Figure 4.11. Chromatogram of the high boiling compounds of the product of the thermal conversion of indan+thianaphthene at 60 minutes.

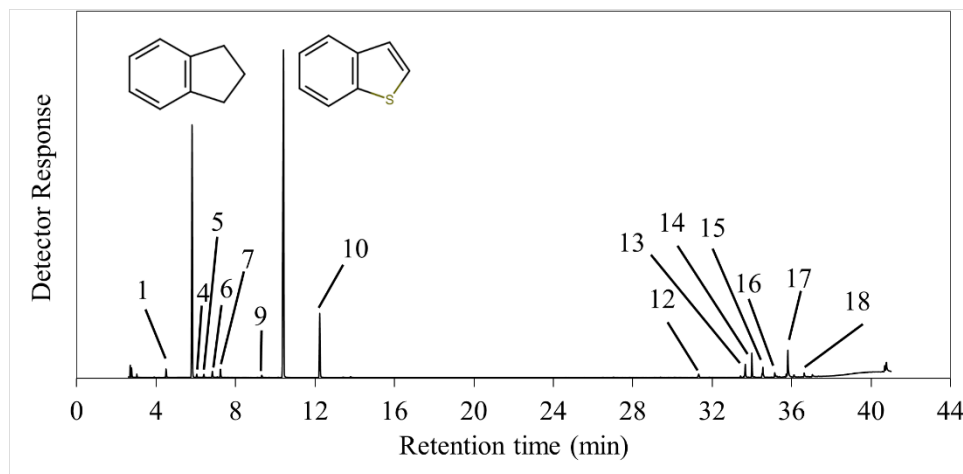
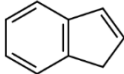
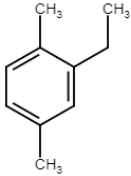
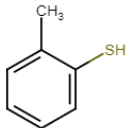
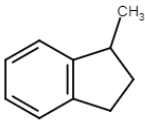
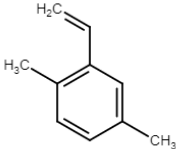
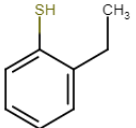
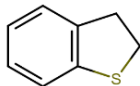
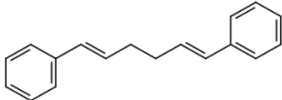
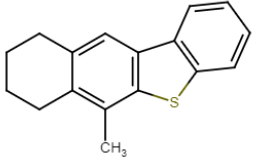
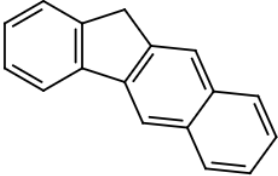
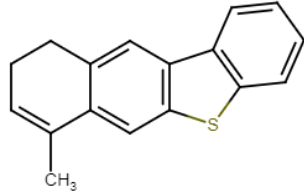
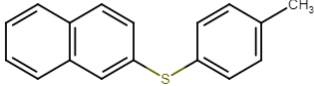
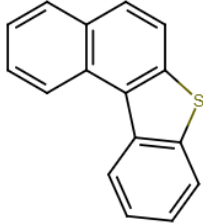
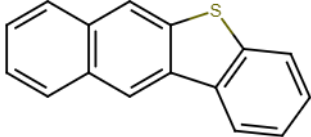


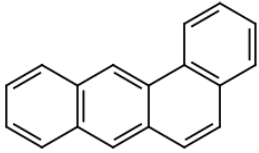
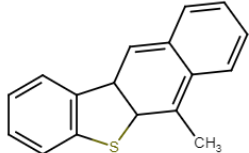
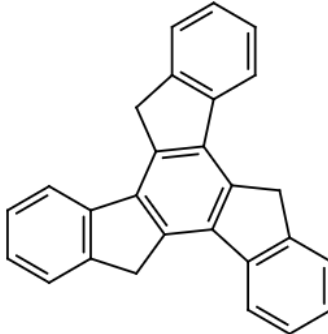
Figure 4.12. Chromatogram of the product of the thermal conversion of indene+thianthrene at 60 minutes.

Table 4.9. Chemical structures of peaks of reaction of indan+thianthrene and indene+thianthrene (Fig 4.10-4.12).

	Retention time (min)	Compound name	Chemical structure
1 ^a	2.504	Benzonitrile	
2 ^a	4.718	1,2,4-trimethylbenzene	
3 ^a	5.453	1,3,5-trimethylbenzene	

4 ^a	6.008	Indene	
5 ^c	6.549	2-Ethyl-1,4-dimethylbenzene	
6 ^d	6.749	2-methylbenzenethiol	
7 ^c	7.244	1-methylindan	
8 ^c	7.250	Isomers of 2-Ethenyl-1,4-dimethylbenzene	
9 ^d	9.382	2-ethylbenzenethiol	
10	12.235	2,3-dihydrobenzo(b)thiophene	
11 ^c	29.428, 31.333	[(1E,5E)-6-Phenylhexa-1,5-dien-1-yl]benzene	

12 ^c	31.340	-	
13 ^c , 14 ^c , 15 ^c	33.695, 34.046, 34.553	-	  
16 ^c	35.202	Isomers of Benzo[b]naphtho[1,2d]thiophene	 

17 ^c	35.803	benz[a]anthracene	
18 ^c	26.685	5-methylbenzonaphtho<2,3-d>thiophene	
19 ^c	38.817	truxene	

^aPeak present in the pure compound acquired from the supplier as an existing impurity or unidentified compound.

^cThese compounds should be seen only as being indicative of the nature of the products. The true identities of these compounds have not been confirmed.

^dThese compounds have been spiked and identity has been confirmed (Figures B.11, B.12 in Appendix B).

Figure 4.12 shows the chromatogram of the product of the thermally converted indene+thianaphthene mixture. Indan and thianaphthene are the major products. A large amount of indene has been hydrogenated to indan. Some of the indene (peak 4) remains unreacted. Thianaphthene has undergone hydrogenation into 2,3-dihydrobenzo(b)thiophene (peak 10). Thianaphthene has also been cracked into 2-methylbenzenethiol (peak 6) and 2-ethylbenzenethiol (peak 9) which structures have been confirmed (Figures B.11, B.12 in Appendix B). Both thianaphthene and indene (or the formed indan) undergo addition reactions (peaks 11-19). This is in accordance with the asphaltenes content.

4.3.2.4 Quantification of indan and thianaphthene by GC-FID

The amount of indan and thianaphthene in the products were quantified using GC-FID. Calibration curves were built for an accurate quantification. The masses of indan and thianaphthene in the feed and product are shown in Table 4.10. The amount of thianaphthene and indan decreased when

these two compounds were reacted together. Indan (6.6% decrease) is more reactive than thianaphthene (2.8% decrease). In addition, a higher percentage decrease in the amount of thianaphthene was observed when it was reacted with indene (27.43%) than when it was reacted with indan (2.8%). It was not possible to check whether indan reacted or not when mixed with indene since indene also forms indan. The total amount of indan in the product has increased.

Table 4.10. Mass of indan and thianaphthene in the feed and product.

Feed Material	Mass of indan (g)			Mass of thianaphthene (g)		
	Feed	Product	Percentage Decrease	Feed	Product	Percentage Decrease
Indene+Indan	2.553	3.40	-	-	-	-
Indene+Thianaphthene	0	0.98	-	2.504	1.82	27.4
Indan+Thianaphthene	2.503	2.34	6.6	2.523	2.45	2.8

4.3.2.5 High boiling compounds identification using SimDist

Simulated distillation for the *n*-pentane soluble fraction of the products of the mixtures were run. The product of the reaction of indan and thianaphthene, that is also totally soluble in *n*-pentane, boils completely at a temperature less than 210 °C (Figure B.13 in Appendix B). This indicates that all compounds in the *n*-pentane soluble product were visible on the GC-MS.

The *n*-pentane soluble fraction of the product of the reaction of indene and indan shows the same step-shape of self-reaction of indene (Figure B.14 in Appendix B). The distillation curve of the *n*-pentane soluble fraction of the product of indene and thianaphthene (Figure B.15 in Appendix B) confirms the presence of high boiling compounds. The first step in the range of temperatures of 33 to 47 °C corresponds to the *n*-pentane. However, it seems there was an error with this measurement as the curve suggests there was a single heavy product (~40% of the mass) that boiled at 450 °C.

4.3.2.6 Free radical content by ESR

The products of the thermally converted feeds have been analyzed for free radical content. The product of indan+thianaphthene shows no free radicals. The product of indene+thianaphthene has a higher free radical content than that of indene+indan (Table 4.11) though the latter had a higher asphaltenes content. The self-reaction of indene at 60 minutes produces the largest amount of free radicals.

Table 4.11. Free radical content for product of the mixtures of model compounds at 60 min.

Feed material	Free radical content after conversion (10^{18} spins/g)
Indene+Indan	0.74
Indene+Thianaphthene	1.18

4.4 Discussion

4.4.1 Effect of reactor walls on cracking and addition

The self-reaction of indene was conducted in a different study (Chapter 5)³ without the use of a glass vial. Therefore, in that study, the indene was in contact with the reactor walls. Table 4.12 below shows the main differences in the results for indene between the previous and current study.

Table 4.12. Self-reaction of indene with and without glass vial.

	Reaction time (min)	% <i>n</i> -pentane insoluble in products	Final boiling point of the <i>n</i> -pentane soluble fraction as obtained by the SimDist (°C)
Self-reaction of indene without vial ³	30	45	698
	60	83	699
Self-reaction of indene with a vial	30	35	587
	60	72	588

The formation of asphaltenes in the self-reaction of indene shows that there are reactions that happened. This is in accordance with the GC-MS and SimDist results. Even though a vial was used inside the reactor, indene was able to self-react. This proves that the contact with the reactor walls was not the initiator of the reaction discussed in Chapter 5.³ The amount of asphaltenes and coke has, however, decreased when the indene was not in contact with the reactor walls. Simulated distillation results also confirm the decrease in the amount of poly-aromatics when using a glass vial in the reactor. It can be observed that the metals in the reactor, mainly iron, chromium and nickel, are potentially playing the role of the catalyst in some of the reactions, in a way that favors free radical addition reactions in the case of the self-reaction of indene. Alternatively, the higher wall temperature resulted in increased free radical addition reactions. Control experiments were not performed to confirm the difference or the reason for the difference.

4.4.2 Self-reactivity of model compounds

While indene shows high susceptibility to self-react, compounds such as indan, indole and thianaphthene are more thermally stable on their own.

Indene has been previously used for the formation of truxene⁵ which was identified as a trimerization of the indene molecule and that was accompanied by the formation of indan. The process of formation of indan from indene was described as an “autoreduction” since the hydrogens released to form truxene have been used by another indene molecule to hydrogenate into indan. In the current study, many other carbon rich compounds that are precursors of asphaltenes have been formed from indene. Indene undergoes clear hydrogen disproportionation. The large amount of hydrogen released in the transformation of indene to condensed poly-aromatic rings led to the formation of a high percentage of indan as shown by the GC-MS and SimDist results.

Indan does not self-react, indicating that this molecular structure is highly stable in the absence of hydrogen donor compounds. No compounds, besides indan, were detected in the product after conversion. There were also no free radicals in the product. The suggested mechanism of free radical formation and termination for the indan molecule is shown in Figure 4.13. It is proposed

that the free radical formed by the loss of hydrogen atom is very unstable that it terminates before any cracking or addition occurs. Slotboom et al.⁶ have performed experiments for the hydrocracking of indan in a flow reactor at around 500 °C and 80 bar in the presence of hydrogen. Cracking occurred following two main trajectories for ring opening: (1) the α -cleavage that produced mainly toluene and lower concentrations of *n*-propylbenzene which can be transformed to methyl benzene via styrene and (2) β -cleavage leading to 2-ethyl toluene which will eventually form *o*-xylene. Kinetics wise, α -cleavage had a higher reaction rate than β -cleavage.

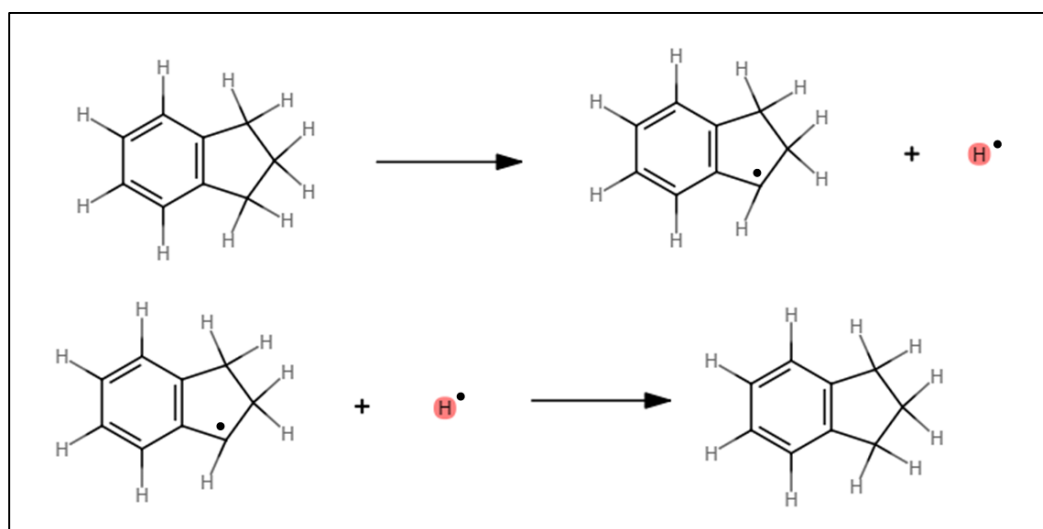


Figure 4.13. Indan free radical formation and termination.

Penninger⁷ conducted cracking of indan in nitrogen at 500 °C and 8 MPa in a flow reactor where indan was continuously injected. The indan was in direct contact with the reactor walls which were reported to play a role of a catalyst in the reaction.⁸ The indan was cracked following a free radical mechanism initiated by the reactor walls. It was concluded⁷ that the cracked products of indan are the same in the presence of either hydrogen or nitrogen with a significantly higher reaction rate with hydrogen. In our study, indan was stable at the operating conditions. That is mainly due to the absence of two factors namely, (a) the walls' catalytic effect due to the use of a glass vial and (b) the hydrogen since experiments were run under nitrogen.

Thianaphthene also showed a high stability when reacted under nitrogen in absence of reactor walls' contact. GC-MS and SimDist show thianaphthene to be the only product confirming that no

reaction happened. This is also confirmed by the physical appearance of the product which resembles the feed as well as the absence of free radicals in the product.

The physical structures of the product after conversion for both indole and benzofuran suggest that reactions took place. This was confirmed by the GC-MS and SimDist results.

There is clear evidence that indole is stable since there is still a large amount unreacted. However, it was observed that polymerization of indole happened but no free radicals were detected in the product (as confirmed by ESR). The cracking of indole is not possible under the operating conditions; rather, it has tendency to polymerize. The rate of polymerization is high enough to form heavy polymerized products (detectable by SimDist) without any dimerization detectable by GC-MS, even at a reaction time of 30 minutes. Indole polymerization is usually conducted in the presence of a catalyst. Bouldin et al.⁹ showed that the route for polymerization of indole, in the presence of the catalyst employed in the study, does not require the abstraction of hydrogen. The indole molecules are rather linked at positions 2 and 3 when undergoing addition reactions. Soylu et al.¹⁰ also suggested that the carbocation mechanism for the polymerization of indole, in the presence of a Lewis acid, takes place on the olefinic carbon of the 5-membered ring.

Benzofuran is stable, since it is the main compound present in the product after conversion. However, part of the benzofuran undergoes cracking as well as addition reactions.

4.4.3 Reactivity of model compounds in mixtures

The amount of asphaltenes formed from the mixtures of model compounds that involve indene (i.e. indene+thianaphthene and indene+indan) (Table 4.8) normalized to indene content is less than the amount of asphaltenes formed from indene alone at the same reaction temperature (Table 4.4). This is mainly due to the domination of cracking reactions rather than free radical addition. Another factor that plays an important role, is the high stability of indan and thianaphthene which remain in large amounts in the products as shown in GC-MS. It has been reported⁷ that the domination of either cracking or addition reactions depends on the concentration ranges of the hydrogen to indan. The lower the ratio of hydrogen to indan, the more the cracking reactions taking

place on the indan molecule and the more the ring opening products. In the current study, the feed contained equal concentrations of indan and indene. Indene is able to attack the indan but only a small amount of indan is reactive.

In this study, it has been shown that both indan and thianaphthene are very thermally stable on their own, but they react in presence of hydrogen donor compounds. Indene is able to open the rings of both indan and thianaphthene. Indene also undergoes addition reactions with them leaving behind persistent free radicals in the product. Thianaphthene ring opening was not found in the presence of indan, but thianaphthene had undergone hydrogenation and addition reactions. This is in accordance with the free radical content. When thianaphthene is reacted, the major low boiling point product formed is when thianaphthene grabs two hydrogen atoms from the matrix to transform to 2,3-dihydrobenzo(b)thiophene. In the case of indene+thianaphthene, the hydrogen disproportionation that indene is capable of constitutes a key initiator for the reactions. For this reason, around 25% of the thianaphthene is consumed when reacted with indene and there are free radicals persisting in the product after reaction.

4.4.4 Sulfur ring-opening

Ring opening for light boiling thiophenes is usually possible using alkali metals like sodium and potassium. Another way to remove sulfur in heavier fractions of the oil is the conventional hydrotreating.¹¹ Cracking of benzofuran, thianaphthene and indole was possible using catalytic hydrotreating.¹² Rhodium catalysis has also been employed for similar purposes.¹³ Ring opening of thianaphthene has been performed using the Birch reduction.^{14,15} Pacut et al.¹⁵ reported that ring opening of thianaphthene occurred to 2-ethylbenzenethiol through the intermediate 2,3-dihydrobenzo[b]thiophene. The mechanism of ring opening involves the formation of carbanions. Bianchini et al.¹⁶ developed a catalyst for cracking of thianaphthene following a free radical mechanism.

In the current study, ring opening of thianaphthene was possible in the absence of direct hydrogen supply, but in the presence of molecules that can lose hydrogen easily. Hydrogen disproportionation occurs during thermal cracking. It has been thus shown, that ring opening is

possible in a non-catalytic cracking process, without contact with reactor walls (i.e. metals) and in the absence of direct hydrogen supply. Indene, undergoing hydrogen disproportionation³ is capable of ring opening of thianaphthene.

4.5 Conclusions

It could be concluded that:

- (1) Indan and thianaphthene are thermally stable on their own. They do not undergo reactions unless a hydrogen donor compound is present.
- (2) Indene and benzofuran are self-reactive. They undergo ring opening as well as addition reactions with a large amount of free radicals in the products.
- (3) Indole ring opening is not possible by self-reaction. Instead, polymerization takes place leaving no traces of free radicals in the product.
- (4) Indan and thianaphthene ring opening and addition are possible in the presence of indene. There is formation of asphaltenes and persistent free radicals.
- (5) Indan and thianaphthene, when reacted together, undergo addition reactions and the products are all soluble in *n*-pentane. Indan ring opening takes place, but thianaphthene remains is not ring-opened in the presence of indan.

Literature cited

- (1) Siddiquee, M. N.; De Klerk, A. Hydrocarbon Addition Reactions during Low-Temperature Autoxidation of Oilsands Bitumen. *Energy and Fuels* **2014**, *28* (11), 6848–6859.
- (2) Siddiquee, M. N.; De Klerk, A. Heterocyclic Addition Reactions during Low Temperature Autoxidation. *Energy and Fuels* **2015**, *29* (7), 4236–4244.
- (3) Tannous, J. H.; de Klerk, A. Asphaltenes Formation during Thermal Conversion of Deasphalted Oil. *Fuel* **2019**, *255*, 1–10.
- (4) Richard J. Lewis, S. *Hawley's Condensed Chemical Dictionary*, Fifteenth.; John Wiley & Sons, 2007.
- (5) Gustav Egloff. *The Reactions of Pure Hydrocarbons*; New York: Reinhold Publishing Corporation, 1937.
- (6) Slotboom, H. W. Mechanism and Kinetics of the Thermal Hydrocracking of Single Polyaromatic Compounds. *Am. Chem. Soc. Symp. Ser.* **1976**, *32*, 444–456.
- (7) Penninger, J. M. L. New Aspects of the Mechanism for the Thermal Hydrocracking of Indan and Tetralin. *Int. J. Chem. Kinet.* **1982**, *14* (7), 761–780.
- (8) Slotboom, H. W.; Penninger, J. M. L. The Role of the Reactor Wall in the Thermal Hydrocracking of Polyaromatic Compounds. *Ind. Eng. Chem. Process Des. Dev.* **1974**, *13* (3), 296–299.
- (9) Bouldin, R.; Singh, A.; Magaletta, M.; Connor, S.; Kumar, J.; Nagarajan, R. Biocatalytic Synthesis of Fluorescent Conjugated Indole Oligomers. *Bioengineering* **2014**, *1* (4), 246–259.
- (10) Soyly, O.; Uzun, S.; Can, M. The Investigation of Acid Effect on Chemical Polymerization of Indole. *Colloid Polym. Sci.* **2011**, *289* (8), 903–909.
- (11) Valla, J. A.; Lappas, A. A.; Vasalos, I. A. Catalytic Cracking of Thiophene and Benzothiophene: Mechanism and Kinetics. *Appl. Catal. A Gen.* **2006**, *297* (1), 90–101.
- (12) Abe, H.; Bell, A. T. Catalytic Hydrotreating of Indole, Benzothiophene, and Benzofuran over Mo₂N. *Catal. Letters* **1993**, *18* (1–2), 1–8.
- (13) Bianchini, C.; Meli, A.; Patinec, V.; Sernau, V.; Vizza, F. Liquid-Biphase Hydrogenolysis of Benzo[b]Thiophene by Rhodium Catalysis. *J. Am. Chem. Soc.* **1997**, *119* (21), 4945–4954.
- (14) Yu, Z.; Verkade, J. G. Reductive Desulfurization of Organosulfur Compounds with Sodium

- in Liquid Ammonia. *Phosphorous, Sulfur, Silicon Relat. Elem.* **1998**, *133* (1), 79–82.
- (15) Pacut, R. I.; Kariv-Miller, E. Birch-Type Reductions in Aqueous Media: Benzo[b]Thiophene and Diphenyl Ether. *J. Org. Chem.* **1986**, *51* (18), 3468–3470.
- (16) Bianchini, C.; Frediani, M.; Vizza, F. Synthesis of the First Polymer-Supported Tripodal Triphosphine Ligand and Its Application in the Heterogeneous Hydrogenolysis of Benzo[b]Thiophene by Rhodium Catalysis. *Chem. Commun.* **2001**, *2* (5), 479–480.

Chapter 5: Asphaltenes formation during thermal conversion of deasphalted oil

Abstract

New asphaltenes are formed during the thermal conversion of heavy oil. When new asphaltenes are formed from deasphalted oil, it erodes the conversion advantage provided by solvent deasphalting prior to visbreaking. The postulate that asphaltenes formation is caused by free radical addition reactions was evaluated. Indene was employed to exacerbate asphaltenes formation during thermal conversion of deasphalted oil at 400 °C. Evidence was provided that indene was involved in addition reactions with itself and with deasphalted oil to produce new *n*-pentane insoluble material. Whether indene induced increases asphaltenes formation, or whether it formed addition products with the deasphalted oil was not resolved. Self-reaction of indene at 400 °C resulted in extensive formation of *n*-pentane insoluble material. Formation of *n*-pentane insoluble material was reduced in mixtures with indan and naphthalene. Using these model systems the presence and nature of addition products was determined. The reported thermal conversion of indene was consistent with reaction chemistry based on molecule-induced homolysis, free radical addition, and propagation / termination by hydrogen transfer. The prevalence of addition reactions and the importance of hydrogen transfer reactions were highlighted, which have implications for modelling reaction chemistry describing thermal conversion of heavy oil.

Keywords: free radical addition, hydrogen disproportionation, molecule-induced homolysis, visbreaking, deasphalted oil, asphaltenes.

5.1 Introduction

One of the undesirable outcomes of the thermal cracking of heavy oils in a visbreaking process is the formation of new asphaltenes and other heavier products during thermal conversion.^{1,2,3,4} Asphaltenes formation is detrimental to downstream processes and a higher asphaltenes content increases the risk of fouling and product instability.

The formation of new asphaltenes is also undesirable for operation of the visbreaking process. Asphaltenes are considered to be a precursor for coke formation.^{5,6,7} The asphaltenes, being a solubility class, can lead to premature phase separation during thermal conversion. Phase separation leading to coke formation is described by Wiehe's phase separation model.⁸ The insolubility of species in the bulk oil is attributed to a combination of high molecular mass and low hydrogen content,⁹ properties that are also attributed to asphaltenes.

In visbreaking, the coke yield must be limited to less than 1% and the maximum conversion that can be achieved by visbreaking is limited by coke formation. One way of enabling higher conversion during visbreaking is to remove the asphaltenes in the oil feed beforehand by solvent deasphalting. For the same oil feed, it is possible to achieve higher visbreaking conversion when the feed is deasphalted. However, the advantage of using a deasphalted oil (DAO) is eroded during visbreaking, because new asphaltenes are formed during thermal conversion.² In fact, the formation of new asphaltenes was also found under residue hydroprocessing conditions,¹⁰ which indicated that new asphaltenes formed as a consequence of thermal conversion and not necessarily due to a lack of available hydrogen.

It was postulated that new asphaltenes are formed by free radical addition reactions during thermal conversion and that an increase in molecular mass was the primary cause of insolubility in the bulk oil, while hydrogen depletion was a secondary cause.¹¹ There is a relationship between the increase in molecular mass and carbon residue (coke) formation of petroleum,¹² but the chemical nature of the materials also change. The new asphaltenes that are formed during thermal conversion, as well as those formed under residue hydroprocessing conditions, were reported to have a lower average molecular mass than the asphaltenes in the straight run bitumen or oil.^{2,10}

Irrespective of the sequence of events, both molecular mass and hydrogen content affect solubility in the bulk oil,⁹ as well as whether the solubility of newly formed heavy products will cause them to be classified as asphaltenes or not.

Four observations were pertinent to the investigation of new asphaltenes formation during visbreaking of DAO: (i) DAO contains persistent free radical species.^{13,14} (ii) Hydrogen transfer reactions take place during visbreaking.¹⁵ (iii) Aromatic hydrocarbons with a 5-membered ring next to an aromatic ring, as found in simple molecules like indan and indene, are prone to free radical addition.¹⁶ (iv) Model compound representatives of complex molecules in asphaltenes were shown to form addition products under thermal cracking conditions.¹⁷

It is unlikely that there is only one pathway to form new asphaltenes from DAO. The aim of this study was to explore the possible contribution of addition reactions of lighter products leading to the formation of asphaltenes. It was postulated that some intermediate products produced by hydrogen transfer and/or thermal cracking reactions would be more prone to chain propagation by addition reactions than chain propagation or termination by hydrogen transfer reactions.

To evaluate the contribution of addition reactions, indene was employed as a surrogate for reactive species present in DAO or formed in DAO by thermal conversion. Indene has an olefinic functional group, but it is also an aromatic. An indene sub-structure, when present as part of larger molecules in DAO, was suspected to undergo free radical addition reactions due to the nature of the free radical that it forms. The carbon free radical formed by hydrogen transfer from indene is in both a benzylic and an allylic position, as shown in Figure 5.1. This position of the free radical enables increased resonance stabilization, making it more likely that such a species will form by hydrogen transfer and that it will persist for longer time.

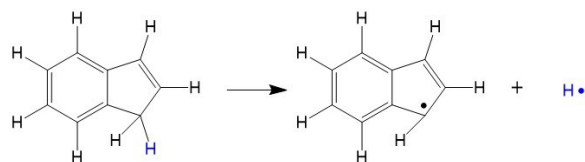


Figure 5.1. Hydrogen transfer from indene leading to the formation of a resonance stabilized indenyl radical. (Note: The hydrogen radical is usually transferred and not released as an isolated free radical species).

In fact, heavier product formation has been observed with less reactive materials. For example, biphenyl was a major product from the thermal conversion of dilute *n*-hexadecane in benzene at 400–450 °C at 14 MPa.¹⁸ Cracking of *n*-hexadecane in the presence of alkyl benzenes resulted in both alkyl aromatic addition products and addition product of olefins to the alkyl aromatics, but no olefin-only addition products.¹⁸

Although DAO obtained from bitumen does not contain indene, it contains species with combined 5- and 6-membered rings.¹⁹ Some of these species have indene-like sub-structures as part of a larger molecule, or can form an indene-containing sub-structure during thermal conversion by hydrogen transfer. This study evaluated whether indene, as a representative sub-structure of larger molecules in DAO, could form asphaltenes under thermal conversion conditions despite its low normal boiling point temperature. Likewise, the study evaluated whether the formation of indene-like products by thermal cracking could result in reactions to produce heavier products that are not necessarily asphaltenes.

The formation of heavier products from material in the distillate boiling range has direct implications for models describing visbreaking without reaction pathways from lighter products to heavier products, e.g.^{20,21,22} A reaction pathway to produce asphaltenes from non-asphaltenes was included in a few models only, e.g.^{23,24} Depending on the nature of addition product formation, it might be necessary to revisit model descriptions used for visbreaking.

5.2 Experimental

5.2.1 Materials

The reactions were performed with indene ($\geq 90\%$, Sigma-Aldrich) and an industrial vacuum residue deasphalted oil (VR DAO). The purity of the indene was determined by gas chromatography with flame ionization detector and it was found to be $97.71 \pm 0.05\%$ based on total response area without response factor correction (average \pm standard deviation of six analyses). The VR DAO was obtained from the Nexen Long Lake Upgrader. Nexen is now CNOOC International Ltd. The VR DAO was produced by industrial pentane solvent deasphalting

of the vacuum residue fraction from vacuum distillation of Athabasca oilsands bitumen. Characterization data for the industrial VR DAO feed are shown in Table 5.1. A different sample of VR DAO from the same origin was previously characterized.¹⁴

Toluene (99.9%, Fisher Scientific) was used as solvent for all Electron Spin Resonance (ESR) analyses. The pentane insoluble analysis used *n*-pentane (99.4%, Fisher Scientific) as the solvent. It was also used as the solvent for the chromatographic analyses. Indan (95%, Sigma Aldrich) was used to spike samples for gas chromatography to facilitate peak identification and was used in control experiments. Naphthalene (99%, Sigma Aldrich) was used in control experiments. Carbon disulfide (99.99%, Fisher Scientific) was used as the solvent for analyses by simulated distillation. Nitrogen (99.999 mol%) used for pressurizing the batch reactors was purchased from Praxair as cylinder gas. Chloroform-D (99.8%, Acros Organics) was used as the solvent for the proton nuclear magnetic resonance measurements. Calibration for electron spin resonance spectrometry was performed with 2,2-diphenyl-1-picrylhydrazyl (~90%, Sigma-Aldrich).

Table 5.1. Characterization of the industrial VR DAO feed.

Property	VR DAO
density at 15.6 °C (kg/m ³)	1040
API gravity	4.4
<i>n</i> -pentane insoluble content (wt%)	3.1
<i>n</i> -heptane insoluble content (wt%)	1.2
ash content (wt%)	0.33
microcarbon residue (wt%)	5.7
elemental analysis (wt%) ^a	
carbon	84.3
hydrogen	9.97
sulfur	5.20
nitrogen	0.62
oxygen	0.61
vanadium content (µg/g)	52
nickel content (µg/g)	32
nature of hydrogen (%) ^b	
non-aromatic	92.5
aromatic	7.5
free radical content (spins/g) ^c	0.9×10 ¹⁸
viscosity (cSt)	
40 °C	5.3×10 ⁶
100 °C	1.9×10 ³
150 °C	165
200 °C	96
250 °C	79

^a Elemental analysis does not add to 100%.

^b Based on ¹H NMR analysis.

^c Quantified using ESR calibrated with DPPH.

5.2.2 Equipment and procedure

Visbreaking reactions were carried out in a batch micro-reactor built with 316 stainless steel Swagelok fittings as shown in Figure 5.2. The batch micro-reactors were heated by placing them in a fluidized sand bath heater. All reactions were performed at 400 °C and 2 MPa under nitrogen environment, using 9 g of sample in total. Each reaction was run at three different reaction times, 30, 45 and 60 minutes, and each of the reactions was performed in triplicate.

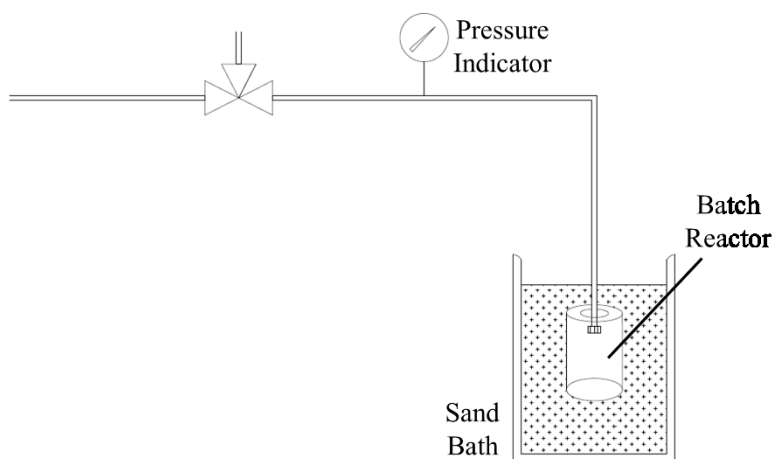


Figure 5.2. Experimental setup used for thermal conversion.

Three different feeds were prepared under nitrogen by mixing VR DAO and indene for 15–20 minutes at a temperature sufficient to increase VR DAO fluidity (typically 85–95 °C), but low enough not to cause indene evaporative loss. The normal boiling point of indene is 182 °C.²⁵ A change in viscosity of the mixture with indene addition could be visually observed. The higher the percentage of the indene added the lower the viscosity of the mixture and the more fluid it became. The prepared feeds are described in Table 5.2.

Table 5.2. Feed materials prepared for thermal conversion experiments.

Feed number	Mass of indene (g)	Mass of VR DAO (g)	Indene concentration (wt%)
1	0	9.0	0
2	0.5	8.5	5.6
3	1.0	8.0	11.1

After thermal conversion, the reaction product was removed without the use of a solvent. The gases produced were collected by depressurization in a gas-bag and the gaseous reaction product was analyzed by gas chromatography (GC). The gaseous products consisted mainly of C₁-C₃ hydrocarbons, with methane being the most abundant on a molar basis. The *n*-pentane insoluble (asphaltenes and coke) content of the liquid product was determined. Products were also characterized using electron spin resonance (ESR) spectroscopy and proton nuclear magnetic resonance (¹H NMR) spectroscopy.

Control experiments were performed at 400 °C under 2 MPa nitrogen pressure for 30 and 60 minutes. The procedure and product characterization was the same as for the experiments that were performed with VR DAO and indene. These control experiments evaluated the reactions of indene, indan, naphthalene and mixtures of indene with indan and indene with naphthalene. The purpose of these control experiments was to assist with interpretation of observations based on reaction in VR DAO. Additionally the *n*-pentane soluble products from the control reactions were characterized by high temperature gas chromatography for simulated distillation and gas chromatography coupled with mass spectrometry for product identification. Prior to analysis, the excess *n*-pentane was evaporated using a rotary evaporator operated at 44 °C and atmospheric pressure.

5.2.3 Analyses

The *n*-pentane insoluble content was determined by mixing 2 g of reaction product with 80 mL of *n*-pentane. The mixture was stirred in a closed jar at room temperature for 1 hour and left to settle

for 23 hours before filtration. Filtration was done using 0.22 μm filter papers. The collected *n*-pentane insoluble precipitates were dried overnight in a fume hood until achieving a constant mass that was employed as a measure of complete drying. The mass of the dried *n*-pentane soluble material was recorded. The percentage of *n*-pentane insoluble material per gram VR DAO in the feed material was calculated. Both the *n*-pentane insoluble and *n*-pentane soluble fractions were further analyzed. The *n*-pentane insoluble material was not further sub-classified to differentiate asphaltenes and coke.

Proton nuclear magnetic resonance spectra were obtained by dissolving 100 mg of the product of each reaction in 700 μL of chloroform-D. The analysis was performed using a 60 MHz NMReady-60 spectrometer from Nanalysis Corporation. Analyses were the average of 32 scans with a scan delay of 20 seconds. The results were analyzed using MestReNova software. The shift values (δ) on the ppm-scale were used to classify the hydrogen as non-aromatic ($\delta < 4.2$ ppm) and aromatic ($\delta > 6.3$ ppm). In oil analysis the intermediate shift values are often associated with hydrogen bonded to olefinic groups.

The free radical content in the products was measured using an Active Spectrum Micro-ESR. For analysis, 20 mg of the sample was diluted in 600 μL toluene, i.e. 4 wt% analyte in toluene. The ESR spectrum was measured at 1.2 Gauss coil amplitude, a digital gain of 12 dB, and a microwave power of 10 mW. The analyses were the average of 7 scans with a sweep delay of 30 seconds. The quantification of the free radical content into number of spins per DAO was possible by the double integration of the ESR peak using a calibration curve of toluene in 2,2-diphenyl-1-picrylhydrazyl (DPPH). The double integration was done using the MicroESR software.

Simulated distillation analysis was performed using an Agilent 7890B high temperature gas chromatograph with a flame ionization detector and DB-HT-SIMDIS column (5 m \times 0.53 mm \times 0.15 μm). The injection volume was 0.5 μL using helium as carrier gas. Sample preparation involved dissolving 100 mg of the reaction product in about 12 g of CS_2 ; the exact mass of the reaction product and CS_2 measured and recorded at 0.1 mg readability. The temperature program started at 50 $^\circ\text{C}$ and temperature was increased at a rate of 15 $^\circ\text{C}/\text{min}$ to 425 $^\circ\text{C}$ at which temperature it was held constant for 10 minutes.

Gas chromatography coupled with mass spectroscopy was used to identify the compounds present in the *n*-pentane soluble reaction products from the control experiments with indene. The apparatus used was an Agilent 7820A coupled with 5977E mass spectrometer. Separation was performed on a HP-5 column (30 m × 0.25 mm × 0.25 μm) using helium as the carrier gas at a constant flow rate of 1 mL/min. The temperature program started at 80 °C, with a hold of time of 5 min, after which the temperature was increased by 5 °C/min up to 200 °C, then held for 2 min at 200 °C, and then increased again at a rate of 5 °C/min until 320°C. The injector is split/splitless and the split ratio is 100:1 with an injection volume of 1 μL.

Refractive index measurements were performed relative to air using the sodium D-line (589 nm) with an Anton Paar Abbemat 200 refractometer.

5.3 Results

5.3.1 Effect of indene on *n*-pentane insoluble content

The hypothesis that new asphaltenes are formed during thermal conversion by free radical addition reactions was tested. The VR DAO feed was spiked with indene, which is a species that is prone to free radical addition. Compared to the VR DAO, which is a vacuum residue fraction, indene is a low boiling species. The *n*-pentane insoluble content was measured after thermal conversion and shown in Figure 5.3.

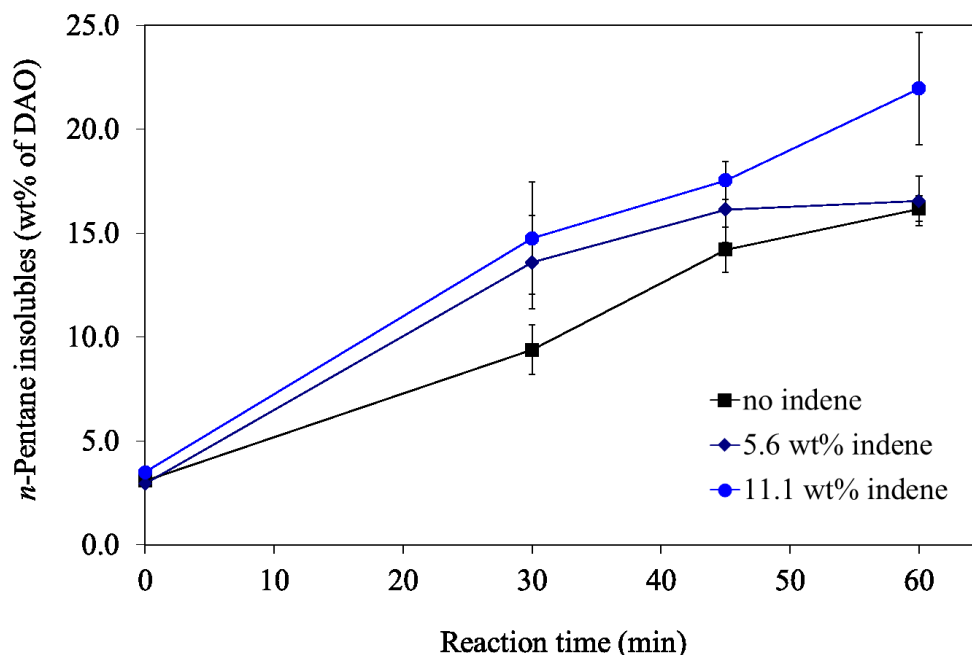


Figure 5.3. *n*-Pentane insoluble content after thermal conversion at 400 °C of VR DAO spiked with no indene (■), 5.6 wt% indene (◆) and 11.1 wt% indene (●). Error bars indicate one sample standard deviation.

In these experiments the *n*-pentane insoluble material was determined, which included both *n*-pentane insoluble asphaltenes and solid materials, i.e. mineral matter and carbonaceous deposits (coke). Only a small amount of mineral matter was present in the feed (Table 5.1). The control experiment with just VR DAO illustrated that new *n*-pentane insoluble material formed over time during thermal conversion, as mentioned in the introduction. When indene was added to the VR DAO, the amount of *n*-pentane insoluble material increased compared to that of VR DAO conversion on its own.

The differences that were observed in Figure 5.3, were not due to changes that took place in the feed prior to thermal conversion. The *n*-pentane insoluble content of the feed materials (Table 5.2) after preparation were confirmed by analysis. The average and sample standard deviation of analyses in triplicate were 3.1 ± 0.1 wt% of VR DAO for the VR DAO feed, 3.0 ± 0.1 wt% of VR DAO for the VR DAO with 5.6 wt% indene, and 3.5 ± 0.1 wt% of VR DAO for the VR DAO with 11.1 wt% indene. Mixtures of VR DAO and indene were stable at ambient conditions for the duration of handling prior to experiments.

A series of control experiments with model mixtures were also performed to better evaluate the results in Figure 5.3. These experiments are reported in Sections 5.3.4 and 5.3.5.

5.3.2 ^1H NMR characterization of products

The hypothesis to explain asphaltenes formation by free radical addition anticipated that hydrogen transfer would take place (Figure 5.1). In order to track changes in the chemical nature of the hydrogen in the products, the products were analyzed by ^1H NMR spectrometry. No peaks were observed in the δ 4.2–6.3 ppm range. For the thermal conversion of VR DAO, with no indene being added, it can be seen that there is a monotonic decrease in the amount of non-aromatic hydrogen with a concomitant increase in the amount of aromatic hydrogen (Figure 5.4). The relative increase in aromatic content between the feed and product after one hour of conversion at 400 °C was 51 %.

Indene has an equal amount of non-aromatic and aromatic hydrogen. However, the hydrogen atoms associated with the olefinic group in the 5-membered ring have ^1H NMR shift values of $\delta_{\text{H-3}} = 6.856$ and $\delta_{\text{H-2}} = 6.498$ ppm respectively.²⁶ The H-3 hydrogen is the hydrogen adjacent to the aromatic. These ^1H NMR shift values were experimentally verified by analysis of the indene feed material.

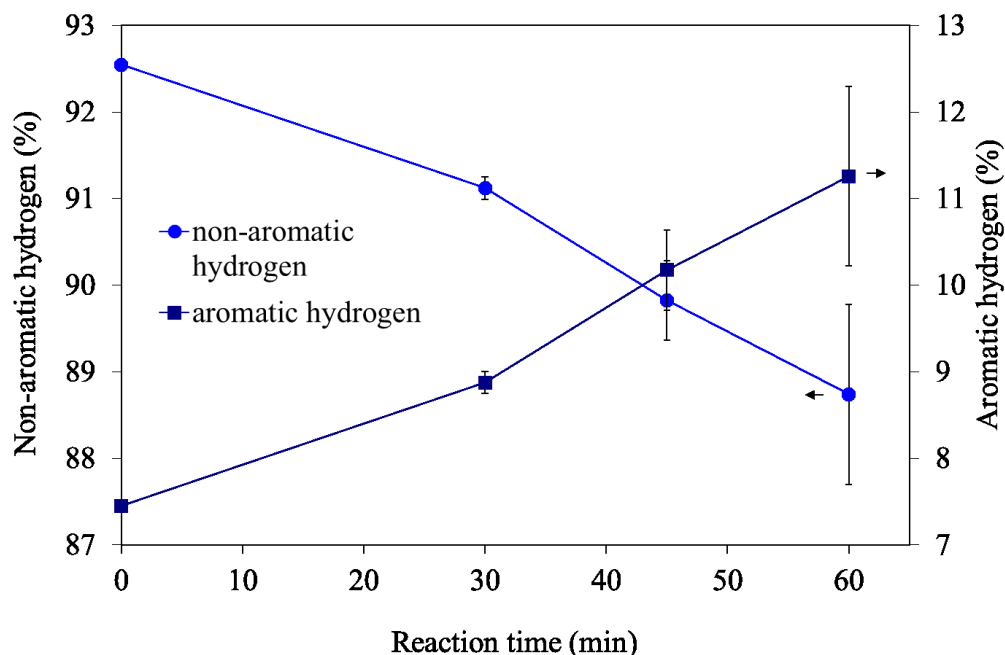


Figure 5.4. Change in the distribution of non-aromatic hydrogen (●) and aromatic hydrogen (■) due to thermal conversion at 400 °C of VR DAO. Error bars indicate one sample standard deviation.

The simple classification of non-aromatic hydrogen ($\delta < 4.2$ ppm) and aromatic hydrogen ($\delta > 6.3$ ppm) provided a poor indication of the nature of the hydrogen when applied to indene. Using the simple classification, the two olefinic hydrogen atoms in indene would be counted as aromatic hydrogen atoms in the ^1H NMR analysis, since both have shift values $\delta > 6.3$ ppm. As a consequence, when the VR DAO feed was spiked with indene (Table 5.2), the overall hydrogen content of the feed that was classified as non-aromatic decreased and the aromatic hydrogen content increased.

The change of the aromatic hydrogen content with reaction time for thermal conversion of the VR DAO feed spiked with indene is shown in Figure 5.5. This is the same trend as the trend that was observed in Figure 5.4 for thermal conversion of VR DAO on its own. The same but opposite trend is seen for the non-aromatic hydrogen content that decreased monotonically with an increase in reaction time (not shown). The ^1H NMR shift values for hydrogen associated with olefins span a wide range, with most of the olefin hydrogen in hydrocarbons being in the δ 4.2–6.3 ppm range.²⁷

No peaks were observed in the δ 4.2–6.3 ppm range of the ^1H NMR spectrum. The relative increase in aromatic hydrogen content between the feed and product after one hour of conversion at 400 °C was 33 % for VR DAO with 5.6 wt% indene and 23 % for VR DAO with 11.1 wt% indene. These changes were relative to a higher aromatic content in the feed than for VR DAO on its own.

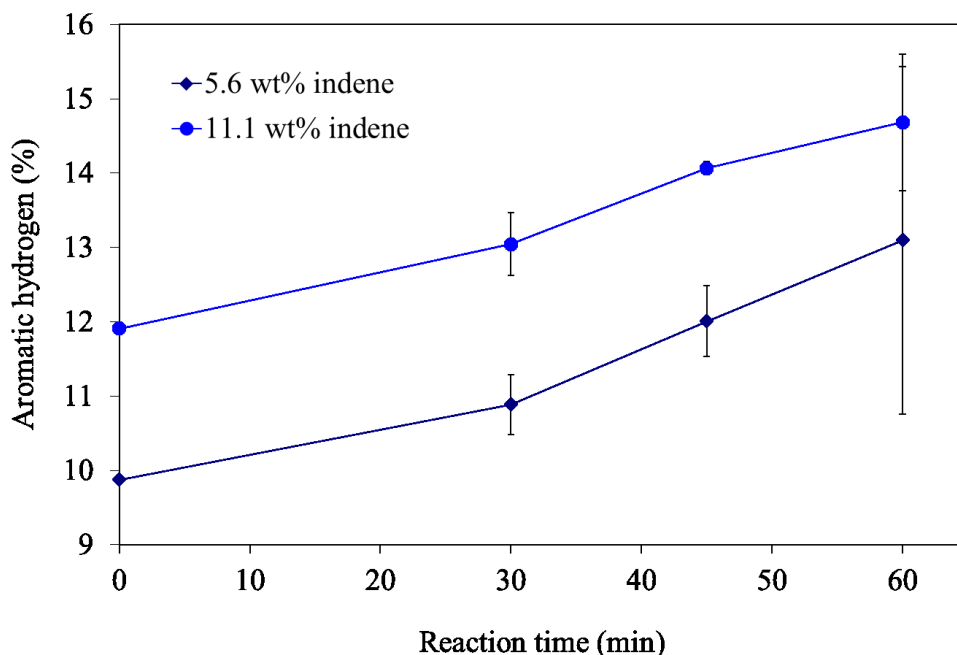


Figure 5.5. Change in the aromatic hydrogen content of VR DAO spiked with 5.6 wt% indene (◆) and 11.1 wt% indene (●) due to thermal conversion at 400 °C. Error bars indicate one sample standard deviation.

The interpretation of the ^1H NMR results in Figure 5.5 is complicated by the shift values of the olefinic hydrogen in indene ($\delta = 6.9$ and 6.5 ppm), which caused these hydrogen atoms to be counted as aromatic hydrogen using the simple classification employed. After reaction of the indene, the chemical environment of the olefinic hydrogen will change. When the indene is involved in an addition reaction, the reaction product could donate hydrogen leading to olefin formation, or it could accept hydrogen to become saturated. The observed aromatic hydrogen content, which also include the olefinic hydrogen associated with indene-type olefinic groups, becomes sensitive to the outcome of the reactions indene is involved in.

5.3.3 ESR characterization of products

Feed characterization (Table 5.1) confirmed the presence of free radicals in the VR DAO feed. It was of interest to see whether thermal conversion also resulted in a change in the free radical content of the product. The free radical content of the products after thermal conversion was quantified (Table 5.3). The sample standard deviation indicated is a measure of the variance in measurement of samples from repeat experiments.

The first observation that can be made from the data in Table 5.3 is that the free radical concentrations in the products are higher than in the VR DAO feed material. The analyses were performed at near similar analyte concentration and the differences could be compared directly. These differences were not large and were at most double. The largest difference was between the reaction product after 30 min reaction with 11.1 wt% indene, 1.8×10^{18} spins/g, compared to 0.9×10^{18} spins/g in the VR DAO feed.

Table 5.3. Free radical content in products after thermal conversion at 400 °C for the reaction times indicated.

Feed material	Free radical content after conversion (10^{18} spins/g VR DAO) ^a					
	30 min		45 min		60 min	
	x	s	x	s	x	s
VR DAO	1.4	0.1	1.5	0.2	1.2	0.0
VR DAO with 5.6 wt% indene	1.2	0.1	1.5	0.2	1.2	0.1
VR DAO with 11.1 wt% indene	1.8	0.1	1.7	0.3	1.6	0.1

^a Average (x) and sample standard deviation (s) of samples from triplicate experiments.

The second observation is that it appears that the free radical content passed through a maximum as the reaction progressed. This observation is more speculative, partly due to the limited data and partly due to the uncertainty indicated by the sample standard deviation. Nevertheless, the VR DAO feed clearly had a lower free radical content than the products and the results indicate that the reaction products after 60 min (Table 5.3) had the lowest free radical content of the converted products.

The data in Table 5.3 also indicated that the products after thermal conversion of the feed material containing a larger amount of indene, i.e. 11.1 wt% indene, had a higher free radical content. The difference is small, within one standard deviation of uncertainty, and statistical confidence in the observation is low. Yet, Figure 5.3 suggested that there might be value to this observation, because the *n*-pentane insoluble content increased due to the addition of 11.1 wt% indene.

The *n*-pentane insoluble fraction that was separated from each of the thermally converted products was analyzed by ESR spectroscopy (Table 5.4). The relative contribution of the VR DAO and indene to *n*-pentane insoluble formation was not known, nor was the amount of *n*-pentane insoluble material the same (Figure 5.3). The results were therefore expressed in terms of spins/g *n*-pentane insoluble material and results were not expressed on a VR DAO feed basis as in the case of Table 5.3.

Table 5.4. Free radical content in *n*-pentane insoluble (asphaltenes) fraction separated from the products after thermal conversion at 400 °C for the reaction times indicated.

Feed material	Free radical content after conversion (10^{18} spins/g) ^a					
	30 min		45 min		60 min	
	x	s	x	s	x	s
VR DAO	3.3	0.7	3.0	2.3	1.5	0.0
VR DAO with 5.6 wt% indene	1.4	0.2	2.2	1.0	1.7	0.3
VR DAO with 11.1 wt% indene	4.1	0.8	2.9	1.3	2.0	0.5

^a Average (x) and sample standard deviation (s) of samples from triplicate experiments.

Similar observations could be made for the free radical content of the *n*-pentane insoluble fractions as for the total products from thermal conversion. The free radical content of the *n*-pentane insoluble material was higher than that of the total product, the free radical content passed through a maximum as reaction progressed, and the *n*-pentane insoluble material obtained from thermal conversion of a feed with 11.1 wt% indene had a higher free radical content.

5.3.4 Refractive index measurement of products

A technique that is useful to measure changes in high boiling mixtures is refractive index. Composition, density, and average molecular mass all affect refractive index. The refractive index measurements of the reaction products are presented in Figure 5.6.

Three observations follow from the results in Figure 5.6. (i) There was a small change in the refractive index due to the thermal conversion of VR DAO; the refractive index of the product decreased slightly with reaction time. (ii) There was considerable sample-to-sample variation in the composition of the products from repeat experiments. The standard deviation of repeat measurements of the refractive index of the same material is usually an order of magnitude lower than was observed for the thermally converted products. (iii) The product from 30 min thermal conversion of VR DAO with 11.1 wt% indene had a meaningfully higher refractive index than any of the other materials, i.e. refractive index passed through a maximum as reaction progressed.

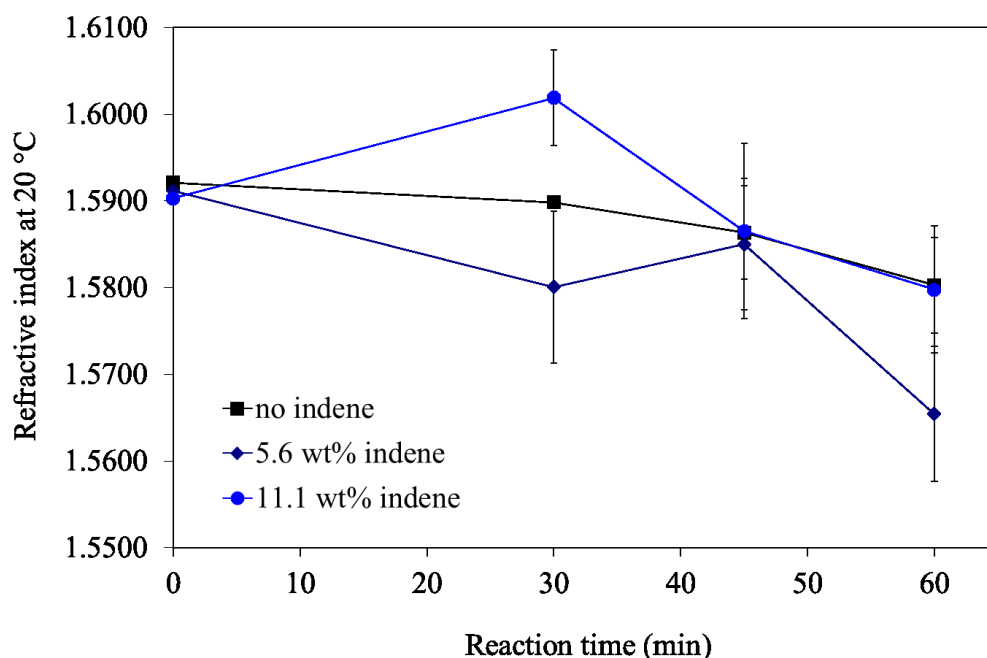


Figure 5.6. Refractive index of total product after thermal conversion at 400 °C of VR DAO spiked with no indene (■), 5.6 wt% indene (◆) and 11.1 wt% indene (●).

Local maxima in the refractive index values for the VR DAO and indene mixtures (Figure 5.6) coincided with local maxima in free radical content (Table 5.3).

5.3.5 Self-reaction of indene

As was postulated in the introduction, indene contributed to formation of *n*-pentane insoluble material during thermal conversion of VR DAO (Figure 5.3). It was also postulated that the way in which *n*-pentane insoluble material was formed was due to an increase in molecular mass caused by free radical addition reactions. If this was indeed the case, then one would anticipate to see evidence of such addition reactions during the thermal conversion of indene on its own.

Control experiments were performed with indene at 400 °C and the results are presented in Table 5.5. Self-reaction of indene at 400 °C caused extensive formation of *n*-pentane insoluble material, with 83 wt% *n*-pentane insoluble material formed after 60 min of thermal conversion.

Table 5.5. Results from the self-reaction of indene by thermal conversion at 400 °C for 30 and 60 min.

Description	Reaction products	
	30 min	60 min
<i>n</i> -pentane insoluble content (wt%)	45	83
nature of hydrogen (%)		
non-aromatic	47	44
aromatic	53	56
free radical content (10^{18} spins/g)		
total reaction product	1.0	1.3
<i>n</i> -pentane insoluble product	1.1	1.1

It was possible to analyze the *n*-pentane soluble fraction after self-reaction of indene by gas chromatography, because indene is a kerosene-range boiling material. Almost no indene remained in the reaction product and the most abundant product after 60 min reaction time that was found in the *n*-pentane soluble fraction was indan. Apart from indan and indene, the products identified

by GC-MS could be grouped into three broad categories. (i) Ring-opened alkylbenzene derivatives with alkyl groups in the C₂–C₄ range. (ii) Dimerization products with a molecular formula of C₁₈H₁₈. (iii) Dimerization products leading to the formation of intramolecular ring-closure to produce multinuclear aromatic species. The formation of products described in (ii) and (iii) were also reported for high temperature self-reaction of indene.²⁸

Some heavier products that could not be eluted and identified using GC-MS analysis could be detected using high temperature gas chromatography. The simulated distillation curves of the reaction product after 30 min (not shown) and 60 min (Figure 5.7) were similar. The simulated distillation analysis showed that the *n*-pentane soluble fraction after 60 min reaction contained about 20 wt% heavier products with normal boiling points in the range 450–700 °C. The reaction product after 30 min reaction contained about 12 wt% material in the 450–700 °C boiling range. Based on the step-type shape of the distillation curve in Figure 5.6, it is inferred that the >450 °C boiling material are products from tri- and tetramerization of indene, analogous to the products from dimerization of indene that could be identified by GC-MS analysis.

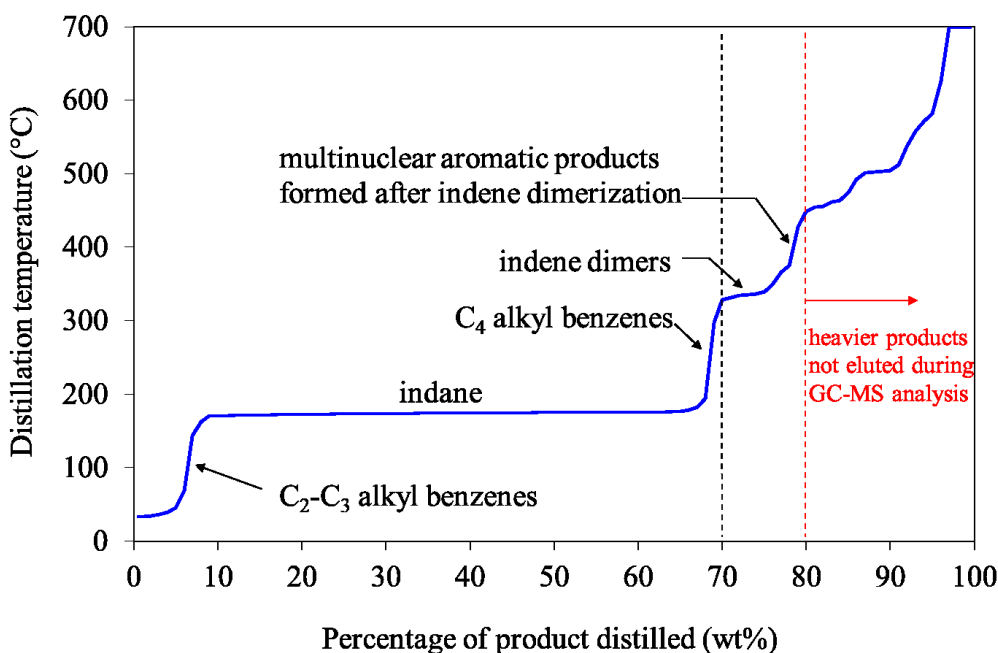


Figure 5.7. Simulated distillation of *n*-pentane soluble product after thermal conversion of indene at 400 °C for 60 min.

More than half of the total *n*-pentane soluble fraction was indan. In the simulated distillation analysis (Figure 5.7) indan is represented by the large near isothermal section with a distillation temperature in the range 170–180 °C. The normal boiling point of indan is 177 °C.²⁵ A summary of the product distribution based on material balance and simulated distillation analysis is presented in Table 5.6.

Table 5.6. Product distribution from self-reaction of indene at 400 °C for 30 and 60 min reaction time.

Product description	Product distribution (wt%)	
	30 min	60 min
<i>n</i> -pentane soluble material		
indene	~ 0	~ 0
indan	35	10
alkyl benzenes	7	2
dimerization products (325-450 °C)	7	2
tri- and tetramerization products	6	3
<i>n</i> -pentane insoluble material ^a	45	83

^a Repeated from Table 5.5.

5.3.6 Impact of dilution on reaction of indene

It was suspected that the extent of addition reactions was partly due to the abundance of indene, which was susceptible to both free radical addition and hydrogen transfer. Another set of control experiments was performed. The indene was mixed in the same mass ratios with indan and naphthalene respectively as substitutes for the VR DAO so that the ratios were the same as shown in Table 5.2. Indan represented a species that could act as a hydrogen donor, but that was also susceptible to addition reactions as a consequence of hydrogen transfer. Naphthalene represented a hydrogen deficient species.

The self-reaction of indan and naphthalene was checked by heating each to 400 °C for 60 min. No *n*-pentane insoluble material was formed by either indan, or naphthalene when they were heated

on their own (Table 5.7). Simulated distillation analyses of the products from self-reaction of indan and naphthalene resulted in final boiling point temperatures at complete recovery of 180 and 212 °C respectively. This indicated that there was no material that was heavier boiling than the starting materials in the products from thermal conversion of indan and naphthalene.

Table 5.7. *n*-Pentane insoluble content after thermal conversion of model mixtures at 400 °C for the reaction times indicated.

Feed material	<i>n</i> -Pentane insoluble content (wt%)	
	30 min	60 min
Indan	-	0 ^a
Indan with 5.6 wt% indene	0 ^a	0 ^a
Indan with 11.1 wt% indene	0 ^a	0.4
Naphthalene	-	0 ^a
Naphthalene with 5.6 wt% indene	0 ^a	0 ^a
Naphthalene with 11.1 wt% indene	0 ^a	3.0

^a Completely soluble in *n*-pentane.

When indan and naphthalene was mixed with indene, at most of the test conditions no *n*-pentane insoluble material was formed (Table 5.7); *n*-pentane insoluble material was found only after 60 min reaction time at 400 °C with mixtures containing 11.1 wt% indene. The amount of *n*-pentane insoluble material formed in the mixture of 11.1 wt% indene with indan was 0.4 wt%, whereas the amount of *n*-pentane insoluble material formed in the mixture of 11.1 wt% indene with naphthalene was 3.0 wt%. These were equivalent to 3.6 and 27 wt% of indene converted to asphaltenes, which were lower than the 83 wt% (Table 5.5) during the self-reaction of indene. Dilution of indene appeared to reduce the number of propagation steps before chain transfer or chain termination took place. Indan was more effective at reducing asphaltenes formation than naphthalene, possibly because it has transferable hydrogen that facilitated chain transfer.

Simulated distillation analysis of the *n*-pentane soluble material showed that there was some *n*-pentane soluble addition products formed after thermal conversion of indene and indan mixtures (Figure 5.8). However, no evidence of *n*-pentane soluble addition products was found in mixtures of indene and naphthalene (Figure 5.8).

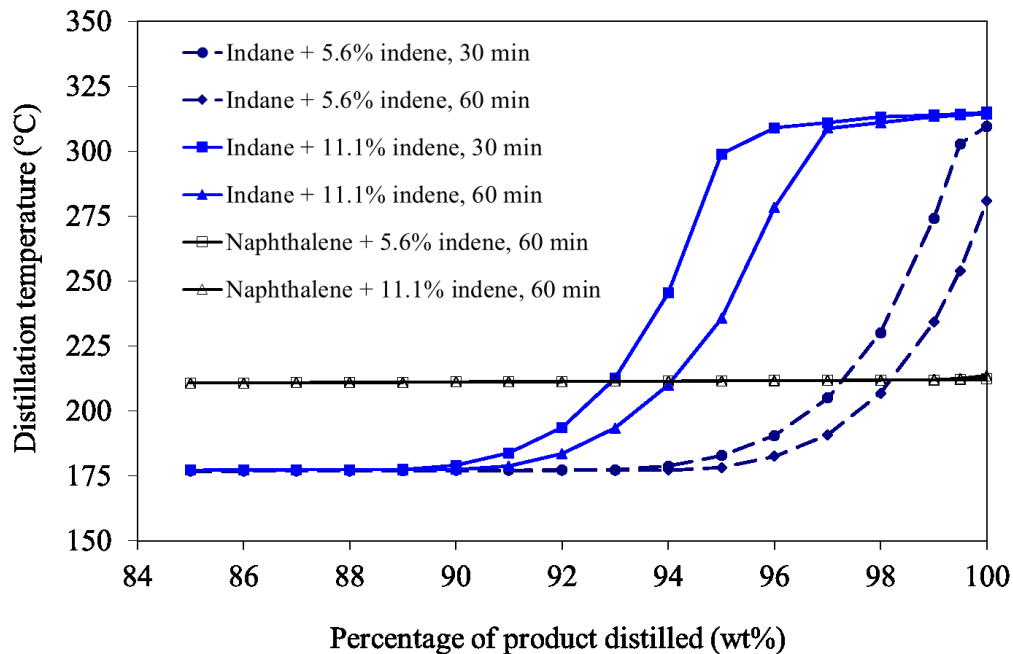


Figure 5.8. Heavy product formation indicated by simulated distillation analysis of the *n*-pentane soluble products after thermal conversion of indene-containing model mixtures at 400 °C.

The GC-MS analysis of the *n*-pentane soluble products from thermal conversion of indan and indene mixtures indicated that the heavier products were found at retention times between 29 and 36 min. This is illustrated by Figure 5.9. The nature of the products from thermal conversion of all indan and indene mixtures contained the products shown in Figure 5.9. The most abundant heavier products were of the molecular formula $C_{18}H_{18}$. A molecular formula of $C_{18}H_{18}$ suggested that these were dimerization products of indene (C_9H_8) and indan (C_9H_{10}). Minor products with molecular formulas of $C_{18}H_{16}$ and $C_{18}H_{12}$ were also found.

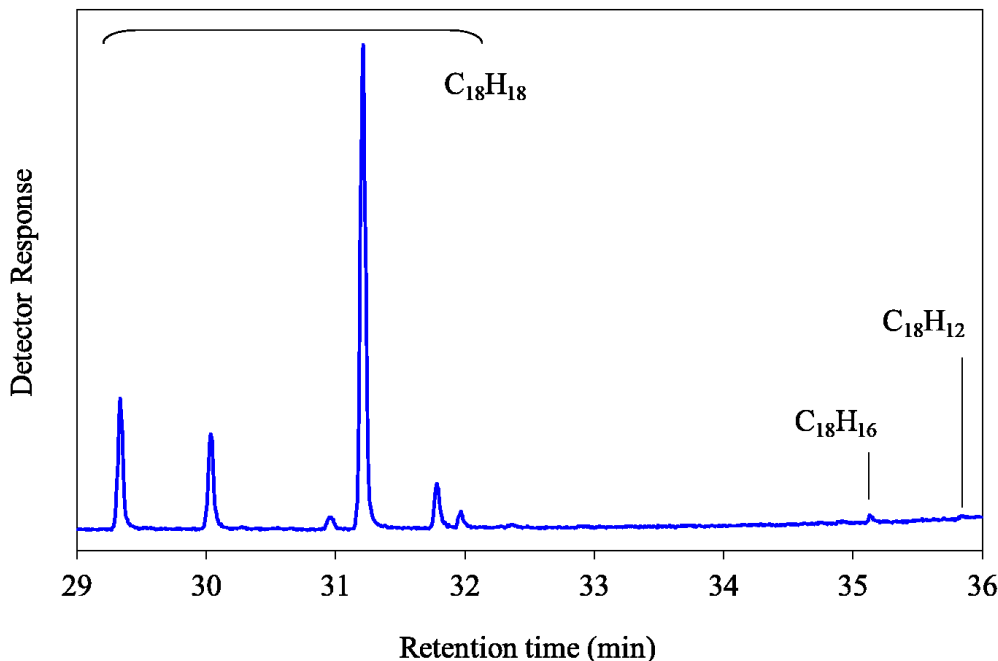


Figure 5.9. Section of the chromatogram from the GC-MS analysis of *n*-pentane soluble product after thermal conversion of an indan with 5.6 wt% indene mixture at 400 °C for 30 min.

The analysis also indicated that indene in the 11.1 wt% indene and indan mixture was substantially converted. The ratio of indene to indan in the feed was 1:8 and after 60 min reaction this ratio changed to 1:30.

Analysis of *n*-pentane soluble products from thermal conversion of naphthalene and indene mixtures by GC-MS confirmed the absence of dimerization products. This corroborated the findings based on the simulated distillation analysis (Figure 5.8) that did not reveal heavier *n*-pentane soluble products. There was no evidence of products from ring-opening of indene.

The total liquid product after thermal conversion of each model mixture was analyzed using 1H NMR and ESR spectroscopy. Little change was seen in the 1H NMR spectra, which was consistent with the minor extent of heavy and *n*-pentane insoluble product formation in the model mixtures. The ESR results showed the presence of $0.5\text{--}0.7 \times 10^{18}$ spins/g of free radicals in the products from thermal conversion of mixtures of naphthalene with 11.1 wt% indene (Table 5.8).

Table 5.8. Free radical content in the total reaction product after thermal conversion of the model mixtures at 400 °C for the reaction times indicated.

Feed material	Free radical content (10^{18} spins/g)	
	30 min	60 min
Indan	-	0 ^a
Indan with 5.6 wt% indene	0 ^a	0 ^a
Indan with 11.1 wt% indene	0 ^a	0 ^a
Naphthalene	-	0 ^a
Naphthalene with 5.6 wt% indene	0 ^a	0 ^a
Naphthalene with 11.1 wt% indene	0.5	0.7

^a None detected and if present was below the detection limit.

All of the reaction products were analyzed using ESR. If free radicals were present in the other products, the concentration was below the detection limit of the instrument, which was of the order 10^{16} spins/g at the sample concentration analyzed.

5.4 Discussion

5.4.1 Heavier product formation during thermal conversion

Thermal conversion of deasphalted oil at 400 °C produced new *n*-pentane insoluble material (Figure 5.3). The industrial VR DAO was not completely free of asphaltenes, but the increase in asphaltenes content was clear and substantial, the *n*-pentane insoluble content increase from 3 to 16 wt% over a reaction period of 60 min.

It has long been recognized that addition reactions, often called condensation reactions, were taking place during thermal conversion in visbreaking processes. For example, Sachanen⁴ wrote: “The formation of high-boiling polycyclic and polymerized hydrocarbons takes place ... These reactions are responsible for the formation of cracked residues boiling above the end point of the original cracking stock.” Heavier boiling material is not necessarily *n*-pentane insoluble, although an increase in boiling point due to an increase in molecular mass increases the likelihood of the materials becoming *n*-pentane insoluble.⁹

The formation of addition products by several model compounds under thermal cracking conditions has been reported in the literature, for example, pyrolysis of *n*-hexadecane,^{29,30} *cis*-decalin,³¹ 1-methylnaphthalene,³² *n*-hexadecane in tetralin, benzene and toluene.^{18,33} There were also some reports on addition reactions of heavy molecules that can be considered precursors to asphaltenes or asphaltenes surrogates.^{17,34}

The fact that addition reactions can and do take place under thermal cracking conditions has been established. This study provided additional corroboration that addition products were formed during thermal conversion at 400 °C, adding indene to the list of model compounds for which addition product formation was reported. Direct evidence of addition product formation was shown by the chromatography results presented in Table 5.6 and Figures 5.7 to 5.9.

5.4.2 Contribution of indene to asphaltenes formation in VR DAO

The reactions involving VR DAO spiked with indene suggested that indene contributed to the formation of asphaltenes (Figure 5.3). Indirect evidence of addition product formation was shown in Figure 5.6, where the refractive index of the products from thermal conversion of VR DAO with 11.1 wt% indene passed through a maximum that was higher than that of the feed.

However, the extent of asphaltenes formation by self-reaction of indene was high (Table 5.5). In addition to uncertainty indicated by standard deviation, the effect of dilution also has to be taken into account, as well as the reactivity of the asphaltenes.^{35,36} Asphaltenes in the VR DAO feed and new asphaltenes formed by reaction could potentially be converted under the reaction conditions investigated. Several possibilities were considered.

The first possibility that was considered was that indene had no impact on asphaltenes formation in VR DAO and that the amount of *n*-pentane insoluble material observed was the sum of asphaltenes produced independently by indene and VR DAO.

The 30 min reaction with 5.6 wt% indene in VR DAO (Figure 5.3) could not be explained in this way. The observed asphaltenes content was 13.6 wt%, but for VR DAO it was only 9.4 wt% and the potential contribution of indene self-reaction was only 2.5 wt% (45×0.056), i.e. $(9.4 \times 0.944 + 45 \times 0.056) = 11.4 < 13.6$. If the dilution effect was to be considered, the contribution of indene in the *n*-pentane insoluble content formation in “indene-DAO matrix” would be 0 wt% instead of 2.5 wt%. At the same conditions and concentration as used in this example, no *n*-pentane insoluble material was detected after 30 min reaction neither with indane nor with naphthalene (Table 5.7).

When taking dilution into account, the 30 and 60 min reaction with 11.1 wt% indene in VR DAO (Figure 5.3) would also serve as examples that could not be explained by independent reactions in parallel. The maximum contribution of indene self-reaction at 11.1 wt% was 3.0 wt% (Table 5.7). To illustrate the point, the *n*-pentane insoluble content after 60 min reaction of 11.1 wt% indene in VR DAO was 22.0 wt%, compared to VR DAO on its own that was 16.2 wt% (Figure 5.3), i.e. $(16.2 \times 0.889 + 3.0) = 17.4 < 22.0$.

The second possibility that was considered was that indene induced increased asphaltenes formation by VR DAO, but the new *n*-pentane insoluble material that formed was formed only by reaction of species in VR DAO. This would be analogous to the formation of biphenyl from benzene when thermally cracked in the presence of a small amount of *n*-hexadecane,¹⁸ as mentioned in the introduction.

This study did not provide direct evidence for the presence or absence of indene incorporation in the *n*-pentane insoluble material from thermal conversion of VR DAO and indene mixtures. To do so would require experiments with isotopically labeled indene. However, considering the extent of *n*-pentane insoluble material from self-reaction of indene (Table 5.5) and even in dilute solution (Table 5.7) it appears unlikely that indene would only induce increased asphaltenes formation by VR DAO.

Furthermore, it was shown that thermal conversion of indene diluted in naphthalene did *not* produce binaphthyl, contrary to the reported formation of biphenyl resulting from thermal conversion of *n*-hexadecane in benzene.¹⁸ The products identified after thermal conversion of

indene diluted in indan (Figure 5.9) included several $C_{18}H_{18}$ species that suggested dimerization of indene with indan took place. These observations support the view that it is unlikely that indene would only induce increased asphaltene formation without participating in asphaltene formation.

The third possibility that was considered was that the addition of indene to species in VR DAO caused an increase in *n*-pentane insoluble material beyond that from either indene self-reaction or VR DAO self-reaction.

The present study provided evidence, to suggest that this might be the case. Although it was not demonstrated that the indene formed addition products with VR DAO, doing so would be an important step towards establishing a link between free radical addition of model compounds and addition reactions to heavy oil fractions leading to asphaltene formation.

5.4.3 Reaction of indene

The self-reaction of indene resulted in surprisingly high yield of *n*-pentane insoluble material within 60 min at 400 °C (Table 5.5). How did indene initiation take place?

Indene has a hydrogen disproportionation pathway that can lead to the formation of two benzylic radicals, shown as pathway (i) in Figure 5.10, but indene does not have a C–C bond that can readily crack, as shown in pathway (ii). Initiation of indene by hydrogen disproportionation appears to be an example of molecule induced homolysis.

Once hydrogen disproportionation takes place, it is likely to lead to the formation of indan by further reaction of the indene molecule that acted as hydrogen acceptor. As anticipated, indan was detected in the *n*-pentane soluble product (Table 5.6).

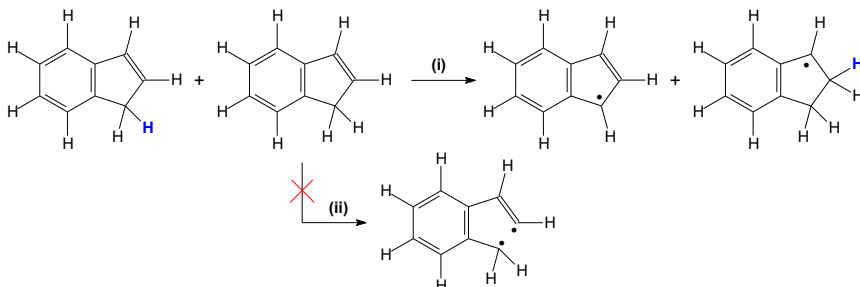


Figure 5.10. Free radical formation by indene by (i) hydrogen disproportionation, but not by (ii) homolytic bond dissociation.

Over time indan could also be thermally converted, as observed from the decrease in the amount of indan in the reaction product from indene self-reaction (Table 5.6). Evidence of the conversion of some indan was also seen in the control reactions with indan and indene mixtures. The major dimerization product was $C_{18}H_{18}$ (Figure 5.9), which was too hydrogen rich to be an indene (C_9H_8) dimer. Only a minor amount of $C_{18}H_{16}$ was found, which corresponds to an indene dimer. The presence of multiple isomers of $C_{18}H_{18}$ (Figure 5.9) suggest that the dimerization reaction is not as specific as shown in Figure 5.10 and that the free radical position is not necessarily on the benzylic carbon as one would anticipate from resonance stabilization.

Another important observation that stems from the conversion of indan with indene, is that it showed that the addition of indene to a molecule with transferable hydrogen could take place, or that indene could induce an addition reaction involving a molecule with transferable hydrogen.

Indan on its own was not thermally converted at 400 °C. The C–C bonds in the 5-membered cycloalkane ring of indan was therefore not susceptible to thermally induced homolysis over the time period studied. In the initial absence of a hydrogen acceptor in the self-reaction of indan, hydrogen transfer was not possible. It also provided corroboration that pathway (ii) in Figure 5.10 was not measurably taking place.

The near complete conversion of indene during self-reaction at 400 °C was observed within 30 min reaction time (Table 5.6). Initiation by hydrogen disproportionation must therefore be a fast process. To put this into context, when tetralin was thermally converted at 400 °C it took 18 h to reach 1 % conversion.³⁷ Tetralin on its own, like indan, could only be converted by thermally

induced homolysis of the C–C in the cycloalkane ring. Homolytic bond dissociation of tetralin at 450 °C was more prevalent and at 450 °C tetralin conversion proceeded after an induction period that is typical of slow free radical initiation.³⁸ A comprehensive discussion on tetralin pyrolysis and pyrolysis kinetics can be found in the paper by Poutsma.³⁹ Initiation by C–C cracking is clearly a much slower process than hydrogen disproportionation as found in reaction with indene.

In dilute solution, indene was still substantially converted. In the control experiments with indan-indene and naphthalene-indene mixtures, there was little unconverted indene left after 60 min at 400 °C. Molecule induced homolysis took place, but there was slower formation and an overall decrease in *n*-pentane insoluble material when the indene was diluted in indan and naphthalene (Table 5.7). It appears that dilution reduced the number of addition steps that took place before chain transfer or chain termination took place, which reduced the amount of *n*-pentane insoluble material. The more significant reduction in *n*-pentane insoluble material when indene was diluted with indan compared to naphthalene (Table 5.7) can be explained by hydrogen transfer from indan that caused chain transfer. The same reaction was not likely in the presence of naphthalene and no evidence was found to indicate that naphthalene transferred hydrogen, i.e. no naphthalene-containing addition products were detected. This will be further explained in section 5.4.4.

The absence of naphthalene-containing addition products was contrary to what was anticipated from literature, where benzene-containing addition products were found under comparable conditions during *n*-hexadecane cracking in benzene.¹⁸

5.4.4 Impact of bulk liquid properties on free radical combination

The *n*-pentane insoluble content (Table 5.7) obtained from the reaction of indene in indan, versus the reaction of indene in naphthalene, suggested that the properties of the bulk liquid had an impact on the chemistry. In other words, the ability of indene to form molecular growth compounds in different media was different in different media even when indene was present at the same concentration.

When indan, a molecule able to donate hydrogen, was abundant in the bulk liquid, the indene was less likely to form chain growth compounds. This was mainly due to the ability of indan with transferable hydrogen to cause chain transfer. Therefore, the probability of terminating chain growth of one chain by hydrogen transfer leading to start of a new chain was increased relative to ongoing chain growth by bonding to another indene or indan radical.

On the other hand, when indene was converted in a mixture with naphthalene, which did not have hydrogen to donate, it “unintentionally” led to more chain growth. When naphthalene does not donate hydrogen to an indene radical to terminate chain growth, it enables the indene radical to persist until it can interact with another indene molecule or radical. This increases the probability of chain growth compared to chain growth in a medium where chain transfer can occur more readily.

This explanation is in accordance with the observed free radical content (Table 5.8), where free radicals were detectable only when indene was reacted in naphthalene, which caused more *n*-pentane insoluble products to be formed. The ability of indan to limit chain growth is higher and the free radicals in products were less than 10^{16} spins/g, which was not the case when naphthalene was the most abundant substance in the bulk liquid.

To put these observations into perspective, DAO contained material with transferable hydrogen and potentially also transferable methyl groups. It is speculated that methyl transfer may occur, like hydrogen transfer. This was not studied in the present work but has been covered by the work by Peña et al.⁴⁰ dealing with the formation of soot. Irrespective, one would anticipate that the reaction of indene in DAO would resemble the behavior observed during the reaction of indene in indan and not naphthalene, i.e. chain growth of indene would be suppressed and indene would be less likely to form heavier products. Yet, when indene was reacted in DAO, the amount of *n*-pentane insoluble material increased (Figure 5.3).

It is worthwhile keeping in mind that when DAO is abundant in the bulk liquid, not only hydrogen transfer is possible. Other functional groups and radicals in the DAO might add to the indene radical and DAO may also affect the rate of diffusion of indene. Whether indene increased free

radical formation in DAO due to chain transfer reactions, or whether indene was incorporated into the heavier products formed in the presence of DAO, was not resolved by this study. However, considering the control experiments with indene in indan and naphthalene, it appeared unlikely that self-reaction of indene would be responsible for the increased *n*-pentane insoluble content during the thermal conversion of indene and DAO mixtures.

5.4.5 Implications for modelling of thermal conversion

The experiments with model compounds and model mixtures demonstrated that addition reactions took place at 400 °C. The reactions could be as simple as dimerization (Figure 5.9), but could also form heavier products (Figure 5.7). It was possible to form *n*-pentane insoluble products (Tables 5.5 and 5.7). Differently put, distilled boiling range materials could be thermally converted to material in the vacuum gas oil and vacuum residue boiling range, as well as products that were *n*-pentane insoluble asphaltenes. With VR DAO as feed, on its own and with indene, new asphaltenes were formed (Table 5.3).

The formation of heavier products can be transient (Figure 5.6), with heavier products again being thermally converted to lighter products. However, the work suggested that models that include terms for heavier product formation, e.g.^{23,24}, reflect the reaction chemistry better. Whether the explicit inclusion of addition reactions in visbreaking models was necessary for an adequate description of visbreaking, was not determined.

The present work also highlighted the importance of hydrogen transfer, including molecule-induced homolysis leading to hydrogen transfer by the self-reaction of indene, as well as reaction of indene in model mixtures with indan and naphthalene.

The importance of hydrogen transfer in cracking kinetics was recognized in some cracking models, for example, the coal pyrolysis model developed by LaMarca, Libanati, Klein, and Cronauer.⁴¹ Evidence of both hydrogen donation and hydrogen accepting behavior has been reported with heavy petroleum fractions,^{42,43,44} and the same is anticipated of VR DAO. Evidence of hydrogen

transfer during thermal conversion of VR DAO can be seen by the decrease in non-aromatic hydrogen content and increase in aromatic hydrogen content with reaction time (Figure 5.4).

5.5 Conclusions

It was shown that new *n*-pentane insoluble material (asphaltenes) was formed during the thermal conversion of VR DAO at 400 °C. The formation of new asphaltenes was increased when VR DAO was converted at the same conditions in the presence of indene.

The self-reaction of indene showed that indene on its own was capable of forming asphaltenes, but that the extent of asphaltenes formation was reduced on diluting the indene. The reduction in asphaltenes formation was more in indan, which has transferable hydrogen, than in naphthalene. This was consistent with reaction chemistry based on molecule-induced homolysis, free radical addition, and propagation / termination by hydrogen transfer.

The prevalence of addition reactions and the importance of hydrogen transfer were highlighted by the work. These observations have implications for representing the reaction chemistry to model thermal conversion of heavy oils.

Literature cited

- (1) León, A. Y.; Guzman, A.; Laverde, D.; Chaudhari, R. V.; Subramaniam, B.; Bravo-Suárez, J. J. Thermal Cracking and Catalytic Hydrocracking of a Colombian Vacuum Residue and Its Maltenes and Asphaltenes Fractions in Toluene. *Energy and Fuels* **2017**, *31* (4), 3868–3877.
- (2) Pevneva, G. S.; Voronetskaya, N. G.; Korneev, D. S.; Golovko, A. K. Mutual Influence of Resins and Oils in Crude Oil from the Usinskoe Oilfield on the Direction of Their Thermal Transformations. *Pet. Chem.* **2017**, *57* (8), 739–745.
- (3) Raseev, S. *Thermal and Catalytic Processes in Petroleum Refining*; Marcel Dekker: New York, 2003.
- (4) Sachanen, A. N. *Conversion of Petroleum: Production of Motor Fuels by Thermal and Catalytic Processes*, 2nd ed.; Reinhold: New York, 1948.
- (5) Joshi, J. B.; Pandit, A. B.; Kataria, K. L.; Kulkarni, R. P.; Sawarkar, A. N.; Tandon, D.; Ram, Y.; Kumar, M. M. Petroleum Residue Upgradation via Visbreaking: A Review. *Ind. Eng. Chem. Res.* **2008**, *47* (23), 8960–8988.
- (6) Gary, J. H.; Handwerk, G. E.; Kaiser, M. J. *Petroleum Refining: Technology and Economics*, 5th ed.; CRC Press: Boca Raton, 2007.
- (7) Cooper, T. A.; Ballard, W. P. Thermal Cracking, Visbreaking, and Thermal Reforming. In *Advances in petroleum chemistry and refining. Vol. VI*; Kobe, K. A., McKetta, J. J. J., Eds.; Interscience: New York, 1962; pp 171–238.
- (8) Wiehe, I. A. A Phase-Separation Kinetic Model for Coke Formation. *Ind. Eng. Chem. Res.* **1993**, *32* (11), 2447–2454.
- (9) Wiehe, I. A. A Solvent-Resid Phase Diagram For Tracking Resid Conversion. *Ind. Eng. Chem. Res.* **1992**, *31* (2), 530–536.
- (10) Montanari, L.; Bonoldi, L.; Alessi, A.; Flego, C.; Salvalaggio, M.; Carati, C.; Bazzano, F.; Landoni, A. Molecular Evolution of Asphaltenes from Petroleum Residues after Different Severity Hydroconversion by EST Process. *Energy and Fuels* **2017**, *31* (4), 3729–3737.
- (11) Zachariah, A.; De Klerk, A. Thermal Conversion Regimes for Oilsands Bitumen. *Energy and Fuels* **2016**, *30* (1), 239–248.
- (12) Schabron, J. F.; Speight, J. G. Correlation between Carbon Residue and Molecular Weight. *Prepr. Pap.-Am. Chem. Soc., Div. Fuel Chem.* **1997**, *42* (2), 386–389.

- (13) Yen, T. F.; Erdman, J. G.; Saraceno, A. J. Investigation of the Nature of Free Radicals in Petroleum Asphaltenes and Related Substances by Electron Spin Resonance. *Anal. Chem.* **1962**, *34* (6), 694–700.
- (14) Castillo, J.; De Klerk, A. Visbreaking of Deasphalted Oil from Bitumen at 280–400 °C. *Energy and Fuels* **2019**, *33* (1), 159–175.
- (15) Guo, A.; Wang, Z.; Zhang, H.; Zhang, X.; Wang, Z. Hydrogen Transfer and Coking Propensity of Petroleum Residues under Thermal Processing. *Energy and Fuels* **2010**, *24* (5), 3093–3100.
- (16) Siddiquee, M. N.; De Klerk, A. Hydrocarbon Addition Reactions during Low-Temperature Autoxidation of Oilsands Bitumen. *Energy and Fuels* **2014**, *28* (11), 6848–6859.
- (17) Alshareef, A. H.; Scherer, A.; Tan, X.; Azyat, K.; Stryker, J. M.; Tykwinski, R. R.; Gray, M. R. Formation of Archipelago Structures during Thermal Cracking Implicates a Chemical Mechanism for the Formation of Petroleum Asphaltenes. *Energy and Fuels* **2011**, *25* (5), 2130–2136.
- (18) Khorasheh, F.; Gray, M. R. High-Pressure Thermal Cracking of n-Hexadecane in Aromatic Solvents. *Ind. Eng. Chem. Res.* **1993**, *32* (9), 1864–1876.
- (19) Strausz, O. P.; Lown, E. M. *The Chemistry of Alberta Oil Snads, Bitumes and Heavy Oils*; Alberta Energy Research Institute, 2003.
- (20) Singh, J.; Kumar, S.; Garg, M. O. Kinetic Modelling of Thermal Cracking of Petroleum Residues: A Critique. *Fuel Process. Technol.* **2012**, *94* (1), 131–144.
- (21) Aguilar, R. A.; Ancheyta, J. Modeling Coil and Soaker Reactors for Visbreaking. *Ind. Eng. Chem. Res.* **2016**, *55* (4), 912–924.
- (22) Cabrales-Navarro, F. A.; Pereira-Almao, P. Reactivity and Comprehensive Kinetic Modeling of Deasphalted Vacuum Residue Thermal Cracking. *Energy and Fuels* **2017**, *31* (4), 4318–4332.
- (23) Trauth, D. M.; Yasar, M.; Neurock, M.; Nigam, A.; Klein, M. T.; Kukes, S. G. Asphaltene and Resid Pyrolysis: Effect of Reaction Environment. *Fuel Sci. Technol. Int.* **1992**, *10* (7), 1161–1179.
- (24) Yasar, M.; Trauth, D. M.; Klein, M. T. Asphaltene and Resid Pyrolysis. 2. The Effect of Reaction Environment on Pathways and Selectivities. *Energy and Fuels* **2001**, *15* (3), 504–509.

- (25) Hawley, G. . *The Condensed Chemical Dictionary*, 8th ed.; Van Nostrand Reinhold: New York, 1971.
- (26) Nies, H.; Rewicki, D. The Analysis of the High-Resolution ^1H NMR Spectrum of Indene. *J. Magn. Reson.* **1982**, *46* (1), 138–141.
- (27) Chamberlain, N. F. *The Practice of NMR Spectroscopy with Spectra-Structure Correlations for Hydrogen-1*; Plenum Press: New York, 1974.
- (28) Lu, M.; Mulholland, J. A. Aromatic Hydrocarbon Growth from Indene. *Chemosphere* **2001**, *42* (5–7), 625–633.
- (29) Ford, T. J. Liquid-Phase Thermal Decomposition of Hexadecane: Reaction Mechanisms. *Ind. Eng. Chem. Fundam.* **1986**, *25* (2), 240–243.
- (30) Wu, G.; Katsumura, Y.; Matsuura, C.; Ishigure, K.; Kubo, J. Comparison of Liquid-Phase and Gas-Phase Pure Thermal Cracking of n -Hexadecane. *Ind. Eng. Chem. Res.* **1996**, *35* (12), 4747–4754.
- (31) Bredael, P.; Rietvelde, D. Pyrolysis of Hydronaphthalenes. 2. Pyrolysis of Cis-Decalin. *Fuel* **1979**, *58* (3), 215–218.
- (32) Blanchard, C. M.; Gray, M. R. Free Radical Chain Reactions of Bitumen Residue. *Prepr. Pap.-Am. Chem. Soc., Div. Fuel Chem.* **1997**, *42* (1), 137–141.
- (33) Khorasheh, F.; Gray, M. R. High-Pressure Thermal Cracking of n-Hexadecane in Tetralin. *Energy and Fuels* **1993**, *7* (6), 960–967.
- (34) Cardozo, S. D.; Schulze, M.; Tykwinski, R. R.; Gray, M. R. Addition Reactions of Olefins to Asphaltene Model Compounds. *Energy and Fuels* **2015**, *29* (3), 1494–1502.
- (35) Savage, P. E.; Klein, M. T.; Kukes, S. G. Asphaltene Reaction Pathways. 1. Thermolysis. *Ind. Eng. Chem. Process Des. Dev.* **1985**, *24* (4), 1169–1174.
- (36) Lababidi, H. M. S.; Sabti, H. M.; Alhumaidan, F. S. Changes in Asphaltenes during Thermal Cracking of Residual Oils. *Fuel* **2014**, *117*, 59–67.
- (37) Benjamin, B. M.; Hagaman, E. W.; Raaen, V. F.; Collins, C. J. Pyrolysis of Tetralin. *Fuel* **1979**, *58* (5), 386–390.
- (38) Hooper, R. J.; Battaerd, H. A. J.; Evans, D. G. Thermal Dissociation of Tetralin between 300 and 450 °C. *Fuel* **1979**, *58* (2), 132–138.
- (39) Poutsma, M. L. Progress toward the Mechanistic Description and Simulation of the Pyrolysis of Tetralin. *Energy and Fuels* **2002**, *16* (4), 964–996.

- (40) Peña, G. D. J.; Alrefaai, M. M.; Yang, S. Y.; Raj, A.; Brito, J. L.; Stephen, S.; Anjana, T.; Pillai, V.; Shoaibi, ahmed al; Chung, S. H. Effects of Methyl Group on Aromatic Hydrocarbons on the Nanostructures and Oxidative Reactivity of Combustion-Generated Soot. *Combust. Flame* **2016**, *172*, 1–12.
- (41) LaMarca, C.; Libanati, C.; Klein, M. T.; Cronauer, D. C. Enhancing Chain Transfer during Coal Liquefaction: A Model System Analysis. *Energy and Fuels* **1993**, *7* (4), 473–478.
- (42) Kubo, J. Radical Scavenging Abilities of Hydrogen-Donating Hydrocarbons from Petroleum. *Ind. Eng. Chem. Res.* **1998**, *37* (11), 4492–4500.
- (43) Gould, K. A.; Wiehe, I. A. Natural Hydrogen Donors in Petroleum Resids. *Energy and Fuels* **2007**, *21* (3), 1199–1204.
- (44) Naghizada, N.; Prado, G. H. C.; De Klerk, A. Uncatalyzed Hydrogen Transfer during 100–250 °C Conversion of Asphaltenes. *Energy and Fuels* **2017**, *31* (7), 6800–6811.

Chapter 6: Methyl transfer in free radical reactions

Abstract

It was speculated that hydrogen transfer was not the only type of transfer that could take place in free radical reactions and that methyl transfer could also take place. There was a large body of literature on intramolecular methyl migration, but little mention of intermolecular methyl transfer as a potentially important reaction type in free radical systems. The transfer of a methyl group in free radical systems was tested using indene, 2-methylindene and α -methylstyrene. Besides the formation of cumene from α -methylstyrene by hydrogen transfer, evidence of methyl transfer was provided by the formation of products like toluene, ethylbenzene, and *sec*-butylbenzene. Free radical addition reactions to form heavy products took place in reactions of indene with α -methylstyrene and 2-methylindene with α -methylstyrene. The presence of a methylated indene in the feed boosted the formation of products that require methyl transfer like the formation of ethylbenzene from cumene. When methyl transfer was favored by the presence of methylated compounds in the feed, there was less heavy products formed in the vacuum residue range and less free radical content in the products. The type of heavy products formed when methylate indene is in the feed was less compact than when indene is in the feed. This was a noteworthy contribution, because it not only showed the importance of intermolecular methyl transfer in free radical systems, but also indicated that methyl transfer as opposed to hydrogen transfer affected the properties of the reaction product.

Keywords: methyl migration, free radical addition, hydrogen transfer, intermolecular hydrogen transfer.

6.1 Introduction

Hydrogen transfer during thermal conversion increases the likelihood of free radical chain transfer reactions in relation to free radical addition reactions. Hydrogen transfer therefore influences the probability of forming heavier products during thermal conversion by decreasing the chain growth reactions. In the case of petroleum residue conversion processes, the formation of heavier and hydrogen depleted products can ultimately lead to asphaltenes and coke. To suppress such free radical addition reactions, the use of so-called “hydrogen donor solvents” is well established.^{1,2}

Since hydrogen transfer is possible, it was suspected that methyl transfer also takes place during thermal conversion of petroleum. The methyl radical is the second lightest radical produced by hydrocarbons. From a bonding perspective, the homolytic bond dissociation of a carbon-carbon bond requires less energy than the dissociation of a corresponding carbon-hydrogen bond.³

The rule in alkyl shifts, in general, is that the smaller alkyl substituent tends to be the one that shifts. That is why the transfer of a methyl group, or the so-called methyl migration or methyl shift, has been widely discussed in literature. However, most of the literature covers intramolecular methyl transfer, the movement of the methyl group within the same molecule, either by a carbocation or a carbanion mechanism.^{4, 5, 6, 7, 8} The most commonly encountered type of intramolecular shift is 1,2-methylshift. This occurs when a quaternary carbon (carbon #1) is adjacent to a secondary carbocation (carbon #2). In reactions driven by the formation of a cation, the 1,2-methylshift is a carbocation re-arrangement in which the methyl group migrates from carbon #1 to carbon #2. This leads to the formation of a tertiary carbocation on carbon #1 that is more stable than the secondary carbocation on carbon #2.

Intramolecular rearrangement by free radical transfer reactions has been described for several migrating groups,⁹ but these groups did not include methyl migration. Intramolecular methyl migrations, when described, are explained in terms of elimination-readdition.¹⁰

Methyl migration by tautomerism has been reported and many studies^{11, 12, 13, 14} have been done on the two isomers of methylated indene, namely 1-methylindene and 3-methylindene. These

studies evaluated whether the methyl group will take position 1 or 3 upon methylation by different techniques. This originated from the indene molecule itself. There was no clear conclusion on whether the non-benzenoid double bond of the indene is fixed^{15, 16} or is jumping between two positions,¹⁷ as shown in Figure 6.1.



Figure 6.1. Indene double bond alteration.

However, little literature was found that investigated methyl transfer during free radical reactions. Methyl groups form an intermediate in combustion systems; the reactivity of the methyl radical has been tested with oxygen and nitric oxide¹⁸. Peña et al.¹⁹ studied the effect of the methyl substituted aromatics on the formation of soot, that is usually a concern in fuels due to the incomplete combustion. They concluded that the presence of a methyl group on the aromatic fuels led to smaller primary particle size, and smaller lateral size of polyaromatic hydrocarbons present in soot, as well as a more compact nanostructure of the soot that is also less reactive towards oxygen. In another study on soot, the thermodynamic properties have been used to study the shift of the methyl group.²⁰ The binding nature of a methyl radical on graphenes,²¹ and the effect of the position of the methyl group (ortho, meta and para isomers) on the deactivation of aromatic radicals was reported.²²

Conceptually, methyl transfer can take place either by homolytic bond dissociation to release a methyl radical ($\bullet\text{CH}_3$), or by transfer during a concerted reaction that involves simultaneous bond breaking and formation. In a condensed phase and under moderate reaction conditions, it is anticipated that intermolecular transfer reactions take place predominantly by a concerted bimolecular reaction, as was found for hydrogen transfer.²³

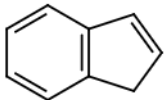
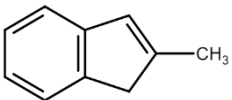
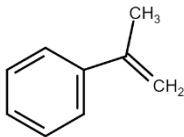
To study methyl transfer in comparison to hydrogen transfer, methylindene and indene were selected as model compounds, due to their propensity for molecule induced homolysis.²⁴

6.2 Experimental

6.2.1 Materials

Reactions involved model compounds of two types. One is a good hydrogen donor (indene and 2-methylindene) and the other one that has the ability to accept transferred hydrogen (α -methylstyrene). For comparison of methyl transfer with hydrogen transfer, the reaction of 2-methylindene and α -methylstyrene was compared to the reaction of indene and α -methylstyrene (Table 6.1). The choice of 2-methylindene instead of a different isomer was pragmatic and based on commercial availability and cost.

Table 6.1. Model compounds purities.

Compound Name	2-D chemical structure	CASRN ^a	Purity (%) ^b	Supplier
Indene		95-13-6	≥ 90 ^c	Sigma-Aldrich
2-methylindene		2177-47-1	98	Sigma-Aldrich
α -methylstyrene		98-83-9	99	Sigma-Aldrich

^a CASRN = Chemical Abstracts Services Registry Number

^b This is the purity of the material guaranteed by the supplier; material was not further purified

^c Purity determined by gas chromatography with flame ionization detector based on peak area, 97.7 %.

The chemicals used to confirm the identity of suspected products during analysis, are listed in Table 6.2.

In addition to these chemicals, toluene (99.9%, Fisher Scientific) and *n*-pentane (99.4%, Fisher Scientific) were used as solvents for the chromatographic analyses. Toluene was also used as the solvent for all electron spin resonance (ESR) analyses. Calibration for electron spin resonance spectrometry was performed with 2,2-diphenyl-1-picrylhydrazyl (~90%, Sigma-Aldrich). The

pentane insoluble analysis used *n*-pentane (99.4%, Fisher Scientific) as the solvent. Carbon disulfide (99.99%, Fisher Scientific) was used as the solvent for analyses by simulated distillation. Nitrogen (99.999 mol%) used for pressurizing the batch reactors was purchased from Praxair as cylinder gas. Chloroform-D (99.8%, Acros Organics) was used as the solvent for the proton nuclear magnetic resonance (¹H NMR) measurements.

Table 6.2. Compounds used for peak identification in GC-MS.

Compound Name	Purity (%) ^a	Supplier
2,5-dimethylstyrene	97	Alfa Aesar
cumene	98	Sigma Aldrich
ethylbenzene	99.8	Sigma Aldrich
indan	95	Sigma Aldrich
propylbenzene	98	Sigma Aldrich
<i>sec</i> -butylbenzene	≥99	Sigma Aldrich

^aThis is the purity of the material guaranteed by the supplier; material was not further purified

6.2.2 Equipment and procedure

Reactions were carried out in a batch micro-reactor built with 316 stainless steel Swagelok fittings. The reagents were placed in the reactor in a glass vial (glass test tube). Reactions were performed at 400 °C and 2 MPa initial pressure of N₂ for 30 minutes. Table 6.3 shows the proportions of each reactant in the mixtures.

The mass balance on the reactor indicated that there were gases formed. This was confirmed by the increase of pressure from 2 MPa initially to around 3 MPa after the reaction. Gases were analyzed using gas chromatography and the presence of methane as the main product was confirmed. Other gases identified were ethane and propane.

Table 6.3. Concentration of model compounds in mixtures.

Sample name	Mass in feed (g)		
	indene	α -methylstyrene	2-methylindene
Indene-MST (4:2)	4.050±0.001	2.057±0.001	-
Indene-MST (3:3)	3.037±0.001	3.012±0.001	-
Indene-MST (2:4)	2.021±0.001	4.027±0.001	-
Indene-MST (1:2)	1.024±0.001	2.012±0.001	-
2MI-MST (1:2)	-	2.092±0.001	1.021±0.001
MST	-	1.025±0.001	-
2MI	-	-	1.022±0.001

6.2.3 Analyses

Gas chromatography coupled with mass spectroscopy (GC-MS) was used to identify the compound classes present in reaction products. The apparatus used was an Agilent 7820A coupled with 5977E mass spectrometer with split/splitless injector. A split ratio of 100:1 with an injection volume of 1 μ L was employed. Separation was performed on a HP-5 column (30 m \times 0.25 mm \times 0.25 μ m) for products of the reaction of indene with α -methylstyrene at (4:2), (3:3), and (2:4) ratios. Separation of the other reaction products employed a longer column, HP-PONA (50 m \times 0.2 mm \times 0.5 μ m). The change in column was not necessitated by this investigation, but by a different investigation sharing the same equipment. For all samples, helium was used as carrier gas at constant flow rate of 1 mL/min with the same temperature program. The temperature program started at 80 °C, with a hold time of 5 min. Then temperature was increased by 5 °C/min to 200 °C, held for 2 min at 200 °C, and then increased again at a rate of 5 °C/min until 320 °C.

It was anticipated that some heavier products would be formed that would not elute during GC-MS analysis. Simulated distillation analysis was performed using an Agilent 7890B high temperature gas chromatograph with a flame ionization detector according to the ASTM D7169 standard test method.²⁵

The *n*-pentane insoluble content was determined by mixing 2 g of reaction product with 80 mL of *n*-pentane. The mixture was stirred in a closed jar at room temperature for 1 hour and left to settle for 23 hours before filtration. Filtration was done using 0.22 μm filter paper. The collected *n*-pentane insoluble precipitates were dried overnight in a fume hood until achieving a constant mass. The *n*-pentane insoluble content does not differentiate between ‘asphaltenes’ (toluene soluble) and ‘coke’ (toluene insoluble).

Proton nuclear magnetic resonance spectra were collected with a 60 MHz NMReady-60 spectrometer from Nanalysis as the average of 32 scans with a scan delay of 20 seconds. The samples were prepared at around 15 % concentration in chloroform-D.

Electron spin resonance spectra were collected with an Active Spectrum Micro-ESR as the average of 7 scans with a sweep delay of 30 seconds. Instrument parameters were 1.2 Gauss coil amplitude, a digital gain of 12 dB, and a microwave power of 15 mW. For analysis, a 20 mg sample was diluted in 600 μL toluene and placed in 5 mm diameter PQ tubes medium wall quartz. Quantification was based using a calibration curve prepared of using 2,2-diphenyl-1-picrylhydrazyl in toluene. The quantification limit on this instrument is 3×10^{16} spins/g and the detection limit is around 10^{16} spins/g.

6.3 Results

6.3.1 Reaction of α -methylstyrene with indene

6.3.1.1 Identification of reaction products by GC-MS

The products from the conversion of indene and α -methylstyrene were analyzed by GC-MS to identify the products that were formed. In the product boiling range that could be eluted by gas chromatography, the products appeared only in two regions of the chromatogram (Figures 6.2a and 6.2b).

When the compounds were identified it was found that the compounds in Figure 6.2a were mononuclear aromatic species that had a boiling point of less than 240 $^{\circ}\text{C}$, whereas the compounds

in Figure 6.2b were addition products. No major products eluted between 10 and 30 minutes retention time.

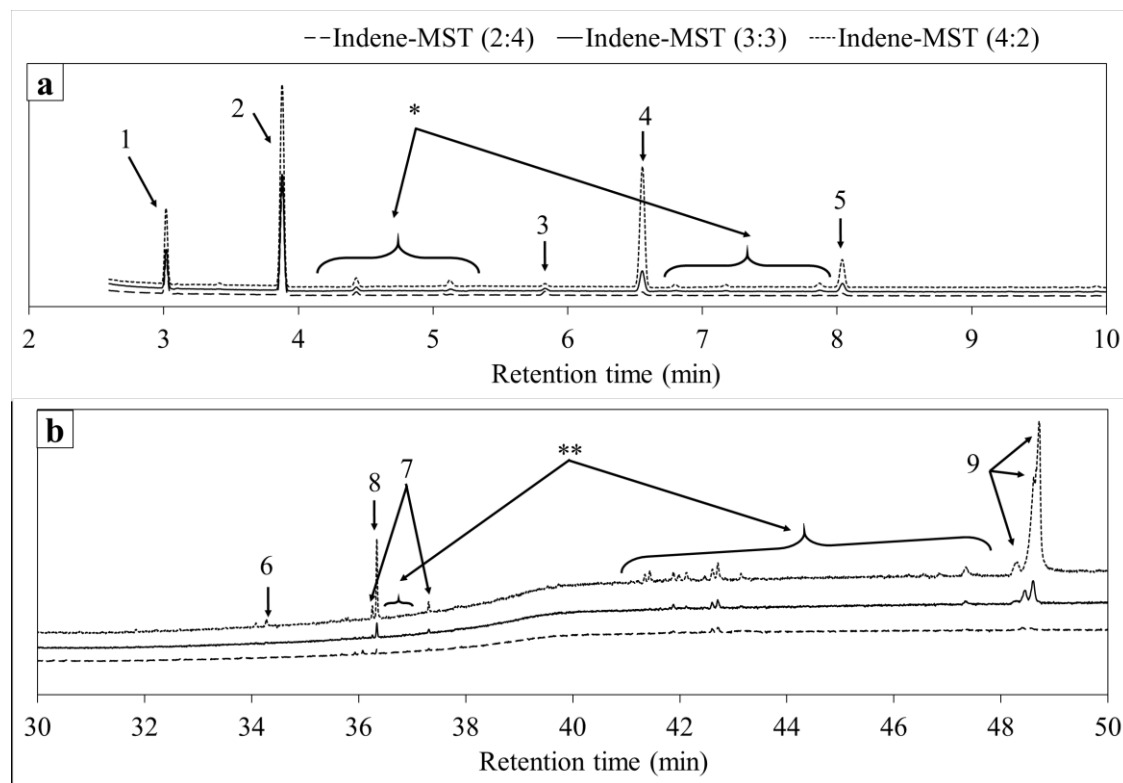
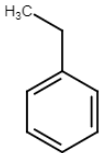
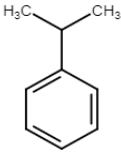
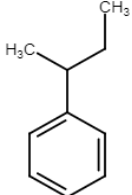
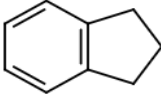
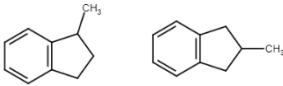


Figure 6.2. Chromatograms of the products of the reactions of indene with α -methylstyrene in different percentages for (a) light products, the solvent delay = 2.5 minutes (b) addition products. Values of intensities in y-axis multiplied by a factor of 1.5 for indene-MST (3:3) and 2 for indene-MST (4:2) for clear presentation.

The identification of the major peaks is provided in Table 6.4, together with the fractional peak area of each. Since the electron impact ionization propensity of the different compounds may differ, the fractional peak area is only a semi-quantitative indication of the abundance of each compound.

The chromatographic analysis found that the main product, regardless of the ratio of indene to α -methylstyrene in the feed, is cumene eluting at around 3.88 min. Cumene is the product from hydrogen transfer to α -methylstyrene. The other two major peaks are ethylbenzene (3.02 min) and indan (6.56 min). The identity of all these compounds have been confirmed using the authentic compounds listed in Table 6.2.

Table 6.4. Compound classes present in the product of the reactions of indene with α -methylstyrene in different percentages.

Peak number	Retention time (min)	Compound name	Chemical structure	Peak Fractional Area (%)		
				Indene-MST (4:2)	Indene-MST (3:3)	Indene-MST (2:4)
1	3.021	Ethylbenzene ^a		7.6	13.4	16.7
2	3.883	Cumene ^a		25.8	49.3	67.5
3	5.834	<i>sec</i> -butylbenzene ^a		0.5	1.4	3.5
4	6.556	Indan ^a		19.8	10.8	2.9
5	8.039	Isomers of methylindan		4.4	4.7	1.7
*	4-8 ^b	Not unambiguously identified and/or impurity in the feed eluting at retention time less than 10 min.		3.7	2.7	3.3
6	34.28	C ₁₇ H ₁₂	-	0.4	0	0
7	36.077 & 37.307	C ₁₉ H ₁₄	-	0.4	0	0.7

8	36.338	C ₁₈ H ₁₂	-	2.6	1.5	0.8
9	48.44- 48.72	C ₂₇ H ₂₀	-	27.0	12.5	0
**	36-49 ^c	Not unambiguously identified and/or column bleeding eluting at retention times greater than 30 min.		7.7	3.6	2.8

^a Chemical structure of these compounds has been confirmed.

^b Retention times (min)= 4.431, 5.072, 5.126, 5.133, 6.796, 7.177, 7.872.

^c Retention times (min)=36.258, 37.307, 41.349, 41.443, 41.884, 41.984, 42.131, 42.606, 42.612, 42.712, 43.147, 47.35, 48.272, 48.305.

Analysis of the toluene solvent on its own revealed that ethylbenzene was present as a trace contaminant. Although it was unlikely that the ethylbenzene in the reaction product was caused by solvent contamination, it was worthwhile confirming whether the ethylbenzene was present in the product, or whether it was just a contaminant introduced by the toluene used as a solvent. Furthermore, since ethylbenzene was found in the product, it was suspected that toluene may also be formed, which could not be observed when toluene was employed as a solvent.

To confirm the presence of ethylbenzene and toluene as reaction products, the *n*-pentane soluble fraction of the products was analyzed using *n*-pentane as the solvent; this will be discussed in more detail in the next section (Section 6.3.1.2). The peak of ethylbenzene was present in high intensity, which confirmed that ethylbenzene was a major product from the reaction between indene and α -methylstyrene. Supporting evidence was obtained from simulated distillation analysis (Section 6.3.1.2). When the *n*-pentane soluble fraction was analysed in the GC-MS, it was also clear that toluene was present in all products. This was also confirmed by the initial boiling point of simulated distillation results. The effort expended to confirm that both ethylbenzene and toluene were indeed reaction products was necessary, because these products imply that methyl groups were removed from α -methylstyrene during reaction.

The heavier addition products eluted at time greater than 30 minutes (Figure 6.2b). It was not possible to identify individual species with certainty in the heavier addition products.

6.3.1.2 Characterization by simulated distillation and *n*-pentane insoluble content

The relative abundance of hydrogen-enriched light products (Figure 6.2a) and the presence of addition products (Figure 6.2b) suggested that to maintain hydrogen-to-carbon balance there must also be heavier and more hydrogen-depleted products. These heavier and more hydrogen-depleted products did not elute during the GC-MS analysis. To evaluate the extent of heavier product formation, the material was analyzed by simulated distillation.

The simulated distillation profile of the total reaction product of indene and α -methylstyrene is illustrated by Figure 6.3. The general shape of the distillation profile was near similar irrespective of the indene to α -methylstyrene ratio. There were three main plateau regions (see Figure 6.3) where the mass loss increased at near constant temperature, which corresponded to ethylbenzene (133-139 °C), cumene (148-155 °C), and indan (170-173 °C). The normal boiling points are: 136 °C for ethylbenzene, 152.4 °C for cumene, and 176.5 °C for indan.²⁶ There was some material with boiling point lower than that of ethylbenzene.

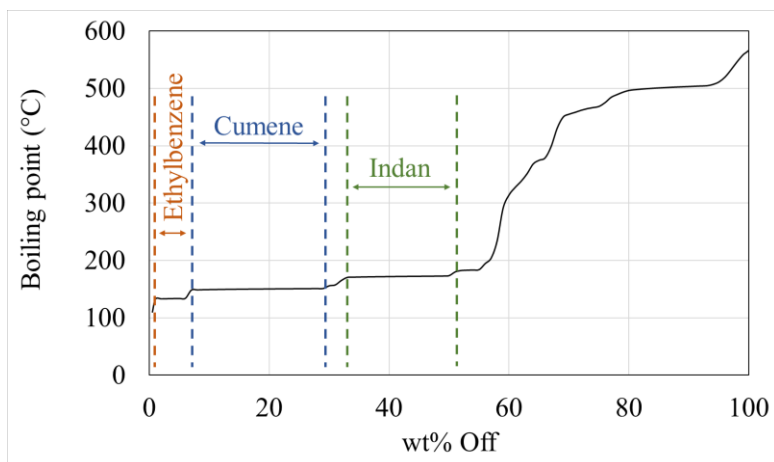


Figure 6.3. SimDist curve for the product of the ratio of indene to α -methylstyrene of 4:2 in feed, showing the main three plateaus.

The simulated distillation results supported the GC-MS results, which indicated that ethylbenzene, cumene and indan were major reaction products (Section 6.3.1.1). It also provided evidence of some lighter material that was present.

The simulated distillation results indicated complete recovery. The initial and final boiling points of each sample as well as the wt% of naphtha, distillate, vacuum gas oil, vacuum residue were tabulated in Table 6.5. The higher the amount of indene in the feed, the higher the initial boiling point of the product. The equimolar ratio of indene and α -methylstyrene formed the lowest amount of products boiling in the naphtha range and the highest amount of products boiling in the vacuum residue range.

Table 6.5. Simulated distillation results for indene-MST (4:2), indene-MST (3:3) and indene-MST (2:4)

Sample name		Indene-MST (4:2)	Indene-MST (3:3)	Indene-MST (2:4)
Temperature (°C)	IBP	110	108	83
	T10	149	149	134
	T30	156	151	151
	T50	174	183	152
	T70	455	481	322
	T90	503	598	508
	T95	511	619	566
	FBP	567	679	602
Wt % of each distillation fraction	Naphtha (<175°C)	50	48	62
	Distillate (175-360°C)	13	11	11
	Vacuum gas oil (360-525°C)	33	24	18
	Vacuum residue (>525°C)	4	17	9
Wt% of the light fraction (<240°C)		58	54	66

The amount of *n*-pentane insoluble content (asphaltenes) present in the products of these reactions was determined and is reported in Table 6.6. These results were surprising, because it indicated that most of the vacuum gas oil and vacuum residue products formed by the reaction of indene and α -methylstyrene were *n*-pentane insoluble. It is also in agreement with the simulated distillation results for the total reaction product (Table 6.5), showing the highest amount of heavy material for the equimolar ratio of indene and α -methylstyrene.

Table 6.6. *n*-pentane insoluble content.

Sample name	<i>n</i> -pentane insoluble content (wt%)
Indene-MST (4:2)	44.8
Indene-MST (3:3)	49.1
Indene-MST (2:4)	36.0

6.3.1.3 Spectroscopy of reaction products

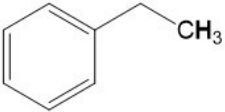
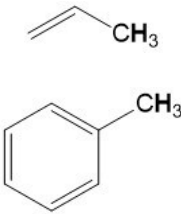
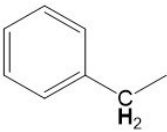
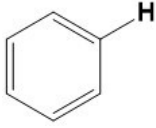
Proton nuclear magnetic resonance results for raw α -methylstyrene show a peak of high intensity at 2.0–2.5 ppm for the three aliphatic hydrogens, two peaks between 5–6 ppm corresponding to the olefinic hydrogens and a triplet at 7–8 ppm for aromatic hydrogens.

The peaks obtained from the analysis of the reaction products by proton nuclear magnetic resonance spectroscopy can be classified into four δ -regions: 1.1–1.6, 1.9–2.5, 2.5–3.2 and 7–8 ppm (Table 6.7). Each region corresponds to a neighbourhood of the hydrogen detected. The peaks corresponding to olefinic hydrogens for both α -methylstyrene and indene are not present anymore in the product indicating that hydrogenation of olefins took place. The percentage of aromatic hydrogens downfield at δ =7–8 ppm is almost the same for all samples. In fact, aromatic hydrogens don't only reflect the heavier portion of the product, i.e. condensed polyaromatic rings, but also hydrogens on the aromatic rings of the light fraction.

The second largest amount of hydrogens corresponds to the most shielded ones with a chemical shift δ =1.1–1.6 ppm. The percentage of hydrogens in this range is higher with a higher amount of

α -methylstyrene in the feed. This is because cumene and ethylbenzene are more abundant in the products. Hydrogens in the range of $\delta=1.9\text{--}2.5$ ppm and $\delta=2.5\text{--}3.2$ ppm are present more in the product with more indene in the feed. In fact, indan has 4 hydrogens on the benzylic position that would show in the $\delta=2.5\text{--}3.2$ ppm region whereas, cumene and ethyl benzene have only 1 and 2 hydrogens respectively that fall in the region of this chemical shift. That is why the intensity is more dependent on the indene content in feed than α -methylstyrene. The other two hydrogens on the cyclopentane ring of indan, are more upfield and show a signal at $\delta=1.9\text{--}2.5$ ppm. Though they are bonded to two alkyls, they are shifted due to the aromatic ring in the indan structure. Indan hydrogen shifts have been confirmed by running indan on its own in chloroform-D. The ^1H NMR spectra confirmed that hydrogen transfer took place. The ^1H NMR spectra also supported the chromatographic analyses that found that cumene, ethylbenzene and indan were the most abundant products in the light fraction.

Table 6.7. Type of hydrogens in the products of indene-MST (2:4), indene-MST (3:3) and indene-MST (4:2).

	Wt% of hydrogen			
	R-CH ₂ -R	R ₃ -CH	R-C \equiv C-H	
				
Chemical Shift				
δ (ppm)	1.1-1.6	1.9-2.5	2.5-3.2	7-8
Indene-MST (2:4)	33	2	8	57
Indene-MST (3:3)	28	3	11	58
Indene-MST (4:2)	22	5	15	58

The high concentration of hydrogen enriched products, such as cumene and indan, gave a clear indication that hydrogen transfer took place. It was of interest to see whether any free radical species could be detected in the reaction products. Electron spin resonance spectroscopy of the reaction products revealed a high concentration of free radical species (Table 6.8), of the order

10^{18} spins/g. The free radical content increased with increasing indene content in the indene and α -methylstyrene feed. No free radicals were detected in the *n*-pentane soluble fraction of the reaction products.

Table 6.8. Analyte spin content in the products of the reactions of indene with α -methylstyrene.

Sample name	Analyte spin content (spins/g) ($\times 10^{18}$)
Indene-MST (2:4)	2.06
Indene-MST (3:3)	3.21
Indene-MST (4:2)	4.42

6.3.2 Reaction of α -methylstyrene with 2-methylindene

The purpose of studying 2-methylindene was to focus more on the possible transfer of the methyl group rather than the transfer of hydrogen. Identification of the species in the reaction products was important, which meant that the study would benefit most from selecting a ratio of 2-methylindene and α -methylstyrene that was shown to have the least heavy product formation. To make comparison easier, the reaction of 2-methylindene with α -methylstyrene and the reaction of indene with α -methylstyrene were performed at 1:2 ratio (Table 6.3) at the same reaction conditions and the reaction products were analyzed in the same way.

6.3.2.1 Identification of reaction products by GC-MS

The chromatogram of the light products of the reaction of 2-methylindene with α -methylstyrene (Figure 6.4) can be compared to the control experiment showing the light products of the reaction of indene with α -methylstyrene (Figure 6.5). The chemical structures of the light compounds corresponding for each peak in Figures 6.4 and 6.5 are provided in Table 6.9. The GC-MS column used for these analyses was longer than the column used for the results in Table 6.4, which provided better chromatographic resolution. All light products eluted before a retention time of 24 minutes.

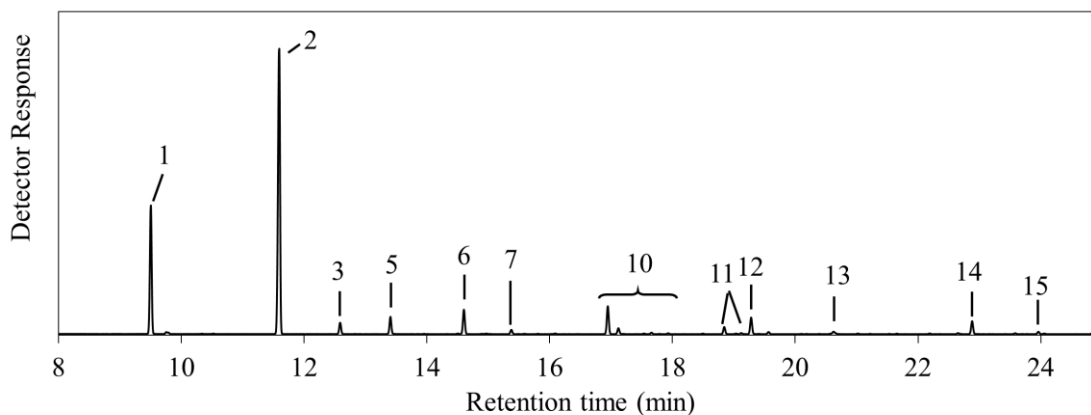


Figure 6.4. Chromatogram of the products of the reaction of 2-methylindene with α -methylstyrene (light products); the solvent delay = 8 minutes.

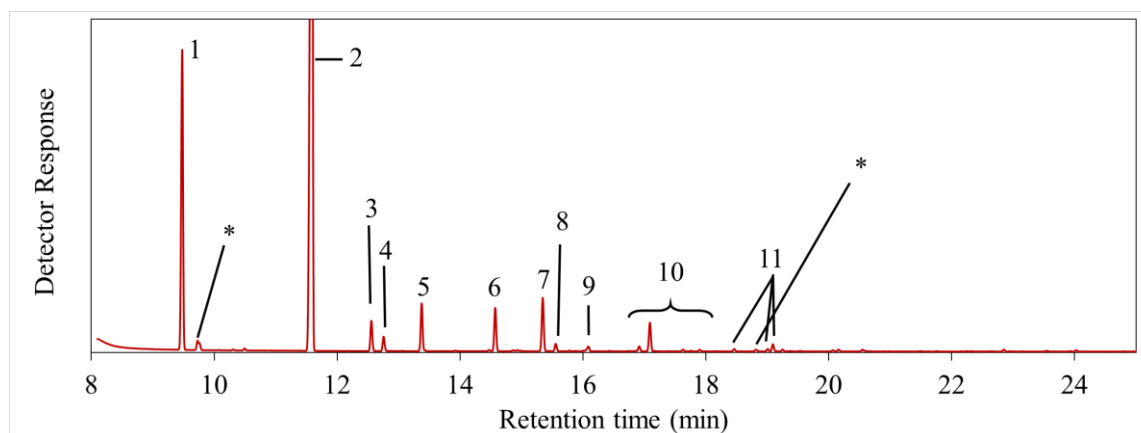
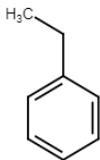
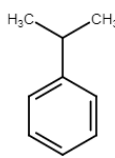
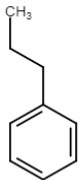
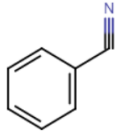
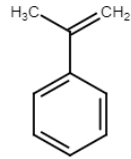
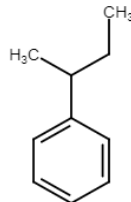
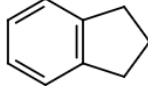
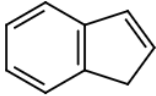
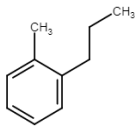
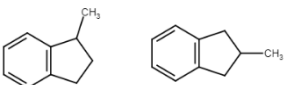
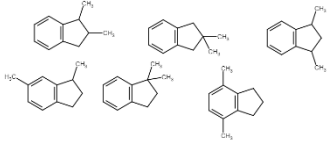
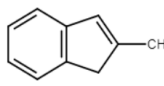
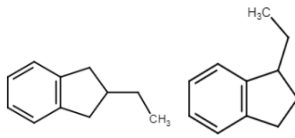
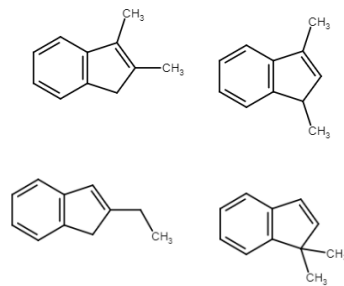
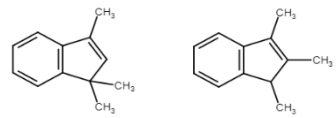


Figure 6.5. Chromatogram of the products of the reaction of indene with α -methylstyrene (light products); the solvent delay = 8 minutes.

Table 6.9. Chemical structure of peaks in chromatogram of Figures 6.5 and 6.6.

Peak number	Retention time (min)	Compound name	Chemical structure	Peak Fractional Area (%)	
				Indene-MST (1:2)	2MI-MST (1:2)
1	9.504	Ethylbenzene ^c		15.3	14.0

2	11.594	Cumene ^c		53.4	35.0
3	12.588	Propylbenzene ^c		1.6	1.3
4	12.757	Benzonitrile ^a		0.8	0
5	13.407	α -methylstyrene ^c		2.5	1.9
6	14.604	<i>sec</i> -butylbenzene ^c		2.3	2.8
7	15.377	Indan ^c		2.9	0.5
8	15.557	Indene ^c		0.4	0
9	16.088	C ₄ -alkylbenzene		0.4	0
10	16.947- 17.896	Isomers of methylindan ^b		1.9	4.0

11	18.464, 18.845, 19.092	Isomers of dimethyl-indan ^b		0.5	0.8
12	19.283	2-methylindene ^c		0	1.9
13	20.625	Isomers of ethylindan ^b		0	0.5
14	22.883	Isomers of dimethyl-indene or ethyl-indene ^b		0	1.5
15	23.963	Isomers of tri- methyl-indene ^b		0	0.3
*	9.73 & 19.008	Not unambiguously identified and/or solvent impurity		0.9	0

^a Compound present as impurity/stabilizer in raw indene.

^b These compounds should be seen only as being indicative of the nature of the products. The true identities of these compounds have not been confirmed.

^c Chemical structure of these compounds has been confirmed.

As mentioned before, it was not possible to identify individual species in the addition products with certainty. Probable structures of the addition products that were detected by GC-MS analysis are shown in Figure 6.6.

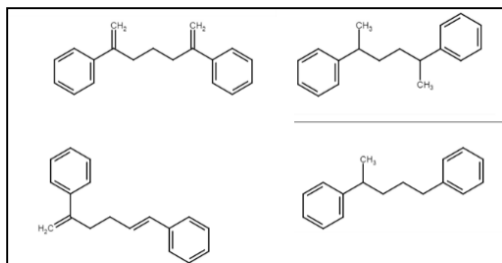


Figure 6.6. Possible structures of addition products that could be detected by GC-MS.

6.3.2.2 Characterization by simulated distillation and *n*-pentane insoluble content

The *n*-pentane insoluble content and simulated distillation results are tabulated below (Table 6.10). The initial boiling point (IBP), final boiling point (FBP) and the temperature at which “x” wt% boiled off (Tx) are presented in the table. The *n*-pentane insoluble content and simulated distillation results are tabulated below (Table 6.10). The reaction of α -methylstyrene with 2-methylindene in the ratio of 2:1 has the lowest amount of asphaltenes in the product (Table 6.10). Therefore, the presence of indene with α -methylstyrene in feed leads to more heavy products than 2-methylindene with α -methylstyrene in feed. However, the presence of indene in the feed yields more material in the light fraction in the product than 2-methylindene. When indene is in the feed, the naphtha and vacuum residue fractions are higher whereas the distillate and vacuum gas oil fractions are lower.

Table 6.10. *n*-pentane insoluble and Simulated distillation results for indene-MST (1:2) and 2MI-MST (1:2).

		Indene-MST	2MI-MST
		(1:2)	(1:2)
Temperature (°C)	IBP	108	108
	T10	135	134
	T30	151	151
	T50	152	182
	T70	330	374
	T90	577	536
	T95	613	597
	FBP	662	672
Wt % of each distillation fraction	Naphtha (<175°C)	61	49
	Distillate (175-360°C)	10	19
	Vacuum gas oil (360-525°C)	15	20
	Vacuum residue (>525°C)	14	12
<i>n</i> -pentane insolubles (wt%)		22.2	13.4
Wt% of the light fraction (<240°C)		66	58

The SimDist curves of both reactions indene-MST (1:2) and 2MI-MST (1:2) are shown in Figure 6.7. The SimDist curves for both reactions did not have a change in the boiling temperature in the range of 0-43 wt% off. From 43-74 wt% off, the boiling temperature for 2MI-MST (1:2) was consistently higher than that of indene-MST (1:2). Beyond this point, the boiling temperature for indene-MST (1:2) becomes consistently higher than that of 2MI-MST (1:2). For instance, the wt% of materials boiling at a temperature below 240 °C (light fraction) is less for indene-MST than for 2MI-MST. However, beyond the meeting point (dashed line) of the two curves, the behaviour of curves changes. At that point, the two curves intersect showing that the amount of compounds boiling below ~395 °C for both reactions is equal (~74 wt%). This will further be discussed in Section 6.4.5.

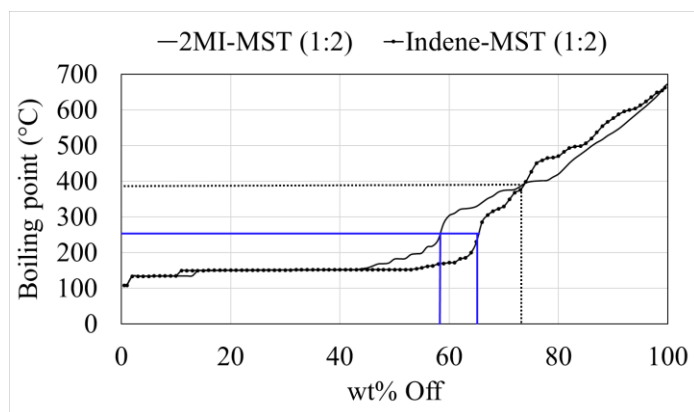


Figure 6.7. SimDist curves for the reactions indene-MST (1:2) and 2MI-MST (1:2).

6.3.2.3 Spectroscopy of reaction products

The distribution of hydrogen types obtained from NMR is similar for both products (Table 6.11). The abundance of cumene in the products gives a high percentage for hydrogens in the range of $\delta=1.1\text{--}1.6$ ppm. NMR spectra show not much difference between indene and 2-methylindene in the light and heavy fractions.

Table 6.11. Type of hydrogens in the products of indene-MST (1:2) and 2MI-MST (1:2).

	Wt% of hydrogen			
	R-CH ₂ -R	R ₃ -CH	R-C≡C-H	
Chemical Shift				
δ (ppm)	1.1-1.6	1.9-2.5	2.5-3.2	7-8
Indene-MST (1:2)	30	5	11	55
2MI-MST (1:2)	30	4	10	56

The number of free radicals in the product is higher when indene is reacted with α -methylstyrene (2.6×10^{18} spins/g) than when 2-methylindene is (2.4×10^{18} spins/g), that is in accordance with the *n*-pentane insoluble content (Table 6.12). The *n*-pentane soluble fraction of both products did not have any signal (i.e. no free radicals or amounts lower than the detection limit of instrument). Therefore, the free radicals are mainly located in the heavy fraction. Indene-MST (1:2) having a higher amount of compounds boiling in the vacuum residue range (Table 6.10) contains more persistent radicals in the product than 2MI-MST (1:2).

Table 6.12. Analyte spin content in the products of the reactions of indene with α -methylstyrene and 2-methylindene with α -methylstyrene.

Sample name	Analyte spin content (spins/g) ($\times 10^{18}$)
Indene-MST (1:2)	2.6
2MI-MST (1:2)	2.4

6.3.3 Self-reactions

In the self-reaction of α -methylstyrene, GC-MS results show a large amount of the reactant left. The main products formed from highest to lowest amounts are: cumene, ethylbenzene and sec-butylbenzene. It was surprising to find styrene, even if in smaller amounts, in the product of the self-reaction of α -methylstyrene. Styrene could not be detected in the product from the reaction of indene or 2-methylindene with α -methylstyrene, though it might have formed as an intermediate. The self-reaction of 2-methylindene has a large amount of reactant unreacted and forms mainly isomers of methylindan, indan, isomers of diethylindene and isomers of dimethylindan, these products are listed from most to least abundant. The self-reactions of indene have been previously studied and indene was found to undergo addition reactions and form *n*-pentane insoluble materials.²⁴

The simulated distillation results of the self-reactions reveal that 2-methylindene is capable of forming a large amount of compounds in the vacuum residue range. This is in accordance with the

free radical content in the products showing that the self-reaction of 2-methylindene has the highest amount, followed by indene then α -methylstyrene (Table 6.13).

Table 6.13. Analyte spin content in the products of the self-reactions of indene, α -methylstyrene and 2-methylindene

Sample name	Analyte spin content (spins/g) ($\times 10^{18}$)
Indene	1.22*
MST	0.97
2-MI	1.57

*Value obtained from the self-reaction of indene at the same conditions

6.4 Discussion

6.4.1 Reaction chemistry taking place in the reaction of indene with α -methylstyrene

GC-MS data has been combined with SimDist results in order to estimate the approximate percentage of each light liquid product (i.e. b.p. < 240 °C and eluting before 10 minutes) in the light fraction. All calculation details and assumptions are stated in Appendix C.1. Cumene has been used as a reference as explained in the appendix. The summary of the wt% of each light product in the light fraction for all reactions of indene with α -methylstyrene is represented in the histogram in Figure 6.8.

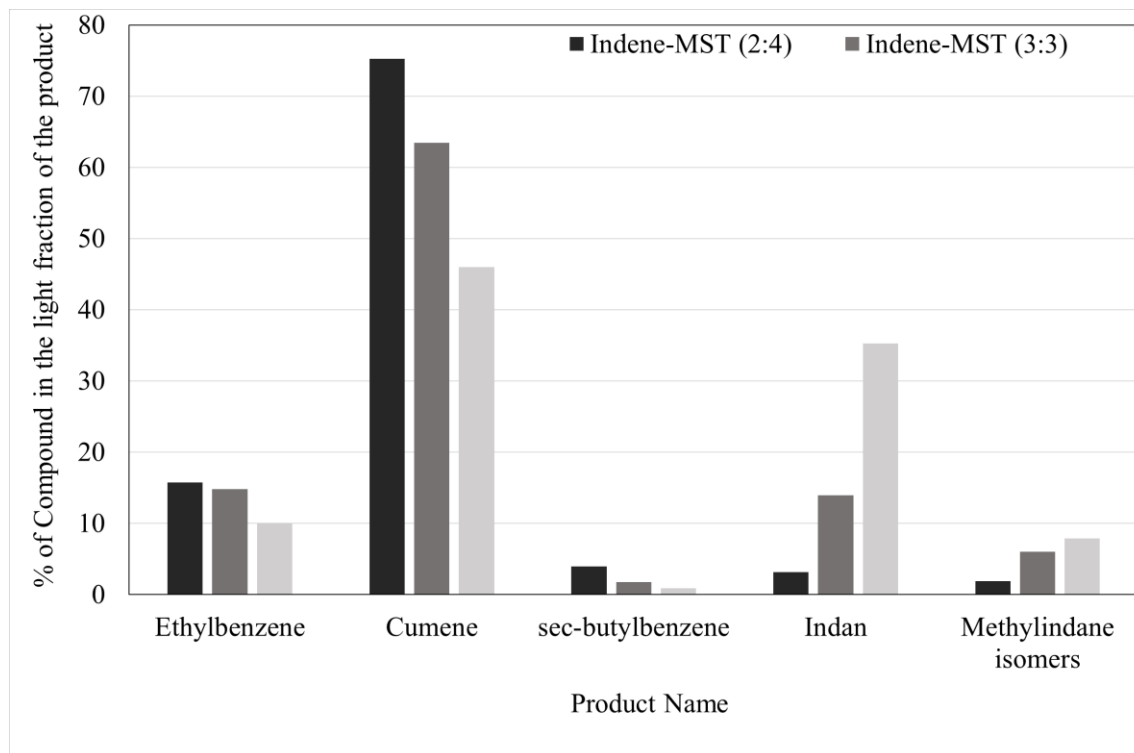


Figure 6.8. wt% of each light product in the light fraction for all reactions of indene with α -methylstyrene.

The main light products originating from α -methylstyrene are ethylbenzene and cumene. This is because the amount of ethylbenzene and cumene in the product increases with the increase of the α -methylstyrene content in the feed (Figure 6.9). They are also products of the self-reaction of α -methylstyrene. Cumene is formed by gaining two hydrogen atoms that is favourable due to the instability of the double bond in the α -methylstyrene structure (Figure 6.9). The two possible mechanism for the formation of ethylbenzene are through cumene intermediate or styrene intermediate (Figure 6.10). The presence of styrene as a product from the self-reaction of α -methylstyrene indicated that the possibility of formation of ethylbenzene from styrene is valid. The reaction of cumene with indene in ratios of 2g to 1g at the same conditions formed ethylbenzene and toluene. Therefore, the formation of ethylbenzene is independent of the formation of the styrene intermediate. Chemistry-wise, the formation of ethylbenzene from cumene is more favourable, since the rate of hydrogenation of α -methylstyrene is higher than that of the carbon-carbon bond cleavage to form styrene.

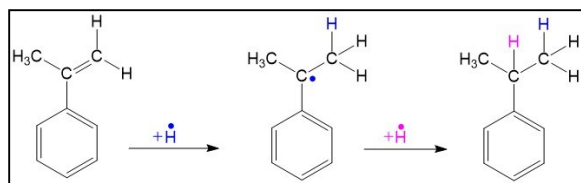


Figure 6.9. Free radical pathway for formation of cumene from α -methylstyrene.

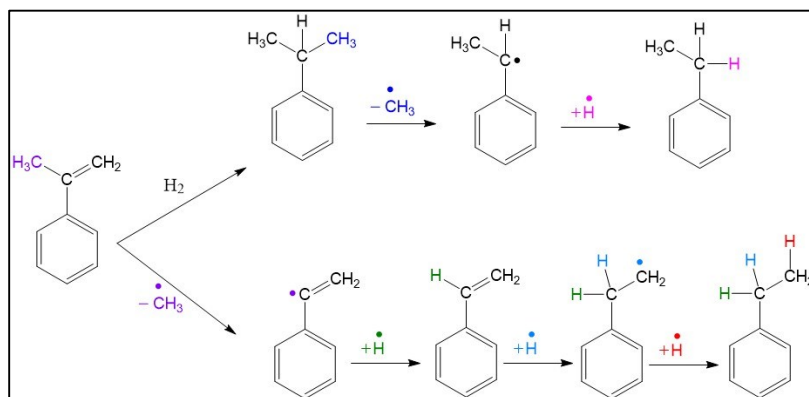


Figure 6.10. Free radical pathway for formation of ethylbenzene from α -methylstyrene.

The product eluting at 5.384 min (*sec*-butylbenzene) is also originating from α -methylstyrene as its amount in the product increases with the increase of the amount of α -methylstyrene in the feed.

On the other hand, indan and methylindan originate from the indene in the feed. Indan is the hydrogenated product of indene which also showed to be the main product in the self-reaction of indene.²⁴ The chemistry suggested for the formation of indan from indene is shown in Figures 6.11.

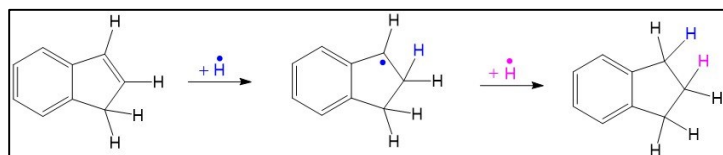


Figure 6.11. Free radical pathway for formation of indan from indene.

The peak of the compound eluting at 8.039 min elutes much later than indan; therefore, it is unlikely to be olefinic C₄-alkylbenzenes as they elute before indan. In addition, this peak has been confirmed not to be 2,5-dimethylstyrene. The only other molecule that has the same number of

carbons and hydrogens as C₄-alkylbenzenes is methylindan. Since methylindan isomers are not available commercially, this peak cannot be spiked, but there is compelling evidence chemistry-wise to say it is methylindan. This peak is present in both the self-reaction of indene and the self-reaction of α -methylstyrene. However, the effect of indene seems to be higher as the amount of this compound in the product is directly proportional to the amount of indene in the feed (Figure 6.8).

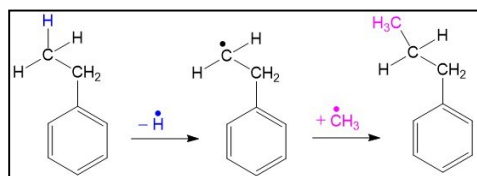
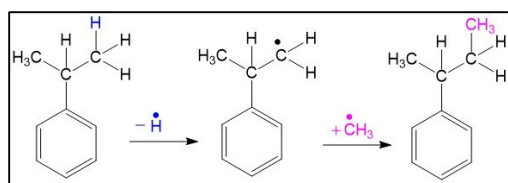
6.4.2 Reaction chemistry taking place in the reaction of 2-methylindene with α -methylstyrene

Using the same calculation steps as before (Appendix C.1), the wt% of each light product in the light fraction has been found and postulated in Table 6.14. The only difference is that the GC-MS column used for these reactions is longer; therefore, it allows one to see more light products. Light products show until a retention time of 25 min.

Some of the α -methylstyrene, indene and 2-methylindene remain unreacted. Propylbenzene is formed from ethylbenzene as shown in Figure 6.12. Whereas, *sec*-butylbenzene is formed from cumene (Figure 6.13). All the substituted indenenes and indans that have gained a methyl group have the same concept of free radical formation (e.g. Figure 6.14). A small amount of indan is formed from 2-methylindene (Figure 6.15).

Table 6.14. wt% of light compounds in light fraction.

Product Name	Wt% of compound in light fraction	
	Indene-MST (1:2)	2MI-MST (1:2)
Ethylbenzene	14.26	22.25
Cumene	69.71	53.77
Propylbenzene	2.10	2.00
α -methylstyrene	3.26	2.96
<i>sec</i> -butylbenzene	3.03	4.36
Indan	3.84	0.79
Indene	0.53	0.00
Isomers of dimethyl-ethylbenzene	0.48	0.00
Isomers of methylindan or isomers of ethyl-styrene	2.44	6.09
Isomers of dimethyl-indan	0.18	1.30
2-methylindene	0.18	2.96
Isomers of ethylindan	0.00	0.77
Isomers of dimethyl-indene or ethyl-indene	0.00	2.33
Isomers of tri-methyl-indene	0.00	0.44

**Figure 6.12.** Free radical pathway for formation of propylbenzene from ethylbenzene.**Figure 6.13.** Free radical pathway for formation of *sec*-butylbenzene from cumene.

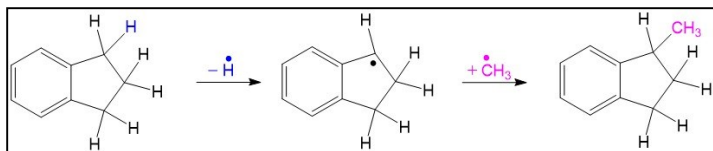


Figure 6.14. Free radical pathway for formation of 1-methylindan from indan.

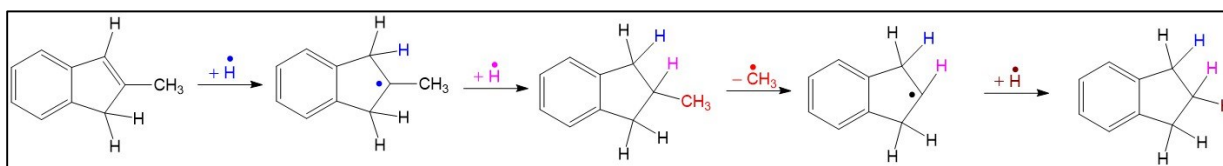


Figure 6.15. Free radical pathway for formation of indan from 2-methylindene.

6.4.3 Comparison of the tendency of indene, 2-methylindene and α -methylstyrene to form asphaltene precursors

The mol% of each feed that reacted to form light products and addition products is shown in Table 6.15. These calculations have been done as shown in Appendix C.2. For the reactions indene-MST (1:2) and 2MI-MST (1:2), only the 10 most abundant light products have been included in the calculations (i.e. those that exist in the amount >1 wt % in light fraction). The rest have been neglected.

These values prove that indene is responsible, by far, for the formation of addition products. In fact, the maximum amount of indene in the feed forming light products is 30% for indene-MST (4:2). The remaining indene is responsible for the formation of condensed polyaromatic rings, precursors of asphaltene as well as asphaltene. On the contrary, α -methylstyrene has tendency to form light fractions.

Table 6.15. mol% of each feed that reacted to form light and heavy products.

Sample name	Feed	Mol% of feed that reacted to form	
		Light fraction (b.p.<240°C)	Heavy fraction (b.p.>240°C)
Indene-MST (4:2)	Indene	31.4	68.6
	α -methylstyrene	84.8	15.2
Indene-MST (3:3)	Indene	17.9	82.1
	α -methylstyrene	76.4	23.6
Indene-MST (2:4)	Indene	8.2	91.8
	α -methylstyrene	81.5	18.5
Indene-MST (1:2)	Indene	11.63	88.37
	α -methylstyrene	84.91	11.99
2-MI-MST (1:2)	2-methylindene	21.51	78.49
	α -methylstyrene	66.96	30.66

Table 6.15 also shows that when the ratio of indene to α -methylstyrene in the feed decreases (i.e. indene becomes more dilute), indene tends to form more light products. This reflects the impact of the bulk liquid on the formation of addition products as observed earlier²⁴ when indene was diluted in indan and naphthalene. This means that the presence of α -methylstyrene in excess in the feed, makes it harder for the indene molecule to react with itself to form addition products. Though indene can still react with α -methylstyrene but this seems not to be the major reason for the formation of heavy products.

2-methylindene has a lower tendency to undergo addition reactions than indene, but it still forms fewer light products than α -methylstyrene does. This is also confirmed by the SimDist results of the self-reaction of α -methylstyrene that shows only 44 wt% of addition products compared to 49 wt% for self-reaction of 2-methylindene.

On another note, the equimolar ratio of α -methylstyrene to indene in the feed, has the highest amount of asphaltenes content in the product (Table 6.6), the lowest wt% of light fraction in

product and the highest final boiling point (Table 6.5). This is an indication that the formation of addition products and molecular weight growth is mainly favoured when each molecule of indene has exactly one molecule of α -methylstyrene to react with and vice-versa. The mol% of α -methylstyrene that reacts to form addition products in indene-MST (3:3) is the highest (Table 6.15). Thus, the high amount of addition products is mainly because of the inability of the α -methylstyrene molecule to react with another α -methylstyrene molecule due to the equimolar ratio with indene in the feed.

6.4.4 Methyl transfer taking place in free radical chemistry

The reaction mechanisms suggested in Sections 6.4.1 and 6.4.2 show that most of the light products are formed by the transfer of a hydrogen or a methyl group between molecules.

The major product in all reactions being cumene shows that hydrogen transfer is the dominating process in the presence of a molecule like α -methylstyrene that can easily gain hydrogens, and indene, a molecule that donates hydrogens. The formation of cumene from α -methylstyrene is, however, not dependent on the indene molecule, as α -methylstyrene can exchange this hydrogen between two of its molecules. The main product in the self-reaction of α -methylstyrene is also cumene. However, GC-MS shows that the amount of α -methylstyrene remaining (i.e. unreacted) in the product of the its self-reaction, is approximately equal to 71% of the amount of cumene by weight. Whereas this value (i.e. ratio of area of α -methylstyrene to cumene) is 4.7 and 5.5 % for indene-MST (1:2) and 2MI-MST (1:2) respectively. Naghizada et al.²⁷ also found the formation of cumene by the self-reaction of α -methylstyrene but their reactions were operated at lower temperatures.

Hydrogen transfer is also taking place in other light products formation (e.g. indan from indene).

An interesting observation in this study, is the large number of products formed due to the transfer of a methyl group. It is, therefore, possible to talk about methyl migration in a free radical mechanism which usually takes place at high temperatures. From a bond dissociation energy point of view, and as mentioned in the introduction, if hydrogen transfer is possible, methyl transfer

should take place. Most of the methyl transfer processes also involve a hydrogen transfer for rearrangement (Figures 6.10,6.12-6.15). Methyl transfer has been observed in molecules like ethylbenzene, propylbenzene and *sec*-butylbenzene that are found in relatively large amounts in the products. The formation of methylated indenenes and indans also requires the migration of a methyl group from one molecule to the other.

In the matrix, many reactions are taking place in parallel. Since it was possible to detect and confirm the structure of the light products by GC-MS, the discussion about hydrogen and methyl transfer is being confined to them. However, hydrogen and methyl transfer also take place in the heavier products during addition reactions. The light fraction constitutes around 54-66 wt% of the whole product, but there are also addition products and asphaltenes being formed at the same time. This makes the availability of a hydrogen radical or methyl radical in the matrix highly probable. There is a large amount of hydrogens released by the formation of condensed polyaromatic rings that have a low H:C ratio. Indene, for example, is the type of molecule that would lose a hydrogen to form addition products mainly. The hydrogen transfer has been proved by NMR results.

6.4.5 Effect of the methyl group in the feed on the formation of light and heavy products

The comparison between indene-MST (1:2) and 2MI-MST (1:2) in Table 6.16 is done based on the type of transfer (i.e. hydrogen or methyl transfer). Since the formation of ethylbenzene, propylbenzene and *sec*-butylbenzene by methyl transfer is not possible unless the cumene molecule is formed first, these three products have been separated. The remaining amount (in wt%) of each sample corresponds to the unreacted reactants as estimated in Table 6.14.

Table 6.16. Hydrogen transfer vs. methyl transfer.

	wt% of light compounds in light fraction that has been formed by			
	Hydrogen transfer only	Methyl transfer (that might include hydrogen re-arrangement)		
		that <i>do not</i> depend on cumene content	that depend on cumene content	Total
Indene-MST (1:2)	74	3 ^a	19 ^c	24
2MI-MST (1:2)	60	6 ^b	29 ^c	35

^aThese compounds include isomers of methylindan, dimethylindan, methylindene, ethylindan, dimethylindene, ethylindene and trimethylindene.

^bThese compounds include isomers of indan, dimethylindan, ethylindan, dimethylindene, ethylindene and trimethylindene.

^cThese compounds include ethylbenzene, propylbenzene and *sec*-butylbenzene.

The quantity of products formed only by hydrogen transfer is more when indene is in the feed (74 wt%). This is because the tendency of indene to donate hydrogens is higher than that of 2-methylindene.

The formation of ethylbenzene, propylbenzene and *sec*-butylbenzene by methyl transfer after formation of cumene is higher for 2MI-MST (29 wt%) than indene-MST (19 wt%) (Table 6.16). This is a clear indication of the role of the methyl group. When a methyl group is present in the feed (i.e. 2-methylindene), the methyl-transfer is boosted due to its high availability. Whereas, in the reaction of indene with α -methylstyrene, the availability of a methyl group depends on other reactions taking place in the matrix. It is not explicitly available in the feed material and therefore is not as readily available in the matrix. It is important to note that the amount of cumene formed in the presence of indene in the feed is higher than that formed in the presence of 2-methylindene in the feed. Therefore, normalizing the values in Table 6.16 of the “wt% of light compounds in light fraction formed due methyl and hydrogen transfer dependent on cumene”, to amount of cumene, will even boost the percentage for 2MI-MST to around twice that of indene-MST.

Table 6.16 also shows that the formation of molecules by methyl transfer (independent of cumene) is higher in the presence of 2-methylindene (6 wt%) in the feed than indene (3 wt%).

Conclusively, the formation of light products that require methyl transfer is boosted in the presence of a methylindene in the feed rather than indene.

On another hand, the presence of the methyl group in the feed contributes to the decrease of the amount of *n*-pentane insoluble portion in the products and the free radical content (Table 6.10). However, the quantity of light products formed when indene is in the feed (66 wt%) is larger than when 2-methylindene is in the feed (58 wt%). There are also slightly more aromatic hydrogens in the product of 2MI-MST (1:2) than in the product of indene-MST (1:2) (Table 6.11). The increase of aromatic hydrogen in the product of the reaction with 2-methylindene (41 % increase) is also larger than that with indene (9% increase).

This can be explained from two perspectives: (i) *the larger amount of light products for indene vs. 2-methylindene is due to the cumene*: Figure 6.7 shows that the main factor that affects the change in the amount of light fraction in the product is the plateau of cumene. While cumene exists in the amount of 44 wt% in the product when indene is used, it is only present in the amount of 29 wt% when 2-methylindene is used. Due to the hydrogen transfer impact discussed earlier, the donation of hydrogen by 2-methylindene is not favourable; therefore, the formation of cumene is not as favourable. This is confirmed by the mol% of α -methylstyrene that reacts to form light products that is lower with 2-methylindene than with indene (Table 6.15). This means that the α -methylstyrene has higher tendency to form addition products when reacted with 2-methylindene than when reacted with indene. (ii) *the presence of 2-methylindene in the feed leads to more medium fraction but less heavy fraction*: though there are more addition products (b.p.>240 °C) when 2-methylindene is used than when indene is, there is clear indication that these addition products are divided into two regions (Figure 6.7). The first region (medium fraction: 240 °C < b.p. < 395 °C) has the curve of 2-methylindene above the one of indene, then there is inversion beyond this point. This means the heaviest fraction is more for indene than 2-methylindene which is in accordance with the asphaltenes content. Asphaltenes is a solubility class whereas SimDist deals with boiling point. It might not be possible to relate asphaltenes to a specific region in SimDist but it is for sure the heaviest there. This is reflected by the higher distillate and vacuum

gas oil range product in 2MI-MST compared to indene-MST and lower vacuum residue range products (Table 6.10). Conclusively, the presence of methyl groups in the feed is leading to more addition products with most of them belonging to the medium fraction (i.e. $240\text{ }^{\circ}\text{C} < \text{b.p.} < 395\text{ }^{\circ}\text{C}$) and are not included in the asphaltenes portion of the product. This might also be an indication of the type of addition products as well as asphaltenes formed when the methyl group is present.

Point (ii) indicates that when 2-methylindene is in the feed, the condensed rings might resemble a structure more like archipelago rather than island. This can be seen from a different perspective: since the methyl group is not available in the feed when indene is used, it must be provided from the matrix itself to form products like propylbenzene, *sec*-butylbenzene or substituted indenenes and indans. The only ways the matrix can provide these methyl groups, is either by the formation of ethylbenzene, or by a molecular weight growth that releases methyl radicals. Since the presence of indene boosts hydrogen transfer and the presence of methylindene boosts methyl transfer, it seems that the need for methyl groups is higher in the matrix. Hence, in the absence of the methyl group in the feed, reactions happen in a way to release methyl radicals, boosting the formation of *n*-pentane insolubles and probably changing the structure of asphaltenes formed to a more compact structure (i.e. island). This has implications to thermal cracking in terms of dependence of the product on the type of feed material. The more the methyl radical is available in the matrix, the less compact the structure of the asphaltenes. This also affects the type of addition products formed. A higher availability of the methyl radical in a DAO matrix can be either reflected by more methyl substituted compounds in the feed or by more methyl radicals released during cracking due to the type of feed or the operating conditions.

6.5 Conclusions

Free radical pathways for products of the reaction of indene with α -methylstyrene have been drawn by reacting different amounts of indene with α -methylstyrene. The formation of cumene from α -methylstyrene is higher in the presence of indene that can donate hydrogens. Indene is responsible for the addition products, whereas most of the α -methylstyrene reacts to form light products.

It has also been demonstrated that the methyl transfer in a free radical mechanism takes place. The presence of a methylated indene in the feed boosts the formation of products that require methyl transfer and decreases the amount asphaltenes and free radicals in the products. The type of heavy products formed when methylated indene is in the feed is less compact than when indene is in the feed.

Literature cited

- (1) Bockrath, B. C. Chemistry of Hydrogen Donor Solvents. In *Coal Science Vol.2*; Gorbaty, M. L., Larsen, J. W., Wender, I., Eds.; Academic Press: New York, 1983; pp 65–124.
- (2) Alemán-Vázquez, L. O.; Torres-Mancera, P.; Ancheyta, J.; Ramírez-Salgado, J. Use of Hydrogen Donors for Partial Upgrading of Heavy Petroleum. *Energy and Fuels* **2016**, *30* (11), 9050–9060.
- (3) Blanksby, S. J.; Ellison, G. B. Bond Dissociation Energies of Organic Molecules. *Acc. Chem. Res.* **2003**, *36* (4), 255–263.
- (4) Nakamoto, M.; Fukawa, T.; Sekiguchi, A. Silylium Ion to Silylium Ion Rearrangement Caused by 1,3-Methyl Migration. *Chem. Lett.* **2003**, *33* (1), 38–39.
- (5) Terheijden, J.; van Koten, G.; Vinke, I. C.; Spek, A. L. 1,2-Methyl Shift between Pt and the Coordinated Aryl Group in the Reaction of Methyl Iodide with 2,6-Bis[(Dimethylamino)Methyl]Phenyl-N,N',C Complexes of Platinum(II). X-Ray Crystal Structure of the Arenonium-Platinum Compound [Pt(o-Tolyl)(MeC₆H₃(CH₂NMe₂)). *J. Am. Chem. Soc.* **1985**, *107* (10), 2891–2898.
- (6) Mawby, R. J.; Basólo, F.; Pearson, R. G. Methyl Migration in the Reaction of Alkyl- and Acylmanganese Carbonyls. *J. Am. Chem. Soc.* **1964**, *86* (22), 5043–5044.
- (7) Maudgal, R. K.; Tchen, T. T.; Bloch, K. 1,2-Methyl Shifts in the Cyclization of Squalene To Lanosterol. *J. Am. Chem. Soc.* **1958**, *80* (10), 2589–2590.
- (8) Collier, W. L.; Macomber, R. S. Tert-Butylacetylene Revisited. An Improved Synthesis. Methyl Migration during Bromination. *J. Org. Chem.* **1973**, *38* (7), 1367–1369.
- (9) Freidlina, R. K.; Terent'ev, A. B. Rearrangement of Short-Lived Radicals in the Liquid Phase. In *Advances in free-radical chemistry Vol.6*; Williams, G. H., Ed.; Heyden: London, 1980; pp 1–63.
- (10) Wilt, J. W. Free Radical Rearrangements. In *Free Radicals Vol. 1*; Kochi, J. K., Ed.; Wiley-Interscience: New York, 1973; pp 333–501.
- (11) Bergson, G.; Weidler, A.-M. Proton-Mobility in the Indene Ring-System. *Acta Chem. Scand.* **1963**, *17* (3), 862–864.
- (12) Bergson, G.; Weidler, A.-M. A Stereospecific Tautomeric Rearrangement. *Acta Chem. Scand.* **1963**, *17* (6), 1798–1799.
- (13) Bergson, G. Proton-Mobility in the Indene Ring-System. *Acta Chem. Scand.* **1963**, *17* (10),

- 2691–2700.
- (14) Nihlgård, B.; Weidler, A.-M.; Bergson, G.; Johansson, L.; Nilsson, L. Hydrogen Isotope Effect on the Rate of an Intramolecular Tautomeric Rearrangement. *Acta Chemica Scandinavica*. 2008, pp 1498–1501.
 - (15) Elleman, D. D.; Manatt, S. L. An NMR Study of Indene Using a Proton-Proton Decoupling Technique. *J. Chem. Phys.* **1962**, *36* (9), 2346–2352.
 - (16) Koelsch, C. F.; Scheiderbauer, R. A. The Tautomerism of Indene. *J. Am. Chem. Soc.* **1943**, *65* (12), 2311–2314.
 - (17) Wawzonek, S.; Laitinen, H. A. The Reduction of Unsaturated Hydrocarbons at the Dropping Mercury Electrode. II. Aromatic Polynuclear Hydrocarbons. *J. Am. Chem. Soc.* **1942**, *64* (10), 2365–2368.
 - (18) Baldwin, A. C.; Golden, D. M. Reactions of Methyl Radicals of Importance in Combustion Systems. *Chem. Phys. Lett.* **1978**, *55* (2), 350–352.
 - (19) Peña, G. D. J.; Alrefaai, M. M.; Yang, S. Y.; Raj, A.; Brito, J. L.; Stephen, S.; Anjana, T.; Pillai, V.; Shoaibi, ahmed al; Chung, S. H. Effects of Methyl Group on Aromatic Hydrocarbons on the Nanostructures and Oxidative Reactivity of Combustion-Generated Soot. *Combust. Flame* **2016**, *172*, 1–12.
 - (20) Rutz, L. K.; Bockhorn, H.; Bozzelli, J. W. Methyl Radical Substitution and Shift Reactions with Aliphatic and Aromatic Hydrocarbons. *Int. Symp. Combust. Abstr. Work. Posters* **2004**, *49*, 451–452.
 - (21) Tachikawa, H. Methyl Radical Addition to the Surface of Graphene Nanoflakes: A Density Functional Theory Study. *Surf. Sci.* **2019**, *679* (June 2018), 196–201.
 - (22) Steglich, M.; Knopp, G.; Hemberger, P. How the Methyl Group Position Influences the Ultrafast Deactivation in Aromatic Radicals. *Phys. Chem. Chem. Phys.* **2019**, *21* (2), 581–588.
 - (23) Billmers, R.; Griffith, L. L.; Stein, S. E. Hydrogen Transfer between Anthracene Structures. *J. Phys. Chem.* **1986**, *90* (3), 517–523.
 - (24) Tannous, J. H.; de Klerk, A. Asphaltenes Formation during Thermal Conversion of Deasphalted Oil. *Fuel* **2019**, *255*, 1–10.
 - (25) ASTM D7169. Standard Test Method for Boiling Point Distribution of Samples with Residues Such as Crude Oils and Atmospheric and Vacuum Residues by High Temperature

- Gas Chromatography; ASTM: West Conshohocken, PA, 2016.
- (26) Weast, R. C.; Astle, M. J.; Beyer, W. H. *CRC Handbook of Chemistry and Physics (Vol. 69)*; Boca Raton, FL: CRC press., 1988.
- (27) Naghizada, N.; Prado, G. H. C.; De Klerk, A. Uncatalyzed Hydrogen Transfer during 100-250 °C Conversion of Asphaltenes. *Energy and Fuels* **2017**, *31* (7), 6800–6811.

Chapter 7: Synthesis of carbon-labelled indene

Abstract

Tracing compounds in complex matrices, like thermal cracking, is challenging. Providing direct evidence on a molecular level to show that species prone to free radical addition are incorporated in product species during thermal conversion of bitumen and deasphalted oil is crucial. The proposed strategy was to make use of ^{13}C -labelled compounds to track the incorporation of light addition prone species. A new way of synthesis of ^{13}C -labelled indene was evaluated. The synthesis of ^{13}C -labelled indene provided a method to use labelled compounds to track addition reactions in bitumen and deasphalted oil. This work can serve as the starting point for future investigations related to heavy products formation in free radical systems.

Keywords: indene, ^{13}C -labelled compounds, synthesis, benzene, tracing.

7.1 Introduction

In our previous study (Chapter 5), it was proved that indene, when mixed with deasphalted oil (DAO), leads to higher asphaltenes content than that formed by DAO alone or indene alone. However, it was not possible to demonstrate whether indene incorporated in the formation of *n*-pentane insoluble material or not. In other words, did indene induce the formation of heavier compounds when mixed with DAO by actually participating in the reactions? or by just being present in the matrix? This question could only be answered if a labelled indene was used.

This required, thus, the purchase of ^{13}C -labelled or ^{14}C -labelled indene and test products using either ^{13}C -NMR or a radio tracer to detect the radioactive carbon isotope, respectively. Unfortunately, one gram of ^{13}C -labelled indene costs around C\$ 150,000. Since the price of this chemical is not within the budget of this research study, a suggested pathway for synthesis of indene has been proposed, tested and a cost estimation has been performed.

The first concern about the synthesis of a labelled indene, was the position of the labelled carbon. The label could either be inside the benzene ring of the indene molecule or on one of the carbons of the cyclopentene ring. However, when indene is reacted, the part of the molecule that is subject to reaction (e.g. addition or cracking) is the cyclopentene part since the benzene ring is very stable. In other words, there is almost no chance the benzene ring will open in any kind of reaction. In order to better track this molecule in a complex matrix like DAO, the label had to be on the stable part of the molecule (i.e. the benzene ring).

For that reason, it was decided to start with a labelled benzene and synthesize indene. The label in Figure 7.1 is represented by a red star. Fortunately, ^{13}C -labelled benzene costs around C\$ 400 / 1g and was purchased from Sigma Aldrich with all carbons on the ring being carbon-13 instead of carbon-12 (i.e. 99% atom ^{13}C). The synthesis pathway suggested consists of converting benzene to indanone and then reduce it to indene. By converting benzene to indanone, the value of the product will be increased to C\$ 12,500 / 1g, that is the cost of labelled indanone.

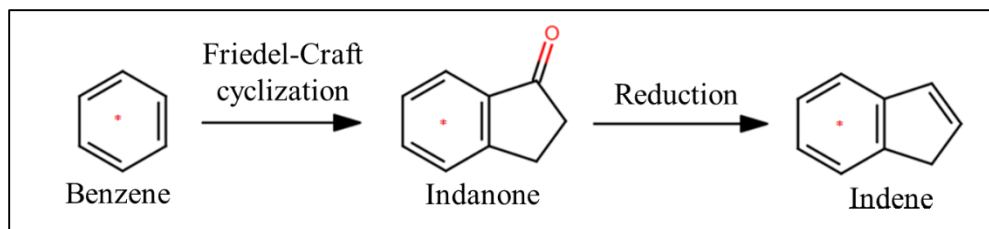


Figure 7.1. Pathway for synthesis of ^{13}C -labelled indene.

The synthesis of radioactive indene was done for different applications. Badger et al.¹ discussed the formation of indene starting with 2-bromoethyl benzene and adding ^{14}C after forming the Grignard reagent. Therefore, the label in the indene molecule is located on one carbon present on the cyclopentene ring. ^{14}C -labelled indene was also used for tracing indene in a biocatalytic process.² The suggested pathway for formation of indene starts with benzene passing through intermediates indanone and the corresponding enol-triflate (Figure 7.2). In the current study, the procedure described by Yanagimachi et al.² was tested. However, below is the detailed explanation of what reactions worked and what did not work. Consequently, a synthesis with new pathways has been suggested and tested and is mentioned at the end of this study. All syntheses below have been tested using unlabelled compounds.

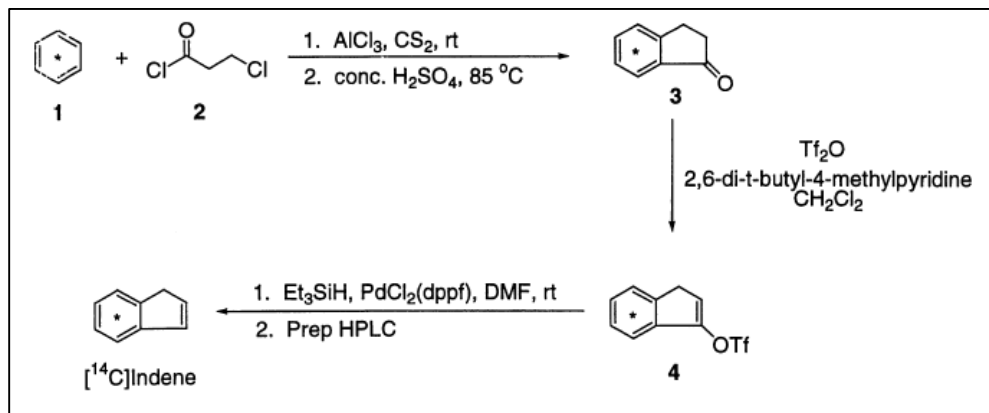


Figure 7.2. Synthesis of radioactive indene from benzene.²

7.2 Experimental

Syntheses steps and glassware were described in Section 7.3.

The synthesized products were identified using an Agilent 7820A Gas Chromatography coupled with and Agilent 5977E Mass Spectroscopy. Separation is performed on a HP-5 column (30 m × 0.25 mm × 0.25 μm) using helium as the carrier gas at constant flow of 1 mL/min. The temperature program starts at 80 °C, with a hold of time of 5 min, after which the temperature is increased by 5 °C/min up to 200 °C and then held for 2 min, then increased again at a rate of 5 °C/min until 320 °C. The injector is split/splitless and the split ratio is 100:1 with an injection volume of 1 μL.

The yields of the reactions were calculated using an Agilent 7890A chromatograph and separation occurred in a DB-5MS column (30m x 0.25 mm x 0.25 μm). The temperature program starts at 80 °C, with a hold of time of 5 min, after which the temperature is increased by 5 °C/min up to 200 °C and then held for 2 min, then increases again at a rate of 5 °C/min until 320 °C. The injector is split/splitless and the split ratio is 100:1 with an injection volume of 1 μL.

Synthesized indanone using sulfuric acid has been characterized using Simulated Distillation to identify heavy compounds not detectable by GC-MS. Simulated distillation analysis was performed using an Agilent 7890B high temperature gas chromatograph with a flame ionization detector and DB-HT-SIMDIS column (5 m × 0.53 mm × 0.15 μm). The injection volume was 0.5 μL using helium as carrier gas. Sample preparation involved dissolving 100 mg of the reaction product in about 12 g of CS₂; the exact mass of the reaction product and CS₂ were measured and recorded with 0.1 mg readability. The temperature program started at 50 °C and temperature was increased at a rate of 15 °C/min to 425 °C at which temperature it was held constant for 10 minutes.

7.3 Results and Discussion

7.3.1 Synthesis of 3-chloropropiophenone from benzene

In order to transform benzene into indanone, the first step was to create the 3-chloropropiophenone intermediate. The formation of 3-chloropropiophenone was conducted by Friedel-Craft acylation³ by adding an acyl halide (3-chloropropionyl chloride) to a benzene ring as shown in Figure 7.3. The acyl halide is attached to the aromatic ring using a strong Lewis acid AlCl₃. In this step, the electrophile (i.e. AlCl₄⁻) is created due to the presence of the chlorine molecule on the acyl halide.

The attachment occurs on the carbon close to the oxygen since aluminum chloride is attracted by the oxygen. This reaction is not reversible due to strong attraction between oxygen and electrophile.

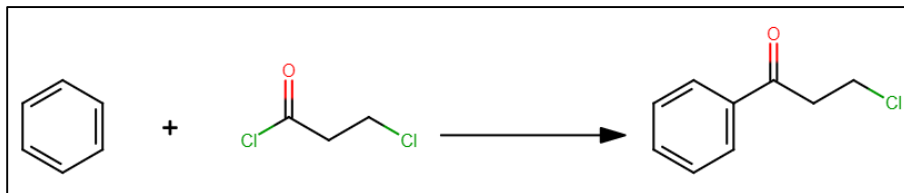


Figure 7.3. Reaction of benzene with 3-chloropropionyl chloride.

The experimental methodology consists of dissolving 0.12 mol (i.e. 16.2 g) of aluminum chloride (99%, Alfa Aesar) in 50 ml dry carbon disulfide solvent (>99%, Fisher). The setup consists of using a 250 ml 3-necked round bottom flask equipped with condenser, stirrer and addition funnel. An equimolar mixture of 0.1 mol (i.e. 7.8 g) of benzene (99%, Alfa Aesar) and 0.1 mol (i.e. 12.7 g) of β -chloropropionyl chloride (98%, Sigma Aldrich) in 25 ml carbon disulfide is added dropwise for 1 hour to the previously prepared mixture with continuous stirring. After all reactants are added, the resultant mixture is stirred for 3 additional hours at room temperature. The mixture is then slowly quenched with ice. In fact, the water molecule reacts with aluminum chloride to produce excessive fumes of hydrogen chloride in the gas form in a very exothermic reaction. Therefore, proper handling and cooling is required especially that carbon disulfide is highly flammable. After addition of ice, the mixture is then extracted with diethylether (>99%, Fisher), that is also added slowly then washed with distilled water, 10% sodium carbonate (>99%, Sigma Aldrich) solution in distilled water, then water and dried over magnesium sulfate (Caledon laboratory chemicals) and filtered using 0.22 μm porosity filter papers. The excess solvent in the resultant mixture is removed using rotary evaporator at 47 $^{\circ}\text{C}$ and atmospheric pressure.

The product obtained is then analyzed in the GC-MS. This synthesis has been repeated multiple time (>10 times) and the switch of solvent to diethylether and methylene chloride or diethylether and toluene instead of only diethylether was tested. The yield of 3-chloropropiophenone is calculated by creating calibration curves using chromatography. It was concluded that products that used only diethylether for liquid-liquid extraction had the highest yields. The yields varied between 83-91%. Though this method is not 100% reproducible, the yield is high enough to proceed to the next step.

Chromatograms of all products have the same peaks. Figure 7.4 shows the chromatogram of one of the samples. There is formation of the by-product 1-phenyl-2-propen-1-one in small amounts (eluting at 9 minutes) and the main product is 3-chloropropiophenone (eluting at around 17 minutes). The chromatogram shows that all reactants are totally consumed.

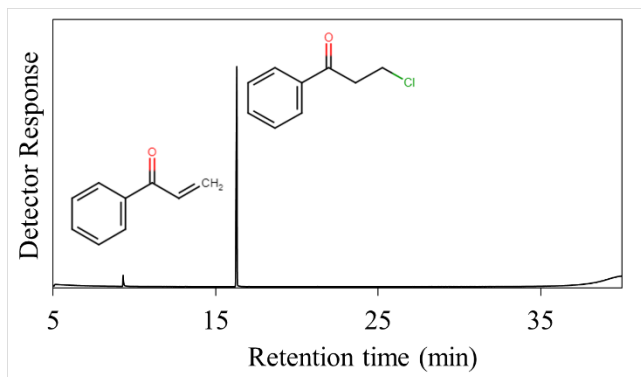


Figure 7.4. Chromatogram of synthesized 3-chloropropiophenone.

7.3.2 Synthesis of indanone from 3-chloropropiophenone

The formation of indanone requires a Friedel-Craft cyclization that converts the 3-chloropropiophenone formed in Section 7.3.1 into the ketone (Figure 7.5). Two different methods were tested.

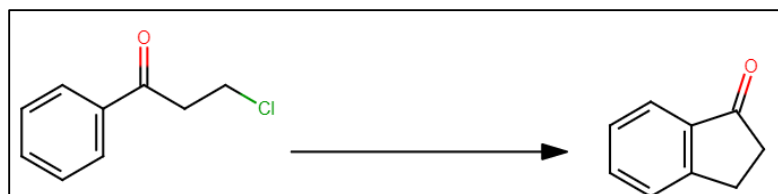


Figure 7.5. Cyclization of 3-chloropropiophenone.

Method 1:

Nguyen et al.⁴ used a mixture of aluminum chloride (AlCl_3) with sodium chloride (NaCl) to convert the 3-chloropropiophenone to indanone. Aluminum chloride acts as the electrophile. The use of sodium chloride was not justified in the paper, but it was suspected that it was rather used to decrease the melting point of the aluminum chloride than to provide an electrophile (i.e. chlorine) for it. In fact, the NaCl partially blocks the interaction of the aluminum chloride with the

nucleophile forming NaAlCl_4 . In this reaction, the electrophile is created using the chlorine atom in the 3-chloropropiophenone. The melting point of AlCl_3 is $192\text{ }^\circ\text{C}$ but the mixture of aluminum chloride with sodium chloride melts at $130\text{ }^\circ\text{C}$ or lower which makes it useful to add the sodium chloride.

Experimentally, 0.1 mol of the previously synthesized 3-chloropropiophenone is added to a slurry of 0.1 mol (i.e. 13.34 g) aluminum chloride and 0.06 mol (i.e. 3.5 g) NaCl (Fisher) at $130\text{ }^\circ\text{C}$. The mixture was stirred at $180\text{ }^\circ\text{C}$ for 2 hours. The mixture was then cooled to room temperature and quenched with ice followed by concentrated HCl (1N, Acros Organics). The resulting mixture was extracted with methylene chloride (HPLC grade, Fisher) then dried over magnesium sulfate (Caledon laboratory chemicals) and filtered using $0.22\text{ }\mu\text{m}$ porosity filter paper. The solvent was removed using rotary evaporator at $47\text{ }^\circ\text{C}$ and atmospheric pressure.

This procedure has been repeated 3 times and all products were analyzed in the GC-MS. In the first trial, there was some indanone formed in trace amounts and the rest was some unreacted 3-chloropropiophenone and an indanone dimer. The second trial only produced the indanone dimer with no sign of indanone. Whereas in the third trial, the product solidified immediately after reaction and prior to extraction. It was not possible to extract the product even with concentrated HCl.

Conclusively, this method seems not reproducible. Another challenge with working with this method is to completely dry the 3-chloropropiophenone previously produced (i.e. totally remove the solvents used for extraction in the previous step, namely diethylether and carbon disulfide). It is also suspected that the reaction might depend on the moisture in the air on the day of the run that might affect the catalyst activation. Consequently, another method was used.

Method 2:

Khalaf et al.³ used concentrated sulfuric acid in a neat matrix (i.e. solvent-free) to convert the 3-chloropropiophenone into indanone. In a 3-necked round bottom flask equipped with a condenser and stirrer, and to every 0.01 mol of 3-chloropropiophenone, 10 ml of concentrated sulfuric acid (99.9%, Fisher) is added. The mixture is stirred for 1 hour at $90\text{ }^\circ\text{C}$. The mixture is then cooled to room temperature and quenched with ice slowly. The acid is added to the ice not the opposite. The product is then extracted with diethylether (>99%, Fisher), then washed with distilled water, 10%

sodium carbonate (>99%, Sigma Aldrich) solution in water, then water and dried over magnesium sulfate (Caledon laboratory chemicals) and filtered using 0.22 μm filter paper. The excess solvent in the resultant mixture was removed using a rotary evaporator at 47 $^{\circ}\text{C}$ and atmospheric pressure.

There were three main challenges in this reaction: (i) the previously synthesized 3-chloropropiophenone has to be completely dry (no solvent) because the sulfuric acid is so concentrated and is heated; therefore any solvent present might interfere and solidify the mixture at high temperatures, (ii) it is extremely difficult to keep the temperature at 90 $^{\circ}\text{C}$ in the reaction mixture. In fact, as soon as the concentrated sulfuric acid is added to the 3-chloropropiophenone at room temperature, the mixture becomes hot. Throughout the reaction, that is exothermic, the mixture is easily overheated to beyond 90 $^{\circ}\text{C}$. Therefore, keeping the oil bath at 90 $^{\circ}\text{C}$ does not guarantee that the reaction inside is at 90 $^{\circ}\text{C}$. For that reason, a glass thermometer was introduced into the reaction mixture and the temperature of the oil bath was controlled during the 1 hour of stirring in a way to keep the inside temperature at 90 $^{\circ}\text{C}$ despite all temperature fluctuations, (iii) when working with 0.2 moles of 3-chloropropiophenone, the amount of concentrated sulfuric acid is around 200 ml which requires large amounts of water and solvents in the extraction step. This makes handling very difficult especially due to high concentration of hot sulfuric acid.

This synthesis has been repeated 12 times (Table 7.1) at slightly different conditions for the purpose of increasing the yield. The yield of indanone was calculated using the calibration curves created in the GC-NPD. The yield takes into account the conversion of the 3-chloropropiophenone and the selectivity towards indanone (i.e. $\text{yield} = \text{selectivity} * \text{conversion}$).

Table 7.1. Indanone synthesis at different conditions.

Sample Name	Reaction Temperature (°C)	Reaction time (min)	Yield of indanone (%)	Results
Indanone-1 ^a	70 ^b	30	-	GC-MS shows only some indanone dimer being formed and some reactant left
Indanone-2 ^a	90 ^b	40	-	GC-MS shows equal amounts of indanone and indanone dimer produced and a small amount of reactant left
Indanone-3 ^a	70 ^b	40	-	GC-MS shows only trace amounts of indanone and the rest is unreacted reactant
Indanone-4 ^c	90	40	-	Thermometer used. GC-MS shows only indanone in the product. However SimDist results show that 50 wt% of product is indanone and 40 wt% is the dimer
Indanone-5 ^c	90	50	33.8	Thermometer used. GC-MS shows only indanone in the product. However SimDist results show that 63 wt% of product is indanone and 34 wt% is the dimer.
Indanone-6 ^c	80	50	27.6	Thermometer used. GC-MS shows some reactant left.
Indanone-7 ^c	90	40	50.0	Thermometer used. GC-MS shows only indanone. SimDist shows only 3wt% of dimer and the rest is indanone. The extraction was done

				with both diethylether and toluene in equal amounts.
Indanone-8 ^a	110	40	17.5	Thermometer used. GC-MS shows both indanone and dimer.
Indanone-9 ^a	90	40	7.3	Thermometer used. GC-MS shows both indanone and dimer.
Indanone-10 ^a	90	40	13.1	Thermometer used. GC-MS shows both indanone and dimer. Temperature fluctuation happened reaching 110 °C.
Indanone-11 ^a	90	40	11.0	Thermometer used. GC-MS shows mainly indanone and traces of dimer. SimDist shows around 52 wt% of dimer in the product.
Indanone-12 ^a	90	40	26.1	Thermometer used. GC-MS shows mainly indanone and traces of dimer. The extraction was done with diethylether and toluene (ratio of 1:2). SimDist shows around 13 wt% of dimer in the product.

^aThe feed is the previously synthesized 3-chloropropiophenone.

^bTemperature reflects the temperature of the oil bath. No thermometer was used inside the reaction flask.

^cThe feed is 3-chloropropiophenone purchased from Sigma Aldrich with 98% purity.

GC-MS results for indanone-7 are shown in Figure 7.6. The structure of the indanone dimer might not be exactly as presented. The by-product formed in the previous step (phenyl vinyl ketone) was still present in the mixture but in very low amounts.

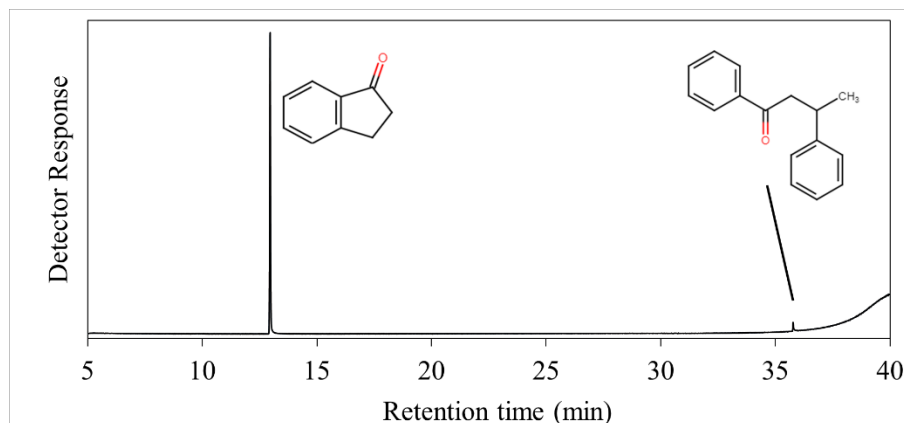


Figure 7.6. Chromatogram of the product of indanone-7.

Table 7.1 shows that amongst samples that used synthesized 3-chloropropiophenone, indanone-12 had the highest yield (26.1 %). Amongst samples that used commercial 3-chloropropiophenone, indanone-7 had the highest yield (50%). Both indanone-7 and 12 used diethylether and toluene for extraction instead of only diethylether which was suggested by Khalaf et al.³. The low yield in these reactions is due to the following reasons: (i) if previously synthesized 3-chloropropiophenone is to be used, some of the solvents and the by-product formed in the previous step might be present (ii) there is a large loss in the volume of product obtained due to the multiple extractions that need to be done especially when dealing with large volumes, as well as the rotary evaporator losses (iii) the dimerization is almost impossible to avoid and that decreases the selectivity to indanone (iv) the nature of the reaction that is highly exothermic and that leads to temperature fluctuations.

Looking back at the literature, the synthesis of phenyl vinyl ketone from benzene has been first discussed by Moureu^{5,6} using acryloyl chloride and aluminum chloride. The yield was 4%. Later, Kohler⁷ repeated Moureu's experiment not believing that what Moureu synthesized was unsaturated (i.e. phenyl vinyl ketone). He concluded that whatever was synthesized back then by Moureu was 1-indanone. Kohler also claimed that the trajectory for synthesis of 1-indanone can pass by either the phenyl vinyl ketone intermediate or the 3-chloropropiophenone intermediate. However, the latter has a higher yield for 1-indanone because of the halogen. He mentioned that the preparation of 1-indanone is very challenging and was a very slow reaction with a high yield of dimers. Hart et al.⁸ were the first to introduce the use of one-step synthesis without isolation of the intermediate. They mentioned that the yield was lower than doing both steps separately. In their procedure, they added the sulfuric acid to the obtained product immediately after reaction,

before any washing or liquid-extraction. The washing is usually used to remove the aluminum chloride that stays connected to the oxygen of the 3-chloropropiophenone and blocks any future reactions. However, Hart et al.⁸ claim that the addition of the sulfuric acid directly to the 3-chloropropiophenone-aluminum chloride complex will decompose this complex and a quick ring closure will take place. This procedure has been tried and was not successful. Indanone was not obtained. Later, this method has been optimized and better explained by Khalaf et al.³ that is the procedure that worked. In a recent study by Zhou et al.⁹, the one-step synthesis of indanone from benzene using acryloyl chloride and aluminum chloride was tested. Different reaction conditions have been considered, but the highest yield of isolated indanone that could be found was 20% and the rest of the reactions either did not form any indanone or formed traces. The dominating product was the indanone dimer.

7.3.3 Synthesis of indene from indanone

Three different pathways were suggested for the synthesis of indene from indanone.

7.3.3.1 Through the enol triflate intermediate

It was suggested that passing through the enol-triflate intermediate (Figure 7.7), it was possible to convert indanone to indene.²

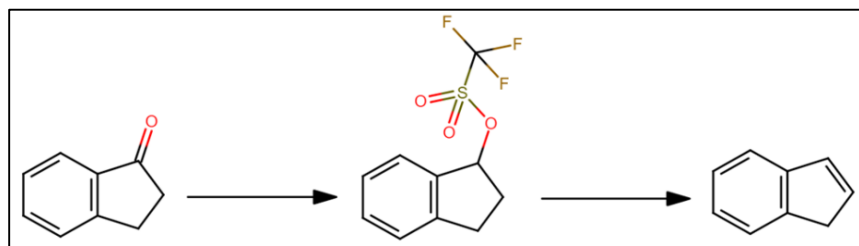


Figure 7.7. Enol intermediate for synthesis of indene from indanone.

7.3.3.1.1 Indanone to enol-triflate

The first part was to synthesize the enol triflate from indanone. Two methods have been tested:

Method 1:

This method was developed using two previous cited syntheses.^{10,11} In a 250 ml round bottom flask, equipped with reflux condenser and stirrer, 30 mmol (i.e. 3.96 g) of indanone ($\geq 99\%$, Sigma Aldrich) is dissolved in 100 ml of dichloromethane solvent (99.9%, Fisher). To the mixture was added 32 mmol (MW=282.13 g/mol) of triflic anhydride ($\geq 99\%$, Sigma Aldrich) and 33 mmol (MW=205.34 g/mol) of 2,6-di-*t*-butyl-4-methylpyridine (97%, Alfa Aesar). Two different combinations of reaction time and temperature were used: 28 °C for 12 hours (Otf-1) and 40 °C for 1 hour (Otf-2).

The solvent is then removed in a rotary evaporator at 555.7 mbar at 23 °C and the residue combined with 150 ml of pentane (switch of solvent to pentane). The pentane solution is washed with 150 ml of HCl (1N, Acros Organics) and with 50 ml of a 1 M saturated sodium chloride (Crystalline, Fisher) solution and is dried over magnesium sulfate (Caledon laboratory chemicals) and filtered using 0.22 μm filter paper then concentrated using a rotary evaporator.

GC-MS shows that Otf-1 product had a 50-50 mixture of indanone and enol triflate. Whereas Otf-2 product had mainly unreacted indanone and a small peak for the enol-triflate. It was worthwhile trying a different method.

Method 2:

The procedure performed by Udayakumar et al.¹² was tried. 7.56 mmol of 1-indanone ($\geq 99\%$, Sigma Aldrich) in 50 ml dichloromethane (99.9%, Fisher) was added to 9.07 mmol (1.2 equiv.) N,N-Diisopropylethylamine (Alfa Aesar). 9.07 mmol (1.2 equiv.) of triflic anhydride ($\geq 99\%$, Sigma Aldrich) was then added dropwise and the mixture stirred at 40 °C for 1 h. The mixture was then washed with distilled water and extracted with dichloromethane. The organic layer was then dried over magnesium sulfate (Caledon laboratory chemicals) and filtered using 0.22 μm filter paper, then concentrated under reduced pressure (rotary evaporator). The product of this synthesis is called Otf-3.

For Otf-3, GC-MS results showed that enol-triflate and indanone were in the product in the ratio of 50-50. The enol triflate formed by these reactions is not part of the mass spectrometer library. Therefore, a fragmentation of the mass spectrum has been done manually to confirm the structure as shown in Figure 7.8. The last peak in the mass spectrum shows 264 that is the molecular weight of the enol-triflate formed. The three other peaks showing in the mass spectrum (i.e. 77, 103 and 131) correspond to the molecular weights of three fragments of the enol-triflate as shown in Figure 7.8.

The results were also combined with GC-DFPD (Dual Flame Photometric Detector) that has a sulfur detector. Otf-3 product shows a peak for sulfur. In conclusion, even if some enol-triflate was formed using both methods, a large amount of indanone remains unreacted.

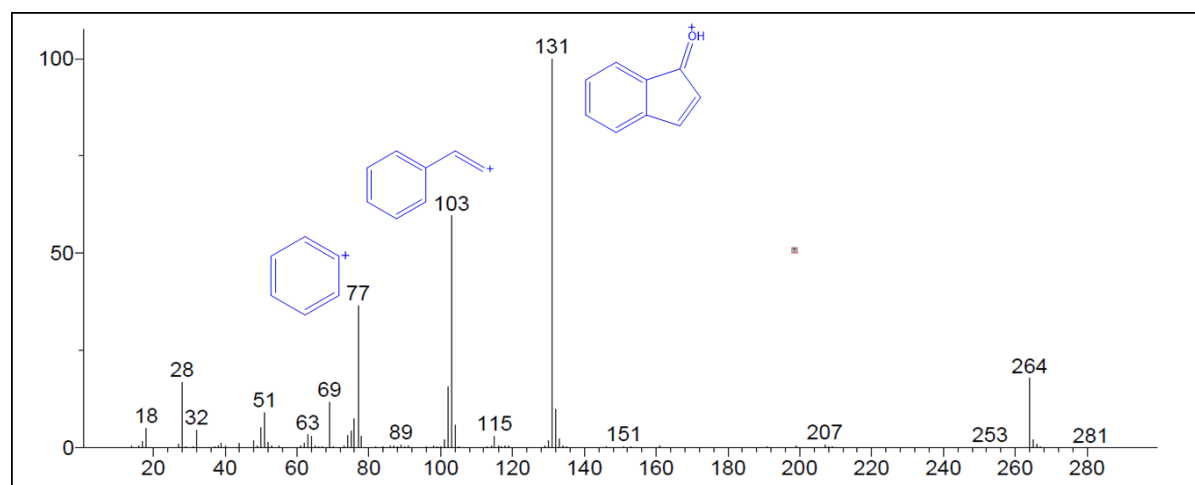


Figure 7.8. Manual fragmentation of mass spectrum of the peak of the enol-triflate.

7.3.3.1.2 Enol-triflate to indene

The second part is the synthesis of indene from the formed enol triflate (Otf-3) using the procedure suggested by Kotsuki et al.¹³ To 10 mmol of previously formed enol-triflate (i.e. 2.64 g) at 60 °C was added 0.2 mmol (i.e. 45 mg) of palladium (II) acetate (47.5%Pd, Acros Organics) and 0.2 mmol (i.e. 80 mg) of dppp (1,3-Bis(diphenylphosphino)propane) (97%, Sigma Aldrich) in 50 mL of dimethylformamide (99.5%, Fisher). The mixture was stirred. 25 mmol (i.e. 4 ml) of triethylsilane (99%, Acros Organics) was then added and the mixture stirred for 5 hours at 60°C. After the reaction was done, the mixture was diluted in diethylether (>99%, Fisher) then washed with distilled water, then saturated aqueous sodium bicarbonate (>99.5 %, Sigma Aldrich)

solution, then saturated aqueous sodium chloride (Crystalline, Fisher) solution. The mixture is then dried over magnesium sulfate (Caledon laboratory chemicals) and filtered using 0.22 μm filter paper and the filtrate was concentrated by removing the solvent.

The major product obtained from this reaction (Figure 7.9) was the hexaethyl-disiloxane (eluting at around 15 minutes) that is due to the reaction between the unconsumed indanone, from Otf-3, with triethylsilane. Therefore, this step cannot be done unless the previous product (Otf-3) is purified and indanone removed. This is also because the enol-triflate intermediate is not available commercially for purchase. However, the separation of indanone and the enol-triflate seems not to be feasible especially given that properties of the indanone enol-triflate compound are not known (e.g. boiling point).

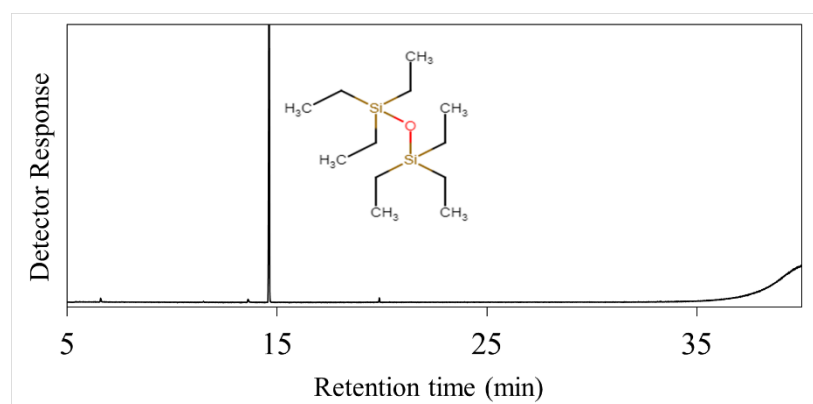


Figure 7.9. Chromatogram showing hexaethyl-disiloxane as main product.

7.3.3.2 Direct synthesis of indene from indanone

The direct synthesis of indan from indanone has been previously done.^{14,15,16} However, there was only one paper found for the direct synthesis of indene from indanone. This synthesis was described by Imai et al.¹⁷ and consists of using neopentyl glycol and p-toluenesulfonic acid.

In the paper by Imai et al.,¹⁷ the experimental methodology described seemed so simple and it was described as follows: a solution of 3.8 mmol of 1-indanone (i.e. 0.5 g), 15.6 mmol neopentyl glycol (i.e. 1.53 g) and 100 mg of p-toluenesulfonic acid in 6 ml benzene was stirred at 80 °C for 36 h. The mixture was then washed with 5 ml of a saturated aqueous sodium carbonate solution and then extracted with diethylether and the product concentrated using a rotary evaporator.

Table 7.2. Indene synthesis at different conditions.

Sample Name	Reaction Temperature (°C)	Reaction time (hrs)	Mass of NPG (g)	Mass of PTS (g)	GC-MS Results
Indene-1 ^a	80	24	1.53	0.1	Most of them had traces of indene except for one that had peaks of indene, indanone and indanone dimer in the ratio of (1:2:4)
Indene-2	80	36	1.53	0.1	Large amount of indanone unreacted, traces of indene and some dimer formed.
Indene-3	80	30	1.53	0.1	Mainly indanone and some dimer formed.
Indene-4	80	18	1.53	0.1	Mainly indanone and some dimer formed.
Indene-5	80	24	1.53	0.32	Traces of indene with equal amounts of indanone and indanone dimer
Indene-6	80	24	1.53	0.62	Traces of indene with equal amounts of indanone and indanone dimer
Indene-7	80	24	0.53	0.32	Only indanone with traces of the dimer
Indene-8	80	24	0.51	0.62	Mainly dimer with traces of indanone.

^aThis has been repeated 4 times.

This procedure was tried multiple times using commercial indanone ($\geq 99\%$, Sigma Aldrich), neopentyl glycol (NPG) (99% , Sigma Aldrich) and p-toluene sulfonic acid monohydrate (PTS) ($\geq 98.5\%$, Sigma Aldrich) but using toluene instead of benzene as the solvent. From the paper, it was

not clear whether the reaction time is 24 hours or 36 hours as it was mentioned differently in different places in the paper. Many trials have been done at different conditions (Table 7.2) trying to increase the yield of indene. In all trials, 0.5 grams of indanone was used.

It was obvious from all these trials, that the method described¹⁷ is not accurate and the yields reported were not possible to obtain as only traces of indene were formed. This method was thus discarded.

7.3.3.3 Through the indanol intermediate

The third method consists of synthesizing indanol as an intermediate (Figure 7.10). It converts the ketone structure (i.e. indanone) into an alcohol (i.e. indanol) and then reduces it into an alkene (i.e. indene). It is divided into two steps:

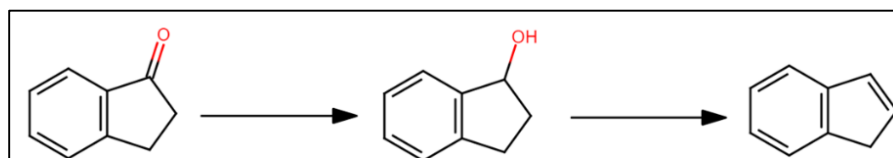


Figure 7.10. Synthesis of indene from indanone through the indanol intermediate.

7.3.3.3.1 Synthesis of indanol from indanone

Synthesis of indanol from indanone has been widely covered in literature (e.g.^{18,19,20}). However, the only procedure that was tried was the one by Teitelbaum et al.¹⁸ and was successful with a high yield. In a jacketed 500 ml 2-necked round bottom flask, and to a solution of 4.54 mmol (i.e. 1.26 g, 0.2 equivalent) of (R)-(+)-2-methyl-CBS-oxazaborolidine ($\geq 95\%$, Sigma Aldrich) in 108 ml of tetrahydrofuran (THF) (Fisher) at 0 °C was added a 14 ml of a borane dimethyl sulfide solution (2 M in THF, Sigma Aldrich) (1.2 equivalent). After stirring for 15 min, a solution of 22.7 mmol (i.e. 3g, 1.0 equivalent) of indanone ($\geq 99\%$, Sigma Aldrich) in 108 ml THF was added dropwise into the reaction mixture. The resultant mixture was stirred for 30 min, then quenched by the addition of 36.5 ml of methanol (HPLC grade, Fisher). The product was concentrated using a vacuum rotary evaporator at 357 mbar at 44 °C to remove the solvent.

Indanol was identified using GC-MS. The chromatogram in Figure 7.11 was obtained. Indanol being the only product is eluting at around 12 minutes. No by-products were obtained and the peak at around 14 minutes corresponds to the remaining reactant (namely, indanone). The peak at around 20 minutes is due to a stabilizer present in the solvent used for the analysis (THF).

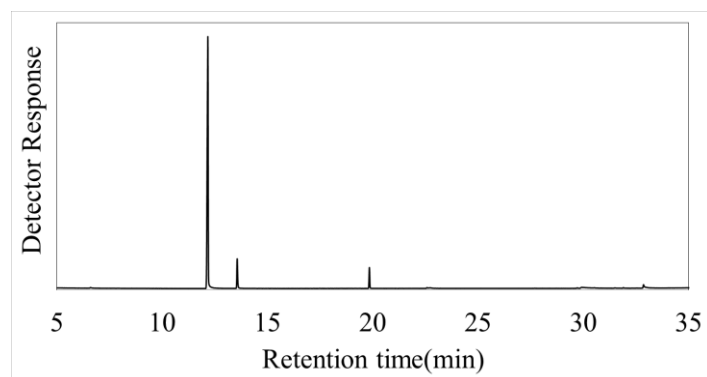


Figure 7.11. Chromatogram of synthesized indanol.

The yield was obtained to be around 90% with 100% selectivity towards indanol. This method has been repeated twice and the reproducibility has been confirmed.

7.3.3.3.2 Synthesis of indene from indanol

The reduction of an alcohol on an aromatic ring to the corresponding alkene has been covered in the literature.^{21,22,23,24} However, the procedure done by Braun et al.²² has been chosen and re-developed by modifying some parameters and tested. The following is the experimental methodology that was followed: 7.45 mmol (i.e. 1 g) of 1-indanol (98%, Sigma Aldrich) was added to 0.46 mmol (88 mg) of *p*-toluenesulfonic acid ($\geq 98.5\%$, Sigma Aldrich) in 50 ml toluene and was stirred at 80 °C for 40 min. The mixture was then cooled to room temperature, then a saturated aqueous saturated sodium carbonate ($>99\%$, Sigma Aldrich) solution was added, and the product was extracted with diethylether ($>99\%$, Fisher). The mixture was dried over magnesium sulfate (Caledon laboratory chemicals) and filtered using 0.22 μm filter paper. The diethylether and toluene were removed carefully using a rotary evaporator at 77 mbar and 45 °C.

Indene was identified using GC-MS (Figure 7.12). The indene peak is showing at around 7 minutes as the major product. The only by-product formed and detected by GC-MS is an addition product

of indene showing at around 33 minutes. The peak showing at around 20 minutes is a stabilizer present in the solvent used for chromatography.

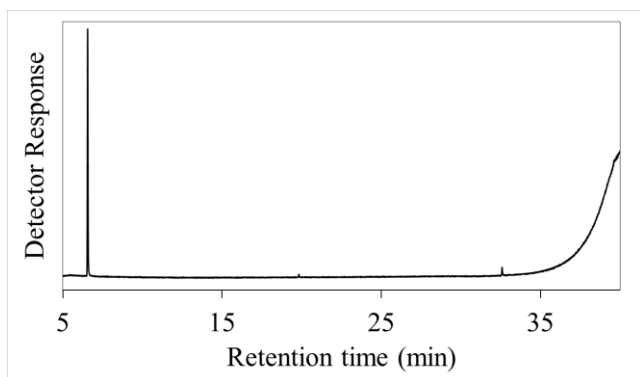


Figure 7.12. Chromatogram of synthesized indene.

The yield of indene was obtained to be around 79%. Part of the indene is being lost during solvent removal due to the volatility of indene. The yield of indene before solvent removal was calculated to be 85% using the same apparatus and same program. Around 6% of the indene is therefore lost due to solvent removal. The reproducibility of this method has also been tested and confirmed.

7.4 Finalized synthesis of indene from benzene and challenges

The pathway of synthesis of indene from benzene has been finalized using the previous set of reactions. It was described as a four-steps synthesis (Figure 7.13).

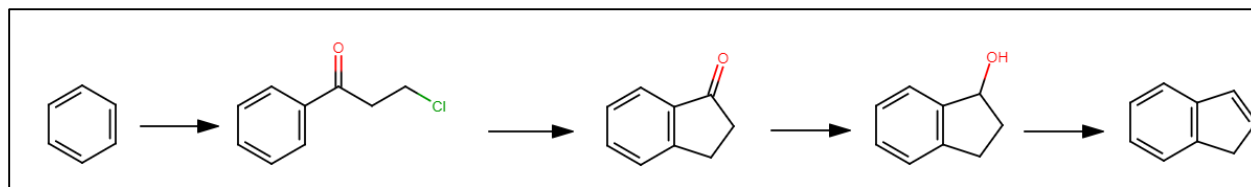


Figure 7.13. Finalized pathway for synthesis of indene from benzene.

The first step consists of synthesizing 3-chloropropiophenone from benzene by Friedel-Craft acylation following the procedure described in Section 7.3.1 (Yield=83-91%). Step 2 consists of having a Friedel-Craft cyclization to the indanone using method 2 of Section 7.3.2 as done for indanone-7 (Yield=50%). Step 3 consists of converting indanone to indanol as described in Section 7.3.3.3.1 (Yield=90%). Step 4 reduces the indanol to indene using Section 7.3.3.3.2 procedure (Yield=79%). All yields of the steps are acceptable except for step two. 50% was the highest yield

that could be obtained for this reaction. This was mainly due to the dimerization of indanone. Therefore, one major challenge in this synthesis is step 2. The low yield might not be a big issue if one starts with a larger amount of initial reactant (i.e. benzene). However, one major challenge in this final synthesis lies in the fact that the indanone dimer formed in step 2 has to be separated from the indanone in order to proceed to the next step. When indanone and indanone dimer mixture was used to form indanol, the reaction was not successful.

Since indanone and its dimer have two very broad boiling points, it should not be impossible to perform the separation (i.e. the indanone purification). Three methods for the separation are suggested: (i) the use of a rotary evaporator at reduced pressure in order to evaporate the indanone and collect it, but this was tried and the separation was not successful, (ii) the use of thin-layer chromatography, which was tried using Silica Gel 60 (particle size 0.040-0.063 nm, 230-400 mesh ASTM, EM Science) as the bed in the ratio of 30 grams silica for every 1 gram indanone, in a 2.3 cm diameter column, with an 8:2 ratio of hexane to ethyl acetate, this was also not successful, (iii) the use of distillation which was not tried as it was not available in our lab.

7.5 Cost estimation of synthesis of ^{13}C -labelled indene

A cost estimation for the synthesis of 1 gram of ^{13}C -labelled indene using the suggested pathway in Section 7.4 has been done (Table 7.3).

Table 7.3. Cost estimation for synthesis of 1 gram of ^{13}C -labelled indene.

Chemical name	Amount needed	Cost (C\$)
^{13}C -labelled benzene	2.24 g	829
3-chloropropionyl chloride	3.64 g	5
Aluminum Chloride	4.59 g	1
Sulfuric Acid	24 ml	6
Borane dimethyl sulfide solution (2M in THF)	7.4 ml	7
(R)-(+)-2-methyl-CBS-oxazaborolidine	0.66 g	61
p-toluene sulfonic acid monohydrate	0.11	1
Solvents and extraction chemicals ^a	-	600
TOTAL	-	1,510

^aThis is a rough estimation of the cost of all solvents used for reactions and extractions (e.g. toluene, diethylether, carbon disulfide, THF, etc.) and all chemicals used for extractions (e.g. magnesium sulfate, sodium carbonate, etc.).

In the cost estimation, the cost of glassware was not included. The cost of chemicals is a rough estimation and usually reflects the maximum cost. In order to synthesize 1 gram of ^{13}C -labelled indene, the back calculation for the initial mass of ^{13}C -labelled benzene needed, using the yields of 83%, 50%, 90% and 79% for steps 1 to 4 respectively, is 2.24 grams. The total cost for synthesis of 1 gram of labelled indene where all the carbons in the benzene ring are ^{13}C -labelled, is no more than C\$ 1,510 compared to C\$ 150,000 for purchase of ^{13}C -labelled indene.

7.6 Conclusions

A new pathway for the synthesis of indene from benzene has been developed. The synthesis consists of passing through 3-chloropropiophenone, indanone and indanol as intermediates. The ^{13}C labels are present on all carbons of the benzene ring to be capable to track the indene molecule in all types of complex matrices. The synthesis costs only around C\$ 1,510 / g.

Literature cited

- (1) Badger, G. M., Jolad, S. D., & Spotswood, T. M. The Formation of Aromatic Hydrocarbons at High Temperatures. XXV. The Pyrolysis of [3-¹⁴C] Indene. *Aust. J. Chem.* **1966**, *19* (1), 85–93.
- (2) Yanagimachi, K. S.; Stafford, D. E.; Dexter, A. F.; Sinskey, A. J.; Drew, S.; Stephanopoulos, G. Application of Radiolabeled Tracers to Biocatalytic Flux Analysis. *Eur. J. Biochem.* **2001**, *268* (18), 4950–4960.
- (3) Khalaf, A.A., Abdel-Wahab, A.A., El-Khawaga, A.M. & El-Zohry, M. . Modern Friedel-Crafts Chemistry XIII. Intra- and Intermolecular Cyclization of Some Carbonyl Derivates under Friedel-Crafts Conditions. *Bull. Chem. Soc. Fr. II* **1984**, No. 5(2), 285–291.
- (4) Nguyen, P.; Corpuz, E.; Heidelbaugh, T. M.; Chow, K.; Garst, M. E. A Convenient Synthesis of 7-Halo-1-Indanones and 8-Halo-1-Tetralones. *J. Org. Chem.* **2003**, *68* (26), 10195–10198.
- (5) Moureu, C. Action Du Chlorure d'acryle Sur Le Benzène En Présence Du Chlorure d'aluminium. *Bull. le Soc. Chim. Paris* **1893**, *3* (9), 570–572.
- (6) Moureu, C. Action Du Chlorure d'acryle Sur Le Benzène En Présence Du Chlorure d'aluminium. *Ann. Chim. Phys.* **1894**, *7* (2), 198–201.
- (7) Kohler, E. P. Vinylphenyl Ketone and Some of Its Homologues. *Am. Chem. J.* **1909**, *42*, 376–380.
- (8) Hart, R. T.; Tebbe, R. F. Acylation-Alkylation Studies. I. *J. Am. Chem. Soc.* **1950**, *72* (7), 3286–3287.
- (9) Zhou, Y.; Li, X.; Hou, S.; Xu, J. Facile Synthesis of Dihydrochalcones via the AlCl₃-Promoted Tandem Friedel-Crafts Acylation and Alkylation of Arenes with 2-Alkenoyl Chlorides. *J. Mol. Catal. A Chem.* **2012**, *365*, 203–211.
- (10) Peter J. Stang, W. T. Single-Step Improved Synthesis of Primary and Other Vinyl Trifluoromethanesulfonates. *Synthesis (Stuttg)*. **1980**, No. 04, 283–284.
- (11) Jigajinni, V. B., & Wightman, R. H. Hydrogenolysis of Enol Triflates; A New Method for the Reduction of Ketones to Methylene Compounds. *Tetrahedron Lett.* **1982**, *23* (1), 117–120.
- (12) Udayakumar, V.; Gowsika, J.; Pandurangan, A. A Novel Synthesis and Preliminary in Vitro Cytotoxic Evaluation of Dihydropyrimidine-2,4(1H, 3 H)-Dione Derivatives. *J. Chem. Sci.*

- 2017, *129* (2), 249–258.
- (13) Kotsuki, H., Datta, P. K., Hayakawa, H., & Suenaga, H. An Efficient Procedure for Palladium-Catalyzed Reduction of Aryl/Enol Triflates. *Synthesis (Stuttg)*. **1995**, No. 11, 1348–1350.
- (14) Kalutharage, N.; Yi, C. S. Scope and Mechanistic Analysis for Chemoselective Hydrogenolysis of Carbonyl Compounds Catalyzed by a Cationic Ruthenium Hydride Complex with a Tunable Phenol Ligand. *J. Am. Chem. Soc.* **2015**, *137* (34), 11105–11114.
- (15) Surya Prakash, G. K.; Do, C.; Mathew, T.; Olah, G. A. Reduction of Carbonyl to Methylene: Organosilane-Ga(OTf)₃ as an Efficient Reductant System. *Catal. Letters* **2011**, *141* (4), 507–511.
- (16) Olah, G. A., Arvanaghi, M., & Ohannesian, L. Synthetic Methods and Reactions; 126. Trifluoromethanesulfonic Acid/Triethylsilane: A New Ionic Hydrogenation Reagent for the Reduction of Diaryl and Alkyl Aryl Ketones to Hydrocarbons. *Synthesis (Stuttg)*. **1986**, No. 9, 770–772.
- (17) Imai, M.; Morais, G. R.; al-Hindawi, B.; al-Sulaibi, M. A. M.; Meetani, M.; Thiemann, T. Acid Catalysed Reaction of Indanones, Tetralones and Benzosuberone with Neopentyl Glycol and Other Alkanediols under Forced Conditions. *J. Chem. Res.* **2010**, *34* (6), 325–329.
- (18) Teitelbaum, A. M.; Meissner, A.; Harding, R. A.; Wong, C. A.; Aldrich, C. C.; Rimmel, R. P. Synthesis, PH-Dependent, and Plasma Stability of Meropenem Prodrugs for Potential Use against Drug-Resistant Tuberculosis. *Bioorganic Med. Chem.* **2013**, *21* (17), 5605–5617.
- (19) Zheng, L. S.; Llopis, Q.; Echeverria, P. G.; Féraud, C.; Guillamot, G.; Phansavath, P.; Ratovelomanana-Vidal, V. Asymmetric Transfer Hydrogenation of (Hetero)Arylketones with Tethered Rh(III)-N-(p-Tolylsulfonyl)-1,2-Diphenylethylene-1,2-Diamine Complexes: Scope and Limitations. *J. Org. Chem.* **2017**, *82* (11), 5607–5615.
- (20) Clerici, A.; Pastori, N.; Porta, O. ChemInform Abstract: Reduction of Aliphatic and Aromatic Cyclic Ketones to Sec-Alcohols by Aqueous Titanium Trichloride/Ammonia System. Steric Course and Mechanistic Implications. *ChemInform* **2010**, *33* (15), no-no.
- (21) Zhu, Z.; Espenson, J. H. Organic Reactions Catalyzed by Methylrhodium Trioxide: Dehydration, Amination, and Disproportionation of Alcohols. *J. Org. Chem.* **1996**, *61* (1),

- 324–328.
- (22) Braun, M., & Bernard, C. Einfache Darstellung von B-Tetralonen Und B-Indanonen Durch 1, 2-Carbonylgruppenverschiebung. *Liebigs Ann. der Chemie* **1985**, No. 2, 435–437.
- (23) Bagheri Marandi, G.; Pourjavadi, A.; Hosseinzadeh, H. Solvent-Free Dehydration of Alcohols Using LiCl-Acidicalumina. *Orient. J. Chem.* **2012**, 28 (3), 1141–1145.
- (24) Dey, J.; O'Donoghue, A. M. C.; More O'Ferrall, R. A. Equilibrium Constants for Dehydration of Water Adducts of Aromatic Carbon-Carbon Double Bonds. *J. Am. Chem. Soc.* **2002**, 124 (29), 8561–8574.

Chapter 8: Conclusions

8.1 Introduction

With the increased interest in heavy oils as a source of energy, the disadvantage of formation of heavier products as side-reactions during thermal conversions persists. This was of particular relevance to visbreaking, since conversion in visbreaking is limited by heavy product formation leading to the onset of coking. It was postulated that a fundamental understanding of the free radical chemistry taking place in the visbreaker is crucial. More studies that aim to clarify the thermal cracking system and the equilibrium between cracking and addition is essential to rationally develop strategies to limit heavy product formation and suppress coke formation.

The purpose of this study was to provide a better understanding of the free radical chemistry in visbreaking with an emphasis on free radical addition reactions.

8.2 Major conclusions and insights

The study on the quantification of free radical content of several oil fractions has set the grounds for studies on free radical systems. It has been demonstrated that the solvent and bulk liquid properties play an important role in shifting the radical formation-radical combination equilibrium. This was the main contribution of this study. In addition, this demonstration suggested that the reported free radical concentrations must be interpreted by considering the nature of the bulk liquid that was analyzed. This has a direct implication on free radical systems including thermal conversions. One way of manipulating the free radical concentrations is by modifying the bulk liquid properties of the matrix, this might shift the equilibrium between cracking and addition reactions. This was a noteworthy contribution, because it provided a new avenue to explore ways to suppress heavy product formation.

The number of free radicals were found to be highest in the heaviest fractions (10^{17} – 10^{18} spins/g), whereas lighter fractions such as the lighter gas oil fractions had free radical concentrations in the range 10^{16} – 10^{17} spins/g. These observations were aligned with previous reports in literature and the main contribution from this work was to update and expand the literature.

The study on the reaction of model compounds at thermal cracking conditions (400 °C, 2 MPa), found that the ability of five-membered ring naphtho-aromatics to undergo free radical addition reactions and forming asphaltenes depended on the nature of the five-membered ring attached to the benzene ring. While indan and thianaphthene were thermally stable on their own, but reactive in mixtures, indene, indole and benzofuran were reactive on their own and in mixtures. The susceptibility of indene to undergo free radical addition reactions and form *n*-pentane insoluble asphaltenes have been proved to be the highest. The chemistry of the behavior of each compound at the reaction conditions was discussed. The main contribution from this work is characterized by the test of reactivity of these model compounds that showed they were susceptible to cracking and addition reactions. This is ultimately related to the cracking-addition equilibrium in the thermal cracking matrix.

Indan ring opening was found to be possible in the presence of indene in the mixture. It could also be concluded that sulfur-ring opening of the thianaphthene structure was possible in the absence of direct hydrogen supply, catalyst and oxygen but in the presence of hydrogen donors, such as indene. The major products from ring-opening were 2-methylbenzenethiol and 2-ethylbenzenethiol. The conversion towards ring opening could be increased by addition of hexachlorobenzene. The value of the study on the thermochemistry of the five-membered ring naphtho-aromatics was to provide evidence of likely reaction pathways that are important, and in particular, the role of intermolecular transfer reactions. The ability to open a sulfur ring without the use of neither direct hydrogen supply, nor a catalyst was a new contribution to the literature of sulfur ring-opening.

When indene was employed to exacerbate asphaltenes formation during thermal conversion of deasphalted oil, it was found that indene was involved in addition reactions with itself and with deasphalted oil to produce new *n*-pentane insoluble material. This indicated that distillate (175-350 °C) boiling range materials could be thermally converted to material in the vacuum gas oil (350-525 °C) and vacuum residue (>525 °C) boiling range, as well as products that were *n*-pentane insoluble asphaltenes.

The effect of bulk liquid on free radical addition reactions of indene was highlighted. It was also found that the formation of *n*-pentane insoluble material was reduced in mixtures with indan and naphthalene. It was shown that new asphaltenes are formed from the thermal conversion of de-asphalted oil. The prevalence of addition reactions and the importance of hydrogen transfer reactions by molecule-induced homolysis were highlighted, which have implications for modelling reaction chemistry describing thermal conversion of heavy oil.

The change of the bulk liquid between indan and naphthalene highlighted the effect of the solvent on chain transfer and chain growth reactions. The relevance of this work was that it demonstrated the importance of the bulk liquid properties in affecting the product distribution (including heavy product formation) from thermal conversion. It also highlighted the importance of including light-to-heavy product forming reactions in models describing visbreaking.

Collectively, the investigation of the thermochemistry of five-membered ring naphtho-aromatics and heavy product formation induced by indene, suggested that methyl transfer might also be an important transfer reaction. A study of the reaction of α -methylstyrene with both indene and 2-methylindene, provided direct experimental evidence of intermolecular methyl transfer. The chemistry emphasized the importance of the transfer of hydrogen and methyl during thermal reaction.

It has been concluded that the methyl migration in free radical systems is possible and is increased by the presence of methylated groups in the feed. It was also shown that the composition of the feed in terms of methyl groups might have an impact on the type of heavy products and *n*-pentane insoluble material formed. This was a noteworthy and a new contribution, because intermolecular methyl transfer has not been recognized as a major reaction type in the description of liquid phase thermal conversion chemistry.

It was suggested that ^{13}C -labelled compounds could be used to track addition and cracking reactions in thermal conversion. This was of interest, because it could provide direct evidence of incorporation of reactive species in products. In order to track changes in the thermal cracking of deasphalted oil, it was suggested to co-feed ^{13}C -labelled indene. A new method of synthesis of

^{13}C -labelled indene from ^{13}C -labelled benzene was developed and tested. Only the protocol for this work was developed to provide a useful starting point for subsequent investigation.

This PhD study provided a new perspective for interpretation of free radical systems, typical of thermal cracking processes. The study showed that the bulk liquid properties affect both the free radical content and the free radical addition reactions in the matrix. These two concepts constitute the base of understanding the formation of heavy products, that are precursors of coke. This has implications to modelling visbreaking reactions. In addition, this work has provided evidence on the importance of intermolecular methyl transfer in thermal conversion processes, which in turn, highlights the effect of methyl group on the formation of heavy products.

8.3 Recommended future work

8.3.1 Impact of bulk liquid properties on free radicals

The study on free radicals' quantification revealed that the radical-solvent interactions could not be neglected. It would be vital to further study this effect. A study designed to probe the nature of the solvent interaction may have a contribution to the literature. It is vital to know the exact manner in which dilution in specific solvents affects the shift of equilibrium between free radical formation and free radical combination to neutral molecules. In addition, it is essential to know the effect of this equilibrium shift on the quantification of free radicals.

On the other side, one could change the bulk liquid properties to study their effect on the free radical species in thermal conversions. In such processes, when the bulk liquid is considered as a solvent for the free radical species, changes in the bulk liquid properties can be used to manipulate the free radical concentration independent of temperature. Changing the properties of the matrix may be done either by changing the reaction or by co-feeding other material, or by both. This will affect the concentration and the reactive availability of free radical species, which could be tested using electron spin resonance spectrometry.

Another implication of the impact of bulk liquid composition is that it might be worthwhile revisiting the interpretation of thermal conversion data in the published literature. Some results

could potentially be explained by changes in the available reactive free radical concentration as a consequence of the changed bulk liquid properties.

8.3.2 Sulfur-ring opening

The sulfur ring opening in the presence of indene opened the door to several research leads. For instance, it would be worthwhile investigating whether indene is the type of molecule that would be capable of ring opening for other challenging compounds. This is mainly because indene was also capable of indan ring opening. Indene is commercially available and relatively cheap. However, to generalize this observation, it showed how compounds that were reactive for hydrogen transfer could be employed at milder conditions than industrially used for visbreaking to perform otherwise difficult reactions.

In addition, the presence of hexachlorobenzene even in very small amounts in the feed led to the increase in the conversion of thianaphthene to form 2-methylbenzenethiol and 2-ethylbenzenethiol. A more detailed study of the chemistry resulting from a halogenated compound and the reason why this increase in yield took place may produce more research leads on how to perform uncatalyzed desulfurization.

8.3.3 Synthesis of ^{13}C -labelled indene

A new method for the synthesis of ^{13}C -labelled indene from ^{13}C -labelled benzene was suggested (Chapter 7). However, the separation of indanone and its dimer, formed in the second step of the suggested synthetic protocol, constitutes an obstacle. In the future, a method for separation of the two compounds needs to be found. It is likely that distillation would be an adequate method of separation. The synthesis process needs to be tested again and yields re-calculated using the synthesized compounds as reactants for each step.

8.3.4 Application of ^{13}C -labelled indene in oil systems

Once the ^{13}C -labelled indene is successfully synthesized, it could be employed for reaction in the deasphalted oil matrix. The study in Chapter 5 did not indicate whether indene induced increased

asphaltenes formation, or whether it formed addition products with the deasphalted oil. This could be resolved by using different percentages of indene with deasphalted oil. In fact, the ^{13}C -labelled indene and the ^{13}C -labelled products originating from it could be tracked using ^{13}C -NMR. This technique will allow quantification of the amount of addition products and cracked products formed from indene specifically in the indene-DAO mixture fed.

The same could be applied to compounds in the DAO that are suspected to undergo free radical addition reactions. This will provide a contribution to the literature in terms of the compound classes in the feed responsible for heavier products.

8.3.5 Tracking of methyl group in oil systems

^{13}C -labelled methylindene with the label on the methyl group attached to the five-membered ring cyclopentene, could be synthesized and used to track the methyl group in complex matrices. One major application of synthesized ^{13}C -labelled methylindene is in the visbreaker matrix.

When ^{13}C -labelled methylindene is co-fed with DAO, the comparison of results with the co-feeding of ^{13}C -labelled indene with DAO, may yield insights on the effect of the methyl group in the feed. This study would ultimately have an added value to understand how the formation of heavier products by free radical addition reactions can be limited by modifying feed properties.

Bibliography

Abe, H.; Bell, A. T. Catalytic Hydrotreating of Indole, Benzothiophene, and Benzofuran over Mo₂N. *Catal. Letters* **1993**, *18* (1–2), 1–8.

Abell, P. I. Addition to Multiple Bonds. In *Free radicals Vol.2*; Kochi, J. K., Ed.; John Wiley & Sons, 1973; pp 63–68.

Adams, J. Q.; Altgelt, K. H.; LeTourneau, R. L.; Lindeman, L. P. Free Radical Concentrations in Gel Permeation Fractions of Asphaltenes from Different Crude Oils. *Prepr. Pap.-Am. Chem. Soc., Div. Pet. Chem* **1966**, *12*, B140–B144.

Aguilar, R. A.; Ancheyta, J. Modeling Coil and Soaker Reactors for Visbreaking. *Ind. Eng. Chem. Res.* **2016**, *55* (4), 912–924.

Alemán-Vázquez, L. O.; Cano-Domínguez, J. L.; García-Gutiérrez, J. L. Effect of Tetralin, Decalin and Naphthalene as Hydrogen Donors in the Upgrading of Heavy Oils. *Procedia Eng.* **2012**, *42*, 532–539.

Alemán-Vázquez, L. O.; Torres-Mancera, P.; Ancheyta, J.; Ramírez-Salgado, J. Use of Hydrogen Donors for Partial Upgrading of Heavy Petroleum. *Energy and Fuels* **2016**, *30* (11), 9050–9060.

Alshareef, A. H.; Scherer, A.; Tan, X.; Azyat, K.; Stryker, J. M.; Tykwinski, R. R.; Gray, M. R. Formation of Archipelago Structures during Thermal Cracking Implicates a Chemical Mechanism for the Formation of Petroleum Asphaltenes. *Energy and Fuels* **2011**, *25* (5), 2130–2136.

ASTM D7169. Standard Test Method for Boiling Point Distribution of Samples with Residues Such as Crude Oils and Atmospheric and Vacuum Residues by High Temperature Gas Chromatography; ASTM: West Conshohocken, PA, 2016.

Badger, G. M., Jolad, S. D., & Spotswood, T. M. The Formation of Aromatic Hydrocarbons at High Temperatures. XXV. The Pyrolysis of [3-14C] Indene. *Aust. J. Chem.* **1966**, *19* (1), 85–93.

- Bagheri Marandi, G.; Pourjavadi, A.; Hosseinzadeh, H. Solvent-Free Dehydration of Alcohols Using LiCl-Acidicalumina. *Orient. J. Chem.* **2012**, *28* (3), 1141–1145.
- Baldwin, A. C.; Golden, D. M. Reactions of Methyl Radicals of Importance in Combustion Systems. *Chem. Phys. Lett.* **1978**, *55* (2), 350–352.
- Benjamin, B. M.; Hagaman, E. W.; Raaen, V. F.; Collins, C. J. Pyrolysis of Tetralin. *Fuel* **1979**, *58* (5), 386–390.
- Bergson, G. Proton-Mobility in the Indene Ring-System. *Acta Chem. Scand.* **1963**, *17* (10), 2691–2700.
- Bergson, G.; Weidler, A.-M. A Stereospecific Tautomeric Rearrangement. *Acta Chem. Scand.* **1963**, *17* (6), 1798–1799.
- Bergson, G.; Weidler, A.-M. Proton-Mobility in the Indene Ring-System. *Acta Chem. Scand.* **1963**, *17* (3), 862–864.
- Bianchini, C.; Frediani, M.; Vizza, F. Synthesis of the First Polymer-Supported Tripodal Triphosphine Ligand and Its Application in the Heterogeneous Hydrogenolysis of Benzo[b]Thiophene by Rhodium Catalysis. *Chem. Commun.* **2001**, *2* (5), 479–480.
- Bianchini, C.; Meli, A.; Patinec, V.; Sernau, V.; Vizza, F. Liquid-Biphase Hydrogenolysis of Benzo[b]Thiophene by Rhodium Catalysis. *J. Am. Chem. Soc.* **1997**, *119* (21), 4945–4954.
- Bielski, B. H. J.; Gebicki, J. M. Atlas of Electronspin Resonance Spectra. Academic Press: New York, 1967.
- Billmers, R.; Griffith, L. L.; Stein, S. E. Hydrogen Transfer between Anthracene Structures. *J. Phys. Chem.* **1986**, *90* (3), 517–523.
- Blanchard, C. M.; Gray, M. R. Free Radical Chain Reactions of Bitumen Residue. *Prepr. Pap.-Am. Chem. Soc., Div. Fuel Chem.* **1997**, *42* (1), 137–141.
- Blanksby, S. J.; Ellison, G. B. Bond Dissociation Energies of Organic Molecules. *Acc. Chem. Res.* **2003**, *36* (4), 255–263.

Bockrath, B. C. Chemistry of Hydrogen Donor Solvents. In *Coal Science Vol.2*; Gorbaty, M. L., Larsen, J. W., Wender, I., Eds.; Academic Press: New York, 1983; pp 65–124.

Bouldin, R.; Singh, A.; Magaletta, M.; Connor, S.; Kumar, J.; Nagarajan, R. Biocatalytic Synthesis of Fluorescent Conjugated Indole Oligomers. *Bioengineering* **2014**, *1* (4), 246–259.

Braun, M., & Bernard, C. Einfache Darstellung von B-Tetralonen Und B-Indanonen Durch 1, 2-Carbonylgruppenverschiebung. *Liebigs Ann. der Chemie* **1985**, No. 2, 435–437.

Bredael, P.; Rietvelde, D. Pyrolysis of Hydronaphthalenes. 2. Pyrolysis of Cis-Decalin. *Fuel* **1979**, *58* (3), 215–218.

Brons, G.; Yu, J. M. Solvent Deasphalting Effects on Whole Cold Lake Bitumen. *Prepr. Chem. Soc. Div. Pet. Chem.* **1995**, *40* (4), 785–793.

Cabrales-Navarro, F. A.; Pereira-Almao, P. Reactivity and Comprehensive Kinetic Modeling of Deasphalted Vacuum Residue Thermal Cracking. *Energy and Fuels* **2017**, *31* (4), 4318–4332.

Cardozo, S. D.; Schulze, M.; Tykwinski, R. R.; Gray, M. R. Addition Reactions of Olefins to Asphaltene Model Compounds. *Energy and Fuels* **2015**, *29* (3), 1494–1502.

Carlson, C. S.; Langer, A. W.; Stewart, J.; Hill, R. M. Thermal Hydrogenation. Transfer of Hydrogen from Tetralin to Cracked Residua. *Ind. Eng. Chem.* **1958**, *50* (7), 1067–1070.

Castellanos, J.; Cano, J. L.; Del Rosal, R.; Briones, V. M.; Mancilla, R. L. Kinetic Model Predicts Visbreaker Yields. *Oil gas J.* **1991**, *89* (11), 76.

Castillo, J.; De Klerk, A. Visbreaking of Deasphalted Oil from Bitumen at 280-400 °C. *Energy and Fuels* **2019**, *33* (1), 159–175.

Chamberlain, N. F. *The Practice of NMR Spectroscopy with Spectra-Structure Correlations for Hydrogen-1*; Plenum Press: New York, 1974.

Chang, H.-L.; Wong, G. K.; Lin, J.-R.; Yen, T. F. Electron Spin Resonance Study of Bituminous Substances and Asphaltenes. In *Asphaltenes and asphalts. Vol. 2*; Yen, T. F., Chilingarian, G. V., Eds.; Elsevier: Amsterdam, 2000; pp 229–280.

Chong, Y. K.; Rizzardo, E.; Solomon, D. H. Confirmation of the Mayo Mechanism for the Initiation of the Thermal Polymerization of Styrene. *J. Am. Chem. Soc.* **1983**, *105* (26), 7761–7762.

Clarke, P. F.; Pruden, B. B. Asphaltene Precipitation from Cold Lake and Athabasca Bitumens. *Pet. Sci. Technol.* **1998**, *16* (3–4), 287–305.

Clerici, A.; Pastori, N.; Porta, O. ChemInform Abstract: Reduction of Aliphatic and Aromatic Cyclic Ketones to Sec-Alcohols by Aqueous Titanium Trichloride/Ammonia System. Steric Course and Mechanistic Implications. *ChemInform* **2010**, *33* (15), no-no.

Collier, W. L.; Macomber, R. S. Tert-Butylacetylene Revisited. An Improved Synthesis. Methyl Migration during Bromination. *J. Org. Chem.* **1973**, *38* (7), 1367–1369.

Cooper, T. A.; Ballard, W. P. Thermal Cracking, Visbreaking, and Thermal Reforming. In *Advances in petroleum chemistry and refining. Vol. VI*; Kobe, K. A., McKetta, J. J. J., Eds.; Interscience: New York, 1962; pp 171–238.

De Klerk, A.; Zerpa Reques, N. G.; Xia, Y.; Omer, A. A. Integrated Central Processing Facility (CPF) in Oil Field Upgrading (OFU). US 9,650,578 B2, 2014.

Dey, J.; O'Donoghue, A. M. C.; More O'Ferrall, R. A. Equilibrium Constants for Dehydration of Water Adducts of Aromatic Carbon-Carbon Double Bonds. *J. Am. Chem. Soc.* **2002**, *124* (29), 8561–8574.

Di Carlo, S.; Janis, B.; Migliorati, P. Tendency of Petroleum Residues to Be Processed in Visbreaking: A Prediction Model. *Prepr. Chem. Soc. Div. Pet. Chem.* **1995**, *40* (4), 730–735.

Doyle, G. Desulfurization via Hydrogen Donor Reactions. *Am. Chem. Soc., Div. Pet. Chem., Prepr.* **1976**, *21*, 165–172.

Eaton, G. R.; Eaton, S. S.; Barr, D. P.; Weber, R. T. *Quantitative EPR*; Springer, 2010.

Elleman, D. D.; Manatt, S. L. An NMR Study of Indene Using a Proton-Proton Decoupling Technique. *J. Chem. Phys.* **1962**, *36* (9), 2346–2352.

Elofson, R. M.; Schulz, K. F.; Hitchon, B. Geochemical Significance of Chemical Composition and ESR Properties of Asphaltenes in Crude Oils from Alberta, Canada. *Geochim. Cosmochim. Acta* **1977**, *41* (5), 567–580.

Erdman, J. G.; Dickie, J. P. Mild Thermal Alteration of Asphaltic Crude Oils. *Prepr. Pap.-Am. Chem. Soc., Div. Pet. Chem.* **1964**, *9*, B69–B79.

Flory, P. J. The Mechanism of Vinyl Polymerizations. *J. Am. Chem. Soc.* **1937**, *59* (2), 241–253.

Ford, T. J. Liquid-Phase Thermal Decomposition of Hexadecane: Reaction Mechanisms. *Ind. Eng. Chem. Fundam.* **1986**, *25* (2), 240–243.

Freidlina, R. K.; Terent'ev, A. B. Rearrangement of Short-Lived Radicals in the Liquid Phase. In *Advances in free-radical chemistry Vol.6*; Williams, G. H., Ed.; Heyden: London, 1980; pp 1–63.

Gajewski, J. J.; Gortva, A. M. Bimolecular Thermal Reactions of 5-Methylene-1,3-Cyclohexadiene (o-Isotoluene) and 3-Methylene-1,4-Cyclohexadiene (p-Isotoluene). *J. Am. Chem. Soc.* **1982**, *104* (1), 334–335.

Gary, J. H.; Handwerk, G. E.; Kaiser, M. J. *Petroleum Refining: Technology and Economics*, 5th ed.; CRC Press: Boca Raton, 2007.

Giese, B. Synthetic Applications of Radical C-C Bond Forming Reactions. *Res. Chem. Intermed.* **1986**, *7* (1), 3–11.

Gordy, W. *Theory and Applications of Electron Spin Resonance (Vol. 15)*; Wiley-Interscience: New York, 1980.

Gould, K. A.; Wiehe, I. A. Natural Hydrogen Donors in Petroleum Resids. *Energy and Fuels* **2007**, *21* (3), 1199–1204.

Gray, M. R. *Upgrading Oilsands Bitumen and Heavy Oil*; University of Alberta Press: Edmonton, AB, 2015.

Gray, M. R.; McCaffrey, W. C. Role of Chain Reactions and Olefin Formation in Cracking, Hydroconversion, and Coking of Petroleum and Bitumen Fractions. *Energy and Fuels* **2002**, *16* (3), 756–766.

Guo, A.; Wang, Z.; Feng, J.; Que, G. Mechanistic Analysis on Thermal Cracking of Petroleum Residue Using H-Donor as a Probe. *Prepr. Chem. Soc. Div. Pet. Chem.* **2001**, *46* (4), 344–347.

Guo, A.; Wang, Z.; Zhang, H.; Zhang, X.; Wang, Z. Hydrogen Transfer and Coking Propensity of Petroleum Residues under Thermal Processing. *Energy and Fuels* **2010**, *24* (5), 3093–3100.

Gustav Egloff. *The Reactions of Pure Hydrocarbons*; New York: Reinhold Publishing Corporation, 1937.

Harmony, J. A. K. Molecule-Induced Radical Formation. In *Methods in free-radical chemistry vol. 5*; Huyser, E. S., Ed.; Marcel Dekker, Inc: New York, 1974; pp 101–176.

Hart, R. T.; Tebbe, R. F. Acylation-Alkylation Studies. I. *J. Am. Chem. Soc.* **1950**, *72* (7), 3286–3287.

Hawley, G. . *The Condensed Chemical Dictionary*, 8th ed.; Van Nostrand Reinhold: New York, 1971.

Hiatt, R. R.; Bartlett, P. D. The Thermal Reaction of Styrene with Ethyl Thioglycolate; Evidence for the Termolecular Thermal Initiation of Styrene Polymerization. *J. Am. Chem. Soc.* **1959**, *81* (5), 1149–1154.

Hooper, R. J.; Battaerd, H. A. J.; Evans, D. G. Thermal Dissociation of Tetralin between 300 and 450 °C. *Fuel* **1979**, *58* (2), 132–138.

Huyser, E. S. Solvent Effects in Free-Radical Reactions. In *Advances in free-radical chemistry. Vol. 1*; Williams, G. H., Ed.; Academic Press: London, 1965; pp 77–135.

Ignasiak, T. M.; Strausz, O. P. Reaction of Athabasca Asphaltene with Tetralin. *Fuel* **1978**, *57* (10), 617–621.

Imai, M.; Morais, G. R.; al-Hindawi, B.; al-Sulaibi, M. A. M.; Meetani, M.; Thiemann, T. Acid Catalysed Reaction of Indanones, Tetralones and Benzosuberone with Neopentyl Glycol and Other Alkanediols under Forced Conditions. *J. Chem. Res.* **2010**, *34* (6), 325–329.

Jamaluddin, A. K. M.; Nazarko, T. W.; Sills, S.; Fuhr, B. J. Deasphalted Oil - A Natural Asphaltene Solvent. *SPE Prod. Facil.* **2007**, *11* (03), 161–165.

Jigajinni, V. B., & Wightman, R. H. Hydrogenolysis of Enol Triflates; A New Method for the Reduction of Ketones to Methylene Compounds. *Tetrahedron Lett.* **1982**, *23* (1), 117–120.

Joshi, J. B.; Pandit, A. B.; Kataria, K. L.; Kulkarni, R. P.; Sawarkar, A. N.; Tandon, D.; Ram, Y.; Kumar, M. M. Petroleum Residue Upgradation via Visbreaking: A Review. *Ind. Eng. Chem. Res.* **2008**, *47* (23), 8960–8988.

Kalutharage, N.; Yi, C. S. Scope and Mechanistic Analysis for Chemoselective Hydrogenolysis of Carbonyl Compounds Catalyzed by a Cationic Ruthenium Hydride Complex with a Tunable Phenol Ligand. *J. Am. Chem. Soc.* **2015**, *137* (34), 11105–11114.

Keesom, B.; Gieseman, J. *Bitumen Partial Upgrading 2018 Whitepaper*; Report AM0401A for Alberta Innovates, rev.8, April 13, 2018.

Khalaf, A.A., Abdel-Wahab, A.A., El-Khawaga, A.M. & El-Zohry, M. . Modern Friedel-Crafts Chemistry XIII. Intra- and Intermolecular Cyclization of Some Carbonyl Derivates under Friedel-Crafts Conditions. *Bull. Chem. Soc. Fr. II* **1984**, No. 5(2), 285–291.

Khorasheh, F.; Gray, M. R. High-Pressure Thermal Cracking of n-Hexadecane in Aromatic Solvents. *Ind. Eng. Chem. Res.* **1993**, *32* (9), 1864–1876.

Khorasheh, F.; Gray, M. R. High-Pressure Thermal Cracking of n-Hexadecane in Tetralin. *Energy and Fuels* **1993**, *7* (6), 960–967.

Khulbe, K. C.; Mann, R. S.; Lamarche, G.; Lamarche, A.-M. Electron Spin Resonance Study of the Thermal Decomposition of Solvent Extracted Athabasca Tar Sand Bitumen. *Fuel Process. Technol.* **1992**, *31* (2), 91–103.

Khulbe, K. C.; Mann, R. S.; Lu, B. C. Y.; Lamarche, G.; Lamarche, A. M. Effects of Solvents on Free Radicals of Bitumen and Asphaltenes. *Fuel Process. Technol.* **1992**, *32* (3), 133–141.

Koelsch, C. F.; Scheiderbauer, R. A. The Tautomerism of Indene. *J. Am. Chem. Soc.* **1943**, *65* (12), 2311–2314.

Kohler, E. P. Vinylphenyl Ketone and Some of Its Homologues. *Am. Chem. J.* **1909**, *42*, 376–380.

Kopecky, K. R.; Lau, M. P. Thermal Reaction between 5-Methylene-1,3-Cyclohexadiene and Styrene. *J. Org. Chem.* **1978**, *43* (3), 525–526.

Kotsuki, H., Datta, P. K., Hayakawa, H., & Suenaga, H. An Efficient Procedure for Palladium-Catalyzed Reduction of Aryl/Enol Triflates. *Synthesis (Stuttg.)* **1995**, No. 11, 1348–1350.

Kubo, J. Radical Scavenging Abilities of Hydrogen-Donating Hydrocarbons from Petroleum. *Ind. Eng. Chem. Res.* **1998**, *37* (11), 4492–4500.

Lababidi, H. M. S.; Sabti, H. M.; Alhumaidan, F. S. Changes in Asphaltenes during Thermal Cracking of Residual Oils. *Fuel* **2014**, *117*, 59–67.

LaMarca, C.; Libanati, C.; Klein, M. T.; Cronauer, D. C. Enhancing Chain Transfer during Coal Liquefaction: A Model System Analysis. *Energy and Fuels* **1993**, *7* (4), 473–478.

Langer, A. W.; Stewart, J.; Thompson, C. E.; White, H. T.; Hill, R. M. Hydrogen Donor Diluent Visbreaking of Residua. *Ind. Eng. Chem. Process Des. Dev.* **1962**, *1* (4), 309–312.

León, A. Y.; Guzman, A.; Laverde, D.; Chaudhari, R. V.; Subramaniam, B.; Bravo-Suárez, J. J. Thermal Cracking and Catalytic Hydrocracking of a Colombian Vacuum Residue and Its Maltenes and Asphaltenes Fractions in Toluene. *Energy and Fuels* **2017**, *31* (4), 3868–3877.

Levinter, M. E.; Medvedeva, M. I.; Panchenkov, G. M.; Agapov, G. I.; Galiakbarov, M. F.; Galikeev, R. K. The Mutual Effect of Group Components during Coking. *Chem. Technol. Fuels Oils* **1967**, *3* (4), 246–249.

- Levinter, M. E.; Medvedeva, M. I.; Panchenkov, G. M.; Aseev, Y. G.; Nedoshivin, Y. N.; Finkel'shtein, G. B.; Galiakbarov, M. F. Mechanism of Coke Formation in the Cracking of Component Groups in Petroleum Residues. *Chem. Technol. Fuels Oils* **1966**, 2 (9), 628–632.
- Li, S.; Liu, C.; Que, G.; Liang, W.; Zhu, Y. Phenomena Occurring before Coke Formation in the Thermal Reaction System of Gudau Vacuum Residuum. *Prepr. Chem. Soc. Div. Pet. Chem.* **1995**, 40 (4), 736–740.
- Lu, M.; Mulholland, J. A. Aromatic Hydrocarbon Growth from Indene. *Chemosphere* **2001**, 42 (5–7), 625–633.
- Magaril, R. Z.; Aksenova, E. I. Investigation of the Mechanism of Coke Formation during Thermal Decomposition of Asphaltenes. *Chem. Technol. Fuels Oils* **1970**, 6 (7), 509–512.
- Magaril, R. Z.; Aksenova, E. I. Study of Mechanism of Coke Formation in Cracking of Petroleum Resins. *Int. Chem. Eng.* **1968**, 8 (4), 727.
- Magaril, R. Z.; Ramazaeva, L. F.; Askenova, E. I. Kinetics of Coke Formation in the Thermal Processing of Petroleum. *Khim. Tekhnol. Topl. Masel* **1970**, 15 (3), 15–16.
- Malhotra, V. M.; Buckmaster, H. A. 9 and 34 GHz EPR Study of the Free Radicals in Various Asphaltenes: Statistical Correlation of the g-Values with Heteroatom Content. *Org. Geochem.* **1985**, 8 (4), 235–239.
- Mansoori, G. A.; Jiang, T. S.; Kawanaka, S. Asphaltene Deposition and Its Role in Petroleum Production and Processing. *Arab. J. Sci. Eng.* **1988**, 13 (1), 17–34.
- Maples, R. E. *Petroleum Refinery Process Economics*; PenWell: Tulsa, 2003.
- Martin, J. C. Solvation and Association. In *Free radicals Vol.2*; Kochi, J. K., Ed.; John Wiley & Sons, 1973; pp 493–526.
- Maudgal, R. K.; Tchen, T. T.; Bloch, K. 1,2-Methyl Shifts in the Cyclization of Squalene To Lanosterol. *J. Am. Chem. Soc.* **1958**, 80 (10), 2589–2590.
- Mawby, R. J.; Basólo, F.; Pearson, R. G. Methyl Migration in the Reaction of Alkyl- and Acylmanganese Carbonyls. *J. Am. Chem. Soc.* **1964**, 86 (22), 5043–5044.

Mayo, F. R. Chain Transfer in the Polymerization of Styrene. VIII. Chain Transfer with Bromobenzene and Mechanism of Thermal Initiation. *J. Am. Chem. Soc.* **1953**, *75* (24), 6133–6141.

Meyer, V.; Eaton, S. S.; Eaton, G. R. X-Band Electron Spin Relaxation Times for Four Aromatic Radicals in Fluid Solution and Comparison with Other Organic Radicals. *Appl. Magn. Reson.* **2014**, *45* (10), 993–1007.

Montanari, L.; Bonoldi, L.; Alessi, A.; Flego, C.; Salvalaggio, M.; Carati, C.; Bazzano, F.; Landoni, A. Molecular Evolution of Asphaltenes from Petroleum Residues after Different Severity Hydroconversion by EST Process. *Energy and Fuels* **2017**, *31* (4), 3729–3737.

Morgenthaler, J.; Rüchardt, C. New Hydrogen Transfer Catalysts. *European J. Org. Chem.* **1999**, *1999* (9), 2219–2230.

Moureu, C. Action Du Chlorure d'acryle Sur Le Benzène En Présence Du Chlorure d'aluminium. *Ann. Chim. Phys.* **1894**, *7* (2), 198–201.

Moureu, C. Action Du Chlorure d'acryle Sur Le Benzène En Présence Du Chlorure d'aluminium. *Bull. le Soc. Chim. Paris* **1893**, *3* (9), 570–572.

Nagaishi, H.; Chan, E. W.; Sanford, E. C.; Gray, M. R. Kinetics of High-Conversion Hydrocracking of Bitumen. *Energy and Fuels* **1997**, *11* (2), 402–410.

Naghizada, N.; Prado, G. H. C.; De Klerk, A. Uncatalyzed Hydrogen Transfer during 100–250 °c Conversion of Asphaltenes. *Energy and Fuels* **2017**, *31* (7), 6800–6811.

Nakamoto, M.; Fukawa, T.; Sekiguchi, A. Silylium Ion to Silylium Ion Rearrangement Caused by 1,3-Methyl Migration. *Chem. Lett.* **2003**, *33* (1), 38–39.

National Energy Board. Crude Petroleum Tariff No. 391.

Nellensteyn, F. J. The Colloidal Structure of Bitumens. In *The science of petroleum, Vol. 4*; Dunstan, A. E., Nash, A. W., Brooks, B. T., Tizard, H., Eds.; Oxford university press, 1938; pp 2760–2763.

Nguyen, P.; Corpuz, E.; Heidelbaugh, T. M.; Chow, K.; Garst, M. E. A Convenient Synthesis of 7-Halo-1-Indanones and 8-Halo-1-Tetralones. *J. Org. Chem.* **2003**, *68* (26), 10195–10198.

Nies, H.; Rewicki, D. The Analysis of the High-Resolution ^1H NMR Spectrum of Indene. *J. Magn. Reson.* **1982**, *46* (1), 138–141.

Nihlgård, B.; Weidler, A.-M.; Bergson, G.; Johansson, L.; Nilsson, L. Hydrogen Isotope Effect on the Rate of an Intramolecular Tautomeric Rearrangement. *Acta Chemica Scandinavica*. 2008, pp 1498–1501.

Niizuma, S.; Steele, C. T.; Gunning, H. E.; Strausz, O. P. Electron Spin Resonance Study of Free Radicals in Athabasca Asphaltene. **1977**, *56*, 249–256.

Nonhebel, D. C.; Walton, J. C. *Free-Radical Chemistry: Structure and Mechanism*; 1974.

Olah, G. A., Arvanaghi, M., & Ohannesian, L. Synthetic Methods and Reactions; 126. Trifluoromethanesulfonic Acid/Triethylsilane: A New Ionic Hydrogenation Reagent for the Reduction of Diaryl and Alkyl Aryl Ketones to Hydrocarbons. *Synthesis (Stuttg)*. **1986**, No. 9, 770–772.

Pacut, R. I.; Kariv-Miller, E. Birch-Type Reductions in Aqueous Media: Benzo[b]Thiophene and Diphenyl Ether. *J. Org. Chem.* **1986**, *51* (18), 3468–3470.

Parsons, A. F. *An Introduction to Free Radical Chemistry*; Wiley-Blackwell., 2000.

Payan, F.; De Klerk, A. Hydrogen Transfer in Asphaltenes and Bitumen at 250 °C. *Energy and Fuels* **2018**, *32* (9), 9340–9348.

Peña, G. D. J.; Alrefaai, M. M.; Yang, S. Y.; Raj, A.; Brito, J. L.; Stephen, S.; Anjana, T.; Pillai, V.; Shoaibi, ahmed al; Chung, S. H. Effects of Methyl Group on Aromatic Hydrocarbons on the Nanostructures and Oxidative Reactivity of Combustion-Generated Soot. *Combust. Flame* **2016**, *172*, 1–12.

Penninger, J. M. L. New Aspects of the Mechanism for the Thermal Hydrocracking of Indan and Tetralin. *Int. J. Chem. Kinet.* **1982**, *14* (7), 761–780.

Peter J. Stang, W. T. Single-Step Improved Synthesis of Primary and Other Vinyl Trifluoromethanesulfonates. *Synthesis (Stuttg)*. **1980**, No. 04, 283–284.

Petrakis, L.; Grandy, D. W. An Electron Spin Resonance Spectrometric Investigation of Natural, Extracted and Thermally Altered Kerogenous Materials. *Geochim. Cosmochim. Acta* **1980**, *44* (5), 763–768.

Pevneva, G. S.; Voronetskaya, N. G.; Korneev, D. S.; Golovko, A. K. Mutual Influence of Resins and Oils in Crude Oil from the Usinskoe Oilfield on the Direction of Their Thermal Transformations. *Pet. Chem.* **2017**, *57* (8), 739–745.

Pfeiffer, J. P.; Saal, R. N. J. Asphaltic Bitumen as Colloid System. *J. Phys. Chem.* **1940**, *44*, 139–149.

Poutsma, M. L. Progress toward the Mechanistic Description and Simulation of the Pyrolysis of Tetralin. *Energy and Fuels* **2002**, *16* (4), 964–996.

Pryor, W. A.; Lasswell, L. D. Diels-Alder and 1,4-Diradical Intermediates in the Spontaneous Polymerization of Vinyl Molecules. In *Advances in free-radical chemistry vol.5*; Williams, G. H., Ed.; Academic Press: New York, 1975; pp 27–100.

Rahimi, P. M.; Dettman, H.; Nowlan, V.; DelBianco, A. Molecular Transformation during Heavy Oil Upgrading. *Prepr. Chem. Soc. Div. Pet. Chem.* **1997**, *42* (1), 23–26.

Rahimi, P. M.; Gentiz, T.; Delbianco, A. Application of Hot-Stage Microscopy in the Investigation of the Thermal Chemistry of Heavy Oils and Bitumen: An Overview. *Prepr. Chem. Soc. Div. Pet. Chem.* **2001**, *46* (4), 341–343.

Rahimi, P. M.; Gentzis, T. Thermal Hydrocracking of Cold Lake Vacuum Bottoms Asphaltenes and Their Subcomponents. *Fuel Process. Technol.* **2003**, *80* (1), 69–79.

Rahimi, P.; Gentzis, T.; Fairbridge, C.; Khulbe, C. Chemistry of Petroleum Residues in the Presence of H-Donors. *Prepr. Chem. Soc. Div. Pet. Chem.* **1998**, *43* (4), 634–636.

Rahimi, P.; Gentzis, T.; Kubo, J.; Fairbridge, C.; Khulbe, C. Coking Propensity of Athabasca Bitumen Vacuum Bottoms in the Presence of H-Donors - Formation and Dissolution of Mesophase from a Hydrotreated Petroleum Stream (H-Donor). *Fuel Process. Technol.* **1999**, *60* (2), 157–170.

Raseev, S. *Thermal and Catalytic Processes in Petroleum Refining*; Marcel Dekker: New York, 2003.

Retcofsky, H. L. Magnetic Resonance Studies of Coal. In *Coal Science Vol. I*; Gorbaty, M. L., Larsen, J. W., Wender, I., Eds.; Academic Press: New York, 1982; pp 43–82.

Richard J. Lewis, S. *Hawley's Condensed Chemical Dictionary*, Fifteenth.; John Wiley & Sons, 2007.

Rüchardt, C.; Gerst, M.; Nölke, M. The Uncatalyzed Transfer Hydrogenation of A-Methylstyrene by Dihydroanthracene or Xanthene—a Radical Reaction. *Angew. Chem. Int. Ed. Engl.* **1992**, *31* (11), 1523–1525.

Rutz, L. K.; Bockhorn, H.; Bozzelli, J. W. Methyl Radical Substitution and Shift Reactions with Aliphatic and Aromatic Hydrocarbons. *Int. Symp. Combust. Abstr. Work. Posters* **2004**, *49*, 451–452.

Sachanen, A. N. *Conversion of Petroleum: Production of Motor Fuels by Thermal and Catalytic Processes*; Reinhold Publishing Corporation, 1948.

Sanford, E. C. Influence of Hydrogen and Catalyst on Distillate Yields and the Removal of Heteroatoms, Aromatics, and CCR during Cracking of Athabasca Bitumen Residuum over a Wide Range of Conversions. *Energy and Fuels* **1994**, *8* (6), 1276–1288.

Sanford, E. C.; Xu, C. M. Relationship between Solids Formation, Residuum Conversion, Liquid Yields and Losses during Athabasca Bitumen Processing in the Presence of a Variety of Chemicals. *Can. J. Chem. Eng.* **1996**, *74* (3), 347–352.

Savage, P. E.; Klein, M. T.; Kukes, S. G. Asphaltene Reaction Pathways. 1. Thermolysis. *Ind. Eng. Chem. Process Des. Dev.* **1985**, *24* (4), 1169–1174.

Schabron, J. F.; Speight, J. G. Correlation between Carbon Residue and Molecular Weight. *Prepr. Pap.-Am. Chem. Soc., Div. Fuel Chem.* **1997**, *42* (2), 386–389.

Schabron, J. F.; Speight, J. G. The Solubility and Three-Dimensional Structure of Asphaltenes. *Pet. Sci. Technol.* **1998**, *16* (3–4), 361–375.

Schultz, K. F.; Selucky, M. L. ESR Measurements on Asphaltene and Resin Fractions from Various Separation Methods. *Fuel* **1981**, *60* (10), 951–956.

Shi, B.; Wang, L. Q.; Lin, D. L.; Que, G. H. Hydrogen-Transfer between Hydrogen Donors and Model Compounds with Steady Isotope. *Prepr. Chem. Soc. Div. Pet. Chem.* **2001**, *46* (4), 325–328.

Siddiquee, M. N.; De Klerk, A. Heterocyclic Addition Reactions during Low Temperature Autoxidation. *Energy and Fuels* **2015**, *29* (7), 4236–4244.

Siddiquee, M. N.; De Klerk, A. Hydrocarbon Addition Reactions during Low-Temperature Autoxidation of Oilsands Bitumen. *Energy and Fuels* **2014**, *28* (11), 6848–6859.

Singh, J.; Kumar, S.; Garg, M. O. Kinetic Modelling of Thermal Cracking of Petroleum Residues: A Critique. *Fuel Process. Technol.* **2012**, *94* (1), 131–144.

Slotboom, H. W. Mechanism and Kinetics of the Thermal Hydrocracking of Single Polyaromatic Compounds. *Am. Chem. Soc. Symp. Ser.* **1976**, *32*, 444–456.

Slotboom, H. W.; Penninger, J. M. L. The Role of the Reactor Wall in the Thermal Hydrocracking of Polyaromatic Compounds. *Ind. Eng. Chem. Process Des. Dev.* **1974**, *13* (3), 296–299.

Soylu, O.; Uzun, S.; Can, M. The Investigation of Acid Effect on Chemical Polymerization of Indole. *Colloid Polym. Sci.* **2011**, *289* (8), 903–909.

Speight, J. G. Thermal Cracking of Athabasca Bitumen, Athabasca Asphaltenes, and Athabasca Deasphalted Heavy Oil. *Fuel* **1970**, *49* (2), 134–145.

Srinivasan, N. S.; McKnight, C. A. Mechanism of Coke Formation from Hydrocracked Athabasca Residuum. *Fuel* **1994**, *73* (9), 1511–1517.

Steglich, M.; Knopp, G.; Hemberger, P. How the Methyl Group Position Influences the Ultrafast Deactivation in Aromatic Radicals. *Phys. Chem. Chem. Phys.* **2019**, *21* (2), 581–588.

Storm, D. A.; Barresi, R. J.; Sheu, E. Y. Evidence for the Micellization of Asphaltenic Molecules in Vacuum Residue. *Prepr. Chem. Soc. Div. Pet. Chem.* **1995**, *40* (4), 776–779.

Strausz, O. P.; Lown, E. M. *The Chemistry of Alberta Oil Sands, Bitumens and Heavy Oils*; Alberta Energy Research Institute: Calgary, Alberta, Canada, 2003.

Subramanian, H.; Landais, Y.; Sibi, M. P. Radical Addition Reactions. *Compr. Org. Synth. Second Ed.* **2014**, *4*, 699–741.

Surya Prakash, G. K.; Do, C.; Mathew, T.; Olah, G. A. Reduction of Carbonyl to Methylene: Organosilane-Ga(OTf)₃ as an Efficient Reductant System. *Catal. Letters* **2011**, *141* (4), 507–511.

Tachikawa, H. Methyl Radical Addition to the Surface of Graphene Nanoflakes: A Density Functional Theory Study. *Surf. Sci.* **2019**, *679* (June 2018), 196–201.

Tannous, J. H.; de Klerk, A. Asphaltenes Formation during Thermal Conversion of Deasphalted Oil. *Fuel* **2019**, *255*, 1–10.

Teitelbaum, A. M.; Meissner, A.; Harding, R. A.; Wong, C. A.; Aldrich, C. C.; Remmel, R. P. Synthesis, PH-Dependent, and Plasma Stability of Meropenem Prodrugs for Potential Use against Drug-Resistant Tuberculosis. *Bioorganic Med. Chem.* **2013**, *21* (17), 5605–5617.

Ten, T. F.; Young, D. K. Spin Excitations of Bitumens. *Carbon N. Y.* **1973**, *11*, 33–41.

Terheijden, J.; van Koten, G.; Vinke, I. C.; Spek, A. L. 1,2-Methyl Shift between Pt and the Coordinated Aryl Group in the Reaction of Methyl Iodide with 2,6-Bis[(Dimethylamino)Methyl]Phenyl-N,N',C Complexes of Platinum(II). X-Ray Crystal Structure of the Arenonium-Platinum Compound [Pt(o-Tolyl)(MeC₆H₃(CH₂NMe₂)). *J. Am. Chem. Soc.* **1985**, *107* (10), 2891–2898.

Thomsen, C. J. *A Guide to Northern Antiquities*; London, 1848.

Tong, Y.; Poindexter, M. K.; Rowe, C. T. Inhibition of Coke Formation in Pyrolysis Furnaces. *Prepr. Chem. Soc. Div. Pet. Chem.* **1995**, *40* (4), 612–617.

Trauth, D. M.; Yasar, M.; Neurock, M.; Nigam, A.; Klein, M. T.; Kukes, S. G. Asphaltene and Resid Pyrolysis: Effect of Reaction Environment. *Fuel Sci. Technol. Int.* **1992**, *10* (7), 1161–1179.

Trukhan, S. N.; Kazarian, S. G.; Martyanov, O. N. Electron Spin Resonance of Slowly Rotating Vanadyls-Effective Tool to Quantify the Sizes of Asphaltenes in Situ. *Energy and Fuels* **2017**, *31* (1), 387–394.

Trukhan, S. N.; Yudanov, V. F.; Gabrienko, A. A.; Subramani, V.; Kazarian, S. G.; Martyanov, O. N. In Situ Electron Spin Resonance Study of Molecular Dynamics of Asphaltenes at Elevated Temperature and Pressure. *Energy and Fuels* **2014**, *28* (10), 6315–6321.

Udayakumar, V.; Gowsika, J.; Pandurangan, A. A Novel Synthesis and Preliminary in Vitro Cytotoxic Evaluation of Dihydropyrimidine-2,4(1H, 3 H)-Dione Derivatives. *J. Chem. Sci.* **2017**, *129* (2), 249–258.

Uemasu, I.; Kushiyama, S. Analysis of 9,10-Dihydroanthracene by Capillary Gas Chromatography for Evaluation of Transferable Hydrogen in Heavy Oils. *J. Chromatogr. A* **1986**, *368* (C), 387–390.

Uzcátegui, G.; Fong, S. Y.; De Klerk, A. Cracked Naphtha Reactivity: Effect of Free Radical Reactions. *Energy and Fuels* **2018**, *32* (5), 5812–5823.

Valla, J. A.; Lappas, A. A.; Vasalos, I. A. Catalytic Cracking of Thiophene and Benzothiophene: Mechanism and Kinetics. *Appl. Catal. A Gen.* **2006**, *297* (1), 90–101.

Varga, J.; Rabo, G.; Zalai, A. Thermal Decomposition of Asphalt-Containing Crude Oils in the Presence of Diluents and Hydrogen. *Brennst.-Chem* **1956**, *37*, 244.

Walling, C. *Free Radicals in Solution*; Wiley, 1957.

Wawzonek, S.; Laitinen, H. A. The Reduction of Unsaturated Hydrocarbons at the Dropping Mercury Electrode. II. Aromatic Polynuclear Hydrocarbons. *J. Am. Chem. Soc.* **1942**, *64* (10), 2365–2368.

Weast, R. C.; Astle, M. J.; Beyer, W. H. *CRC Handbook of Chemistry and Physics (Vol. 69)*; Boca Raton, FL: CRC press., 1988.

Wiehe, I. A. A Phase-Separation Kinetic Model for Coke Formation. *Ind. Eng. Chem. Res.* **1993**, *32* (11), 2447–2454.

- Wiehe, I. A. A Solvent-Resid Phase Diagram For Tracking Resid Conversion. *Ind. Eng. Chem. Res.* **1992**, *31* (2), 530–536.
- Wiehe, I. A. The Chemistry of Coke Formation from Petroleum: A Tutorial. *Prepr. Chem. Soc. Div. Pet. Chem.* **1998**, *43* (4), 612–615.
- Wiehe, I. A. The Pendant-Core Building Block Model of Petroleum Residua. *Energy and Fuels* **1994**, *8* (3), 536–544.
- Wiehe, I. A. Visbreaking. In *Process chemistry of petroleum macromolecules*; Speight, J. G., Ed.; CRC press, 2008; pp 369–376.
- Wiehe, I. A.; Yarranton, H. W.; Akbarzadeh, K.; Rahimi, P. M.; Teclemariam, A. The Paradox of Asphaltene Precipitation with Normal Paraffins. *Energy and Fuels* **2005**, *19* (4), 1261–1267.
- Wilt, J. W. Free Radical Rearrangements. In *Free Radicals Vol. 1*; Kochi, J. K., Ed.; Wiley-Interscience: New York, 1973; pp 333–501
- Wu, G.; Katsumura, Y.; Matsuura, C.; Ishigure, K.; Kubo, J. Comparison of Liquid-Phase and Gas-Phase Pure Thermal Cracking of n -Hexadecane. *Ind. Eng. Chem. Res.* **1996**, *35* (12), 4747–4754.
- Yan, T. Y. Coke Formation in Visbreaking Process. *Am. Chem. Soc. Div. Pet. Chem. Prepr.* **1987**, *32*, 490–495.
- Yanagimachi, K. S.; Stafford, D. E.; Dexter, A. F.; Sinskey, A. J.; Drew, S.; Stephanopoulos, G. Application of Radiolabeled Tracers to Biocatalytic Flux Analysis. *Eur. J. Biochem.* **2001**, *268* (18), 4950–4960.
- Yasar, M.; Trauth, D. M.; Klein, M. T. Asphaltene and Resid Pyrolysis. 2. The Effect of Reaction Environment on Pathways and Selectivities. *Energy and Fuels* **2001**, *15* (3), 504–509.
- Yen, T. F.; Erdman, J. G.; Saraceno, A. J. Investigation of the Nature of Free Radicals in Petroleum Asphaltenes and Related Substances by Electron Spin Resonance. *Anal. Chem.* **1962**, *34* (6), 694–700.

- Yen, T. F.; Sprang, S. R. Contribution of E.S.R. Analysis toward Diagenic Mechanisms in Bituminous Deposits. *Geochim. Cosmochim. Acta* **1977**, *41* (8), 1007–1018.
- Yen, T. F.; Sprang, S. R. ESR G-Values of Bituminous Materials. *Prepr. Pap.-Am. Chem. Soc., Div. Pet. Chem.* **1970**, *15* (2), A65–A76.
- Yu, Z.; Verkade, J. G. Reductive Desulfurization of Organosulfur Compounds with Sodium in Liquid Ammonia. *Phosphorous, Sulfur, Silicon Relat. Elem.* **1998**, *133* (1), 79–82.
- Zachariah, A.; De Klerk, A. Thermal Conversion Regimes for Oilsands Bitumen. *Energy and Fuels* **2016**, *30* (1), 239–248.
- Zachariah, A.; Wang, L.; Yang, S.; Prasad, V.; De Klerk, A. Suppression of Coke Formation during Bitumen Pyrolysis. *Energy and Fuels* **2013**, *27* (6), 3061–3070.
- Zheng, L. S.; Llopis, Q.; Echeverria, P. G.; Féraud, C.; Guillamot, G.; Phansavath, P.; Ratovelomanana-Vidal, V. Asymmetric Transfer Hydrogenation of (Hetero)Arylketones with Tethered Rh(III)-N-(p-Tolylsulfonyl)-1,2-Diphenylethylene-1,2-Diamine Complexes: Scope and Limitations. *J. Org. Chem.* **2017**, *82* (11), 5607–5615.
- Zhou, B.; Liu, Q.; Shi, L.; Liu, Z. Electron Spin Resonance Studies of Coals and Coal Conversion Processes: A Review. *Fuel Process. Technol.* **2019**, *188* (March), 212–227.
- Zhou, Y.; Li, X.; Hou, S.; Xu, J. Facile Synthesis of Dihydrochalcones via the AlCl₃-Promoted Tandem Friedel-Crafts Acylation and Alkylation of Arenes with 2-Alkenoyl Chlorides. *J. Mol. Catal. A Chem.* **2012**, *365*, 203–211.
- Zhu, Z.; Espenson, J. H. Organic Reactions Catalyzed by Methylrhenum Trioxide: Dehydration, Amination, and Disproportionation of Alcohols. *J. Org. Chem.* **1996**, *61* (1), 324–328.

Appendices

Appendix A: Chapter 3 Support Information

A.1 Power saturation study

It is well known that the intensity of the peak obtained during ESR measurements depends on many factors, one of which is the concentration. However, another important factor that potentially affects the intensity and ultimately the quantification in terms of spins per gram, is the microwave power. The phenomenon of saturation should be avoided during measurements in order to make sure quantification is valid. Saturation is reached when the intensity is no longer proportional to the square root of the microwave power. This phenomenon happens when the microwave power is so high so that the relaxation time of the radical in the sample is greater than the signal measurement time. When saturation is reached, saturated free radicals will not be detected and the intensity of the peak decreases or remains constant with the square root of microwave power.¹

It was therefore crucial to check whether saturation has been reached at the operating microwave power (i.e. 15 mW) in this study. For this purpose, analyses were performed by varying the microwave power and fixing all other parameters for a sample of asphaltenes (Asph-8, *n*-pentane insoluble fraction in vacuum residue deasphalted oil, Nexen Long Lake upgrader facility). An asphaltenes sample was selected due to its high free radical content, which would make saturation more apparent when it occurs. The samples were prepared at around 6 wt% concentration in toluene and analyzed using a PQ tube.

The graph of the square root of microwave power versus the maximum intensity of the ESR signal is shown (Figure 1). The maximum intensity value is the maximum of the double integral of the derivative spectrum, which was taken as the average of the maximum intensities of seven scans. The sample standard deviation is indicated, but in most cases so low that it is not visible in Figure 1. The relative standard deviation at low power (1 and 3 mW) and high power (70 mW) was 2-3 %, but was around 1% over the rest of the range.

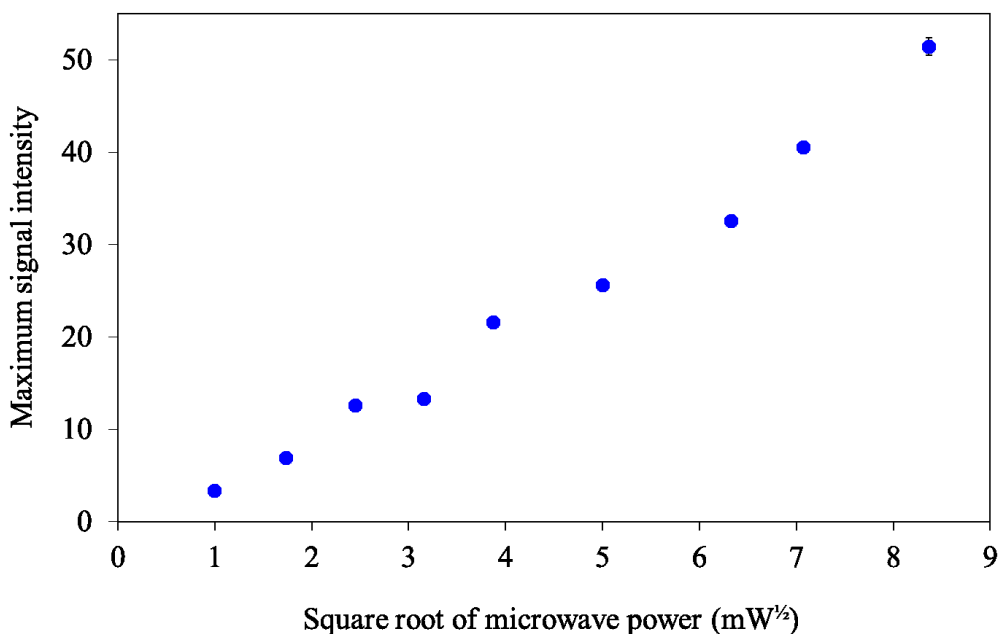


Figure A.1. Microwave power saturation study with an asphaltenes sample.

It could be concluded from Figure 1 that the intensity is proportional to the square root of microwave power over the whole range that was evaluated, i.e. 1 to 70 mW. Saturation was not reached even at the highest microwave power of 70 mW evaluated. Therefore, measurements done at 15 mW (used in this study) are well within the range where saturation is not reached yet.

A.2 ESR tube selection

For quantitative studies it stands to reason that high quality ESR tubes with tight tolerance of manufacturing and high microwave transparency should be used. Yet, there is a cost component to keep in mind, because it is not always possible to reuse the tubes when working with bitumen samples.

To evaluate potential differences, the same bitumen sample (Bit-6, Cold Lake bitumen) diluted to be a 24 wt% in toluene solution, was analyzed using two different tubes each from two different types:

- (i) NMR Norell tube, 5 mm diameter, 18 cm (7 inch) long, 300 MHz Standard Series, concentricity ± 0.010 mm, camber ± 0.038 mm.
- (ii) PQ tube, 5 mm diameter medium wall quartz, 18 cm (7 inch) long, concentricity ± 0.0102 mm, camber ± 0.102 mm.

The ESR instrument parameters were kept the same and the tubes were filled from the same bitumen in toluene solution. The results from the ESR analyses are reported in Table 1.

Table A.1. Comparison of Norell and PQ tubes for quantitative ESR analysis of 24 wt% bitumen (Bit-6, Cold Lake bitumen) in toluene solution at 15 mW microwave power.

Description	ESR double integral area Free radical content (spins/g) ^a			
	Norell	PQ	Norell	PQ
Individual analyses				
tube 1, analysis 1	6469	5063	1.0×10^{18}	9.5×10^{17}
tube 1, analysis 2	5620	5404	9.8×10^{17}	9.7×10^{17}
tube 2, analysis 1	6627	4293	1.0×10^{18}	9.1×10^{17}
tube 2, analysis 2	4948	6250	9.4×10^{17}	1.0×10^{18}
Average	5916	5252	9.9×10^{17}	9.6×10^{17}
Sample standard deviation	783	812	3.7×10^{16}	3.8×10^{16}

^a Based on DPPH calibration in PQ tubes.

The two types of ESR tubes had comparable performance in terms of repeatability. The results also indicated that ESR quantification had a variance in measurements of the order 10–15% when expressed in terms of relative sample standard deviation on double integral area. This was not an exhaustive evaluation, but uncertainty of the order 10% is consistent with the experience of our research group across multiple studies.

The difference between the tubes in terms of microwave transparency could be seen when analyzing samples with a lower spin concentration. To evaluate the signal-to-noise response of the tubes, a maltenes sample (DAO-5, *n*-pentane soluble fraction in vacuum residue deasphalted oil, Nexen Long Lake upgrader facility) was analyzed. The sample was prepared at around 5 wt%

concentration in toluene. The first derivative ESR spectra obtained from the same sample using the different tubes are shown in Figure 2.

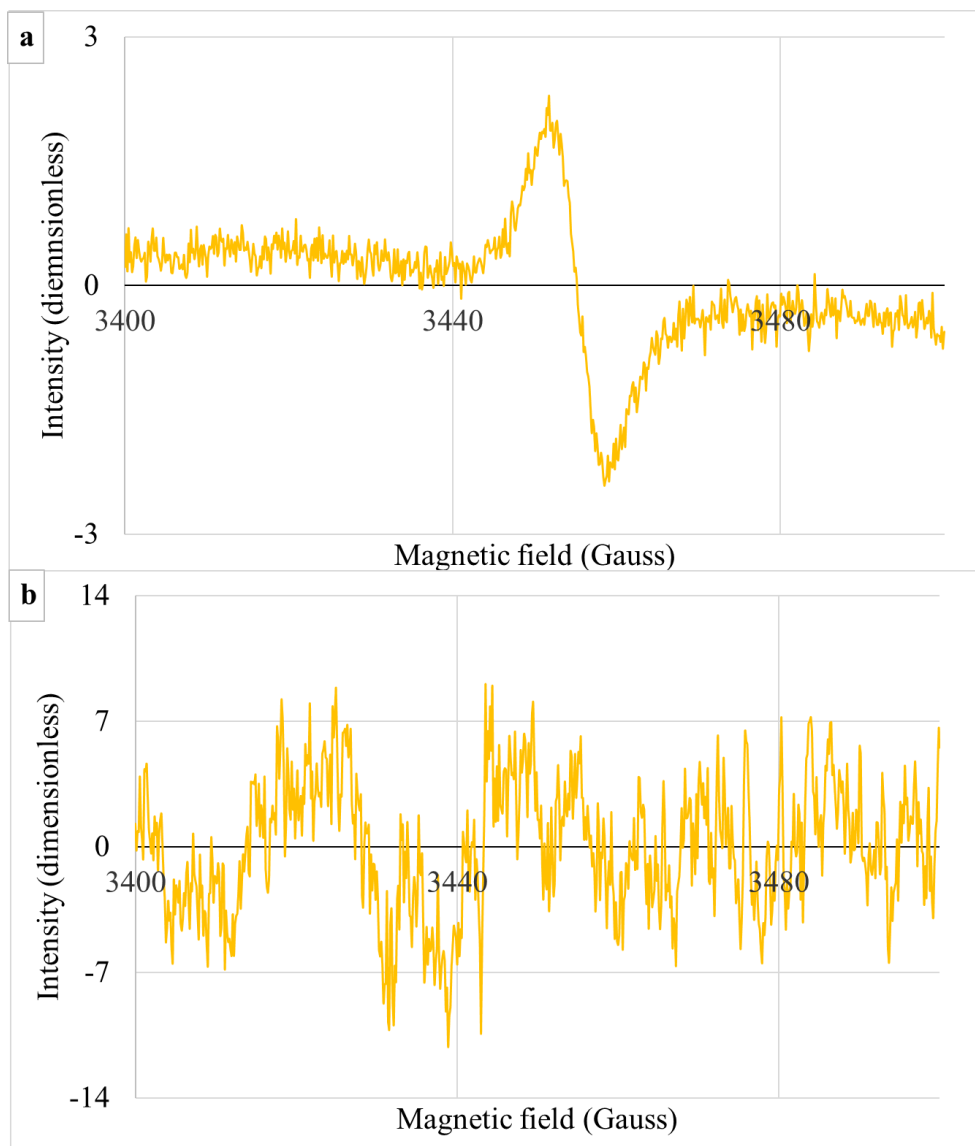


Figure A.2. Comparison of signal-to-noise ratio obtained with (a) Norell tubes (top), and (b) PQ tubes (bottom), for the analysis of an *n*-pentane soluble maltenes sample (DAO-5).

The spectrum obtained using the Norell tube showed only noise (Figure 2 top), i.e. a low signal-to-noise ratio for ESR analysis. The spectrum obtained using the PQ tube had a clear signal (Figure 2 bottom), i.e. a high signal-to-noise ratio.

It was clear that for ESR measurements the tube selection mattered. Although one could use lower quality (cheaper) tubes when dealing with samples having a high free radical content, when analyzing samples with lower free radical content, the microwave transparency of the higher quality (more expensive) tubes is decisive. For all subsequent work in this study PQ tubes were used.

A.3 ESR resonant cavity and probe filling

The signal strength measured by the ESR spectrometer is related to the instrument operating parameters on the one hand and the sample volume (not the sample mass) in the microwave cavity on the other hand. The volume of the microwave cavity itself is not precisely engineered, nor is the quality of the resonant cavity that will be used for signal collection the same from instrument to instrument. There are variations from instrument to instrument even from the same manufacturer.

The resonator quality factor, Q , and the filling factor, η , can be determined.¹ However, when all measurements are performed on the same instrument at the same power conditions, this is not necessary in order to perform quantitative measurements. What is necessary, is to relate the spin concentration in calibration samples to that of samples where the spin concentration is not known. The volume of sample in the microwave cavity affects the filling factor. It is therefore important to always present the same volume of sample for analysis. This is affected by two parameters, namely, the selection of ESR tube and the filling of the ESR tube.

(a) Selection of ESR probe (see Section 2). Unless exactly the same probe will be used for all analyses, it is preferable to make use of probes manufactured with tight control over its internal diameter. In this way one can anticipate that the ESR tubes will have the same internal diameter and cross-section area within a narrow variance, and thus the same volume per unit tube length. Then the inside tube volume that is exposed to microwaves in the cavity will be the same, irrespective of the actual length of the tube section in the resonant cavity.

(b) Filling of the ESR probe. The signal strength is related to the amount of material in the cavity. If two probes are filled from the same stock solution, one should obtain the same signal strength, but only if the same volume of material is analyzed. The amount of material in the cavity = volume in cavity \times concentration; it is therefore very important to make sure that the volume of material in the cavity is the same. Thus, when filling the ESR probe, the volume of the probe that is filled should be sufficient so that the sample extends beyond the microwave cavity. This is illustrated by Figure 3. Sample outside of the volume where signal will be collected does not matter, but if the volume in the cavity from which signal will be collected differs from sample to sample, quantification is impossible.

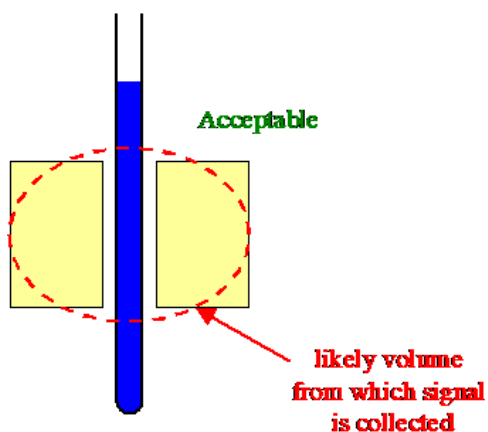
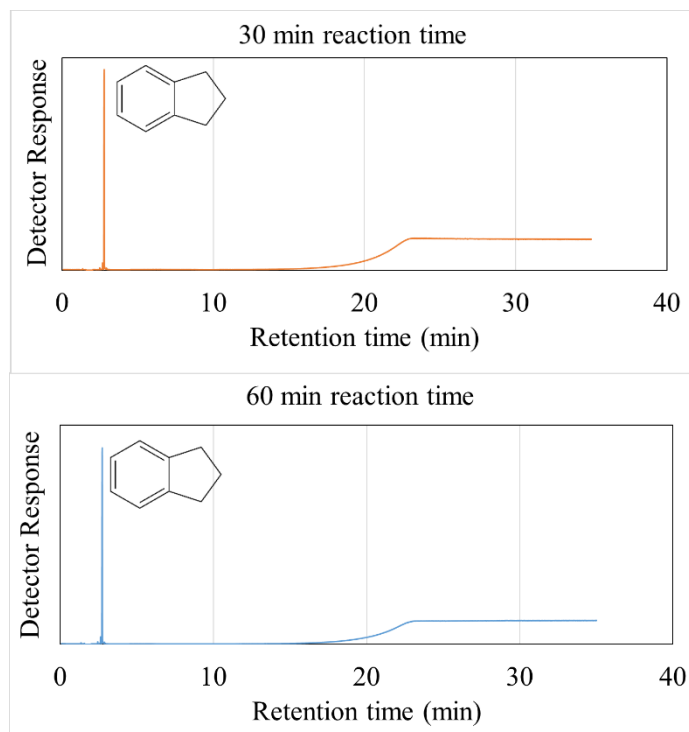


Figure A.3. Illustration of ESR tube filling requirements for quantitative ESR analysis.

In this study attention was paid to both of these aspects.

Appendix B: Chapter 4 Support Information**Figure B.1.** GC-MS of indan product.

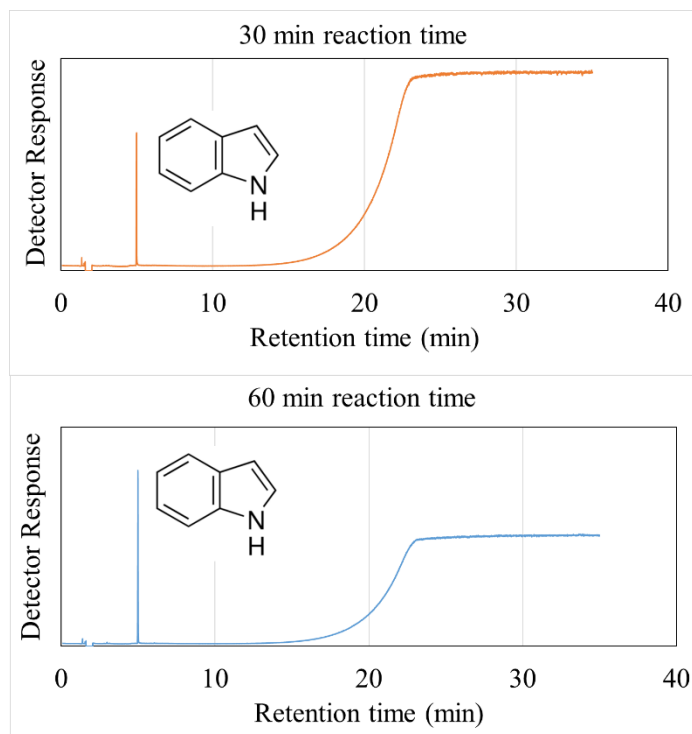


Figure B.2. GC-MS of indole product.

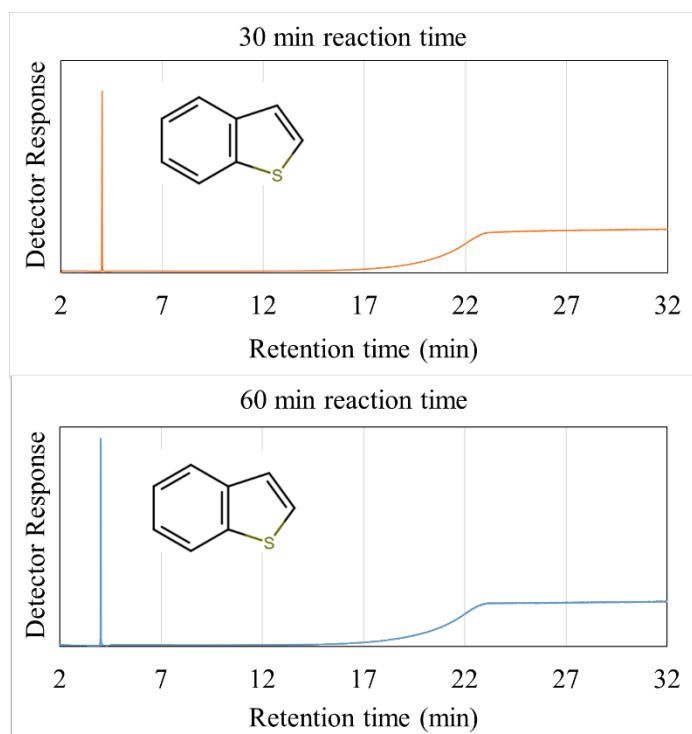


Figure B.3. GC-MS of thianaphthene product.

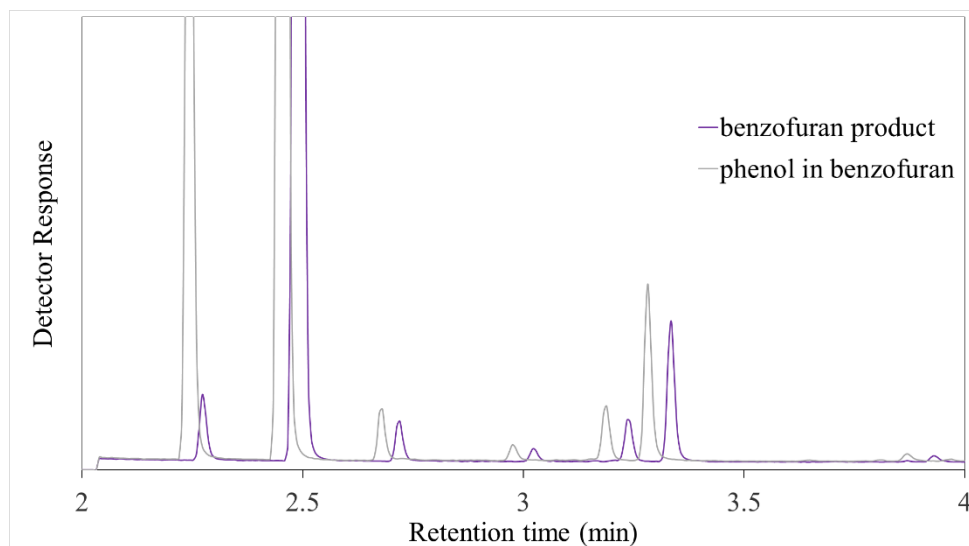


Figure B.4. Chromatogram of benzofuran product spiked with phenol.

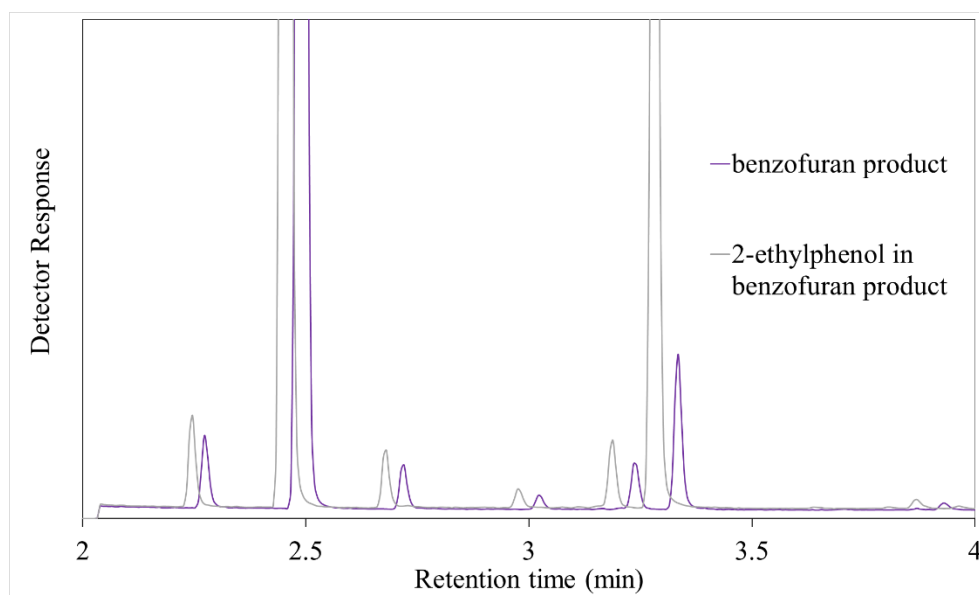


Figure B.5. Chromatogram of benzofuran product spiked with 2-ethylphenol.

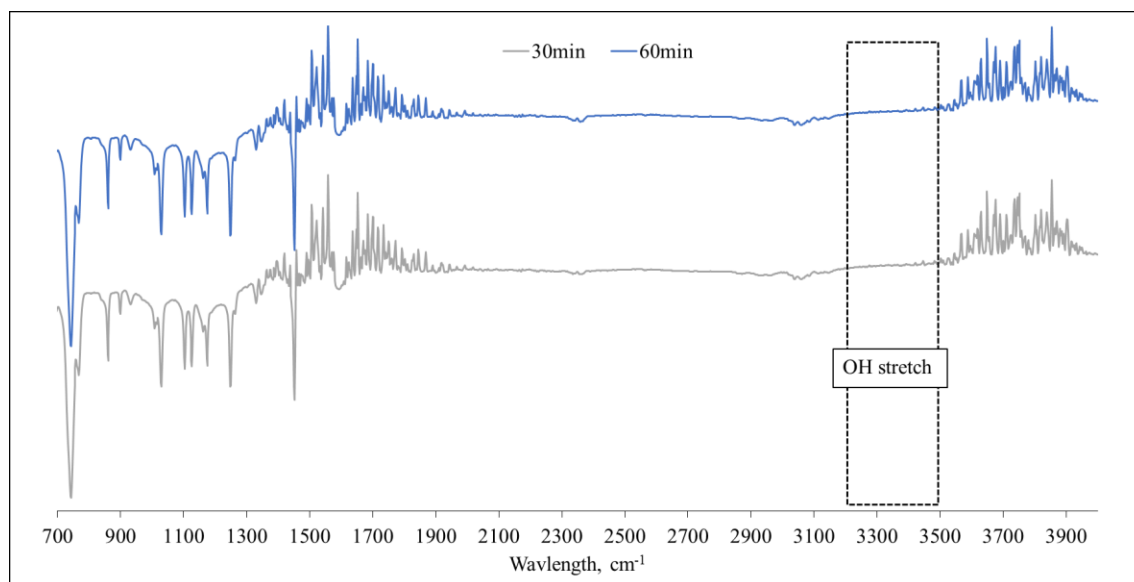


Figure B.6. FTIR results for products of the self-reaction of benzofuran.

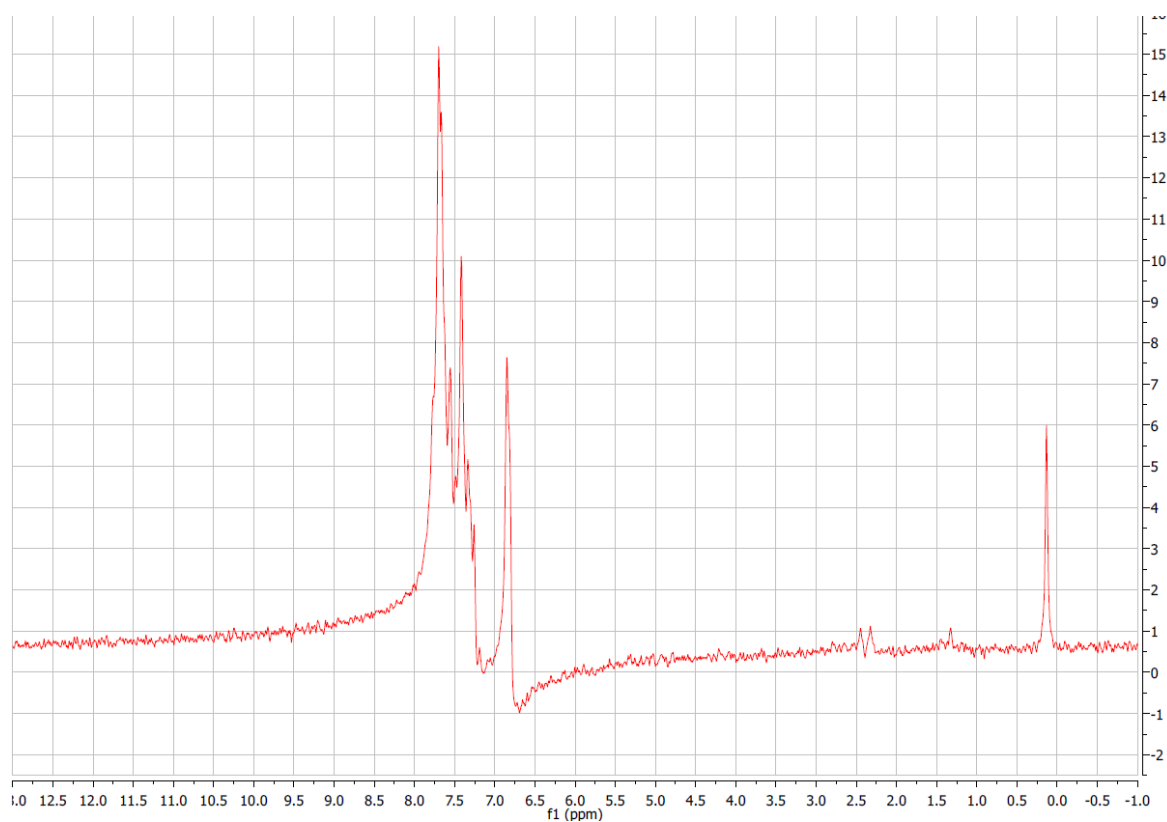


Figure B.7. Screenshot of the Proton-NMR results for products of the self-reaction of benzofuran at 60 minutes.

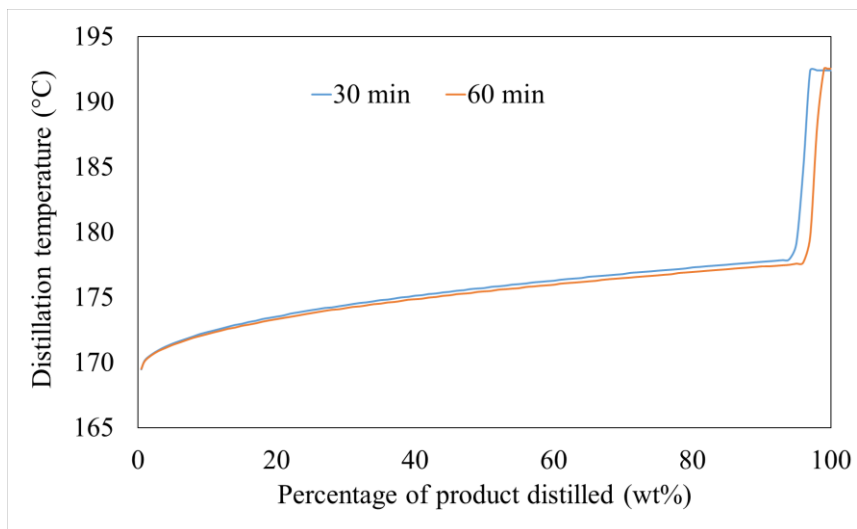


Figure B.8. Distillation curve for the self-reaction of indan product.

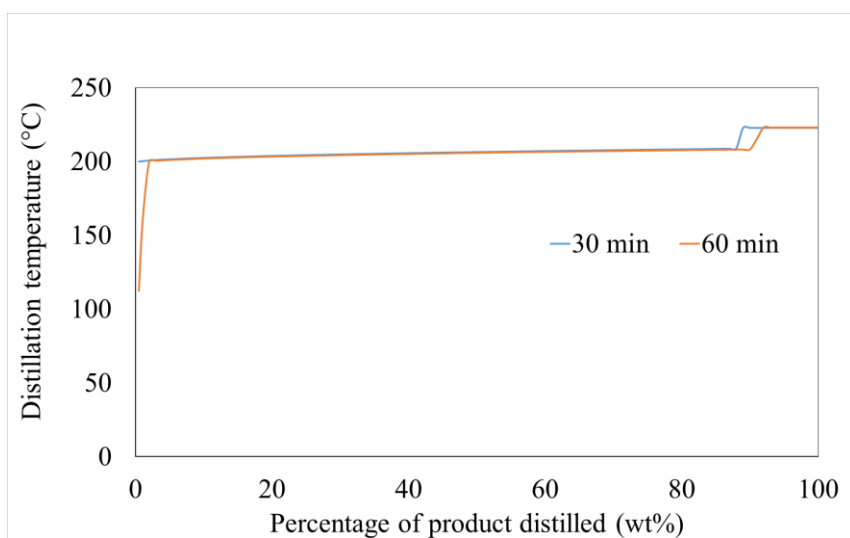


Figure B.9. Distillation curve of the self-reaction of thianaphthene product.

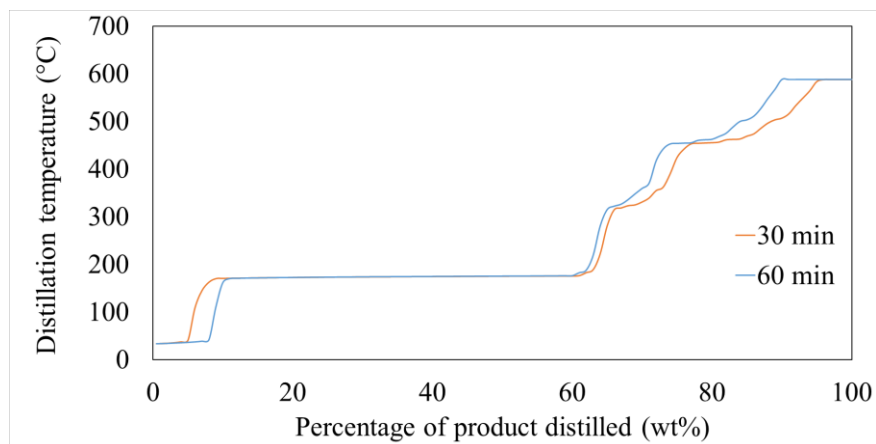


Figure B.10. Distillation curve of the self-reaction of indene product.

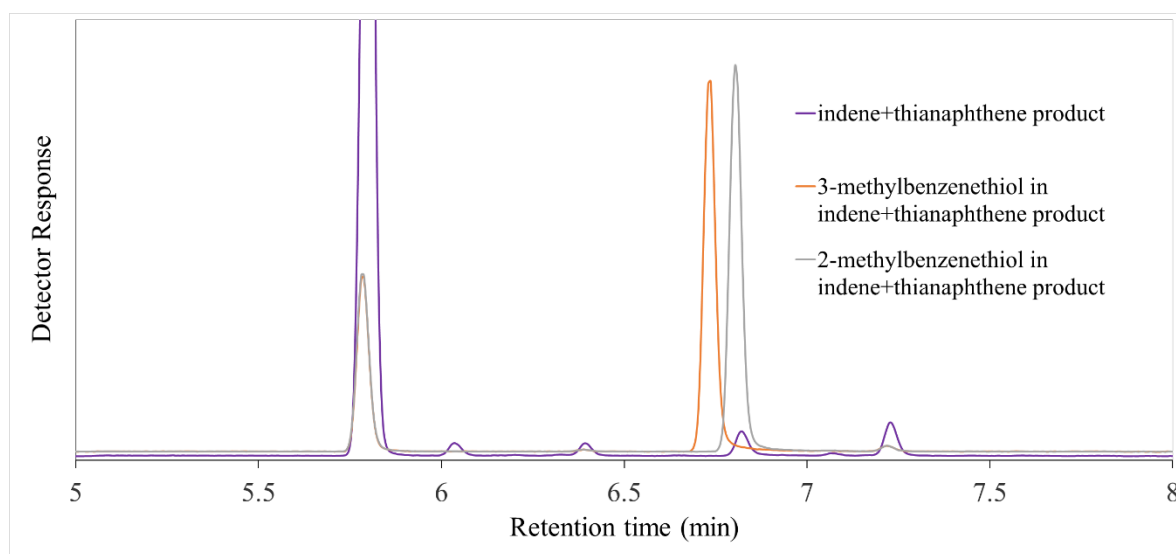


Figure B.11. Chromatograms of the product of indene and thianaphthene along with two other products of the same samples spiked with 2-methylbenzenethiol and 3-methylbenzenethiol.

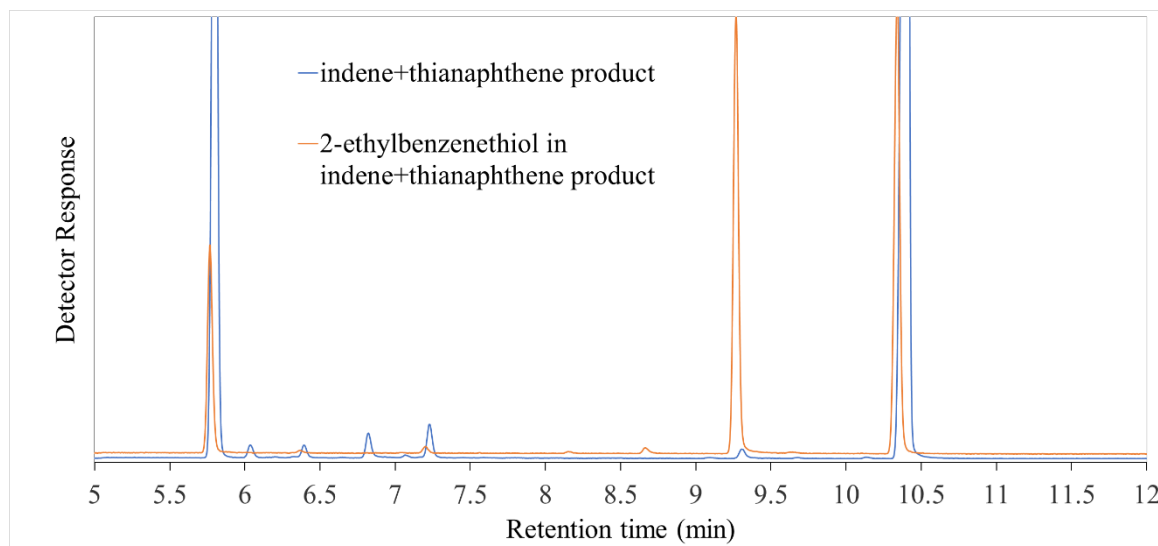


Figure B.12. Chromatograms of the product of indene and thianaphthene along with the same samples spiked with 2-ethylbenzenethiol.

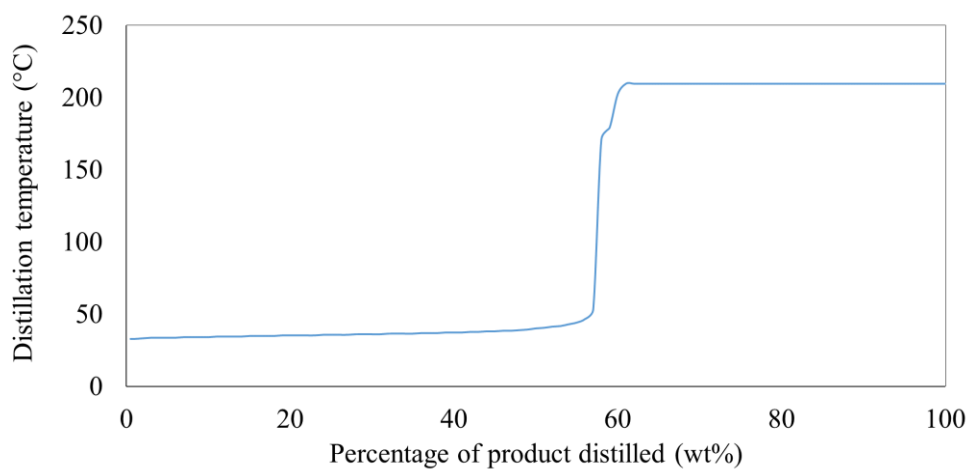


Figure B.13. Distillation curve of the product of the reaction of indan and thianaphthene at 60 min.

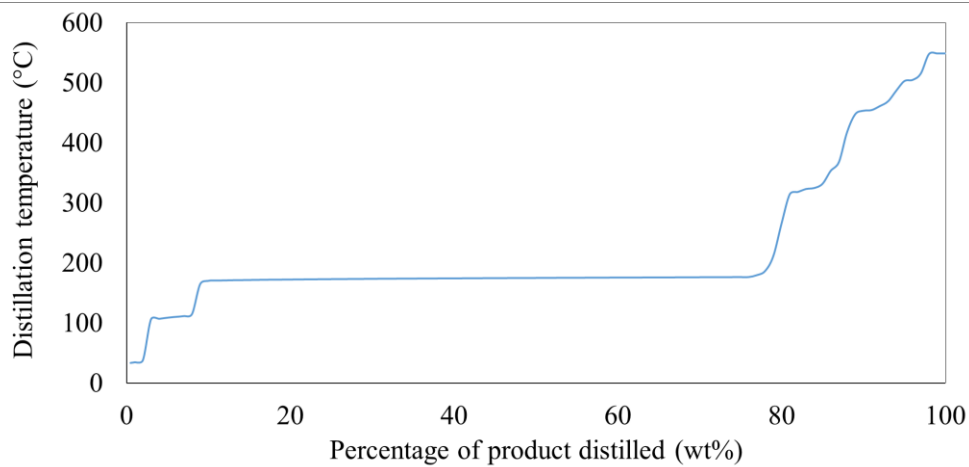


Figure B.14. Distillation curve of the product of the reaction of indene and indan at 60 min.

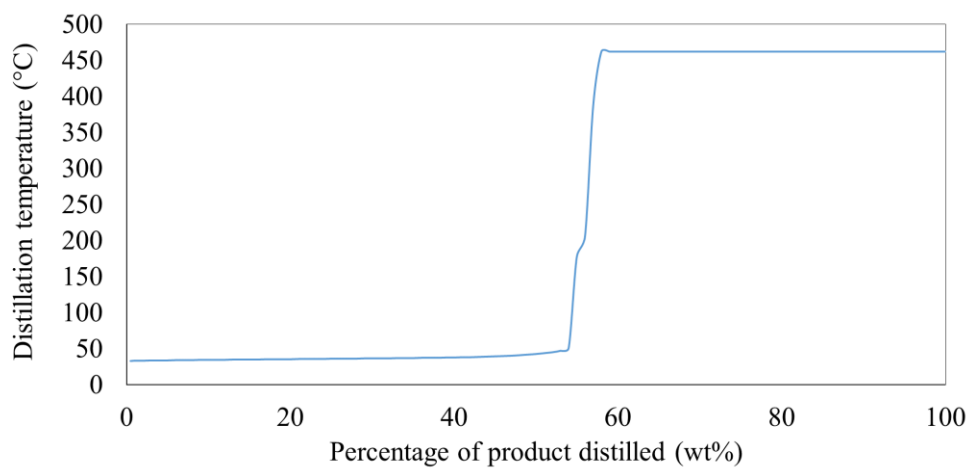


Figure B.15. Distillation curve for the *n*-pentane soluble fraction of the product of the reaction of indene with thianaphthene at 60 min.

Appendix C: Chapter 6 Support Information

C.1: Calculation of the wt% of each light product in the light fraction (b.p < 240 °C excluding gases)

In order to calculate the wt% of each light product in the light fraction, the percentage of cumene in the whole product has been estimated using the SimDist curve. To confirm the correspondence of the plateau (148-155 °C) to cumene, raw cumene has been run in the SimDist.

The percentage of ethylbenzene in the whole product has also been estimated using SimDist, as it is not accurate to use GC-MS for that since the ethylbenzene peak also shows in the chromatographic solvent, toluene, as discussed earlier (section 6.3.1.1). Pure ethylbenzene has also been run in SimDist to confirm the plateau (133-139 °C).

The percentage of the rest of the light elements has been estimated using the relative areas of their peaks with respect to the peak of cumene. We are assuming here that the ionization of all the light fraction in the mass spectrometer is similar as they all belong to the same type of compounds (i.e. substituted aromatics). Therefore, the calculation of relative amounts using peak areas is valid. Cumene peak has been used as the reference since it is the largest peak, reflecting the lowest error.

- Wt% of cumene in the whole product = calculated from SimDist for plateau (148-155 °C)
- Wt% ethylbenzene in the whole product = calculated from SimDist for plateau (133-139 °C)
- Wt% of compound x in the whole product =

$$\frac{(\text{Peak area of compound } x \text{ obtained from GC-MS}) \cdot (\text{Wt\% of cumene in the whole product})}{\text{Peak area of cumene obtained from GC-MS}}$$
- Wt% of compound x in the light fraction =

$$\frac{\text{Wt\% of compound } x \text{ in the whole product}}{\sum \text{Wt\% of all light compounds in the whole product}} * 100$$

C.2: Calculation of the mol% of each feed that reacted to form light fraction and heavy fraction

- mol% of feed y that reacted to form light fraction (i.e. b.p. < 240 °C excluding gases) =
$$\frac{\sum \text{moles of light products originated from feed } y}{(\text{Initial moles of feed } y \text{ in feed}) \cdot (\text{recovery fraction})} * 100$$

Such that

- Number of moles of light compound x originated from feed y =
$$\frac{(\text{Wt\% of compound } x \text{ in the whole product}) \cdot (\text{total mass of product})}{100 \cdot (\text{Molecular weight of compound } x)}$$
- Initial moles of feed y in feed =
$$\frac{\text{Mass of feed } y \text{ in feed}}{\text{Molecular weight of feed } y}$$
- mol% of feed y that reacted to form heavy fraction (i.e. b.p. > 240 °C) = 100 – (mol% of feed y that reacted to form light fraction)

Literature cited

- (1) Eaton, G. R.; Eaton, S. S.; Barr, D. P.; Weber, R. T. *Quantitative EPR*; Springer, 2010.